Summary

Two types of experiments were carried out to study the influence of turbulence in dust-air flame propagation. In the first case, a freely propagating dust-air flame was studied in a vertical tube filled with a pre-suspended dust-air cloud. In the second case, the influence of turbulence was assessed on the burning rate of a dust-air mixture in closed vessels.

Experiments were carried out in a tube 0.19 m inside diameter and 0.91 m long with two ends closed. A dispersion system was developed with a good quality uniform dust suspension and very low level of dispersion-induced turbulence at the moment of ignition. The flame propagation velocity and pressure-time history were measured. The results of measurements of dust flames were compared with that of methane-air flames which were carried out in identical initial and turbulence conditions. The measurements show that the behavior of quasi-laminar dust flames is similar to that of the gas flames. The similarity is based on the similar processes controlling both gas and dust flames. The increase in the maximum overpressure and maximum rate of overpressure rise for dust flames by a factor of two times higher than for gas flames is explained by the increase of combustion efficiency as a result of transition from laminar near-wall combustion to turbulent more uniformly distributed combustion. It was found that the influence of turbulence on the combustion process in a closed tube is more effective in the initial stage of flame propagation along the tube.

Concurrently, experiments have also been carried out to assess the influence of turbulence on the burning rate of cornstarch-air explosions in closed vessels. Different means of varying the turbulence were used, so as to investigate a substantial range of turbulence intensity and a variety of turbulent flow structures.

Since gas-air deflagrations are currently better understood than dust-air deflagrations, all experiments done with the cornstarch-air mixture were replicated with a methane-air mixture, in order to compare the influence of turbulence in explosions in the two media.

The most important finding of the study was that the ratio of the burning rate of the gas-air mixture to that of the dust-air mixture, observed under identical conditions of turbulence, was a constant, independent of the intensity of the turbulence and of the details of the structure of the turbulent flow. This suggests that this ratio is a function of the physico-chemical properties of the mixtures themselves.

Lean flammability limits of gaseous fuel-dust-air mixtures were also studied. The gaseous fuels used were methane and hydrogen. Two different dusts were used in an attempt to determine the influence of volatile content on hybrid limits. Cornstarch was selected for its high volatile content, while iron dust was chosen for its complete lack of volatiles. The experiments were performed in two different apparatus: a 0.18 m^3 cylindrical vessel, and to investigate the effects of scaling, a 5.1 m^3 cylindrical tank. The dust was dispersed by means of an air cylindrical tank. The dust was dispersed by means of an air blast into a hemispherical dust receptacle placed at the bottom of the apparatus. The criterion for self-sustained flame propagation was the evidence of an overpressure in excess of an arbitrarily set limit. For hydrogen-air-cornstarch mixtures, the lean limit of H_2 alone was found to be 4.25% by volume, while that of cornstarch alone was observed to be 70 g/m^3. A line joining these two limits on a graph represents the Le Chatelier limit law (formulated for gaseous homogeneous fuels), which is based on energetics. For the range of mixtures studied, the extension of Le Chatelier's law to hybrid mixtures was shown to be invalid. The deviation of the results from the Le Chatelier law indicates that hybrid lean limits depend more on the mechanism of propagation than on energetics. In fact, it can be seen that in traversing the entire hybrid mixture range from pure dust to pure gas, a crossover region can be identified in which the mode of propagation switches from dust to gas.

Finally, flame quenching in mixtures of cornstarch, aluminum and coal dusts with air has been studied. The experiments were carried out in a vertical tube 0.190 m inside diameter and 1.8 m long with quenching plates held in the middle part. The lean flammability limit determined under constant pressure conditions appears to be several times greater than that determined in constant volume for all dust-air mixtures investigated. The quenching distance was measured in conditions of upward freely propagating flame from the open bottom end of the tube. The minimum quenching distance for flames propagating through dust-air mixtures is 5.5 mm for cornstarch, 10.4 mm for aluminum and about 190 mm for coal dust as compared with 2.0 mm for a stoichiometric methane-air mixture. Because the order of magnitude of the measured quenching distance in cornstarch and aluminum dust flames is the same as in gas flames, it is inferred that processes controlling the flame propagation in all of these flames should be similar. The large value of the quenching distance for coal dust-air mixture can be explained by the large particle size of the coal dust used in the experiments. The quenching distance can be used to identify the controlling processes in laminar premixed coal dust-air flames and hence is one of the most fundamental quantities. This is due to the fact that such quantities as burning velocity and minimum ignition energy are apparatus dependent. Quenching distance determined in limit quenching conditions should not be apparatus dependent.

Resume

Deux types d'experiences ont été effectuées pour étudier l'influence de la turbulence sur la propagation des flammes poussière-air. Dans la première expérience, on a étudié la propagation libre d'une flamme poussière-air dans un tube vertical contenant un nuage de poussière présuspendue dans l'air. Dans la deuxième expérience, on a estimé l'influence de la turbulence sur la vitesse de combustion d'un mélange poussière-air en bombe close.

Les expériences ont été effectuées dans un tube cylindrique fermé aux deux extrémités. Le diamètre intérieur du tube est 0.19 mètre et la longueur du tube 0.91 mètre. On a developpe un système de dispersion permettant d'obtenir une suspension de poussière uniforme tout en limitant la turbulence induite par la dispersion à un niveau minimum avant l'allumage. On a mesuré la vitesse de propagation de la flamme et enregistré la variation de la pression en fonction du temps. Les résultats des mesures sur les flammes poussiere-air ont été compares à ceux des flammes méthane-air effectués dans les mêmes conditions initiales et avec le même degré de turbulence. Les mesures indiquent que le comportement des flammes de poussière quasi-laminaires est semblable à celui des flammes gazeuses. La similarité résulte de la similitude des processus controllant les flammes de poussiere et les flammes gazeuses. La pression maximum et la pente maximum de la variation de surpression pour les flammes de poussiere sont environ deux fois plus grandes que pour les flammes gazeuses. Ces résultats sont attribuables à l'augmentation de l'efficacité de la combustion résultant de la transition de combustion laminaire près des parois en combustion turbulente distribuée plus uniformement. On a observé que l'influence de la turbulence sur le processus de combustion en

tube ferme est plus effective au début de la propagation de la flamme dans le tube.

Parallelement, on a effectué des expériences pour estimer l'influence de la turbulence sur la vitesse de combustion des explosions amidon-air en enceintes fermées. On a utilisé plusieurs méthodes pour varier la turbulence afin d'etudier une gamme suffisante d'intensité de turbulence et une varieté de structures d'écoulement turbulent.

Comme les déflagrations en phase gazeuses sont actuellement mieux connues que les déflagrations de poussiere, toutes les expériences dans le mélange amidon-air ont été reproduites dans le melange méthane-air afin de comparer l'influence de la turbulence sur les explosions dans ces deux mélanges.

Le résultat le plus important de cette étude est que le rapport des vitesses de combustion dans les melanges gaz-air et poussière-air dans les mêmes conditions de turbulence est une constante, indépendentes de l'intensité de la turbulence et des détails de la structure de l'écoulement turbulent. Ceci suggère que ce rapport est une fonction des propriétés physico-chimiques de ces mélanges.

On a également étudié les limites inferieures d'inflammabilité des melanges hybrides: combustible gazeux-poussière-air. Afin de déterminer l'influence de contenu de volatile sur les limites des mélanges hybrides, deux types de poussières ont été utilisées. On a choisi l'amidon pour son contenu élévé en volatile et la poussière de fer pour son absence totale de volatile. Les éxperiences ont été effectuées dans deux appareils differents: une enceinte cylindrique de 0.18 m^3 et pour étudier l'influence de l'échelle, une enceinte cylindrique de 5.1 m^3. La poussiere contenue dans une coupe hémispherique placée au fond de l'appareil était dispersée par une bouffée d'air comprime contenu dans un reservoir cylindrique. On a utilisé comme critère de propagation de flamme autonome l'observation d'une surpression supérieure à une limite fixée arbitrairement. Pour les mélanges hydrogène-air amidon, la limite inferieure d'hydrogène est 4.25% en volume et celle de l'amidon, 70 g/m^3. Une droite joignant ces deux limites sur un graphique représente la loi limite de Le Chatelier (formulée pour les combustibles homogenes gazeux) qui est fondée sur l'énergie. Pour les mélanges etudies, on a observé que la loi de Le Chatelier ne s'applique pas aux mélanges hybrides. La déviation des résultats de la loi de Le Chatelier indique que les limites des mélanges hybrides dépendent du mécanisme de propagation plutôt que de l'énergie. En fait, on peut voir qu'en balayant complètement le domaine des mélanges hybrides entre la poussière pure jusqu'au gaz pur, on peut identifier une région intermédiaire dans laquelle le mode de propagation change de la poussière au gaz.

Finalement, on a étudié l'extinction de flamme dans les mélanges air-amidon, aluminium et poussière de charbon. Les expériences ont été effectuées dans un tube vertical de 0.19 m de diamètre interne et de 1.8 m de long muni de plaques d'extinction dans le milieu du tube. La limite d'inflammabilité inférieure isobarique est plusieurs fois superièure à la limite isochorique pour tous les mélanges air-poussière étudiés. On a mesuré la distance de coincement pour les flammes se propageant librement vers le haut à partir de l'extremité inférieure ouverte du tube. La distance minimum de coincement des flammes poussière-air est 5.5 mm pour l'amidon, 10.4 mm pour l'aluminium et environ 190 mm pour la poussière de charbon. Par contre, cette distance n'est que de 2 mm pour le mélange stoichiométrique méthane-air. Cependant comme la distance minimum de coincement est du même ordre de grandeur dans les flammes de poussière d'amidon et d'aluminum et dans les flammes gazeuses, on en a déduit que les processus qui controlent la propagation de la flamme doivent être semblables. La grande distance de coincement des mélanges poussière de charbon-air peut être attribuée a la taille importante de la poussière de charbon utilisée dans nos expériences. La distance de coincement peut être utilisée pour identifier les processus qui contrôlent les flammes laminaires pré-mélangées de poussière de charbon et d'air. C'est donc un des paramètres fondamentaux. Alors que la vitesse de combustion et l'énergie minimum d'inflammation sont des paramètres qui dépendent de l'appareil expérimental, la distance de coincement obtenue dans les conditions de limites d'extinction devrait etre indépendente de l'appareil expérimental.

5-9080

PROGRESS REPORT

DUST EXPLOSIONS:

1ST 85-00119

Influence of Turbulence on Dust Explosions, the Effect of Methane on Coal-Dust Explosion and Quenching of Dust-Air Flames

by

J.H. Lee
R. Knystautas

Submitted to:

Dr. K. Mintz
Energy, Mines and Resources of Canada
CANMET, MRL

Department of Mechanical Engineering
McGill University
Montreal, Quebec

March 31, 1986

264 pp

MICROMEDIA

THE INFLUENCE OF TURBULENCE ON DUST FLAME PROPAGATION

Submitted by

Y.K. Pu
J.H. Lee
R. Knystautas

McGill University
Montreal, Quebec

March 31, 1986

TABLE OF CONTENTS

I. Introduction

II. Analyses of physical models

1. Proposed model of the structure of a laminar dust flame
2. Proposed model of the influence of turbulence on dust-air flames
3. Review of the physical picture of gas flame propagation in a constant volume tube

III. Experimental details

IV. Experimental results

1. The development of the dispersion system
2. The quasi-laminar dust and gas flame propagation in a constant volume tube with L/D = 4.8 (D = 0.19 m) and the influence of jet-induced turbulence on it.
3. The quasi-laminar dust and gas flame propagation in a constant volume tube with L/D = 9.6 (D = 0.19 m) and the influence of both of jet-induced and obstacle-induced turbulence

V. Summary and conclusions

I. Introduction

The interest in dust explosions, which is by no means new, has been revived by recent major accidental dust explosions in silos, grain elevators, flour mills and coal mines. Dust combustion has become an increasingly important problem both from the point of view of hazard evaluation in coal mines, powder industries, flour mills and grain elevators, as well as in the design of ventilation systems for installations handling combustible dusts. Safety considerations constitute a major motivation for this research. In order to achieve some meaningful assessment of the explosibility of a certain dust-air mixture and guide the design of adequate venting for installations handling combustible dusts, it is necessary to understand the fundamental mechanism of dust flame propagation as well as to acquire reliable data on fundamental explosion parameters such as concentration limits, ignition energies, auto-ignition temperature and burning velocities. A more fundamental understanding of dust explosions will lead to more effective prevention and protection schemes in accidental dust explosion scenarios. All situations of practical interest in the combustion of dust-air mixtures involve some degree of turbulence which also is an intrinsic property for dispersion, mixing and suspension. Therefore, the investigation of the influence of turbulence on dust combustion is becoming an important area of dust combustion research.

Currently, there are two main types of combustion experiments carried out for dust-air mixture; closed bomb experiments and stabilized open flames. Since it is difficult to achieve stationary, adiabatic dust flames for detailed observation, dust combustion has traditionally been studied in constant volume bombs of various sizes and shapes. A considerable amount of data has been accumulated on dust-air explosions, mainly in closed bombs of various shapes and sizes over the past few decades [1-7]. The accumulated data covers factors such as minimum ignition energy, minimum surface ignition temperature, lean concentration limits, maximum overpressure, and the peak rate of overpressure rise (or the K_{St} factor when normalized with respect to the volume of the vessel). All the above mentioned experimental data are somewhat dependent on the apparatus and test procedure, as well as on the physical properties of the dust itself. Little information concerning the flame process can be deduced from these closed bomb experiments. Furthermore, even less is known about the influence of turbulence on the burning rate of a dust flame [7]. In order to correlate these experimental data and achieve some meaningful assessment of the explosibility of a certain dust-air mixture, it is necessary to understand, at least in a qualitative way, the fundamental mechanisms of flame propagation (both laminar and turbulent). Experience with turbulent premixed gaseous flames has already shown that such understanding must be based upon a knowledge of laminar flames. It might be expected that an understanding of turbulent dust flame requires a similar foundation.

The nature of laminar dust flames has been studied in open flame experiments [8-12]. It is fairly difficult to make direct optical observations of the flame structure, since an explosive dust-air mixture is quite opaque. Experimentally, it is also very difficult to produce a uniform laminar flow of a dust-air mixture and to stabilize an adiabatic dust flame on a burner. In view of these difficulties, laminar dust flame structure and mechanisms of laminar flame propagation have not been studied as extensively as gas flames. The U.S. Bureau of Mines has developed a full-scale underground explosion testing facility (with one open end) to study how coal mine explosions are initiated and propagated [13, 14]. Although their experimental results show that the speed of the flame front is increased by turbulence significantly and satisfactory correlations have been developed between dust flame front speed and other flow parameters, it is still not possible to predict the flame front speed itself in terms of the initial conditions, because of the lack of data of the fundamental properties of dust flames and the modelling of dust flame propagation.

Therefore, currently there is no satisfactory empirical relationship linking the burning rate and flame propagation to the relevant parameters of turbulence [15].

In the present study it was thought worthwhile to perform some exploratory experiments in a constant volume tube with L/D as 4.8 and 9.6 respectively to investigate the influence of turbulence on dust flame propagation. There are two reasons to perform dust flame propagation in a constant volume tube. First is that the pressure history in the combustion process can be measured precisely together with the measurement of flame front arrival. Since the pressure history during the combustion process is connected to the energy released during that period, it may be possible to correlate the flame front propagation with the burning rate via pressure data. The second is that in the constant volume tube, the total amount of dust involved in the combustion process is fixed. Because of this, the average dust concentration in the volume can be kept at the same value as initial dust concentration, though the local dust distribtuion has been changed from the initial conditions when the flame starts to propagate. The starting point is based upon a proposed structure and propagation mechanism of laminar dust flames by Bradley and Lee [16]. The assumption made in [16] is that if laminar dust flame propagation for small particle sizes (less than 20 μ m) and high volatile content is governed only by combustion of volatiles, then this kind of laminar dust flame is seen to be rather similar to the laminar gas flame. For homogeneous gases, the fundamental parameters that characterize the explosibility of a mixture are well known and the physical picture of gas flame development in a constant volume tube was observed by Ellis [17, 18] and confirmed by the experiments of Bureau of Mines [3] as well as the effect of turbulence on the propagation for a gas flame is fairly well established [19, 20]. There is no doubt that comparing the experimental data of dust combustion in a constant volume tube to an identical gas combustion can help elucidate the structure and propagation mechanisms of dust flames, since it is fairly difficult to make direct optical observations of the flame structure since it is quite opaque in a typical explosive dust-air mixture. Therefore, combustion of cornstarch-air mixture with size of particles around 15 μm is to be compared to the combustion of methane-air mixture. Such a comparison is used as a means to assess the influence of turbulence on dust flame propagation in the present investigation.

II. The Analyses of Physical Models

1. Proposed model of the structure of a laminar dust flame

The experimental data of laminar dust flame obtained from burners are non-adiabatic and insufficient to study flame structure. Based on the limited studies already made by Smoot, Ballal [21, 22], it would appear that laminar dust flames have burning velocities in the region of 0.3 m/sec, measured flame temperatures of about 1500°K and a flame thickness of the order of 10 mm. Other fundamental parameters that can be related to the flame thickness δ, are the minimum ingition energy and quenching diameter. The careful recent studies of Eckhoff [23] have indicated that the minimum ignition energies of dust mixtures can be as low as the millijoule range. One might find examples that deviate from these typical values but the orders of magnitude of these numbers are about correct. The recent measurements of quenching distance for cornstarch show that the minimum quenching distance for fine cornstarch appears to be 5.5 mm [24]. All these values are comparable with the corresponding ones for homogeneous gas-air mixture, in which the burning velocities for gas flames are about 0.4 ms^{-1}, adiabatic flame temperature about 1800°K and minimum ignition energies in the region of millijoules, the quenching distance as determined in methane-air mixture in [24] is 2.0 mm for the stoichimetric mixture, 9.2 mm for the lean limit and about 20.00 mm for rich limit. From thermal theory of gas flame propagation, it is known that: $u_\ell \sim \alpha/\delta$ or $S \sim \alpha/u_\ell$, where u_ℓ is laminar burning velocity and $\alpha = k/\rho c_p$. If the values for u_ℓ

and α do not differ significantly from those for dust and gas flames then that of δ should also be about the same. Furthermore, the minimum ignition energy, E_{min}, can be shown to be proportional to the cube of the flame thickness. Assuming the same constant of proportionality, if the $(E_{min})_{dust}$ and $(E_{min})_{gas}$ measured are in the same region of millijoules, the δ_{dust} and δ_{gas} must be the same order of magnitude. Finally, it is known from [25] that quenching distance is linked directly to flame thickness. Quenching distance can be determined with relative ease and if properly measured should not be dependent on the apparatus because by definition, it is determined at the limit quenching conditions. It was shown in [24] that the order of magnitude of measured quenching distance in cornstarch-air dust flame is the same as for methane-air gas flame. It would appear from these analyses of the measured data of dust and gas flames, that the effective thickness of a dust flame should have the same order of magnitude as that of a homogeneous gas flame. Because the thickness of flame propagation in cornstarch-air mixture is comparable with thickness of methane-air mixture, the processes controlling flame propagation in these mixtures should be similar even though they have very different physical properties. In the case of cornstarch dust-air flame heat conduction from the high temperature combustion zone raises the particle temperature to start volatilization. The flame propagation is controlled in this case by heat conduction from the hot gas to the particles and by the rate of streamwise molecular diffusion of oxygen and volatiles. This mechanism of flame propagation in premixed laminar dust-air mixtures is supported by the recent investigations of Smoot [21]. Smoot and co-workers [21] reported a series of parametric predictions to identify the controlling processes in premixed fine coal dust-air flame. The method used for their predictions has been systematically developed since 1976 [21] and it has been found that the rate of flame propagation is controlled by the rate of streamwise molecular diffusion of oxygen and volatiles, together with heat conduction from the hot gas to the particles.

It also has been found that radiation, heterogeneous reaction, rates of coal devolatilization and volatile oxidation in the gas phase play a secondary role in the propagation of the flames studied.

A tentative structure of laminar dust flame is proposed as shown in Fig. 1. It consists of three sub-regions; preheat zone, gaseous phase reaction zone, and solid char burning zone. The devolatilization process is taken to be almost entirely within the preheat zone. The effective thickness of the dust flame is determined by the gaseous phase reaction zone. The devolatilization process is largely completed and gas phase reactions occur with high concentration and fast reaction rates of O, OH, H in the gaseous phase zone; also the temperature gradient established by gas phase reactions in this zone is of the same order of magnitude as in the premixed laminar gas flame. The solid char burning zone involves less heat release and a slow burning rate of the solid char with concentration and slow reaction rates of O, OH, H. This solid char burning zone is much thicker than the gaseous phase reaction zone, as a hot tail in the dust flame.

This proposed structure of a dust flame is limited to the small particle size of the fuel (less than 20 μm) with a high volatile content. It would be expected to apply to certain dust materials such as lignites, bituminous coals, vegetable grains and powdered foodstuffs, etc. in which the solid particles are able to emit appreciable amounts of "volatile" gases when heated. The devolatilization process in all of these materials depends mainly on the size of the particles. It is evident that the proposed model is not universal and depends strongly on the nature of the fuel and particularly on the particle size-distribution.

2. Proposed model of the influence of turbulence on dust-air flames

The similarity between laminar dust and gas flames is the starting point in the analysis of the influence of turbulence on dust-air flames in the present study. Therefore, it is necessary to describe the turbulent flow structure and review the influence of turbulence on the burning rate of a flame propagating through a homogeneous gas mixture briefly.

Although there is probably no such thing as a standard turbulent structure we may nevertheless give a simplified picture of isotropic turbulence which contains the essential ingredients of the turbulent flow structure. The turbulent kinetic energy is distributed non-uniformly over a spectrum of the length scales or eddy sizes, the largest of which is of the order of the dimensions of the container, whilst the smallest is the Kolmogorov, dissipative microscale, η. The simplified model in the present study deals with but three scales: the integral length scale, ℓ, associated with the mean eddy size, the Taylor microscale λ, and the smallest dissipative scale η. Turbulent energy is not dissipated uniformly but displays an intermittency as shown in Fig. 2. Tennekes [27] has suggested that dissipative eddies consist of vortex tubes with a diameter of the order of η and a spacing of the order of λ. The simplified model of turbulent flow structure can be described as shown in Fig. 3.

It is known that when a flat laminar gas flame propagates into a container which is filled with turbulent flow, the turbulence will increase the volumetric burning rate ($\dot{\bar{V}}$) of the gas flame in two ways: by increasing the local burning rate, u_ℓ, and by increasing the area of flame surface, A. Then $\dot{\bar{V}}$ is proportional to AU_ℓ. The analysis for the role of turbulence to influence the gas flame propagation is based on the two comparisons. One compares the characteristic length scales associated with the turbulent flow structure, i.e., ℓ, λ, η to the gas flame thickness. Another compares the characteristic time scales associated with the turbulent convection process, i.e. t_ℓ $(=\ell/u_\ell)$, $t_\lambda(=\lambda/u_\ell)$, $t_\eta(=\eta/u_\ell)$ to the characteristic time scale associated with the diffusion process, $t_d(=\delta^2/\alpha)$ in the laminar flame propagation. If the eddy sizes are larger than the flame thickness, the velocity gradients produced by the eddies can increase the area of the flame surface by folding and wrinkling. Otherwise, the flame surface would not be folded by small scale eddies. If the characteristic time scale of the turbulent convection process in the three eddy regions are comparable to the diffusion process in the laminar flame propagation then the diffusion process will be replaced by the turbulent convection process. Otherwise, the local burning rate will not be increased when the laminar flame propagates into the turbulence flow. The detailed analysis is as follows. In the integral eddy regions, if $\ell >> \delta$ and $t_\ell >> t_d$, then the velocity gradients produced by the integral eddies will increase the flame surface by folding but the turbulent convection will not influence the local burning rate, as shown in Fig. 4(1). In the Taylor eddy regions, if $\lambda > \delta$ and $t_\lambda > t_d$, then the velocity gradients produced by Taylor eddies also will increase the flame surface area by wrinkling and the turbulent convection will not influence the local burning rate, as shown in Fig. 4(2). In the Kolmogorov eddy region, if $\eta = \delta$ and $t_\eta = t_d$, then the velocity gradients produced by the Kolmogorov eddies cannot fold the flame surface, but the local burning rate will be increased by turbulent eddy transport instead of the molecular diffusion process, as shown in Fig. 4(3). A physical model of turbulent gas flame propagation can be sketched in Fig. 5.

For the dust flame case, the comparison of charcateristic length scales between dust particles, particle spacing distance to turbulent eddy sizes is sketched in Fig. 6. The comparison of characteristic time scales between the turbulent convection process to the mass diffusion process is described as follows with cornstarch particles of 15 μm diameter and a dust concentration of 500 gm^{-3}, the average inter-particle spacing is about 0.15 mm. If we assume the relative velocity, or slip, between particles and air is about 0.1 ms^{-1} then the associated Reynolds number is 1.5×10^{-2}. Thus we may ignore the influence of turbulence on the local transport rates around the dust particles. If the particle size is much smaller than the diameter of dissipative vortex tube (i.e. η), then the intense shear in these regions is unlikely to influence the transport processes involving the particles. However, in the Kolmogorov eddy regions (η), if the turbulent convection time is comparable to the mass diffusion time among the particles, then turbulence will increase the diffusion rate of the emitted gases from hot particles into the surrounding air and the gas phase burning rate among the particle is increased. In the Taylor eddy regions (λ) if the turbulent convection time is longer than the mass diffusion time among the particles, then turbulence will not increase the diffusion rate of the emitted gases from the hot particles into the surrounding air. Therefore the strong burning regions only occur in the smallest eddies and they will spread from small eddies across the distance λ with the speed of λ^2/ν like the diffusion rate of vorticity, since diffusion of mass, heat and vorticity have the same rates. In the integral eddy regions (ℓ), if turbulent convection time is much longer than the mass diffusion time among the particles, then turbulence will not increase the diffusion rate of the emitted gases from the hot particles into the surrounding air, but the flame is expected to wrinkle as in the case of the gas flame if the effective thickness of a dust flame is estimated of the same order as that for a gas flame and is much less than the integral scale of the turbulent eddies. A physical model of a turbulent dust-air flame is proposed as in Fig. 7.

3. Review of the physical picture of gas flame propagation in a constant volume tube.

Although a large number of data has been gathered on combustion in closed vessels over the past 60 years, most of them studied combustion in closed spherical vessels [28, 29]. The combustion processes in a closed cylindrical tube is very different from that in a closed spherical vessel, but this kind of combustion ever since the time of pioneering investigations of Ellis [17, 18] until now still has not been fully recognized. In the tube, the flame after ignition can propagate only in the direction of its axis. Because of this, one can distinguish two different stages of flame propagation in a closed tube shown in Fig. 8 and Fig. 9. In the first stage, the flame speed is augmented by the expansion of hot gases when the ignition is located at one of the closed ends of the tube. The flame accelerates while its surface develops from a hemispherical to an increasingly elongated semi-ellipsoidal shape. The axial velocity of the flame increases gradually until the flame surface area reaches a maximum value whereas the radial velocity in plane of the upstream end of the tube gradually decreases. In a given mixture, the velocity of the fresh gas obviously depends on the dimensions of the tube. Consider two tubes of equal diameter but of different length L. In the short one, after the initial movement of the flame, the presence of a downstream end wall fairly close to the ignition point impedes axial expansion of the burned gas. Therefore, the flame assumes a less elongated shape than in the long one. According to [30, 31], increased length of the tube increases the maximum flame surface area and the axial velocity of flame. However, if the tube is long enough the flame development will be identical regardless of the value of the length of the tube. The second stage starts while the flame (with cylindrical surface) reaches the side walls of the tube. Then heat losses increase and the area of flame surface decreases very rapidly because the roughly cylindrical part of its surface vanishes. The cooling by conduction to the wall decreases the temperature and causes the density of the product gases to increase. Both of these effects cause a decrease in the apparent velocity of the flame front. Deceleration causes the flame to become unstable in the sense of the Taylor-Markstein instability and the central region becomes cusp-shaped. Taylor [32] showed that a contact discontinuity between two fluids of different density is unstable to acceleration in a direction perpendicular to its orientation if the acceleration is directed toward the light fluid. Figure 10 shows a clear picture of a pure Taylor instability of the flame propagating in a lean methane-air mixture from the closed to the open end of the tube in the direction of gravitational acceleration. The Markstein instability can be discussed in terms of two different processes in nature. The first is related to the cellular structure of the flame observed during its laminar propagation. The second is related to the interaction of the compression or rarefaction wave with the flame, which can be observed during the very strong combustion process in a rather long tube.

The stability of laminar spherical flames was analyzed by Markstein [31], and Istratov and Librovich [33] who used the theory of Landau [34]. Their analysis shows that the onset of instability occurs at a critical Reynolds number which is a function of the expansion ratio. The values of Reynolds number they predicted are in the range of 1000-2000. Real values of critical Reynolds numbers measured in [35] are reported to be in the range 3070-3950. When the Taylor and Markstein cellular instability interacts with the acoustic instability of the tube, acceleration of the flame front can be provided and as a result, an increased rate of pressure rise attained.

The effect of instability related to the interaction of the compression or rarefaction waves with the flame was investigated by Markstein [36]. For a short length of tube, where the compression waves emitted by the laminar flame do not have time to merge into a shock wave, the flow of fresh gases is controlled mainly by the gas movement which is caused by the rarefaction wave reflected from the downstream end. Because of the relative long duration of the first stage of flame propagation, the rarefaction wave travelling in the unburned gases is the first to reach the flame front, in spite of the higher speed of sound in the burned gases as compared with its speed in the fresh gases. For a long length of tube with strong turbulent combustion, the shock wave can be produced, the rarefaction waves travelling in the burned gases reach the flame front first. This wave is partly transmitted into the unburned gases as a rarefaction wave, causing a flow of these gases towards the flame, and partly reflected as a rarefaction wave within the burned gases. The reflected wave returns toward the flame front after a further reflection at the upstream end, and this may occur several times before the rarefaction wave coming from the side of the unburned gas reaches the flame. The latter wave transmits a rarefaction wave into the hot gases, that ultimately reinforces the effect of the original rarefaction wave. It also gives rise to a weak reflected compression wave in the cold gases which will reduce the flow velocity of these gases towards the flame front. Figure 11 shows a clear picture of the Markstein instability as a result of the interaction of a shock wave and a laminar flame.

The effect of any kind of instability is very important when a flame propagates in enclosures, because the increased area produced by an unstable flame causes a more rapid rate of pressure rise than in an open vessel.

The critical value of the ratio of L/D is considered from the point of view of the maximum distance passed by an undisturbed flame during the first stage of its propagation. Experimental results of laminar flame propagation carried out by Ellis [17, 18] shown in Fig. 8 were used to plot dependence between dimensionless length of the first stage of combustion and the ratio of the length of the tube to its diameter (Fig. 12). For a small ratio L/D, an increased length of the tube substantially increases the length of the first stage of flame propagation. However, when the tube is long enough, the length of the first stage will be determined by the cooling effect of the tube walls and will be identical for all the tube lengths.

III. Experimental Details

In general, it is known that the dust flame zone is much thicker than gas flame zone, therefore the apparatus for investigating the influence of turbulence on combustion of dust-air mixture has to have the appropriate geometric parameters. The test tube used in the present experiments has a diameter of 0.19 meter and two different lengths of 0.91 and 1.82 meters. It is obvious that getting a uniform dust dispersion along a long vertical tube involves many difficulties. Experiments not only require uniform spatial distribution of the dust particles along the tube axis, but the particles must remain suspended for the duration of the combustion process. In order to obtain a uniform axial dust concentration distribution, a long vertical test tube can be cascaded in several segments. Each segment contains its own dust dispersion system and has the same construction as the others as shown in Fig. 13. With the configuration, the global non-uniformity along the length of the tube is negligible. Figure 14 shows the structure of one segment. It consists of a 0.19 meter diameter test tube with two ends closed; a dispersion tube (14 mm ϕ x 0.91 mm long) and an additional tube (14mm ϕ x 0.91 m long) for generating jet turbulence within it.

The dispersion system also is shown in Fig. 14. A 14 mm ϕ dispersion tube runs along the wall of the main tube, containing a series of small dispersion holes (the diameters of the holes are 1.0, 1.5 and 2 mm). In front of the dispersion tube there is a 9.5 mm ϕ circular cross section bar to deflect the dust jets. The dispersion tube is connected upstream to a dust vessel which is a small cavity, a solenoid valve and an air reservoir, respectively. Prior to dispersion, a measured quantity of dust is loaded into the dust vessel. The air reservoir is 230 cm^3 and is pressurized to 10 bar overpressure. When the solenoid valve is opened, the dust is convected from the cavity through the dispersion tube. The impulsive jets emerging from the dispersion holes blow the dust against the bar and disperse it uniformly throughout the test tube. In the dispersion process there is a fast decay of the dispersion-induced-turbulence existing within the test tube. Systematic testing and measuring was done to study the uniformity of dust concentration distribution which is dispersed by the dispersion system designed as shown in Fig. 14. The uniformity of the dust particle suspension along the test tube was evaluated by light transmission measurements shown in Fig. 15. Transmission data were obtained by photomultiplier with a laser beam passing through the dust-air mixture perpendicular to axis of the test tube. Results show that if the diameter of the dispersion tube is fixed as 14 mm ϕ, the uniformity of the dust concentration between the top and bottom sections depends on the arrangement of the diameter and the number of the small dispersing holes, the shape and size of the bar which is in front of the dispersion tube, and the gap beween the dispersion tube and bar. Results in Fig. 16 show that initially there is more dust suspended in the top cross-section than in the bottom one. Experimental data also show that in both the top and bottom cross-sections, the dust particle suspension lasts at least 0.5 seconds. Therefore, a fairly uniform dust suspension is considered to be have been achieved for the duration of the dust combustion process which lasts about 0.5 seconds.

The other 14 mm diameter tube in the test tube is the jet-turbulence generator. It contains four series of small holes along its length with diameters ranging from 0.5 to 1 mm. Four series of small holes are equally spaced on a 90° arc. The turbulence tube is connected upstream to a solenoid valve and to another bigger air reservoir (1500 cm^3). In the system, when the solenoid valve is opened, the pressurized air in the reservoir is released into the turbulence tube. The turbulence jets emerging from the holes cover a great percentage of the tube cross-sectional area. The intensity of the jet-induced turbulence is related to the initial pressure in the reservoir (3.5 to 10 bar) and can be determined from the mean velocities of the jets by the experimental correlations of Wygnanski and Fiedler [37]. The average velocities of the jet along the jet centre-line are determined in four positions by the experimental data of the dust particle time of arrival from the light transmission measurements. It is assumed that the dust particles have the same velocity as the air jets. The exit velocities of four line jets are derived from the measured data of average jet velocity gradient according to the profiles of the mean velocities along the jet centre-line which are given by the experimental studies of Wygnanski and Fiedler [37] and Knystautas [38]. As an example, a jet exit mean velocity of 30 m/sec, which corresponds to 10 bar initial overpressure in the reservoir, decreases rapidly to 6 m/sec, 30 mm away from holes, to 2 m/sec at 60 mm, which is the center position of the test tube and decreases more slowly to 1 m/sec beyond half the tube diameter. The intensities of u', v', w' fluctuations in the jet centre-line decrease according to the same law as the mean velocity. All of these results are shown schematically in Fig. 17.

Ignition of the dust-air mixture at the centre of the bottom part of the tube is by a black powder ignitor. A dust flame starts to propagate and develops upwards along the constant volume tube. The air jet-induced turbulence can be added to the original dust combustion process after an appropriate time delay to investigate the influence of turbulence on dust flame propagation. The time delay between dispersion and ignition is controlled by means of an electronic timer and the time delay between ignition and turbulence addition is controlled by a mechanical timer. During the combustion process, the pressure-time history is measured by a PCB quartz pressure transducer. The maximum rate of overpressure rise is calculated from the slope of a tangent to the pressure-time curve through its inflection point. The flame front time of arrival is measured by ionization gauges which are located at three positions along the length of one tube.

The dust used in the present study was cornstarch, a natural polymer of dextrose, with formula $(C_6H_60_5)_n$. Peraldi [39] has measured its heat of combustion to be 631.5 kcal/mole and its heat of formation 222 kcal/mole. The literature seems to contain no information on the devolatilization properties (i.e. products, rate and enthalpy of devolatilization) of cornstarch. Commercially available starch usually contains about 10% moisture by weight. In the present study, the cornstarch was placed in an oven at 90° C for about 18 hours prior to experiments, to eliminate the moisture and thus help produce a more uniform dispersion. Also a fluidizing agent (CAB-0-sil) was mixed with the cornstarch in the proportion of 0.5% of fluidizing agent per unit mass of mixture, to further improve the dispersion. A particle size analysis obtained via direct imaging with an optical image analyzer showed the average size of the particles to be 14.7 microns, with a standard deviation of 5.1 microns. Scanning electron micrographs shown in Fig. 18 showed the particles to be remarkably spheroidal in shape. The following table summarizes the properties of cornstarch that are relevant to its combustion chararcteristics.

Chemical formula:	$(C_6H_{10}0_5)_n$
Mole weight of manomer:	162
Density:	1.5 gm/cm^3
Stoichiometric concentration (theoretical):	253.7 gm/m3
Heat of combustion:	631.5 kcal/mole
Heat of formation:	222 kcal/mole

IV. Experimental results

1. The development of a dispersion system

The study of the influence of turbulence on dust combustion appears to involve contradictory experimental requirements with respect to the dispersion system. To disperse the dust effectively for a uniform suspension of dust-air mixture at a definable and reproducible concentration, an intense flow producing turbulence in every dispersion system is required. On the other hand the investigation of the influence of turbulence on dust combustion requires a quiescent mixture at the initial conditions of dust combustion. Thus the coupling of the combustion process with dispersion-induced turbulence presents some difficulty isolating the influence of turbulence on dust combustion in the investigation. It is necessary to design a compromise dispersion system with good quality uniform dispersion of dust and as low level of dispersion-induced turbulence as possible at the moment of ignition. Such a dispersion system satisfying these conditions has been systematically developed in the present study. The influence of dispersion-induced turbulence on the maximum overpressure and maximum rate of overpressure rise are shown in Fig. 19. The peak overpressure approaches the maximum level in the range of ignition delay time from 50 to 100 ms (fluctuation can be attributed to nominal dust concentration variations), decreasing slowly thereafter. With an ignition delay time of 250 ms, the peak pressure is at the level of 80% of its maximum value. Because the magnitude of the peak pressure reflects the quantity of dust particles participating in combustion, it can be inferred that 80% of dust particles are still in suspension, and the dust particles settling can be ignored. For delay times longer than 500 ms, the maximum overpressure of the dust combustion is also practically independent of dispersion-induced turublence. The dispersion-induced turbulence influences the maximum rate of overpressure rise of dust combustion to a different degree depending on the ignition delay time and the concentration of the dust-air mixture. It approaches the maximum value when the ignition delay time is 50 ms and decays very fast beyond this point, becoming equal to about 120% of its reference value when ignition delay time is 250 ms. The reference value corresponds to the ignition delay time of 700 ms which is determined by the gas combustion in an identical dispersion-induced turbulence condition. To meet the contradictory requirements of low dispersion-induced turublence level at an acceptable dust suspension level, the ignition delay time 250 ms has been chosen in the experiments as the baseline delay time because at this point the dust is effectively in an initial quasi-laminar suspension. Figure 20 displays the maximum pressure and K_{ST} factor, obtained at the chosen ignition delay time (i.e., 250 ms) versus the cornstarch concentrations against a background of experimental data of other researchers. The maximum overpressure which indicates the quality of the dust suspension is in agreement in present with the work of others. In contrast, the K_{ST} factor which is related to the intensities of the dispersion-induced turbulence is much less at a very low level. It is evident from the experimental results presented in Fig. 20 that the developed dispersion system satisfies the requirement namely that a good quality uniform dust suspension with very low level of dispersion-induced turbulence be achieved.

2. The quasi-laminar dust and gas flame propagation in a constant volume tube with L/D = 4.8 (D = 0.19 m) and the influence of jet-induced turbulence on it

The flame conditions just at ignition whether for a dust or gas mixture at optimum delay time are arbitrarily designated as quasi-laminar for convenience. The experimental data for the speeds of the quasi-laminar flame for both gas (9.5% CH_4-air) mixture and cornstarch dust-air mixture (dust concentration at maximum pressure in closed vessel, $C_d \simeq 500$ g/m_3) show that the development of the flame in a closed tube with L/D = 5 is similar to that observed in the experiments of Ellis [17,18]. Three regions with different propagation velocities and different slopes in the pressure curves are distinguishable as a result of these measurements and are shown in Fig. 21. Combustion in the first stage is characterized by very high propagation velocity of the flame front and slight increase of pressure. In the second stage the slower propagation velocity is accompanied by a substantial pressure increase. In the third stage the increased propagation velocity is accompanied by a further pressure increase, very high for the gas flame and more moderate for the dust flame. The effect of jet-induced turbulence on the quasi-laminar dust flame, in these three different stages of its propagation, has been investigated.

Figure 22 illustrates this influence on maximum overpressure and maximum rate of overpressure rise for both gas and dust flame propagation by adding turbulence in three different time delays indicated by n. The n factor is a ratio of the time delay of turbulence addition after ignition to the duration of the combustion process, which is a period between the time of the peak pressure arrival in the pressure-time history and the time of ignition. Three n values taken in the dust and gas flame propagation correspond to adding turbulence in three different regions previously mentioned. Two phenomena are observed in the above experiments. One is that the dust and gas flames are influenced by jet-induced turbulence to a different degree. The maximum overpressure is 1.5 times higher and the maximum rate of overpressure rise is 2-3 times higher for dust flames than for gas flames. The other is that in both gas and dust combustion the most effective influence of jet-induced turbulence on combustion is observed when turbulence is introduced in the first stages of flame propagation.

As a result of the present experiments, a physical model of quasi-laminar dust flame propagation in a constant volume tube has been suggested. The behavior of the dust flame in this model is similar to that of a gas flame. The similarity is based on the fact that the same processes, which are heat conduction and molecular diffusion, control both gas and dust flames. This similarity between gas and dust flame has been already suggested in the paper of Bradley and Lee [16] mentioned before. This suggestion is also supported by the recent works of Smoot et al [23] and by the recent measurements of quenching distance for cornstarch dust-air mixture by Jarosinski et al [24].

From the points of view of interaction of turbulence with a laminar flame in the closed tube the most interesting event in the present study is the first stage of combustion, both for gas and dust flame. The first stage provides the best conditions for the investigation of the interaction of the turbulence with the flame because they are characterized by a clear gas dynamics model of flame propagation and the small influence of pressure on the combustion process. The second and the third stages of combustion in the closed tube are influenced, according to Strehlow [25], by Taylor-Markstein instability phenomena which turbulize the flame and interfere with an additionally introduced turbulence. Therefore, it is only natural that the most effective influence of additional turbulence on combustion is in the initial stage of the flame propagation.

Relatively high growth of maximum overpressure and higher maximum rate of overpressure rise with increased jet-induced turbulence for dust flame, which are observed from our experiments, can be explained by increase in combustion efficiency, which is defined as a ratio of the amount of energy released to the total amount of energy present in the fuel. It is known that in the quasi-laminar case, the flame shape looks like a paraboloid of revolution in the first stage of its propagation in the closed tube. Most of the dust-air mixture in this flame burns in the neighbourhood of the walls, where combustion is not completed. There are two reasons for incomplete combustion: the cooling effect of the wall and the divergence of streamlines and, hence of the trajectories of the particles. Therefore, some dust particles are settled out due to the effect of gravity before they get completely burned. If turbulence is introduced into the mixture early enough, the structure of the flame will change and its shape will become wrinkled and flatter. Therefore, in the turbulent flame most of the dust particles burn far from the wall and more dust can participate in the combustion process. The interaction of turbulence with the flame during the early stage of its propagation in a constant volume tube should be a subject for further research.

3. The quasi-laminar dust and gas flame propagation in a constant volume tube with L/D = 9.6 (D = 0.19 m) and the influence of turbulence on it

A. Methane-air mixture

Experiments show that laminar gas flame starts to propagate as a hemispherical flame surface, then accelerates and changes its shape to semi-ellipsoidal. Acceleration is due to the "channelled" effect of the tube, then the flame surface is deformed and takes on the shape of the tube. Because of this effect, the total flame surface is greater than in a spherical vessel. Therefore, the flame velocity at the initial stage of its propagation is high. The measured "channelled" axial propagation velocity of the semi-ellipsoidal flame in the present study appears to be about 5 times as large as the spherical propagation velocity (Table 1). The measurements carried out in different points of the tube show that this propagation velocity is a linear function of the mixture composition which changed in the experiments in the range from 6.1% to 9.65% CH_4 as shown in Fig. 23. This result is in agreement with burning velocity measurements reported by Andrews and Bradley [40]. As determined in [40], the burning velocity is also a linear function of mixture composition in the range from lean limit to 9.0% CH_4. It is evident from this comparison of data that the flame at the first stage of its propagation can be considered as adiabatic.

The location of the flame front along the tube as a function of time in Fig. 24 shows two different stages of flame propagation independently of mixture composition. The curve $L = \ell(t)$ changes shape in the region between the second and the third ionization probe. It was found, based on many measurements for the three mixture compositions (6.1%, 7.3% and 9.03% CH_4), that the length of the first stage of flame propagation in the 1.82 m long tested tube is around 0.68 m. The character of $L = \ell(t)$ curves appear to be the same as in the Ellis experiments [17, 18] (see Fig. 8) in which the flame propagation is in the direction of gravity acceleration. To reveal the role of gravity on flame propagation, downward and upward propagating flames were tested. The results presented in Fig. 25 show that the flame propagation velocity and pressure increase are higher for downward propagating flames than for an upward ones. Although there are some differences in amplitudes of measured parameters, the two stage character of flame propagation is the same.

The influence of initial pressure on propagation velocity of the flame for different mixture compositions is shown in Fig. 26. Increased initial pressure decreases propagation velocity. The influence of initial pressure on the flame propagation velocity in a lean mixture is higher than in a rich one. For a very lean mixture (6.1% CH_4) the influence is strong. This kind of influence can be explained by the inversely proportional dependence of burning velocity on pressure [41] ($u_\ell \sim p^{1/2}$).

In the experimental study of the influence of turbulence on flame propagation in an $L/D = 9.6$ ($D = 0.19$ m) closed tube, the turbulence was produced in two different ways, by means of obstacles and jets. The obstacles in the form of concentric rings shown in Fig. 27 were located in the first bottom section of the tube. The turbulence generated by obstacles is determined by the properties of the obstacles and the flow speed of unburned gas in front of the flame. Behind the obstacles, velocity gradients of flow are formed. After the flame reaches the obstacles, it propagates in that turbulent mixture with higher than initial velocity. The scale of turbulence depends on the geometrical characteristics of the obstacles while turbulence intensity is determined both by geometrical properties of obstacles and by the mixture composition, characterized by the laminar burning velocity u_ℓ and the expansion ratio ($\rho_u/\rho_b - 1$). Obstacles used in the present research produced large scale of turbulence. Jet-induced turbulence was produced by a jet-turbulence generator shown in Fig. 14. The flow field produced by the generator can be discussed in terms of several consecutive processes: the generation of steady jet flows close to orifices, the interaction and breaking down of jets to produce turbulence and finally diffusion and decay of this turbulence with distance away from the generating jets. The scale of turbulence produced by jet-turbulence generator was rather smaller than that produced by obstacles.

Figure 28 illustrates the influence of obstacle-induced turbulence on the flame propagation for different mixture composition. Under the influence of turbulence, the combustion process is much faster than for laminar propagation. Although the obstacles are located only in the first section of the tube on the length of the tube from 0 to 90 mm, their influence on the propagation velocity extends up to about 1500 mm. In the region of the 5th ionization probe the flame decelerates and one can also observe some delay time in the pressure increase. Such behavior is similar and independent of the mixture composition.

Figure 29 presents the influence of jet-induced turbulence on flame propagation for different mixture compositions. The turbulence generator occupies the first section of the tube. Its influence is also extended into the second section of the tube and similar to the case of obstacle-induced turbulence, it decreases at the final stages of the tube. The influence of jet-induced turbulence on the propagation velocity of the flame and the pressure in the tube is strong for lean mixtures and weak for near stoichiometric mixtures.

The influence of turbulence on flame propagation velocity along the tube length is shown in Fig. 30. The influence of obstacle-induced turbulence is much stronger than the jet-induced one, especially in the second section of the tube, corresponding to the second stage of propagation of laminar flame. Obstacles increase propagation velocity of the flame 20-30 times, while turbulence from jet generator increases it 5-15 times, compared to laminar propagation. The ratio of the turbulent propagation velocity to the laminar propagation velocity is different in different sections of the tube. For example, for obstacle-induced turbulence, this ratio in the position of the second ionization probe is 2-5 against 20-30 in the position of the third ionization probe.

The influence of turbulence on the rate of pressure increase along the tube length is shown in Fig. 31. Experimental results show that the trend of the influence of turbulence on the rate of pressure increase is the same as the influence on flame propagation velocities in the first stage of flame propagation, but there is different behavior of the rate of pressure increase from the flame propagation velocities for the turbulent flame. The flame propagation velocities approach maximum values at the position of the third ionization probe, then decrease, whereas the rate of pressure increase approaches maximum values around the position of the third ionization probe, then keeps at the high value or increases until the position of 6th ionization probe. This phenomena implies that there may be some volume combustion occurring in the second stage of combustion.

The influence of turbulence on the shape of flame front is also shown in Fig. 33. Experimental results show that in the case of propagation of turbulent flame, the ellipsoidal shape of flame front is eliminated and becomes cusp-shaped.

B. Cornstarch-air mixture

Experiments with flame propagating in cornstarch dust-air mixture show that its behavior and all its characteristics are very similar to that for laminar flame propagation in gas mixture. Figure 34 shows the overpressure and location of the flame front along the tube as a function of time for cornstarch dust-air mixture with concentration of dust 460 g/m^3. Two sections of the $L = \ell(t)$ curves with different slopes indicate to different stages of flame propagation, identical with the case of flame propagating in gas mixture. Also, distribution of propagation velocities along the tube shown in Fig. 35 confirms that a physical model of flame propagation in dust and gas mixture is the same.

The influence of turbulence on dust flame propagation in the closed tube with L/D = 9.6, D ≈ 0.19 m is in the working process.

V. Summary and conclusions

1. A dispersion system was developed which yields a medium of uniform dust suspension and very low level of dispersion-induced turbulence at ignition. This provides relatively quiescent initial conditions of flame propagation to study the influence of turbulence on dust combustion in constant volume tube.

2. A physical two-stage model of quasi-laminar dust flame propagation in a constant volume tube with L/D = 4.8 and 9.6 has been proposed. The measurements show that the behavior of the dust flame in this model is similar to that of a gas flame. The similarity is based on the same processes controlling both gas and dust flames: heat conduction and molecular diffusion.

3. Detailed measurements showed that laminar flame propagating in a closed tube can be considered as adiabatic at the first stage of its propagation.

4. The overpressure Δp as a function of flame location along the tube L is the same for laminar and turbulence flame at the first stage of their propagation for the same mixture composition and the same initial pressure. This means that both processes go in in adiabatic conditions.

5. Turbulent gas flame behaves in different than laminar way during its propagation along the tube. It is probable that it propagates from the beginning as a flat in shape flame, reacting in many zones

distributed at its entire substantial thickness. Propagation velocity of turbulent flame is over one order of magnitude higher than that of laminar one, and cooling effect of the tube wall starts to influence flame propagation at the time when the flame is far from ignitor. Because of this turbulent flame can be passed undistrubed much longer distance of the tube than laminar flame (deceleration of this flame occurs at the end of its propagation).

6. Experiments in one section of the tube with L/D = 4.8 show that influence of turbulence on the combustion process is most effective in the initial first stage of combustion. This was confirmed in the two section tube experiments. The turbulence generated in the first section of the tube influenced the combustion process in the entire tube.

7. Turbulence used in the experiments increased propagation velocity of the flame in the range of 5 to 30 times comparing to laminar propagation velocity. This corresponds to the entire range of changes of the ratio of turbulent burning velocity to laminar burning velocity discussed in a survey paper of Andrews et al [42].

8. It was found that the closed tube is most suitable to investigate the influence of turbulence on dust flame by virtue of clear gas dynamic model of its propagation. The advantage of this kind of investigation lies in its simplicity: the overpressure and the maximum rate of overpressure rise determine sufficiently the efficiency of the combustion process.

References

1. Hartmann, I., Nagy, J., Brow, H.R., U.S. Bureau of Mines, Rept. of Inv. No. 3722, 1943.

2. Hartmann, I., Cooper, A.R., Jacobson, M., U.S. Bureau of Mines, Rept. of Inv. No. 4725, 1951.

3. Nagy, J., Seiler, E.C., Conn, J.W., Verakis, H.C., U.S. Bureau of Mines, Rept. of Inv. No. 7507, 1971.

4. Bartknecht, W., "Explosion-course-prevention-protection", Translated by Bung, H. and Almond, T., Springer-Verlag, New York, 1980.

5. Bartknecht, W., "Brenngas-Und Stousbexplosionen", Forschung-Bericht F45, Bundesinst. f. Arbeitschutz. Kobleng (1971).

6. Bartknecht, W., 18th Annual Loss Prevention Symp., AIChE, Philadelphia, Aug. 19-22.

7. Kauffman, C.W., Srinath, S.R., Tezok, F.I. etc., 20th Symposium (International) on Combustion, 1984.

8. Faraday, M., Lyell, C., Phil. May 26, 16 (1845).

9. Smoot, L.D., Horton, M.D., Prog. Energy Combust. Sci., Vol. 3, pp. 235-258, 1977.

10. Howard, J.B., Essenhigh, R.H., Ind. Eng. Chem. Proc. Des. and Devel. 6, 76 (1967).

11. Howard, J.B., Essenhigh, R.H., 11th Symposium (International) on Combustion, pp. 399-408, 1967.

12. Howard, J.B., Essenhigh, R.H., Combustion and Flame 9, 337 (1965), 10, 92 (1966).

13. Richmond, J.K., Liebman, I., "A Physical description of coal mine explosions", Bureau of Mines, U.S. Department of the Interior.

14. Richmond, J.K., Liebman, I., "A physical description of coal mine explosions Part II", Bureau of Mines, U.S. Department of the Interior.

15. Clark, D.P., Smoot, L.D., Combustion and Flame, 62: 255-269, 1985.

16. Bradley, D., Lee, J.H.S., "On the mechanism of propagation of dust flame", presented at the First International Colloquium on Explosibility of Industrial Dusts, Baranow near Sandomierz, 8-10 November, 1984.

17. Ellis, O.C. des. Fuel. Vo. 7., Nos. 5-12, 1928 (in 8 parts).

18. Ellis, O.C. des. Fuel. Vo. 7, No. 4, 1928, pp. 169-178.

19. Chomiak, J., Prog. Energy Combust. Sci., 5: 207-221, 1979.

20. Libby, P.T., Williams, F.A., Turbulent Reacting Flows, Springer-Verlag, 1980.

21. Smoot, L.D., Horton, M.D., and Williams, G.A., 16th Symposium (International) on Combustion. The Combustion Institute, Pittsburgh, Pa., 375-387, 1976.

22. Ballal, D.R., Proc. R. Soc. Lond. A385, 21-51 (1983).

23. Eckhoff, R.K., Combustion and Flame 24: 53-64, 1975.

24. Jarosinski, J., Lee, J.H.S., Knystautas, R. and Crowley, J.D., Submitted for presentation at the 21st International Combustion Symposium.

25. Jarosinski, J., Combustion and Flame 50: 167-175 (1983).

26. Smoot, L.D., Hedmen, P.O. and Smith, P.J., Prog. Energy Combust. Sci., 10: 359-441, 1984.

27. Tennekes, H., Physics of Fluids 11: 669-670 (1968).

28. Lewis, B., and Von Elbe, G., Combustion and Flame 19: 275-288, 1972.

29. Zeldovich, Ya.B., Barenblatt, G.I., Librovich, V.B., and Makhviladze, G.M., The Mathematical Theory of Combustion and Explosions, Consultants Bureau, Plenum Publishing Corporation, New York, 1985.

30. Bradley, D. and Mitcheson, Combustion and Flame 26: 201-217 (1976).

31. Markerstein, S.H., Ed., "Non-steady flame propagation", Agardograph No. 75, Pergamon Press, 1964.

32. Taylor, S.J., Proc. Roy. Soc., A201: 192, 1950.

33. Istratov, A.G. and Librovich, V.B., Astronautica Acta 14: 453, 1969.

34. Landau, L.D., Acta Physicochim URSS 19: 77, 1944.

35. McCann, D.P.J., Thomas, S.O., and Edwards, D.H., Combustion and Flame 59: 233, 1985.

36. Strehlow, R.A., Combustion Fundamentals, McGraw-Hill Book Company, 1984.

37. Wygnanski, I., Fiedler, H., J. Fluid Mech. (1969), Vol. 38, part 3, pp. 577-612.

38. Knystautas, R., The Aeronautical Quarterly, Vol. XV, Feb. 1964.

39. Peraldi, O., These de Docteur Ingenieur, Universite de Poitiers, 1985.

40. Andrews, G.E. and Bradley, D., Combustion and Flame 19: 275-288 1972.

41. Chomiak, J., Podstawowe Problemy Spalania PWN Warszawa 1977 (in Polish).

42. Andrews, G.E., Bradley, D., and Lwakabamba, S.B., Combustion and Flame 24: 285-304, 1975.

Table 1:

Comparison of propagation velocities between cylinder tube and spherical vessels

CH_4% \ propagation velocities	$(W_{lam.})_{spherical}$	$(W_{lam.})_{cylinder}$	$(W_L)_c / (W_L)_s$
6.1%	1.0 m/sec	4.7 m/sec	4.7
7.3%	1.8 m/sec	9.4 m/sec	5.2
9.05%	3.0 m/sec	16.5 m/sec	5.5

$(W_{lam.})_{cylinder}$: calculated at the base of the experimental data determined in the present tube; the average propagation velocities were measured at length equal to 0.4 m from ignitor.

$(W_{lam.})_{spherical} = U_{lam} \cdot T_{ad}/T_u$,

where $U_{lam.}$ is laminar burning velocity,

T_{ad} is adiabatic temperature after combustion and

T_u is room temperature)

The data of $U_{laminar}$ and T_{ad} for methane-air are obtained from [40].

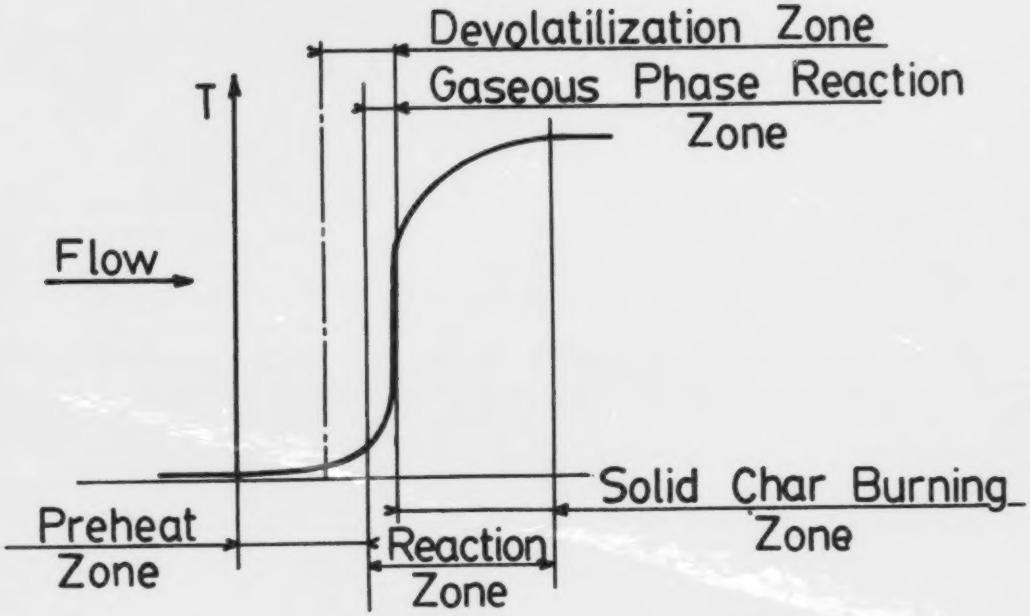
Devolatilization Zone
Gaseous Phase Reaction Zone
T
Flow
Solid Char Burning Zone
Preheat Zone
Reaction Zone

Fig. 1 : The tentative structure of laminar flame.

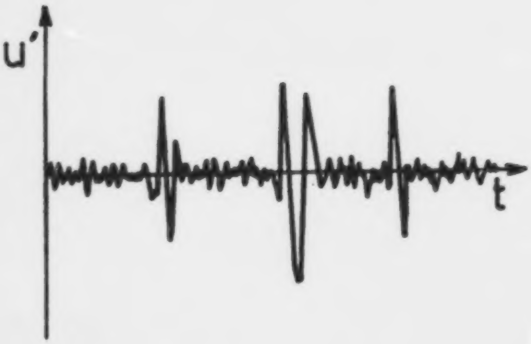

Fig. 2 : Intermittency in turbulence flow.

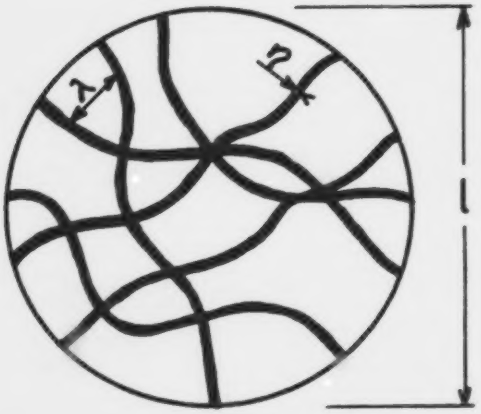

Fig. 3 : Simplified model of turbulence flow structure.

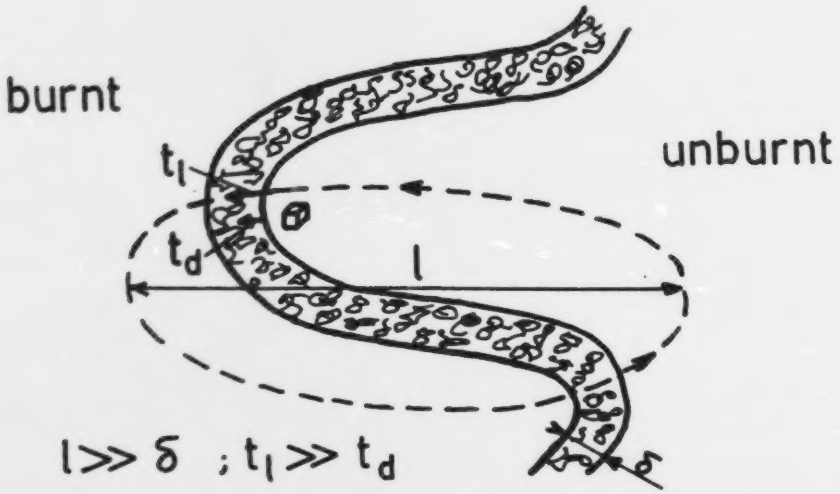
burnt
unburnt
t_l
t_d
θ
l
δ
$l \gg \delta \; ; t_l \gg t_d$

a/ In the integral eddies regions.

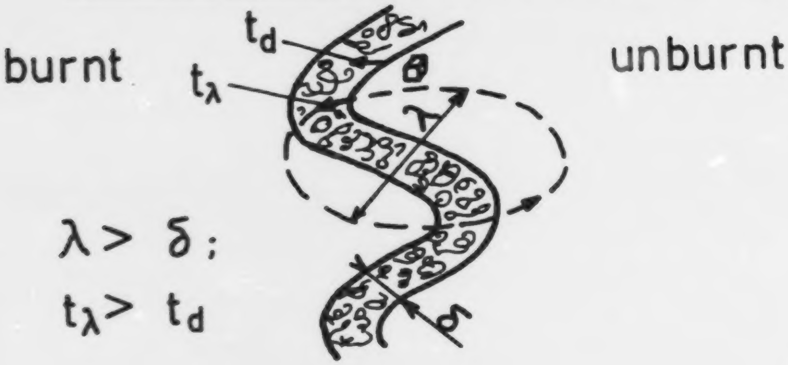
t_d
burnt
unburnt
t_λ
θ
λ
δ
$\lambda > \delta ;$
$t_\lambda > t_d$

b/ In the Taylor eddies regions.

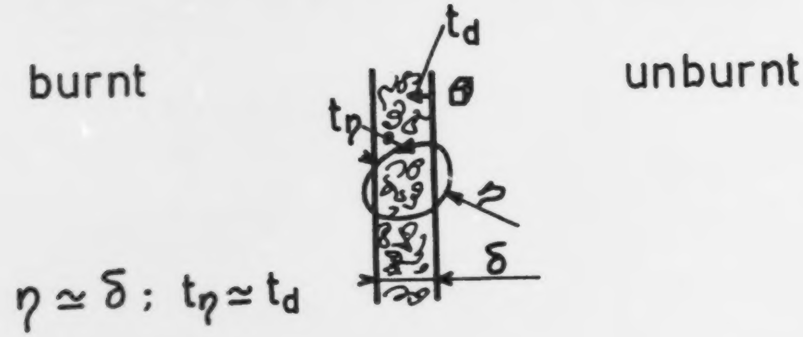
t_d
burnt
unburnt
θ
t_η
η
δ
$\eta \simeq \delta ; \; t_\eta \simeq t_d$

c/ In the Kolomogorov eddies regions.

Fig. 4 : The influence of turbulence on gas flame in three eddies regions.

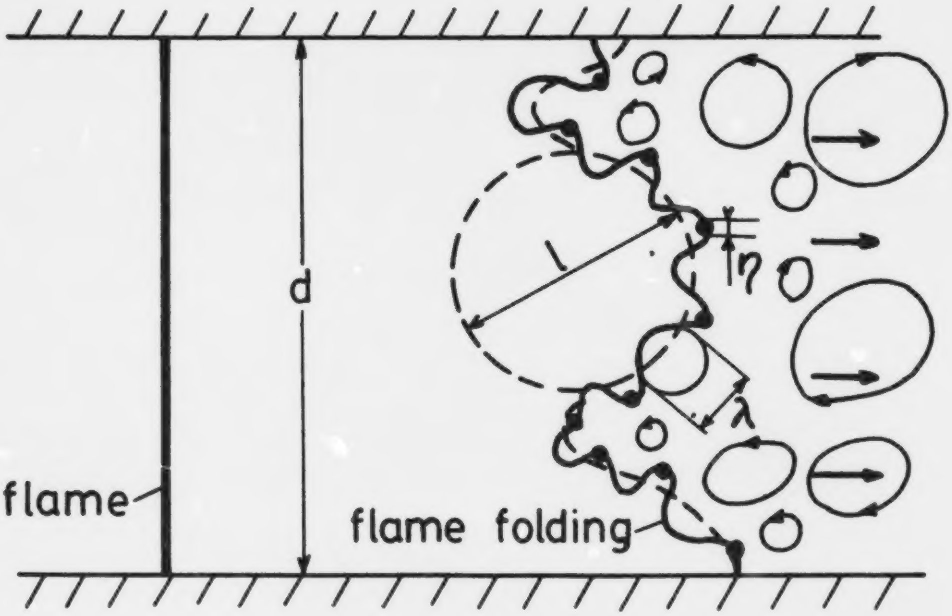
d
l
η
λ
flame
flame folding

Fig. 5 : Physical model of turbulence gas flame propagation.

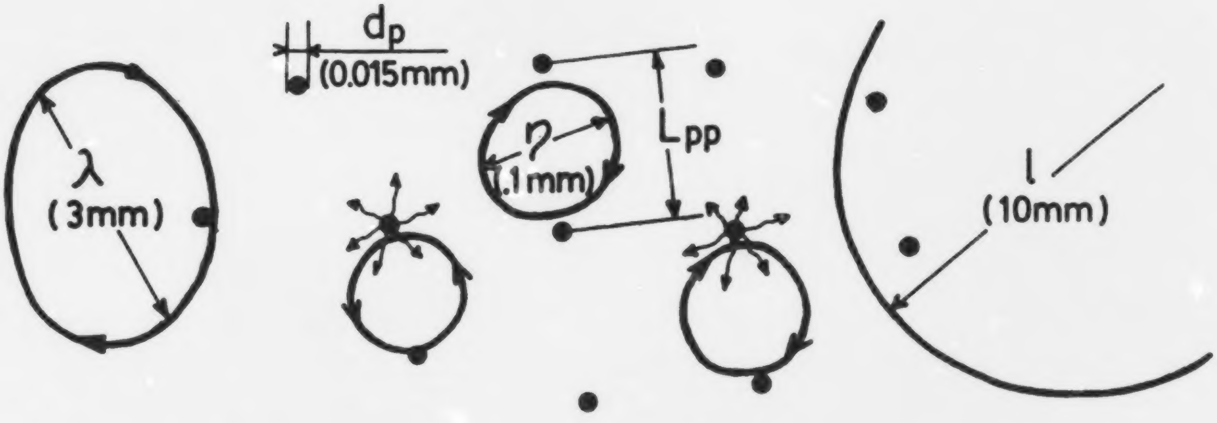
λ
(3mm)
dp
(0.015mm)
η
(.1mm)
Lpp
l
(10mm)

Fig. 6 : The comparison of length scale between dust particles, interparticles spacing and turbulence eddies.

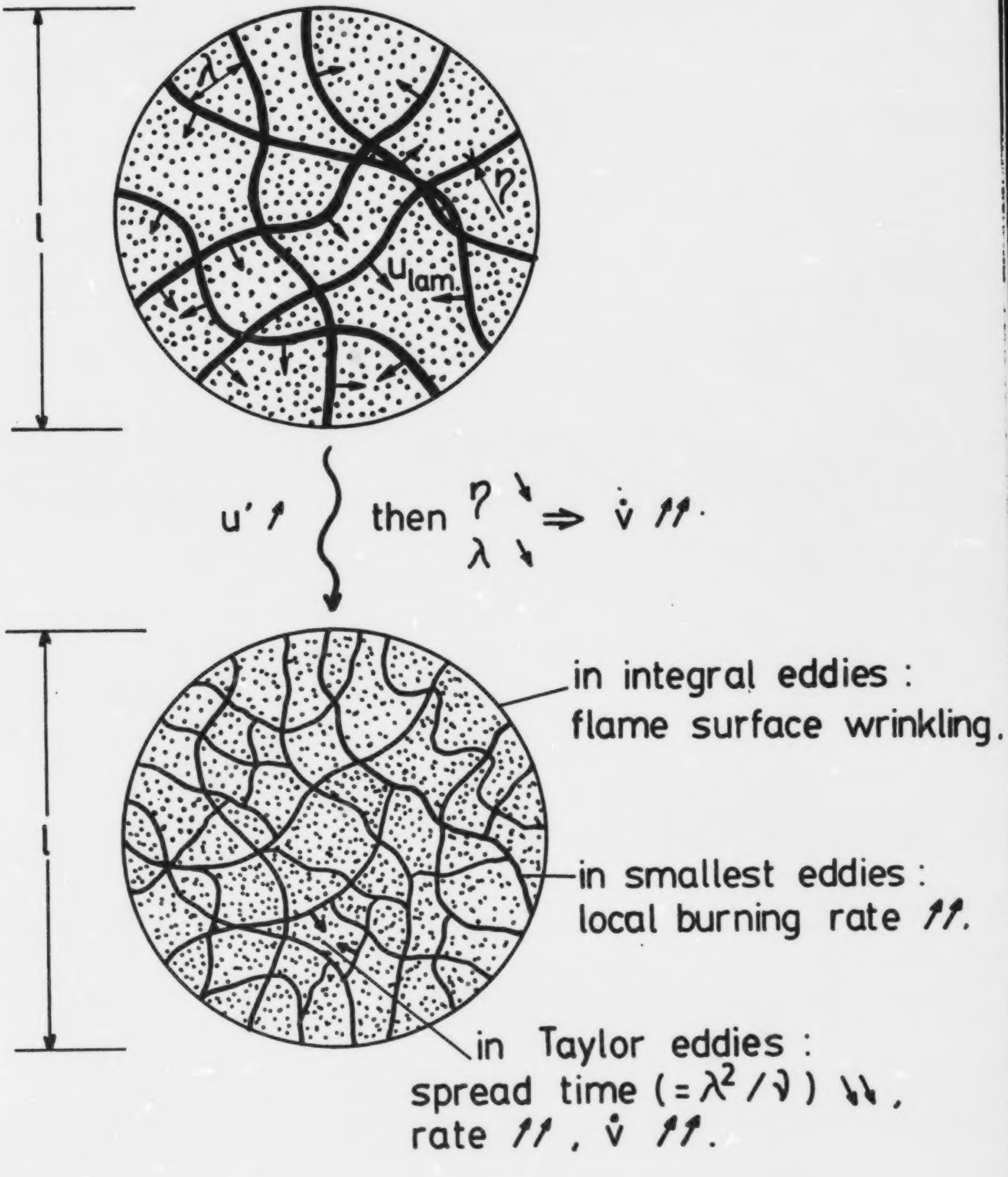
l
λ
η
u lam.
u' ↗ then η ↘ λ ↘ ⇒ v̇ ↗↗.
l
in integral eddies : flame surface wrinkling.
in smallest eddies : local burning rate ↗↗.
in Taylor eddies : spread time (= λ²/ν) ↘↘, rate ↗↗, v̇ ↗↗.

Fig. 7 : The tentative structure of turbulent dust-air flame.

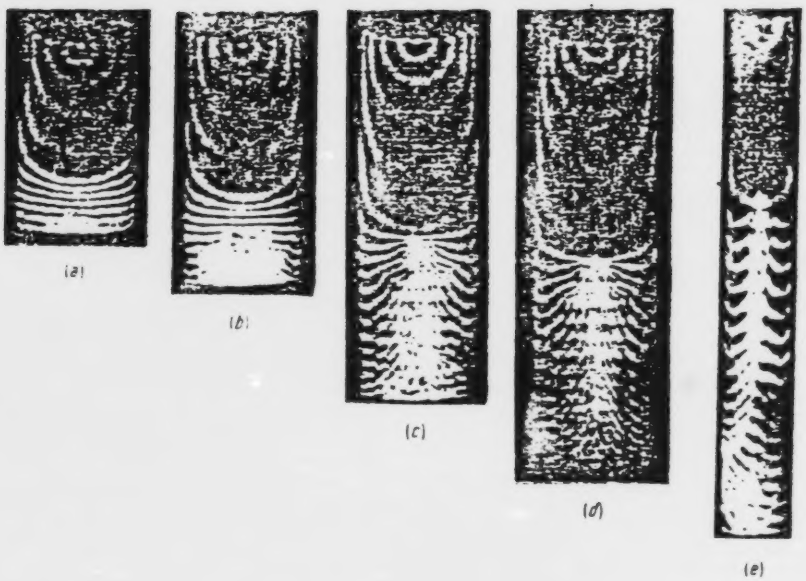

Fig. 8 : The effect of L/D on the growth of Taylor-Markstein instability :
Mixture : 10 parts C O + 1 part O_2 , saturated with water vapor at 15 C,
Cylinder vertical tube closed at both ends,
(a)-(d) : 50 mm diameter, (e) : 25 mm diameter,
Lengths are : (a) 95 mm, (b) 100 mm, (c) 170 mm,
(d) 195 mm, (e) 230 mm.
Ignition is at the top center.
(From O.C. de C. Ellis, Fuel Sci. Pract., Vol. 7, (1928), p. 502, with permission).

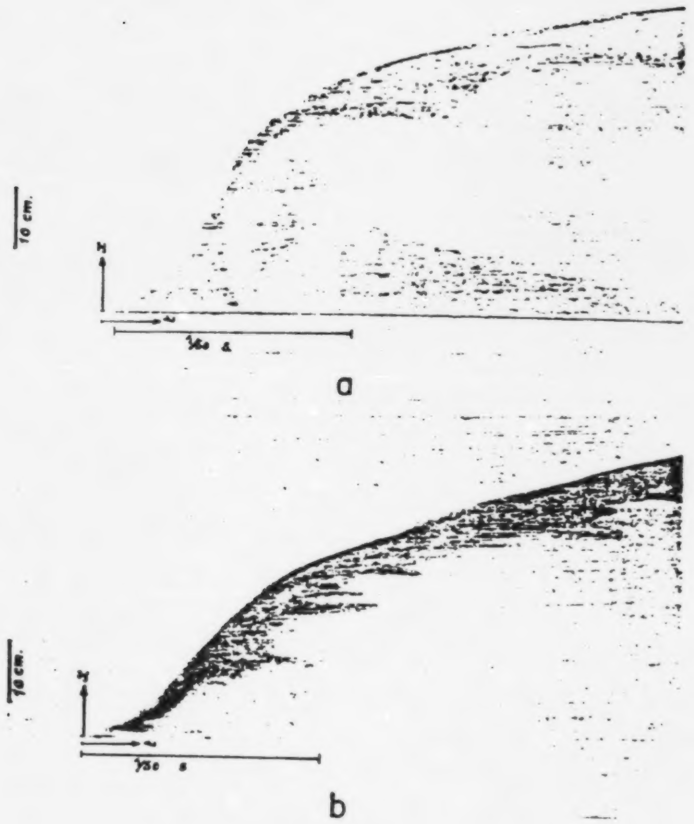

Fig. 9 : Drum-camera records of flame propagation in a tube closed at the both ends of 55 cm length and 5.3 cm diameter, Mixture : 1 part $C_6 H_6$ + 34 parts air, initial pressure 440 mm Hg,
Ignition : (a) hot point source,
(b) extended source (spiral filament).

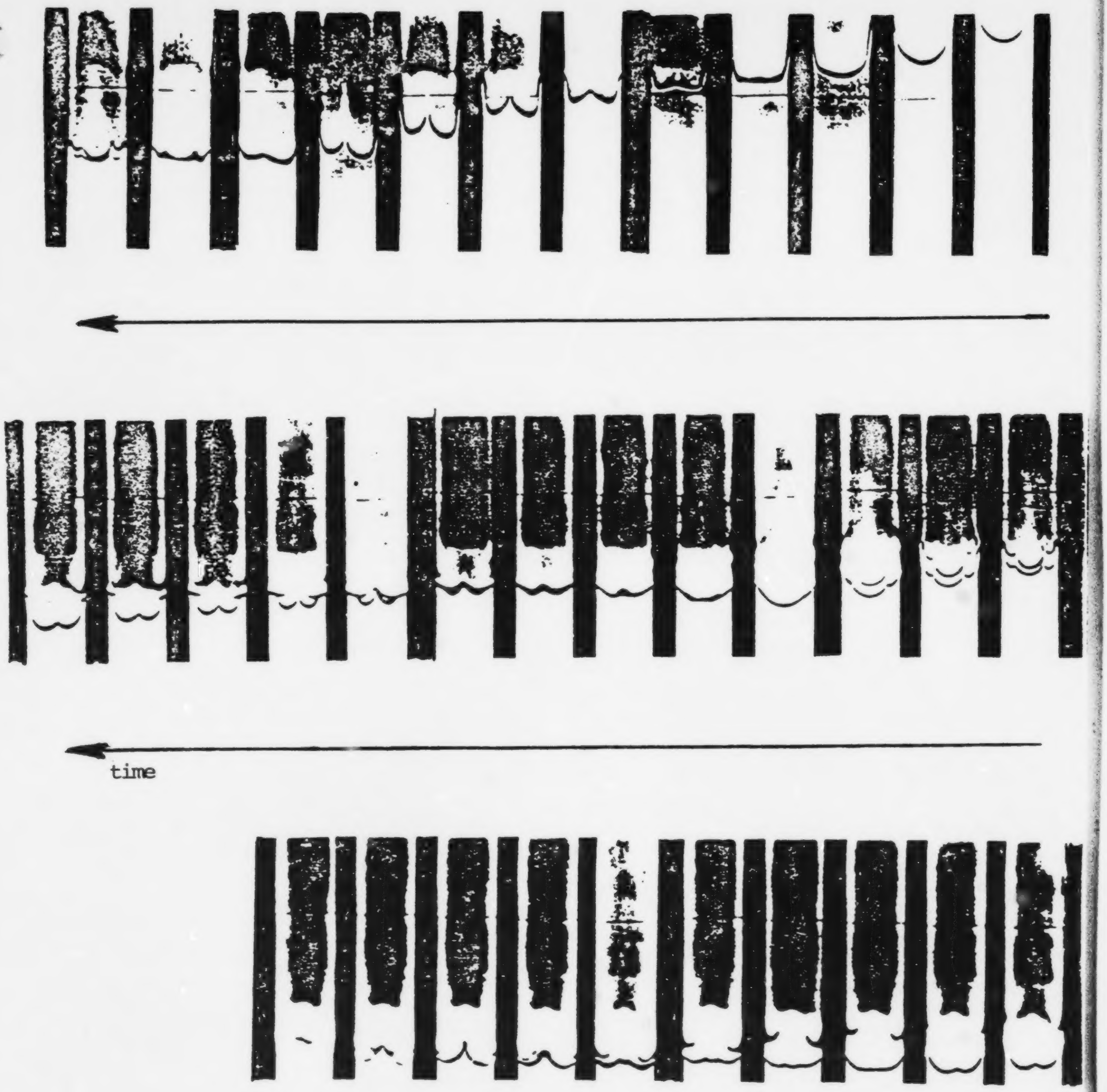

Fig. 10-(a) : History of downward propagation from the closed end of the tube illustrating extinction.

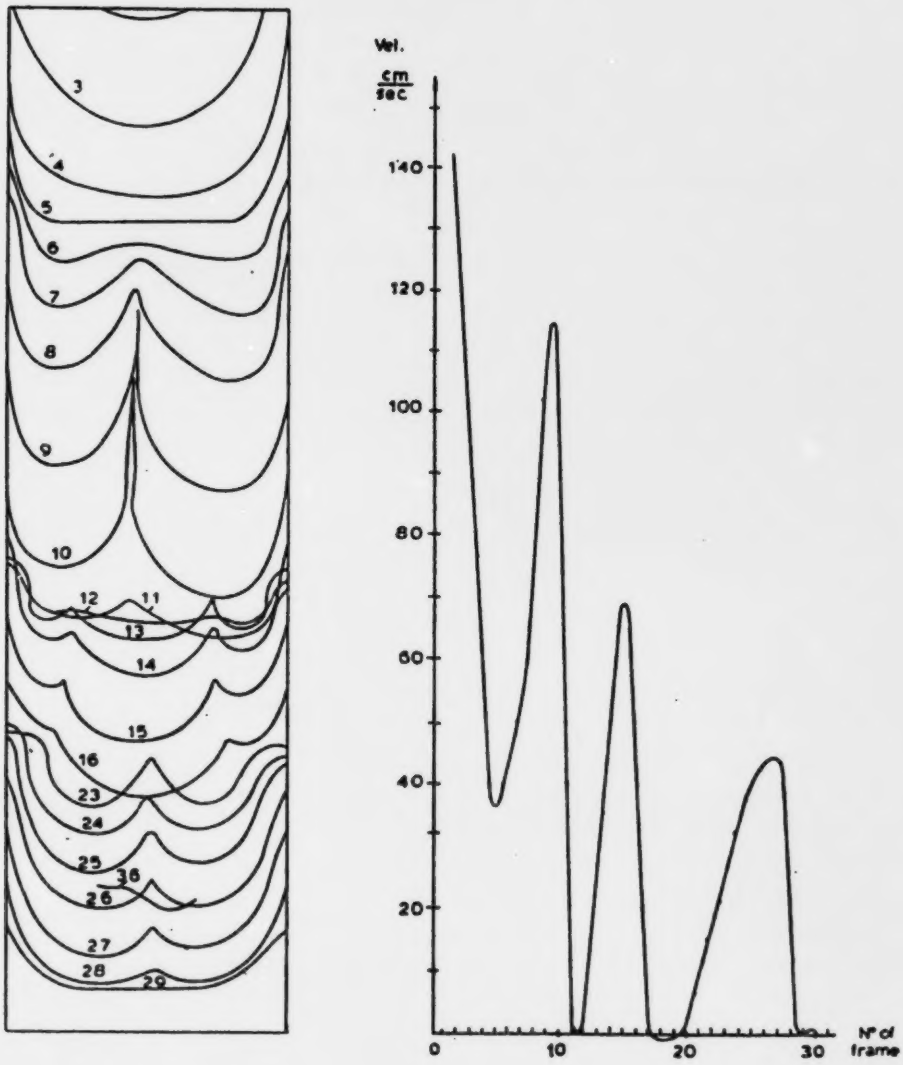

Fig. 10-(b) : Symmetrical oscillations during downward propagation from the closed end just before extinction. (Drawn from Fig. 10-(a)).

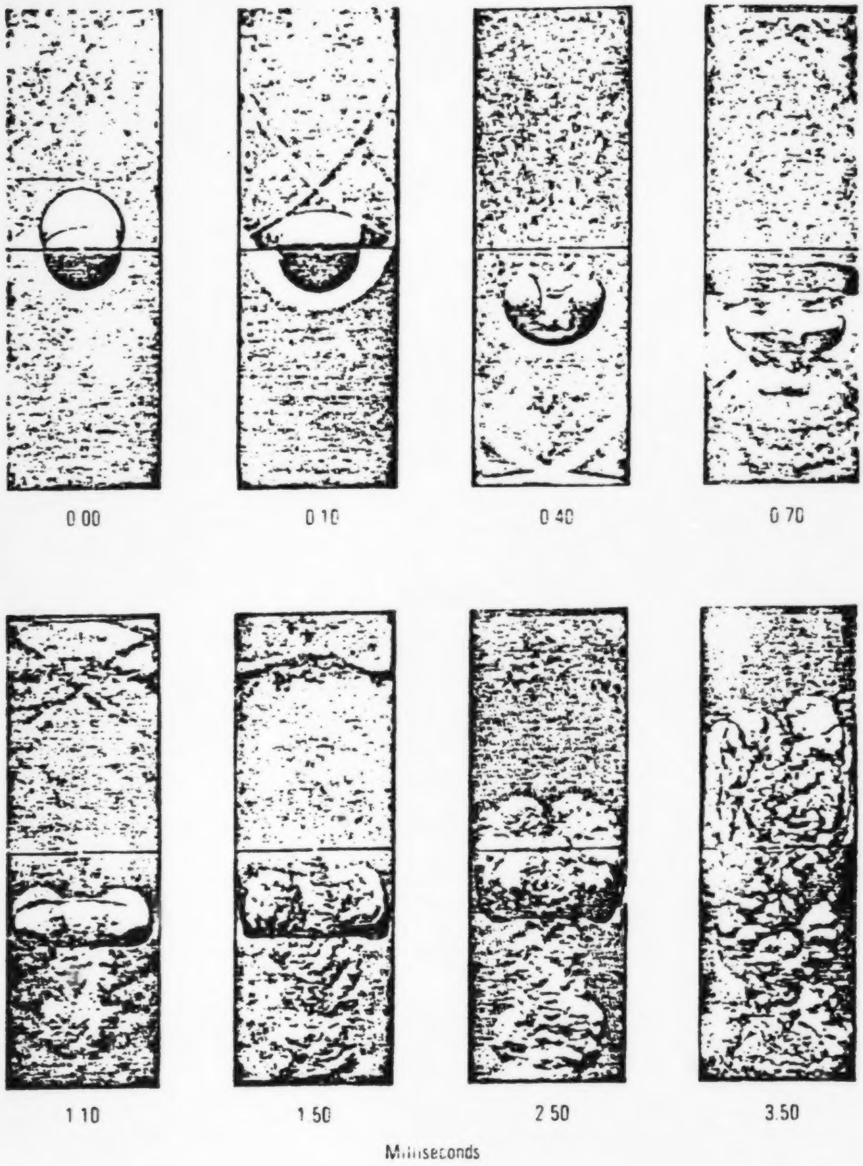

Fig. 11 : Interaction of a shock wave and a flame of initial roughly spherical shape. Pressure ratio of incident shock wave 1.3; stoichiometric butane-air mixture ignited at the center of combustion chamber, 8.7 millisec. origin of the time scale. (Courtesy G.H. Markstein , Factory Mutual Research, Norwood Mass.; originally in Combustion and Propulsion, third AGARD Colloquium , p. 153, Pergamon, 1958, with permission).

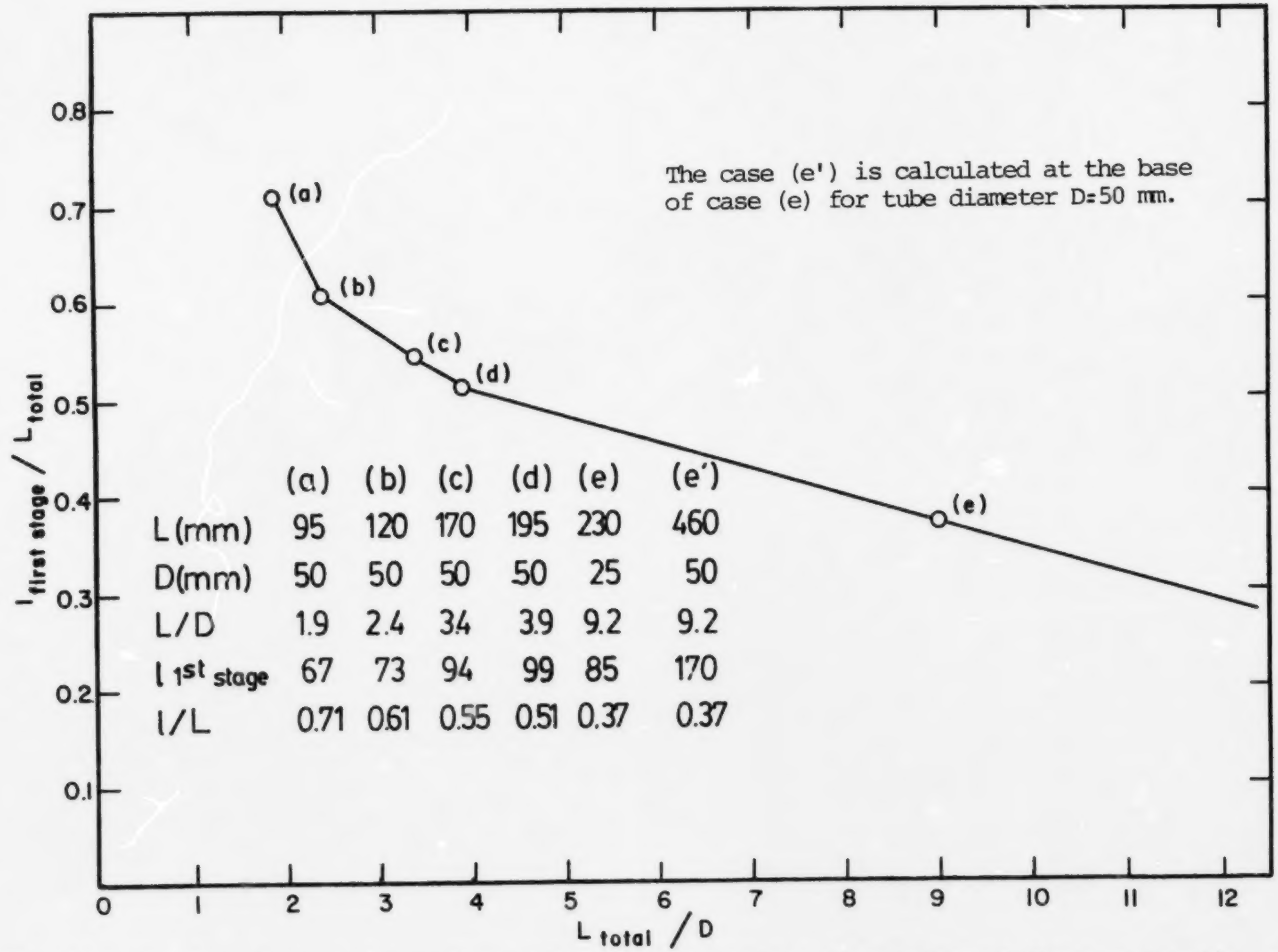

The case (e') is calculated at the base of case (e) for tube diameter D=50 mm.

	(a)	(b)	(c)	(d)	(e)	(e')
L(mm)	95	120	170	195	230	460
D(mm)	50	50	50	50	25	50
L/D	1.9	2.4	3.4	3.9	9.2	9.2
$l_{1^{st}\ stage}$	67	73	94	99	85	170
l/L	0.71	0.61	0.55	0.51	0.37	0.37

Fig. 12 : The dependence between dimensionless length of the first stage of flame propagation and the ratio of the length of the tube to its diameter. (obtained from [17],[18]).

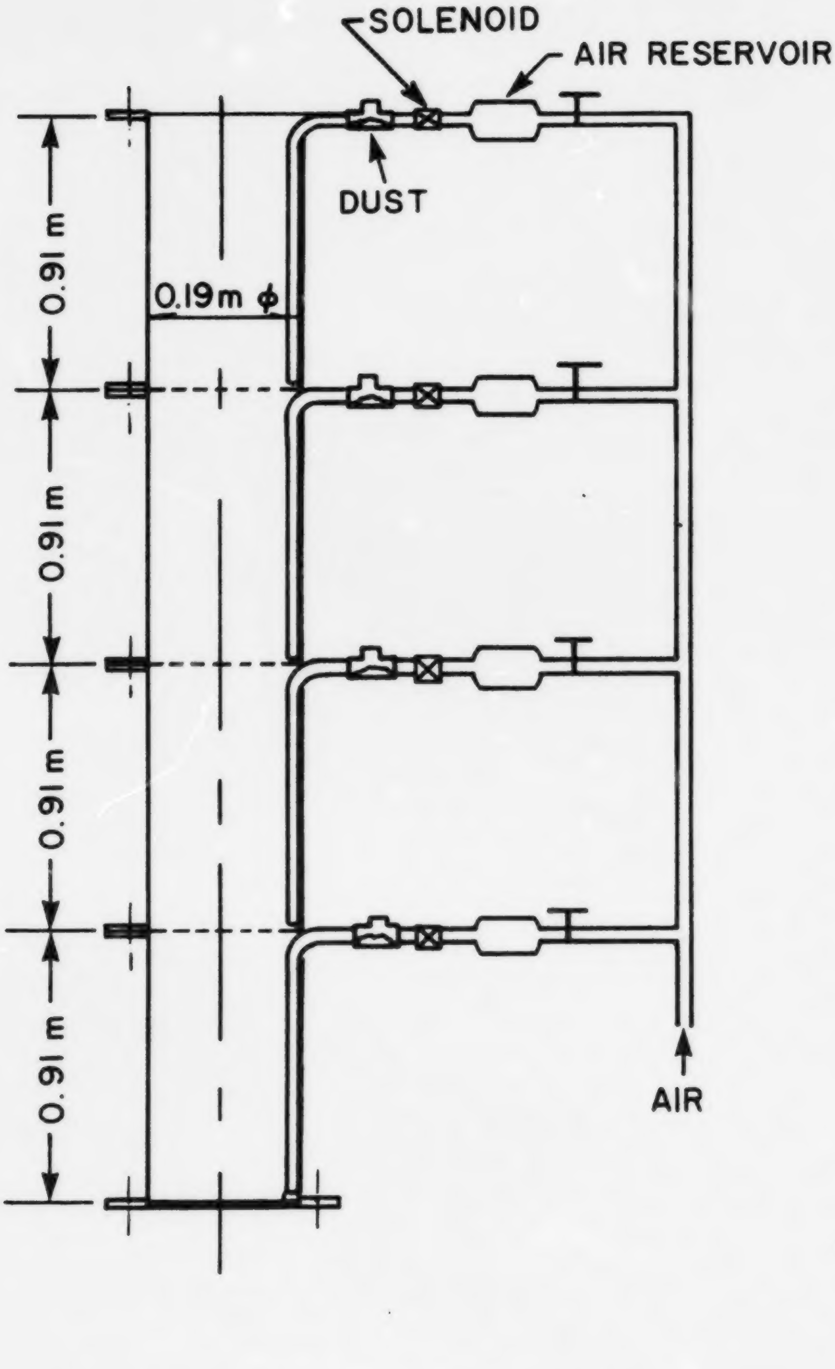
SOLENOID
AIR RESERVOIR
DUST
0.19m ϕ
0.91 m
0.91 m
0.91 m
0.91 m
AIR

Fig. 13 : Test tube for studying dust flame propagation.

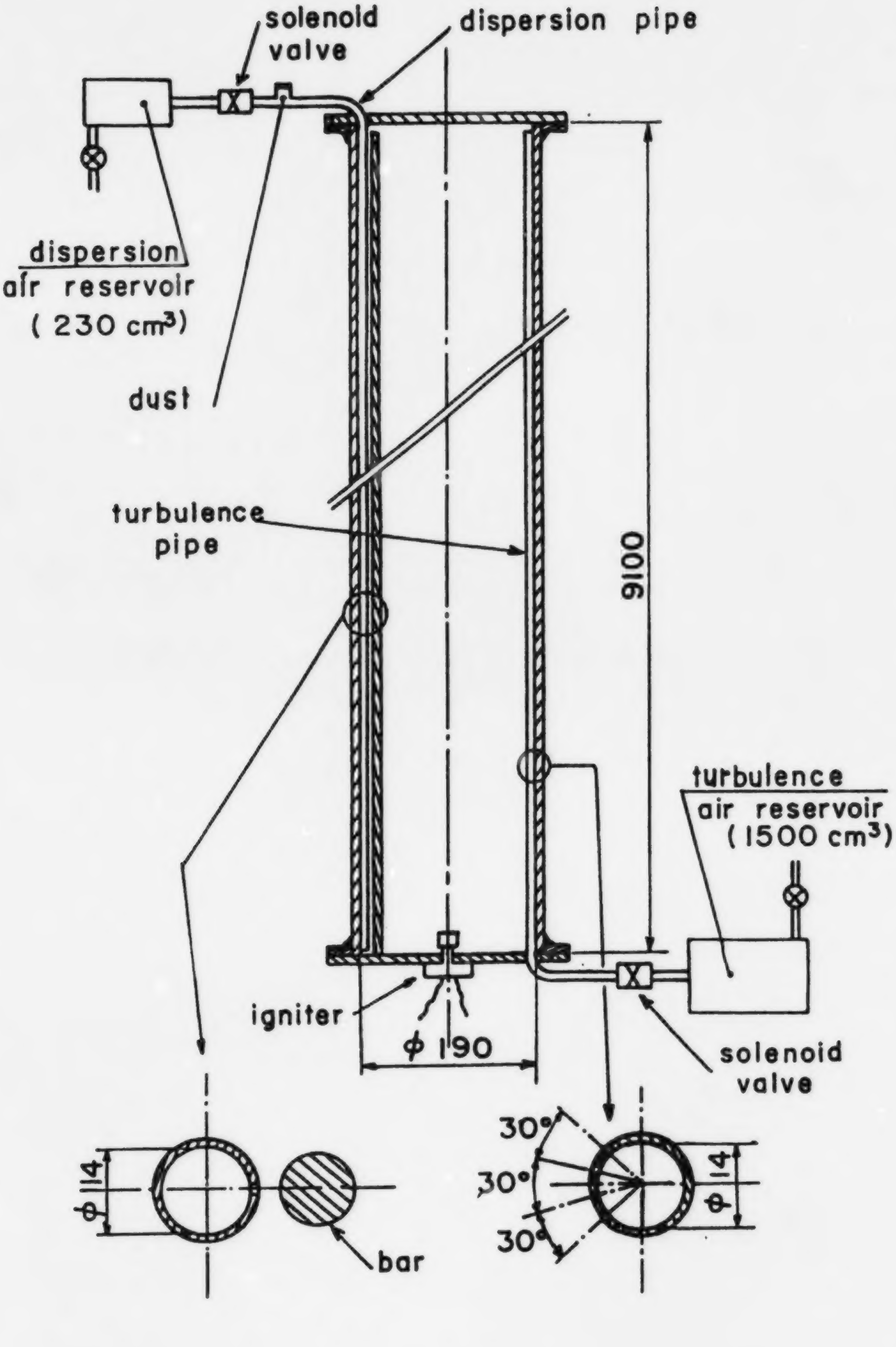
solenoid valve
dispersion pipe
dispersion air reservoir (230 cm³)
dust
turbulence pipe
9100
turbulence air reservoir (1500 cm³)
igniter
ϕ 190
solenoid valve
ϕ 114
bar
30°
30°
30°
ϕ 114

Fig. 14 : Side view of one segment of apparatus.

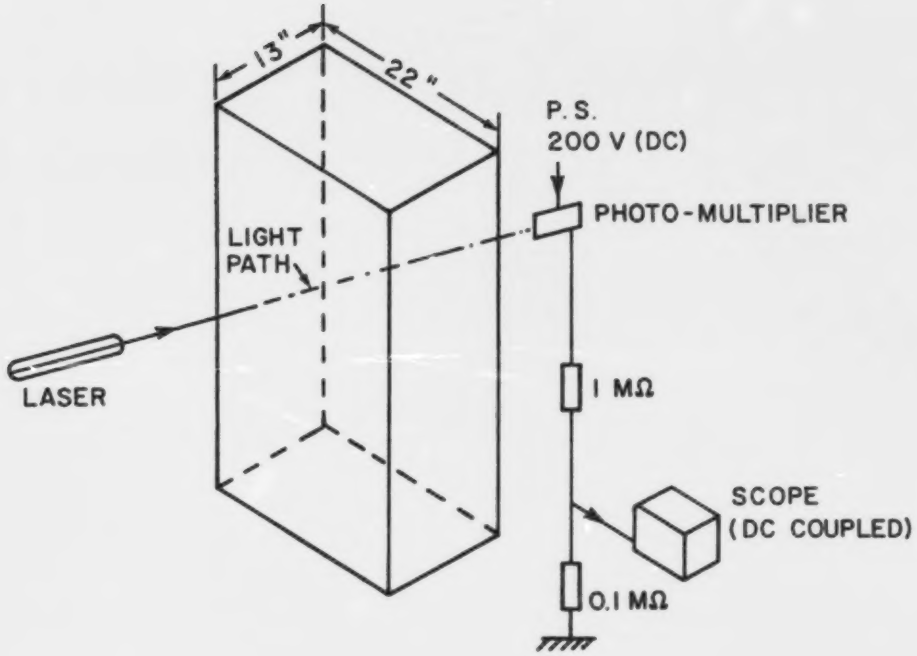
13"
22"
P.S.
200 V (DC)
PHOTO-MULTIPLIER
LIGHT
PATH
LASER
1 MΩ
SCOPE
(DC COUPLED)
0.1 MΩ

Fig. 15 : Optical arrangement of transmission measurements for dust dispersion experiments.

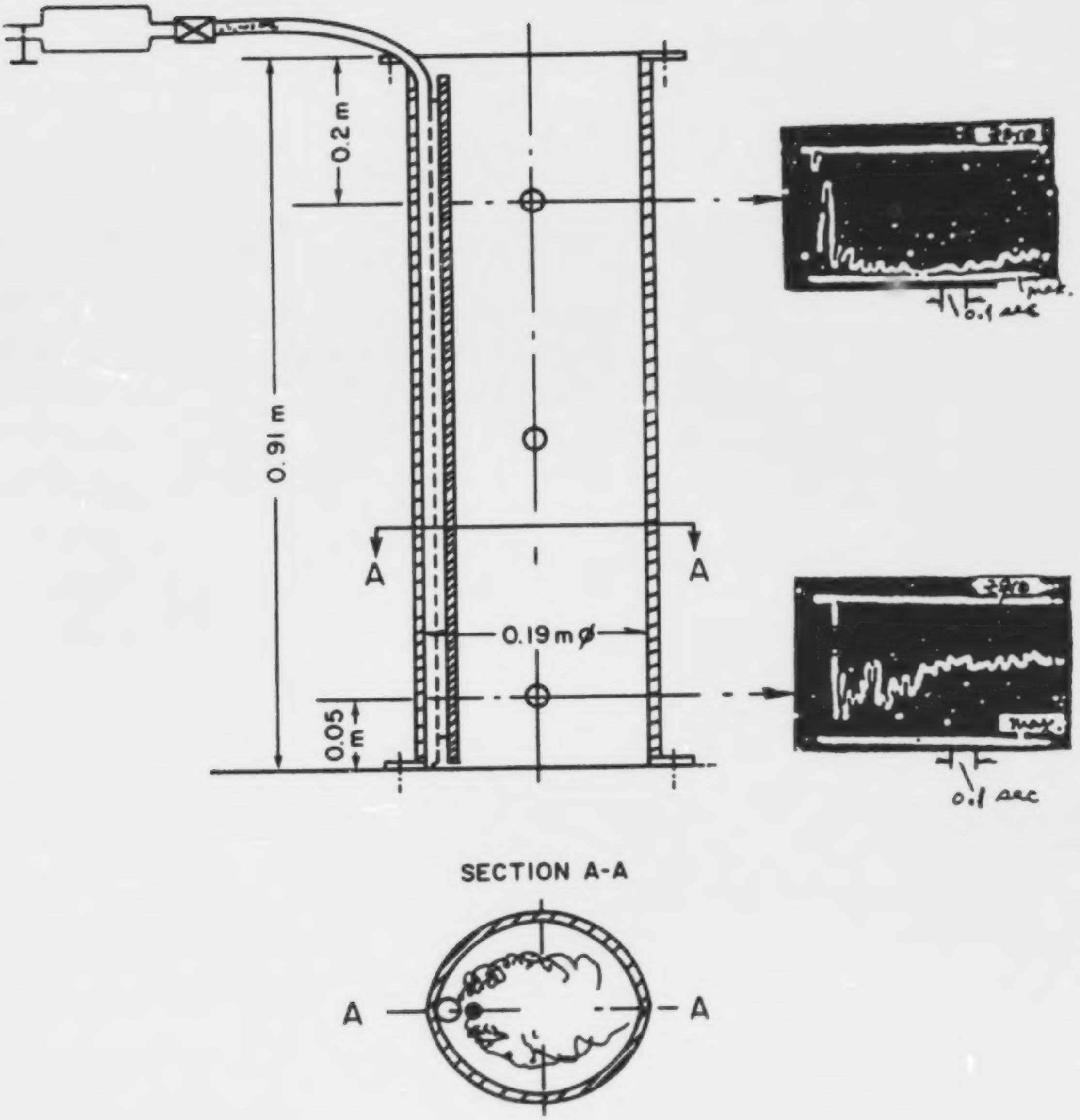
0.2 m
0.91 m
A
A
0.19 m ø
0.05 m
zero
max.
0.1 sec
zero
max.
0.1 sec
SECTION A-A
A
A

Fig. 16 : Relative dust concentration (i.e. light transmission) versus time at top and bottom section respectively.

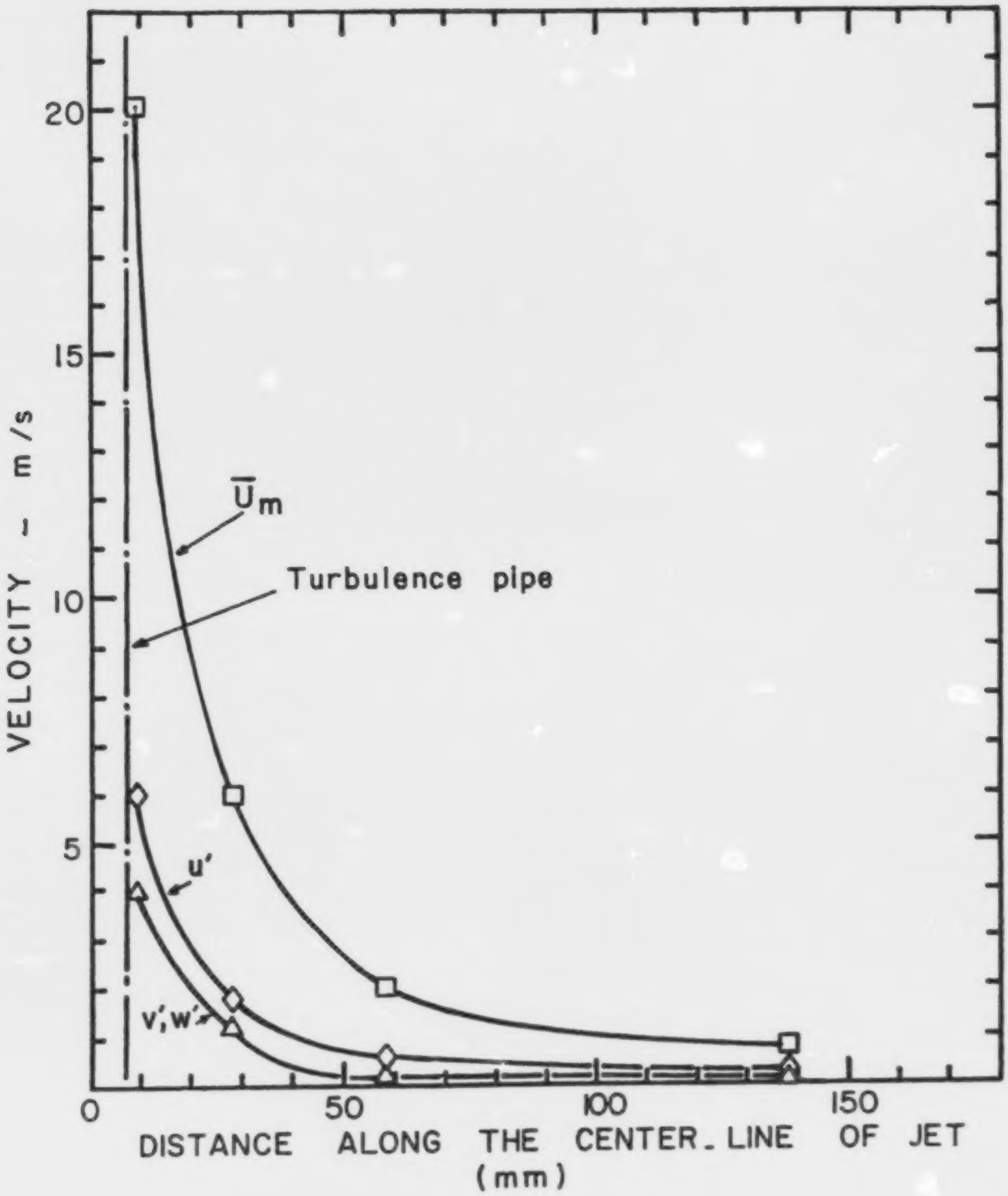

Fig. 17 : The distribution of the mean velocities of the jet (U_m) and the intensities of the jet-induced turbulence of u', v', w' fluctuations in the jet centerline (determined by [37],[38]).

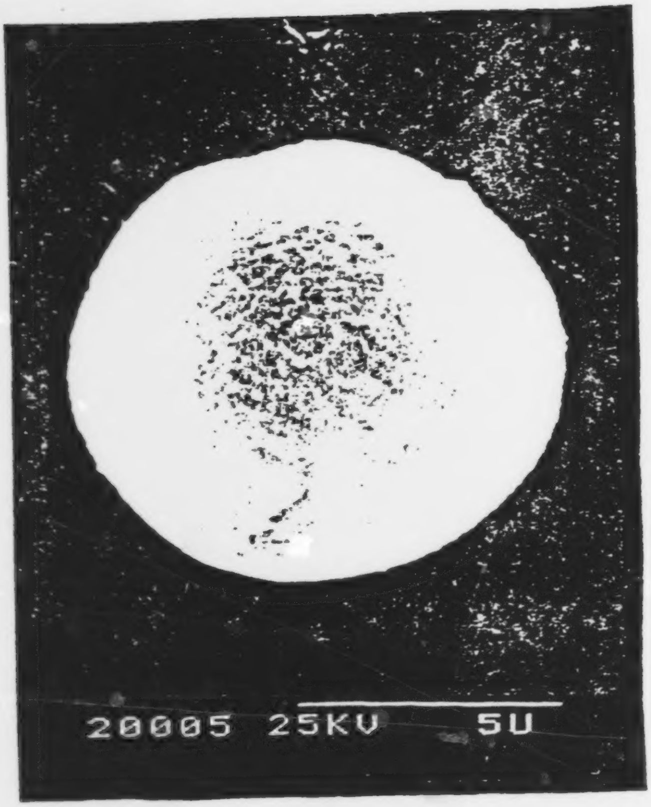
20005 25KV 5U

Fig. 18 : S.E.M. photograph of cornstarch particle.

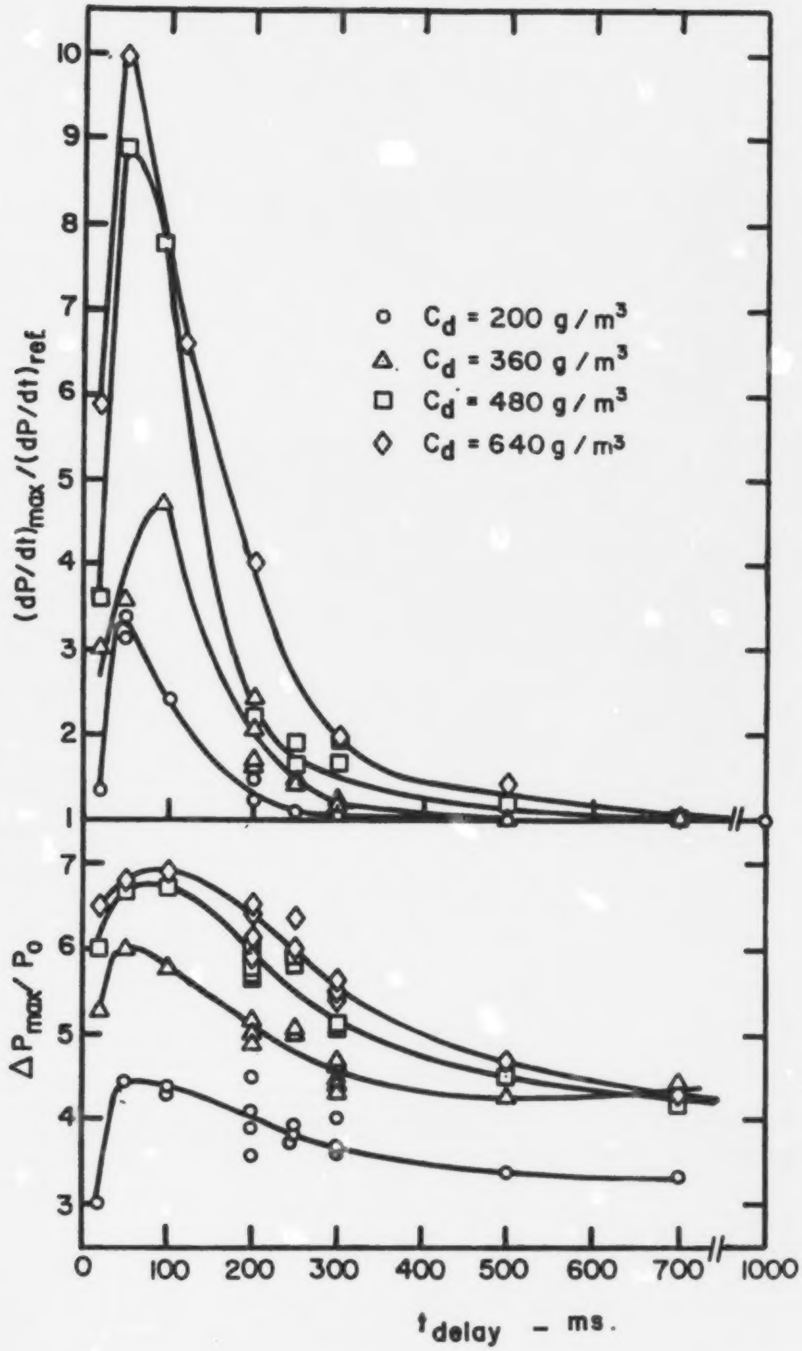

Fig. 19 : Maximum overpressure (ΔP_{max}) and maximum rate of overpressure rise ($[dP/dt]_{max}$) versus ignition delay time (t_d).

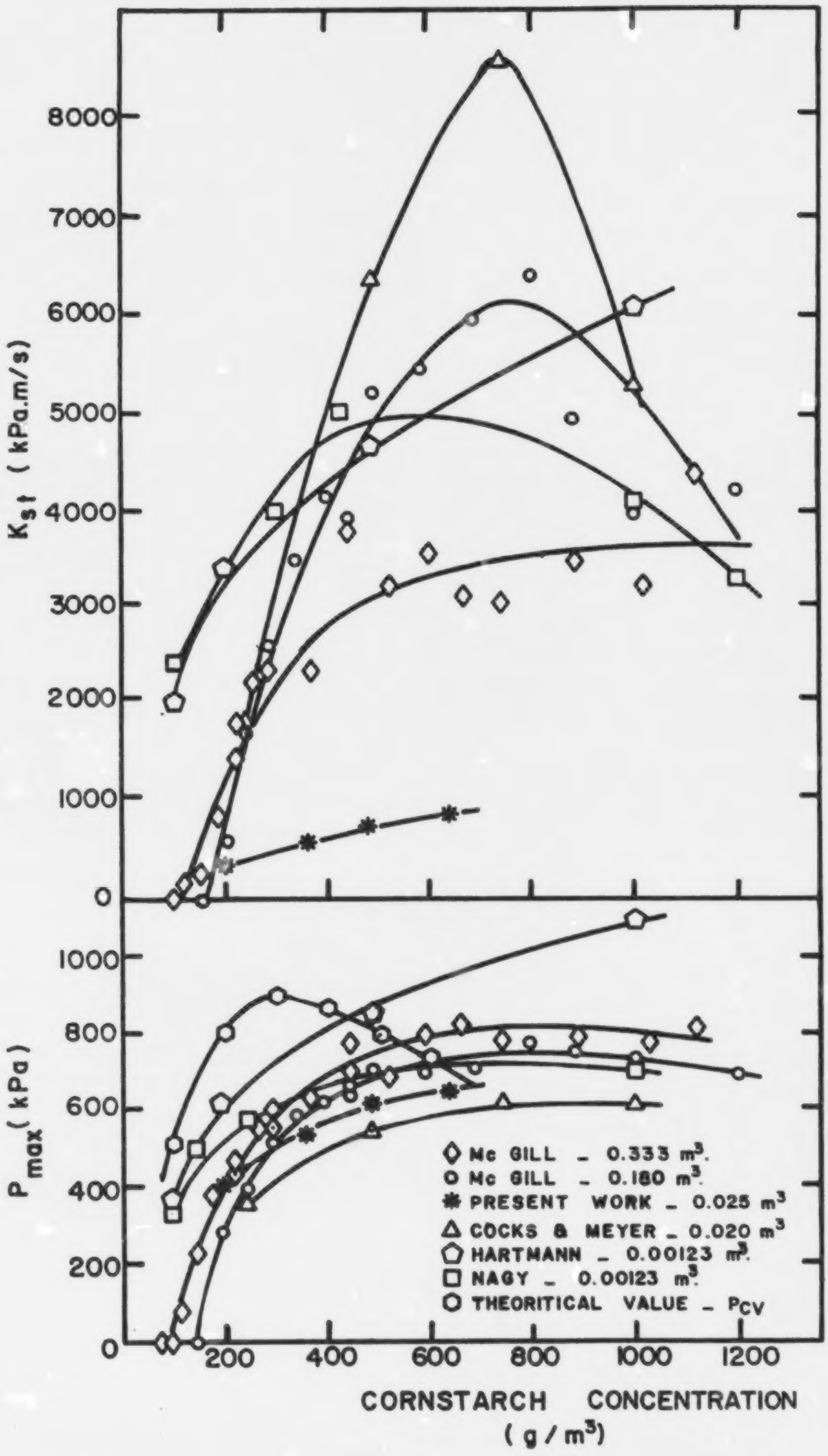

Fig. 20 : The comparison between the present work and the work of the others of the maximum overpressure and K_{st} factor versus cornstarch concentration.

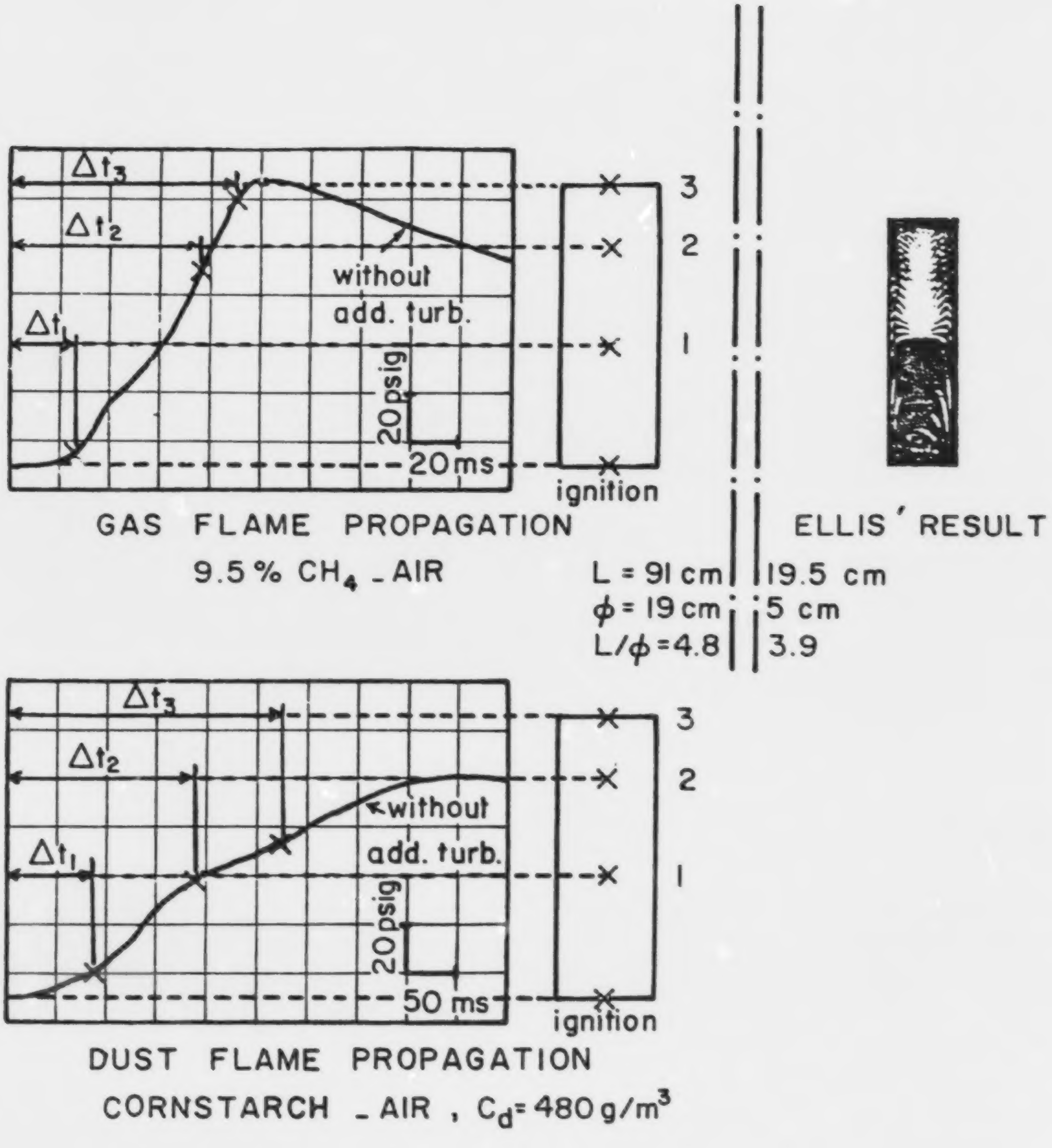

Fig. 21 : The measurements of flame speeds and pressure history in both quasi-laminar gas and dust flames propagation in the closed tube.

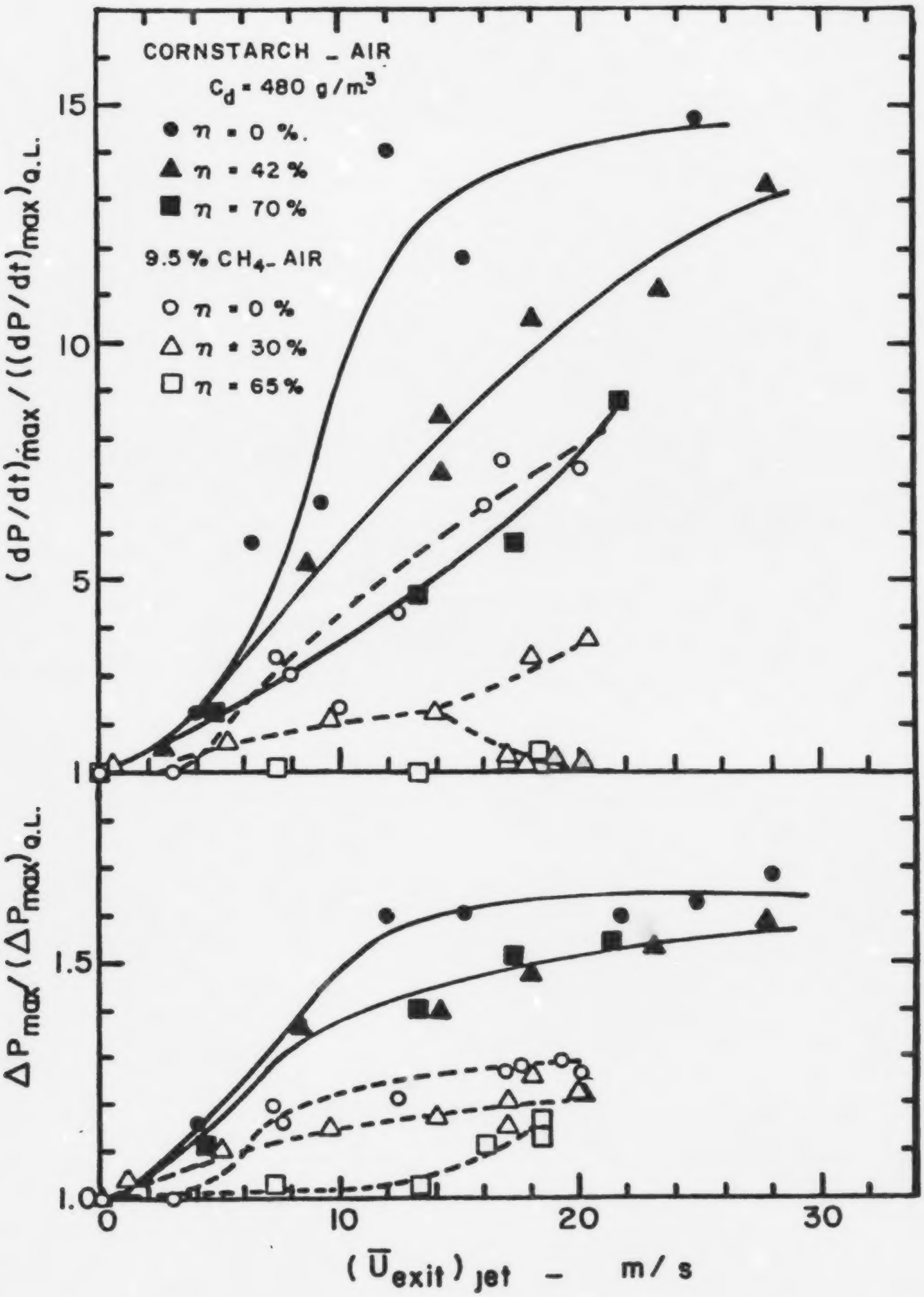

Fig. 22 : The maximum overpressure (ΔP_{max}) and the maximum rate of overpressure rise $(dP/dt)_{max}$ both in gas and dust flame propagation in the closed tube versus intensities of jet-induced turbulence (indicated by exit velocity of jet along its center-line in this figure).

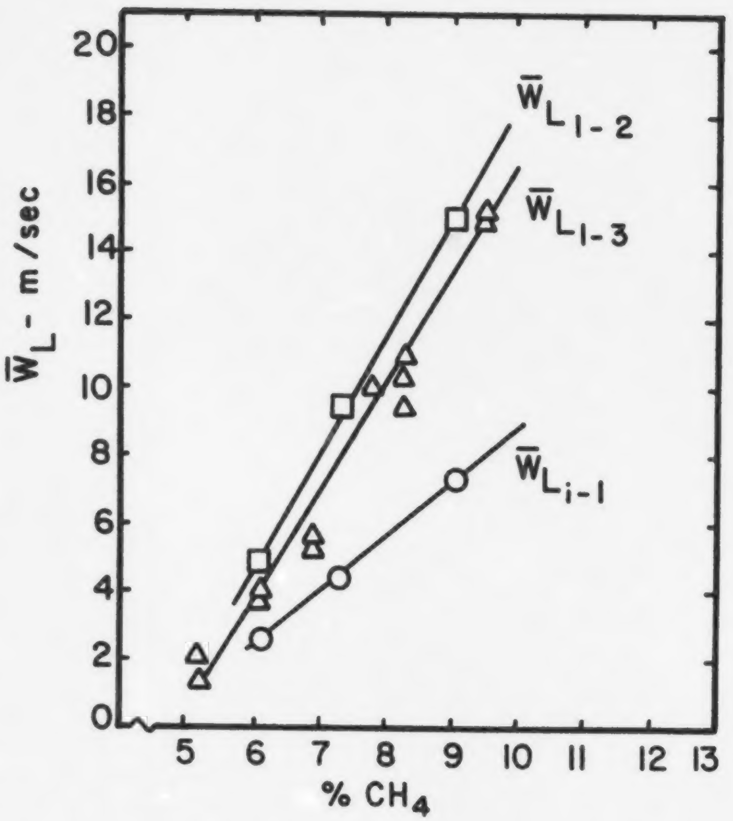

$(W_L)_{1-2}$: average propagation velocities at $l = 0.4$ m from ignitor, between ion gauge $1^{\#}$ and $2^{\#}$.

$(W_L)_{1-3}$: average propagation velocities at $l = 0.45$ m from ignitor, between ion gauge $1^{\#}$ and $3^{\#}$.

$(W_L)_{i-1}$: average propagation velocities at $l = 0.1$ m from ignitor, between ignitor and ion-gauge $1^{\#}$.

Fig. 23 : Mean propagation velocities of the flame front in different points of the tube as a function of mixture composition.

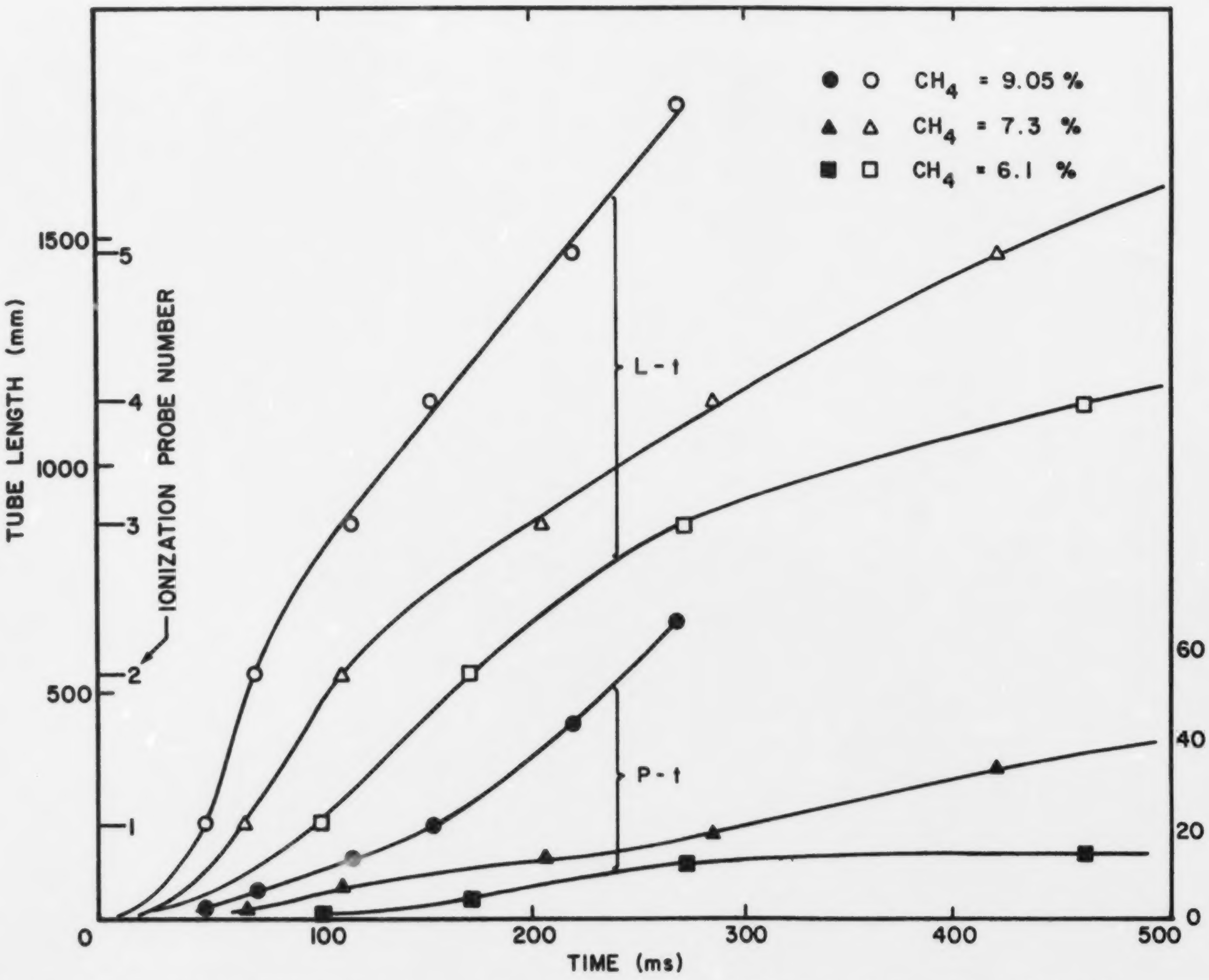

Fig. 24 : History of pressure and flame front locations for different mixture composition in quasi-laminar case.

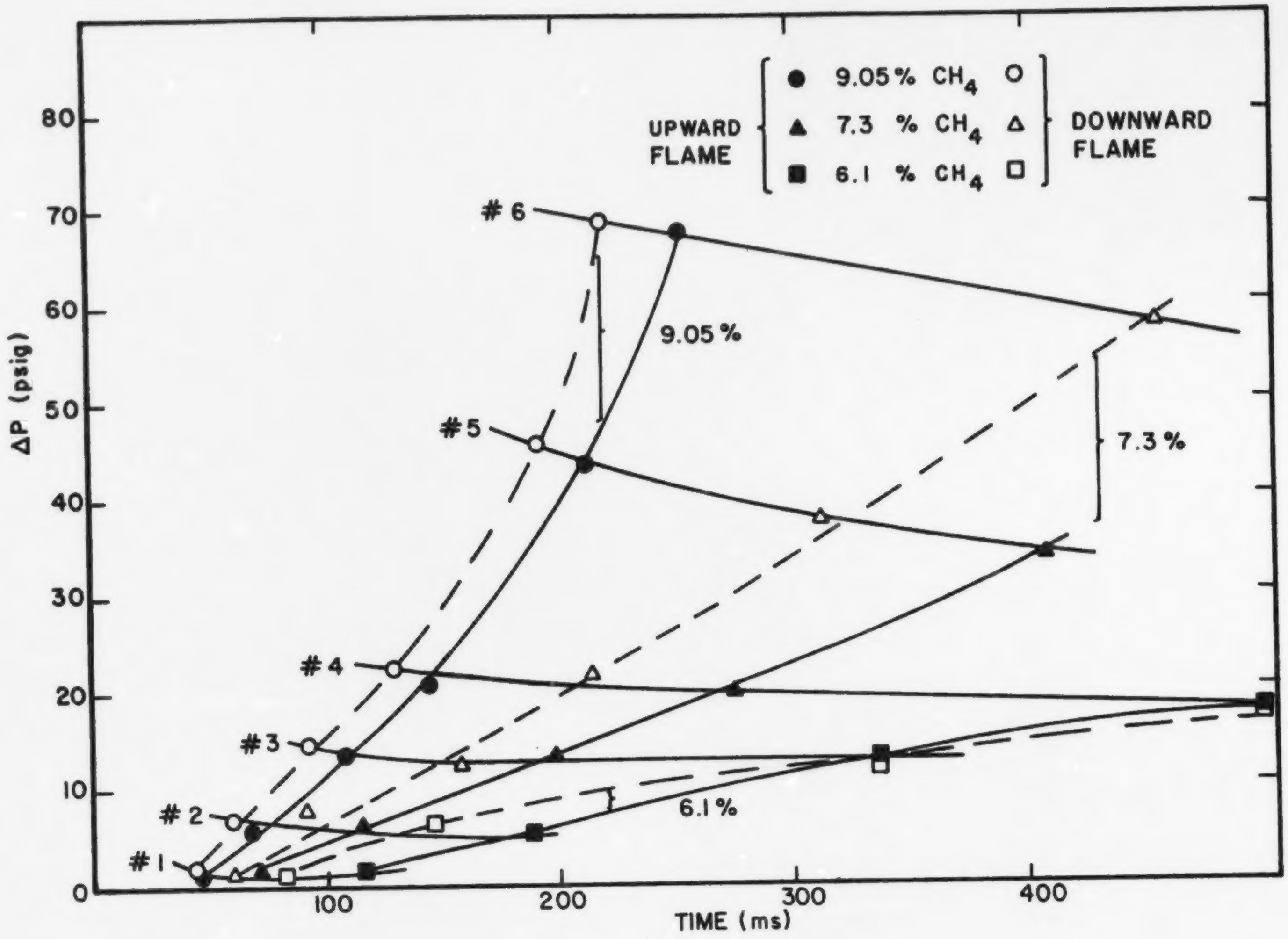

Fig. 25-(a) : Pressure history of upward and downward propagating flame in different mixture composition.

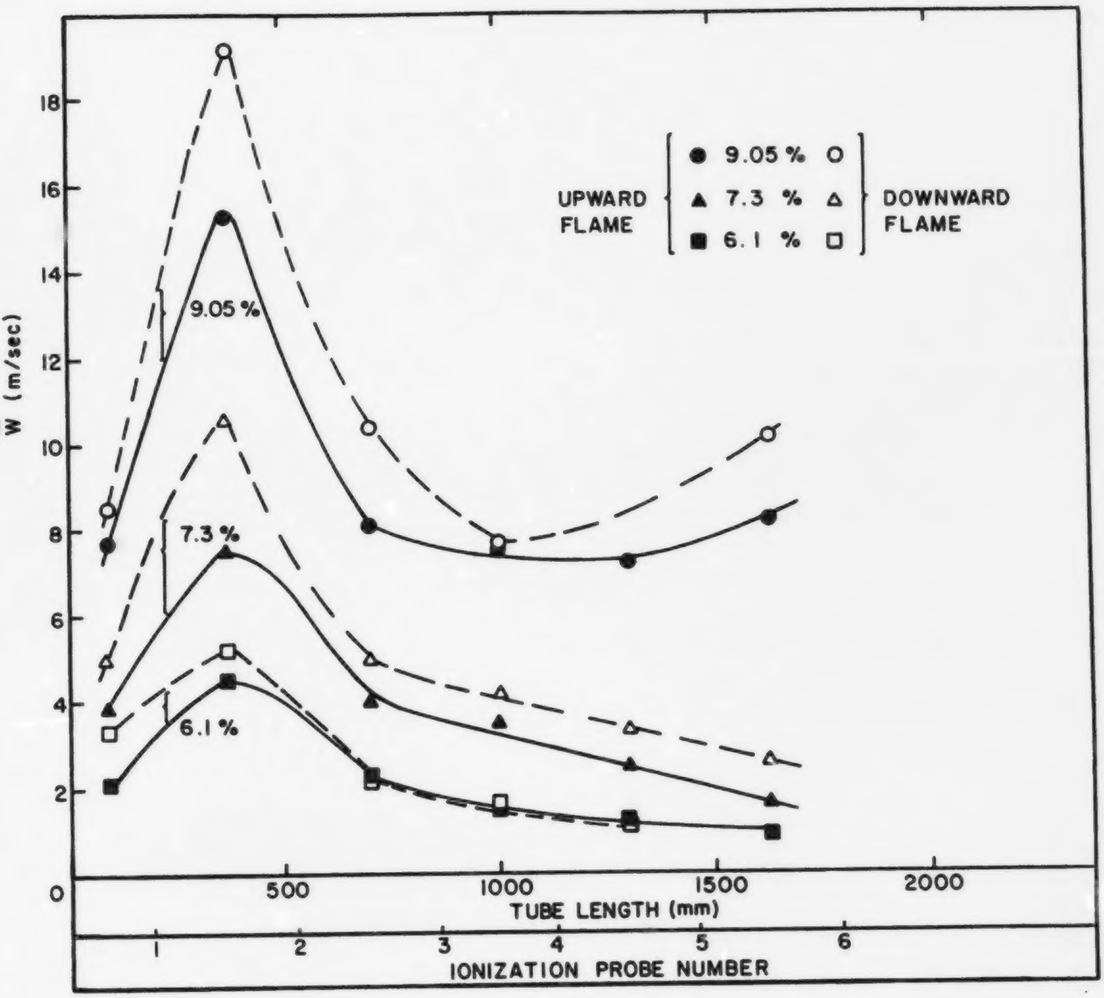

Fig. 25-(b) : Flame propagation velocities as a function of flame location along the tube for upward and downward propagation flame and different mixture composition.

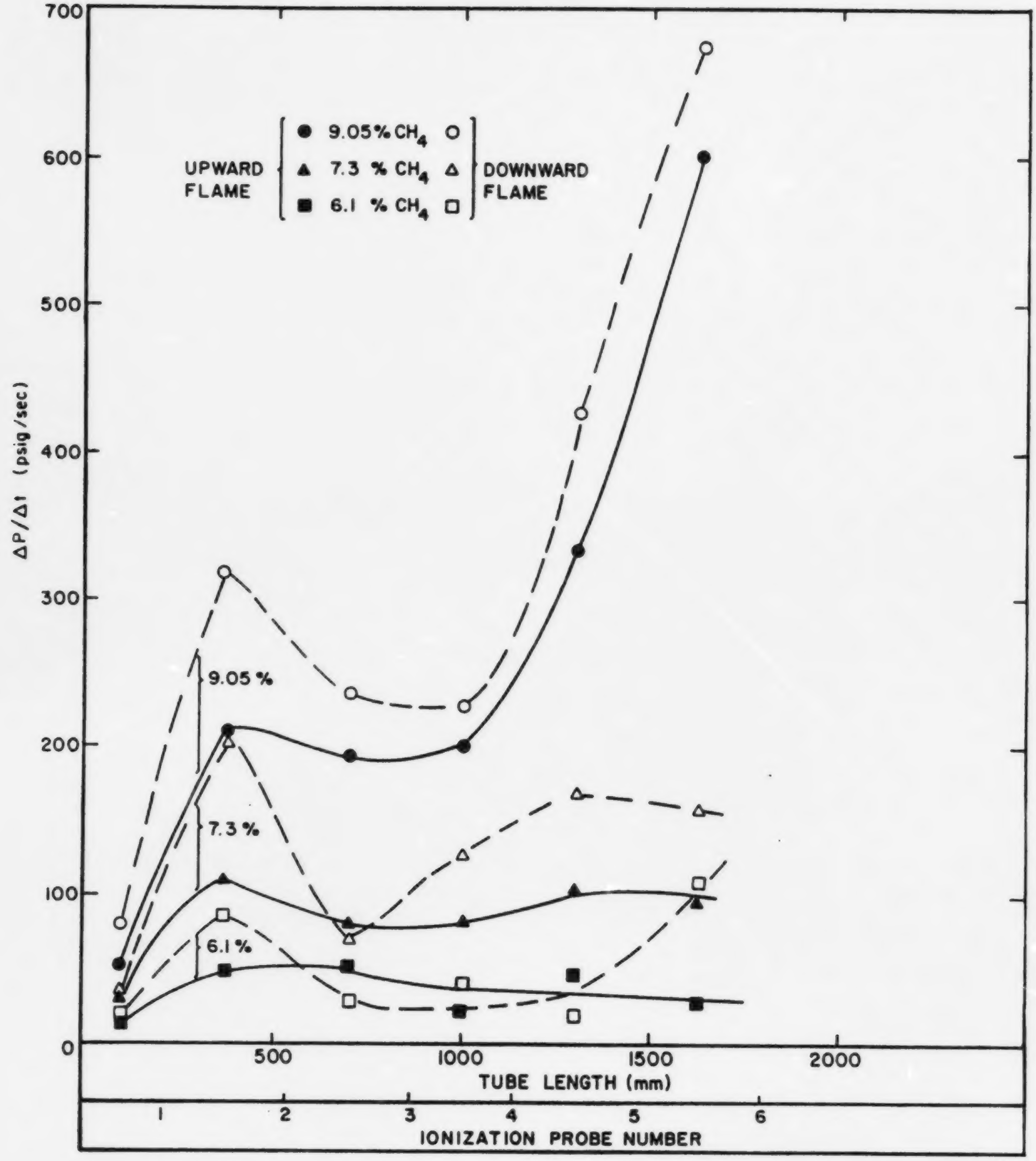

Fig. 25-(c) : The (ΔP/Δt) as a function of flame location along the tube for upward and downward propagating flame and different mixture composition.

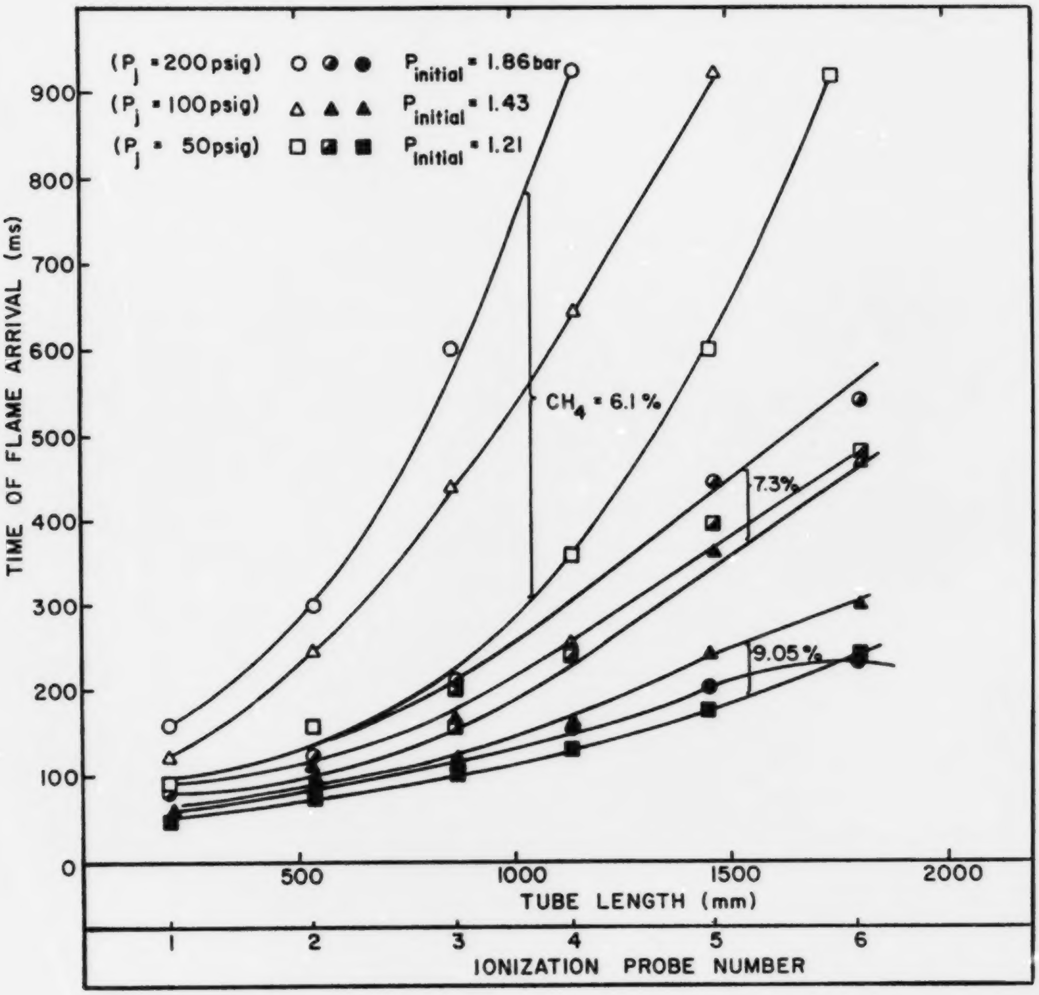

Fig. 26 : Flame front location histories for different initial pressure and different mixture composition.

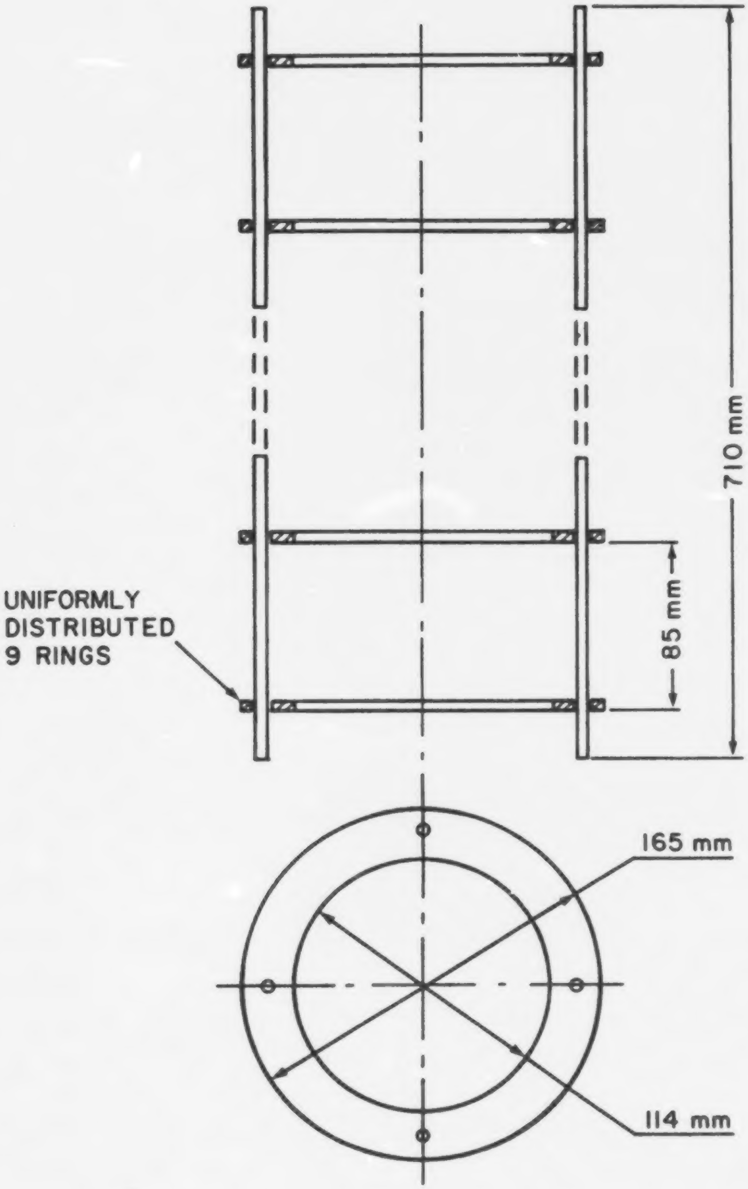
710 mm
85 mm
UNIFORMLY
DISTRIBUTED
9 RINGS
165 mm
114 mm

Fig. 27 : Geometric shape and size of obstacles used in present study.

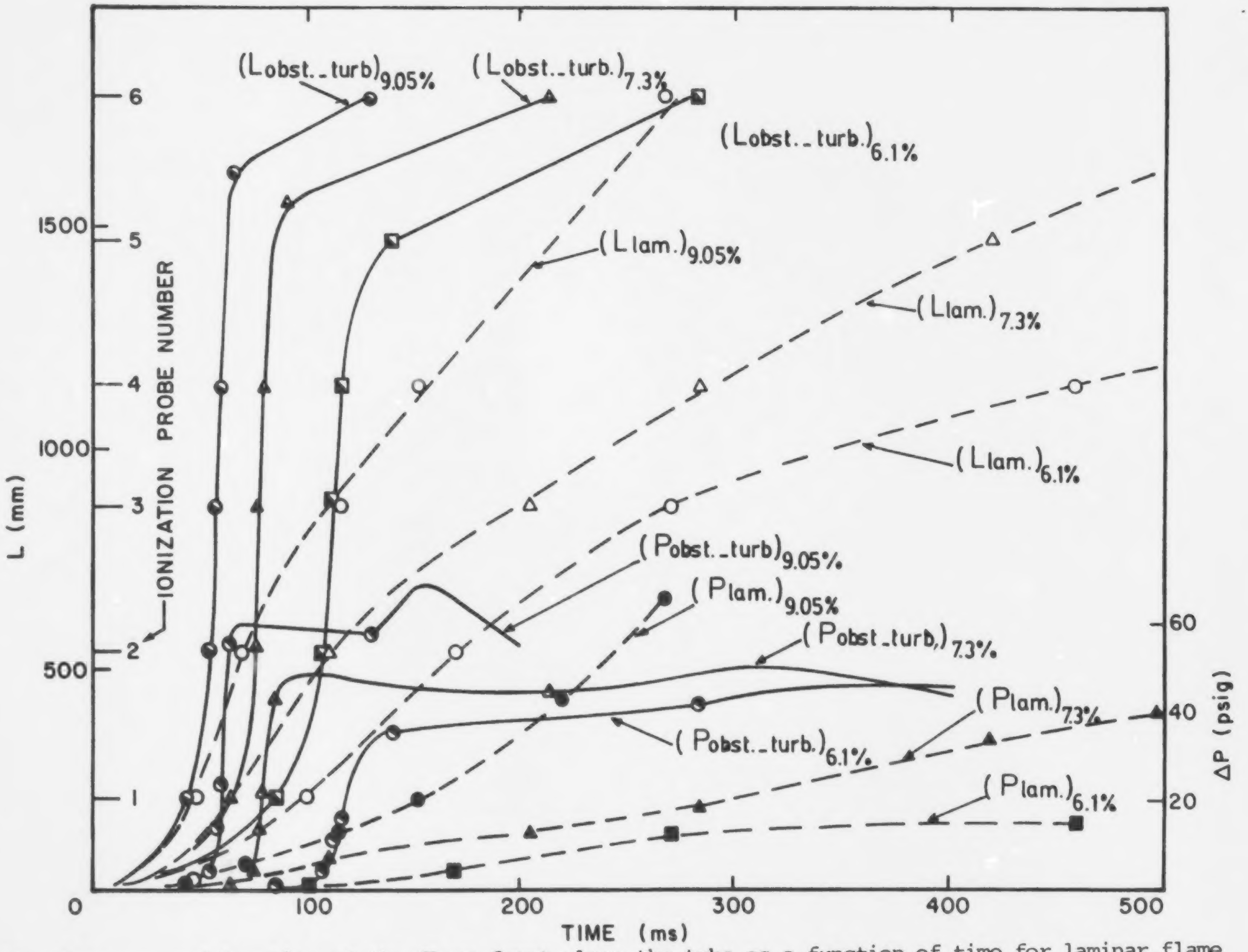

Fig. 28 : Pressure and location of the flame front along the tube as a function of time for laminar flame and for flame propagating through obstacles, for different mixture composition.

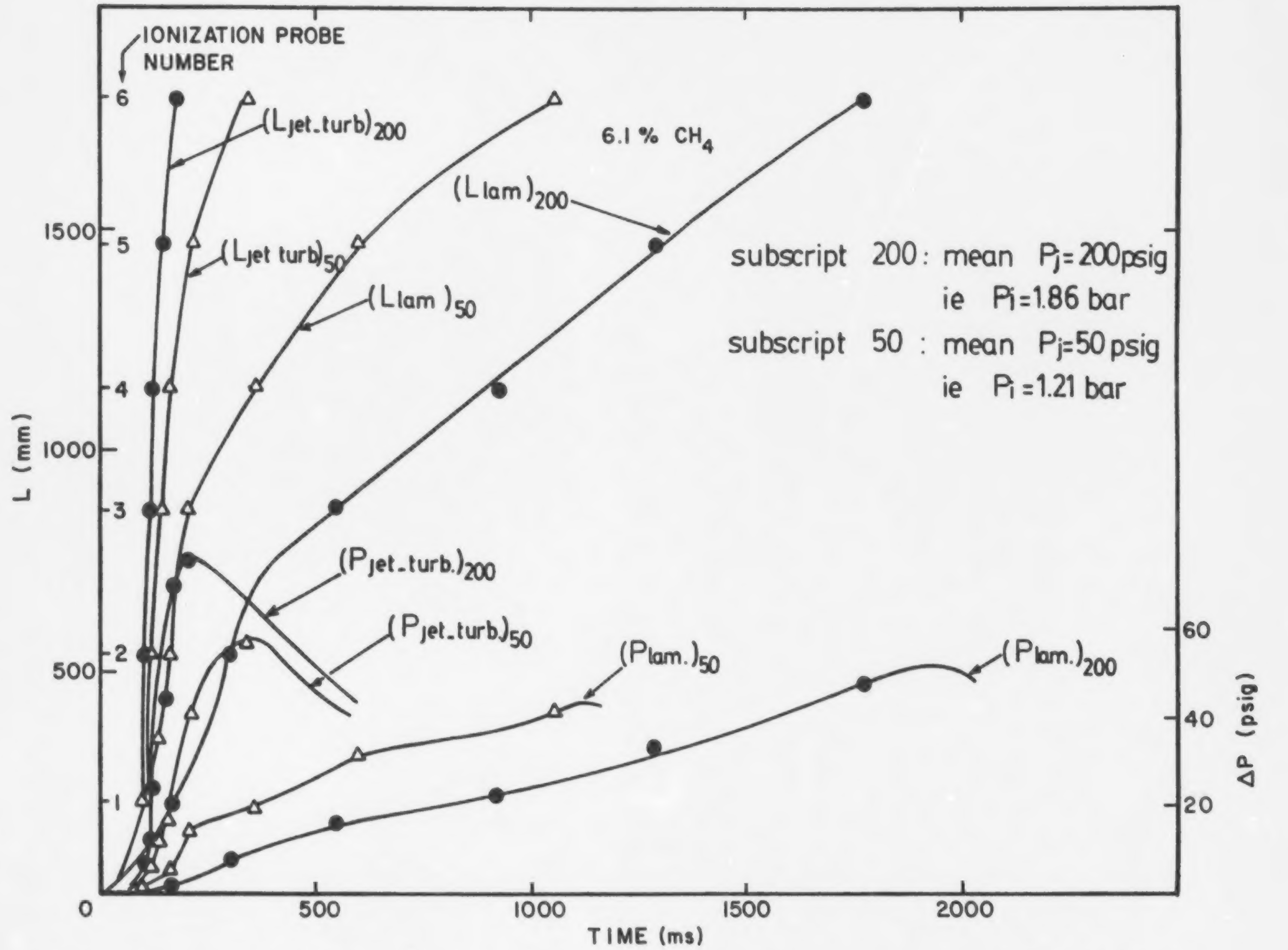

Fig. 29-(a) : Pressure and location of the flame front along the tube as a function of time for laminar flame and for flame influenced by jet-induced turbulence (initial pressure of laminar propagation corresponds to that of turbulence case).

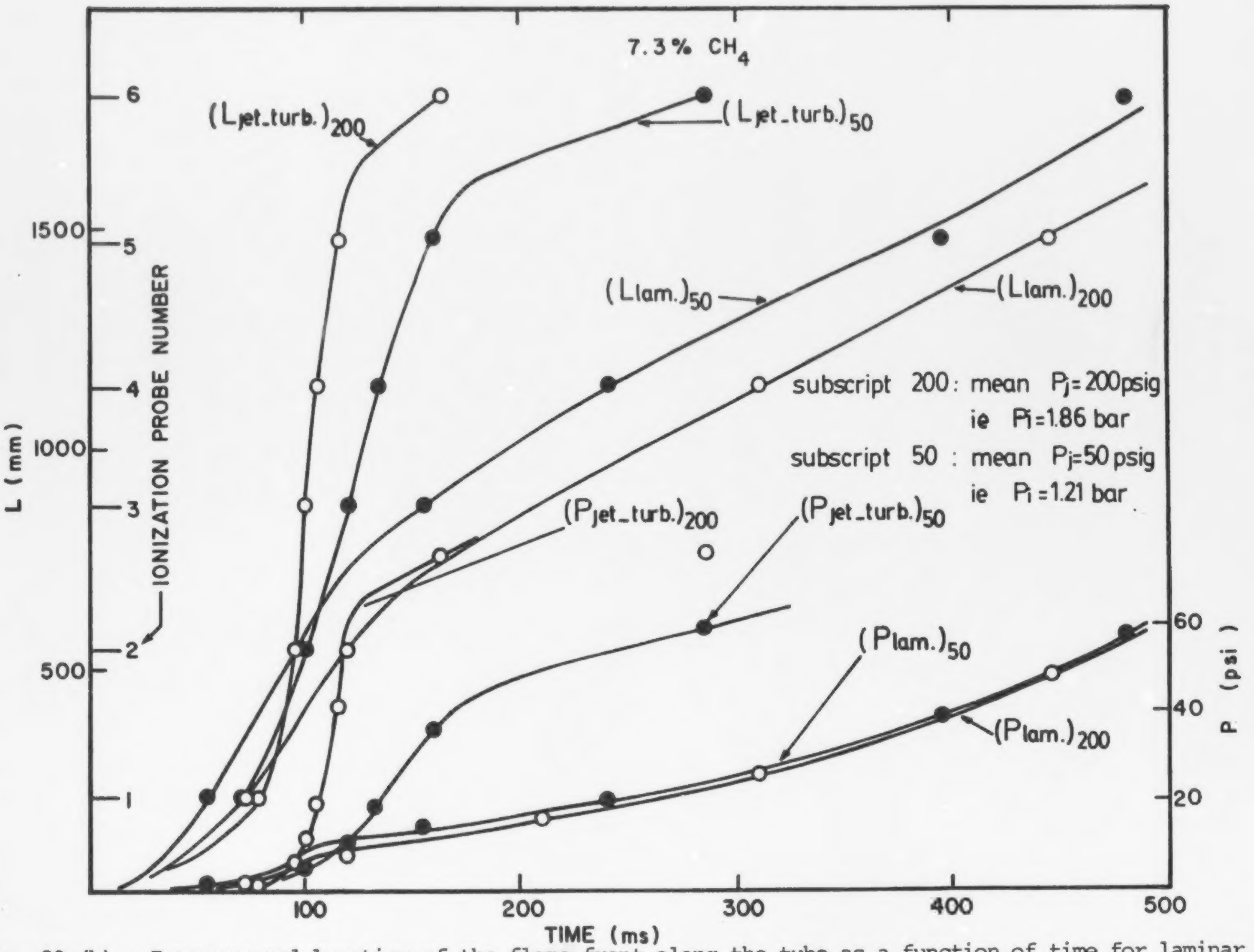

Fig. 29-(b) : Pressure and location of the flame front along the tube as a function of time for laminar flame and for flame influenced by jet-induced turbulence (initial pressure of laminar propagation corresponds to that of turbulence case).

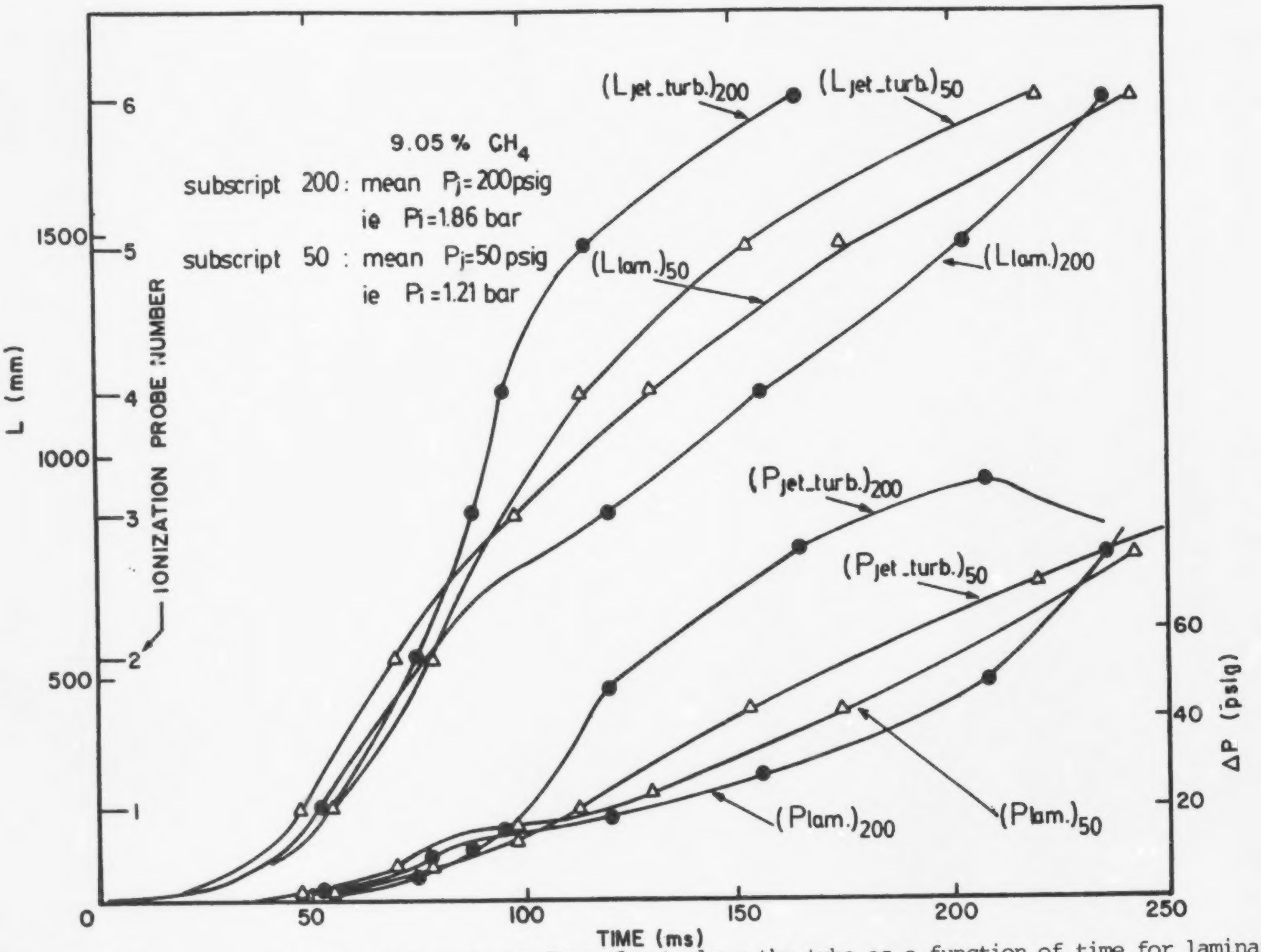

Fig. 29-(c) : Pressure and location of the flame front along the tube as a function of time for laminar flame and for flame influenced by jet-induced turbulence (initial pressure of laminar propagation corresponds to that of turbulence case).

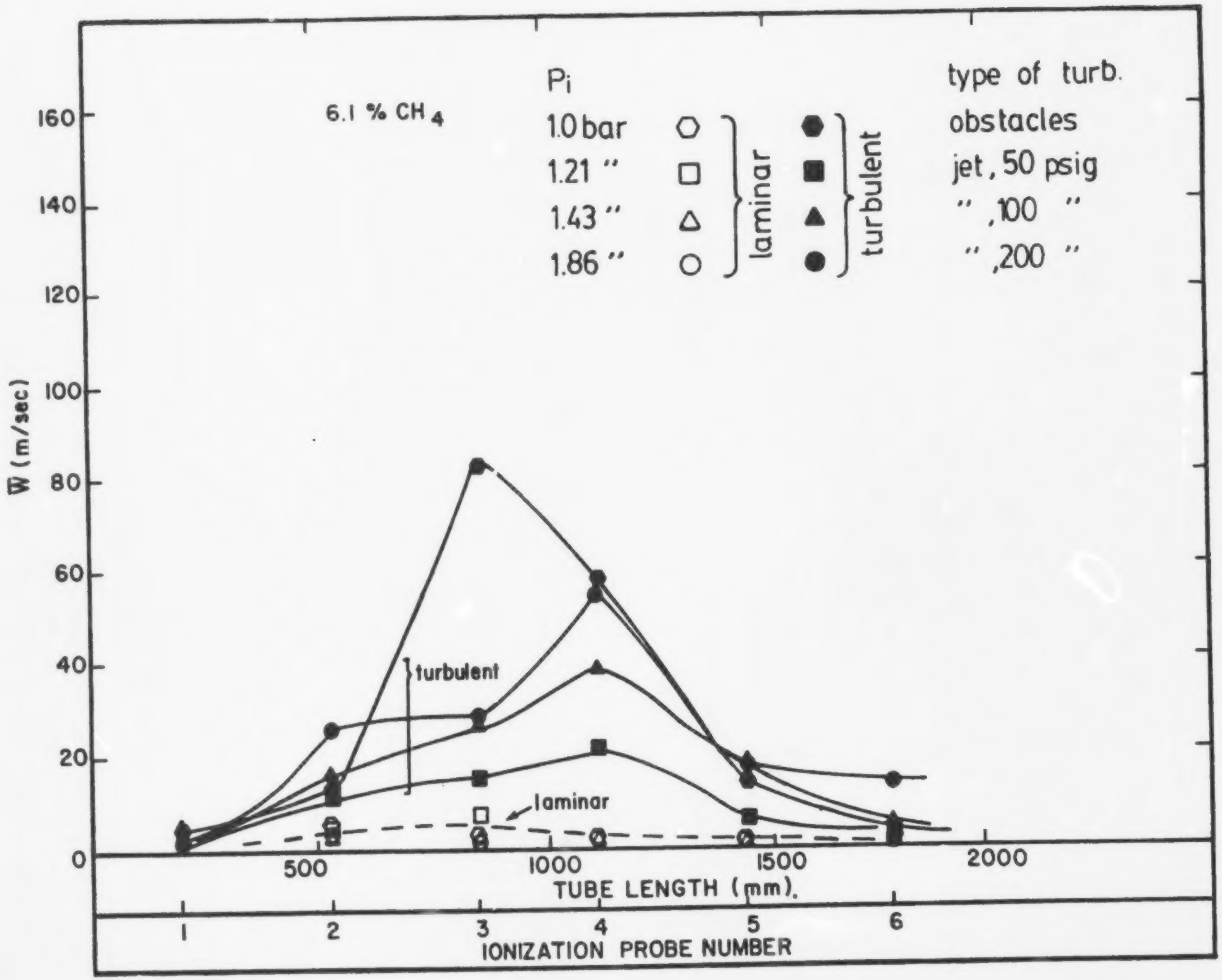

Fig. 30-(a) : Propagation velocities as a function of location of flame along the tube for laminar and turbulent propagation.

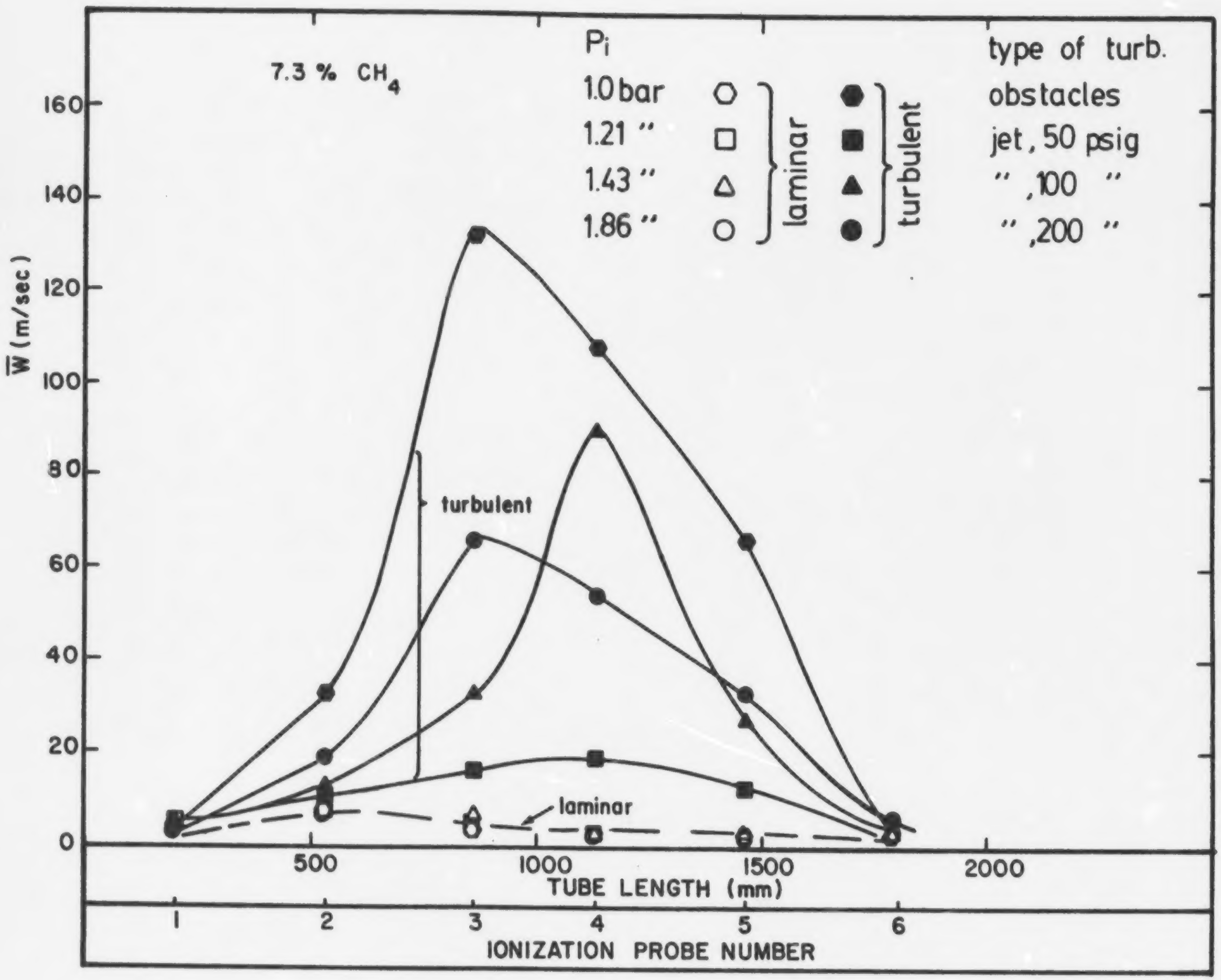

Fig. 30-(b) : Propagation velocities as a function of location of flame along the tube for laminar and turbulent propagation.

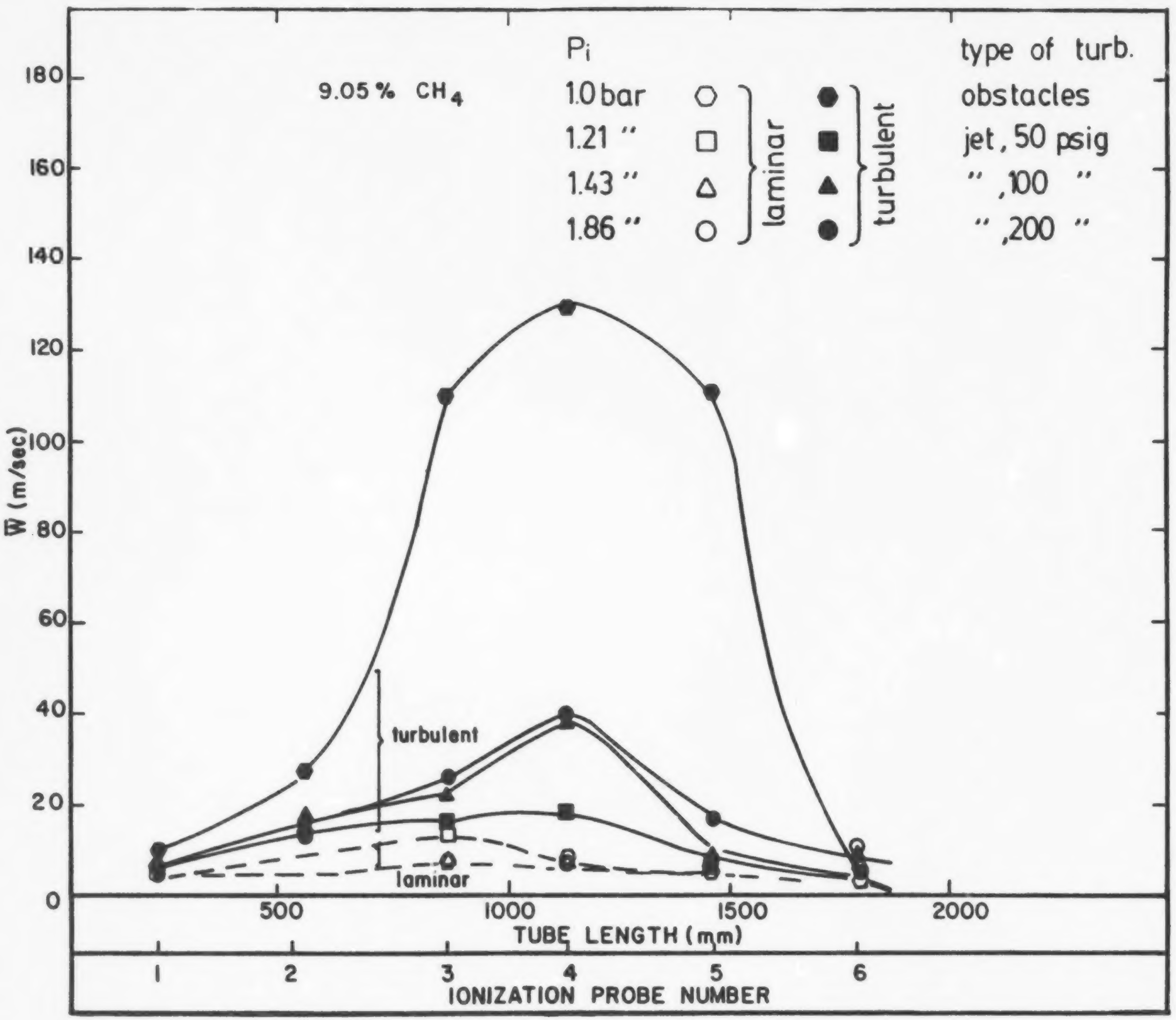

Fig. 30-(c) : Propagation velocities as a function of location of flame along the tube for laminar and turbulent propagation.

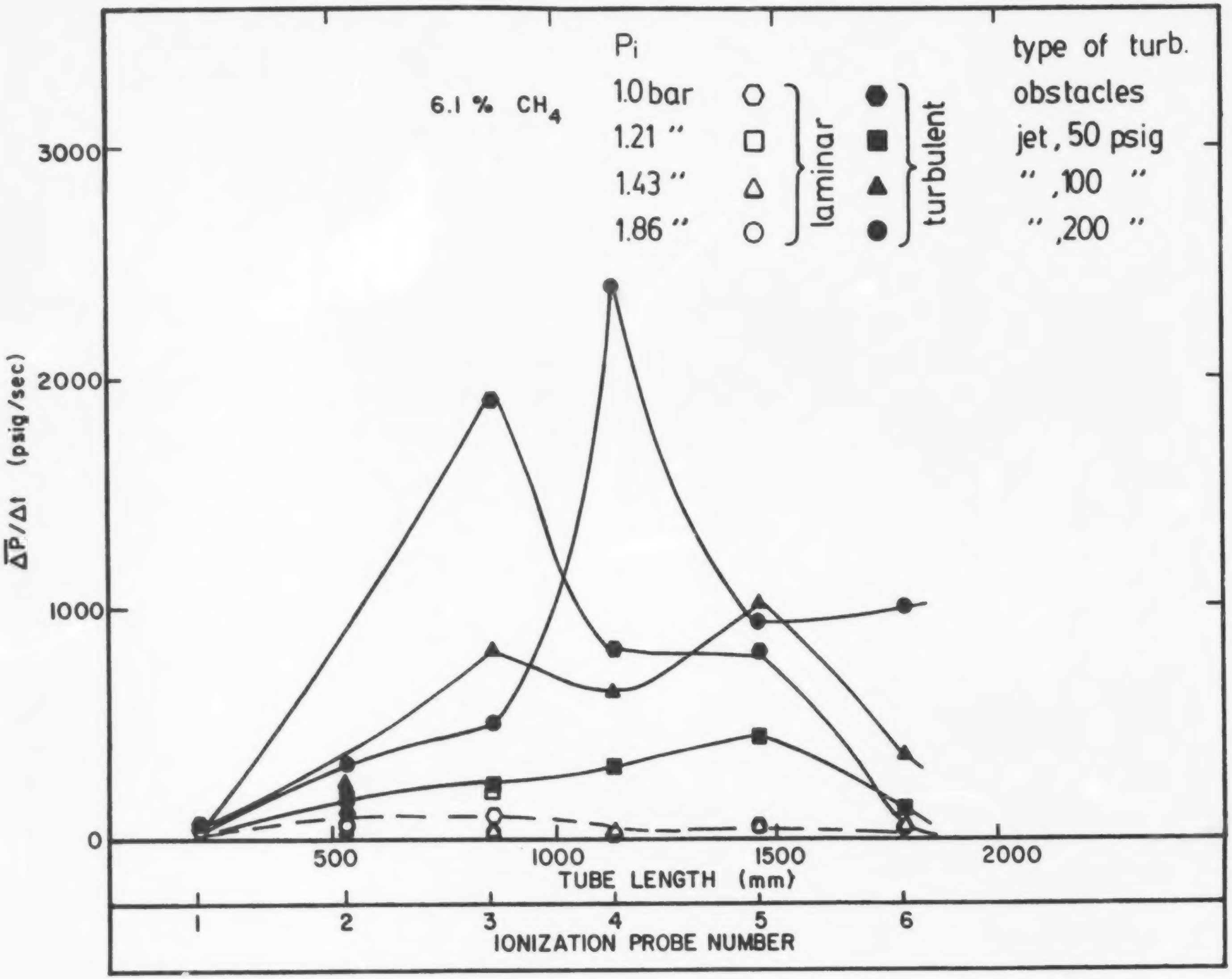

Fig. 31-(a) : The rate of pressure increase ($\Delta P/\Delta t$) as a function of location of flame along the tube for laminar and turbulent propagation.

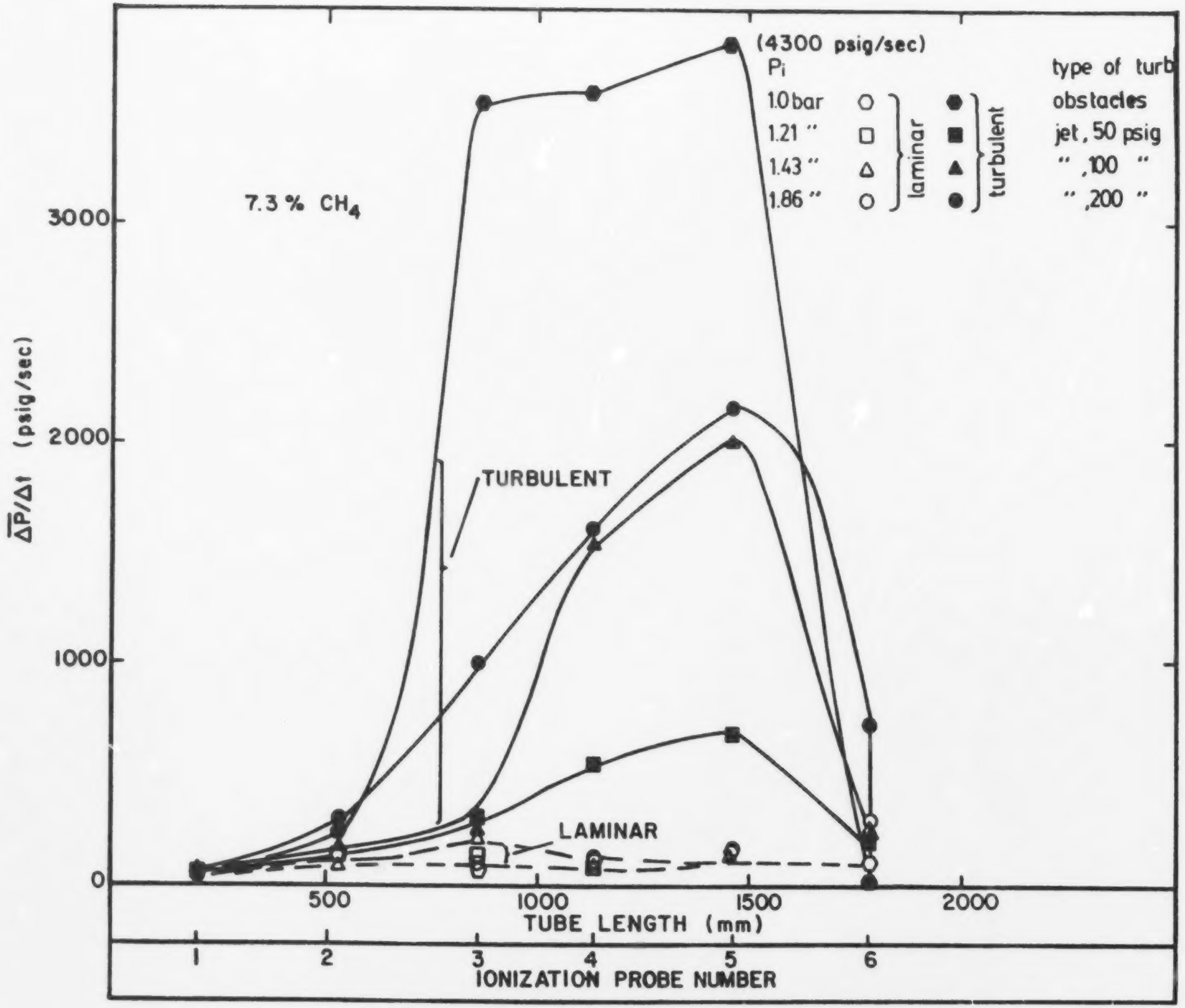

Fig. 31-(b) : The rate of pressure increase ($\Delta P/\Delta t$) as a function of location of flame along the tube for laminar and turbulent propagation.

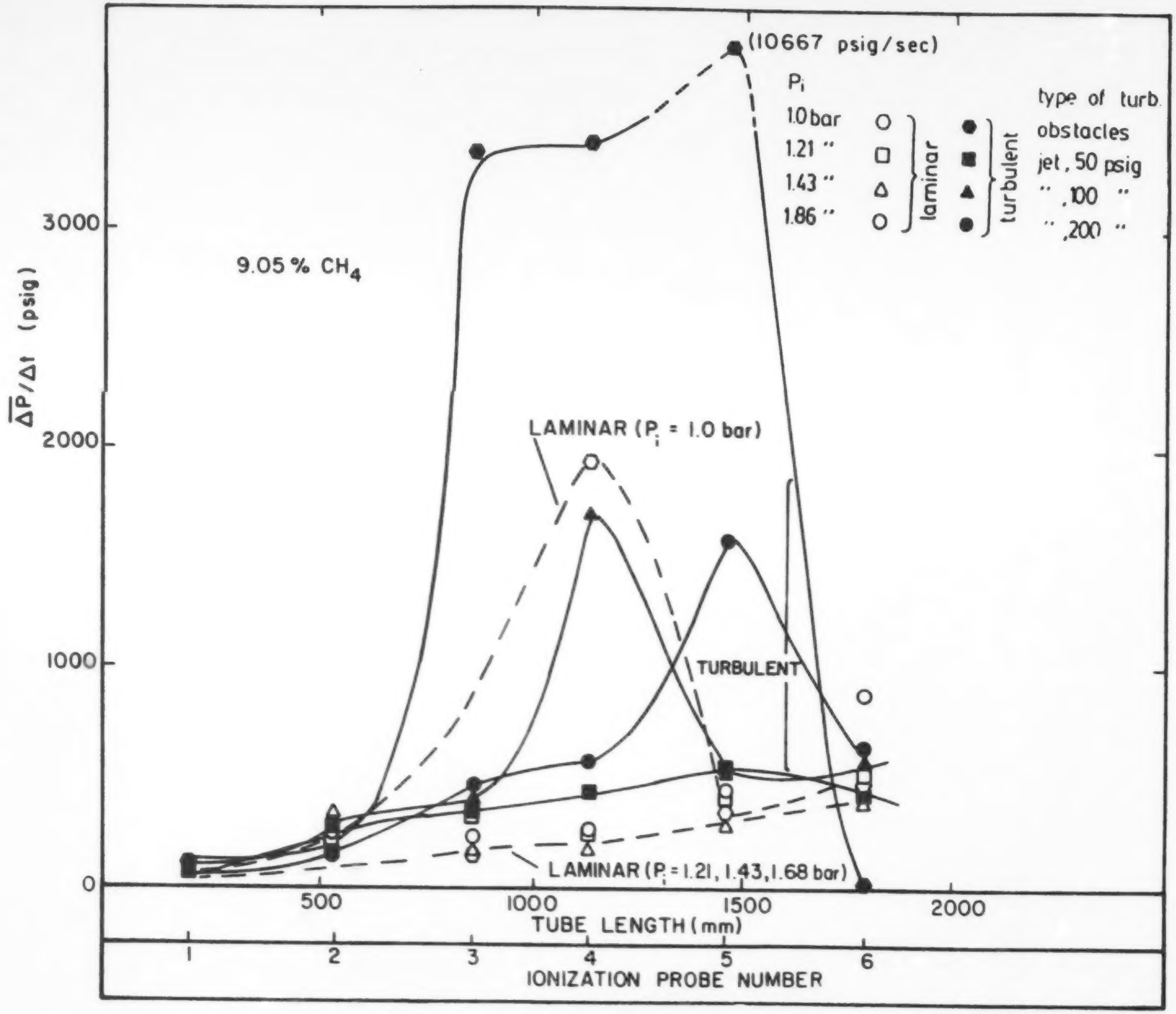

Fig. 31-(c) : The rate of pressure increase (ΔP/Δt) as a function of location of flame along the tube for laminar and turbulent propagation.

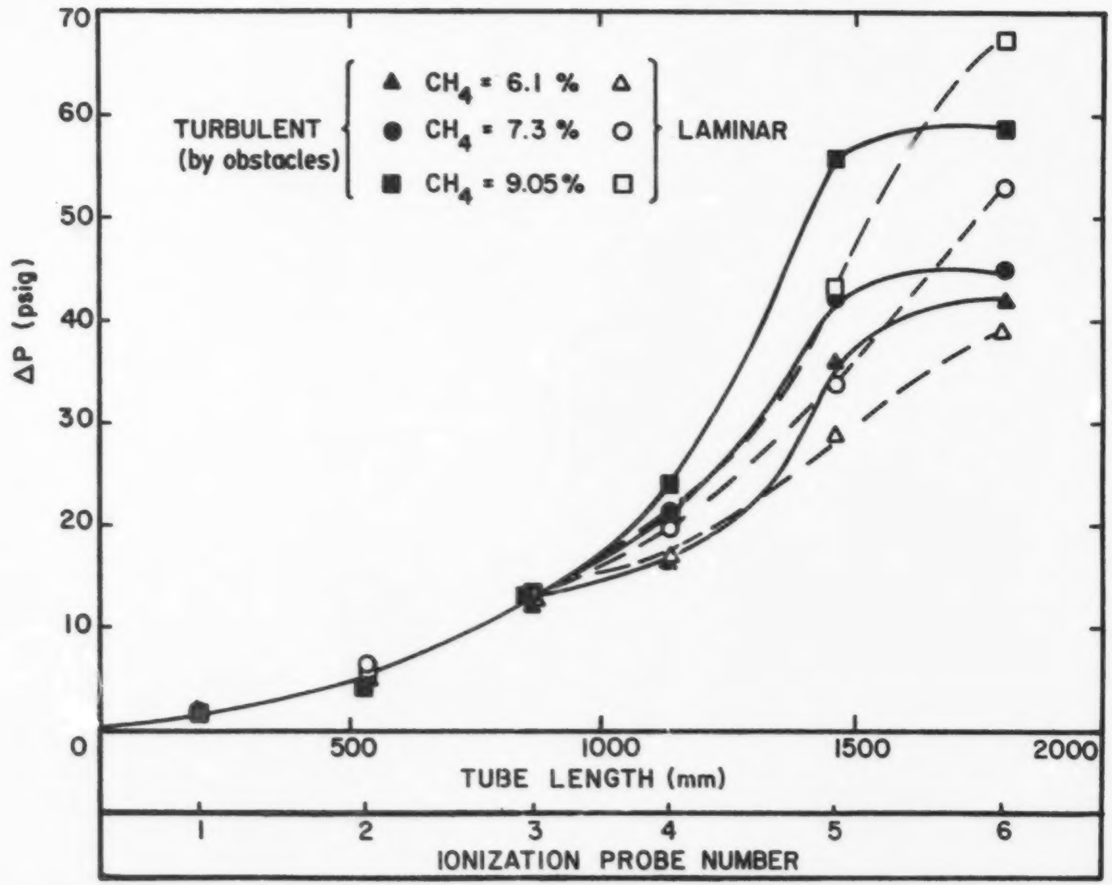

Fig. 32-(a) : Pressure as a function of location of flame along the tube for laminar and turbulent propagation (obstacles-induced turbulence).

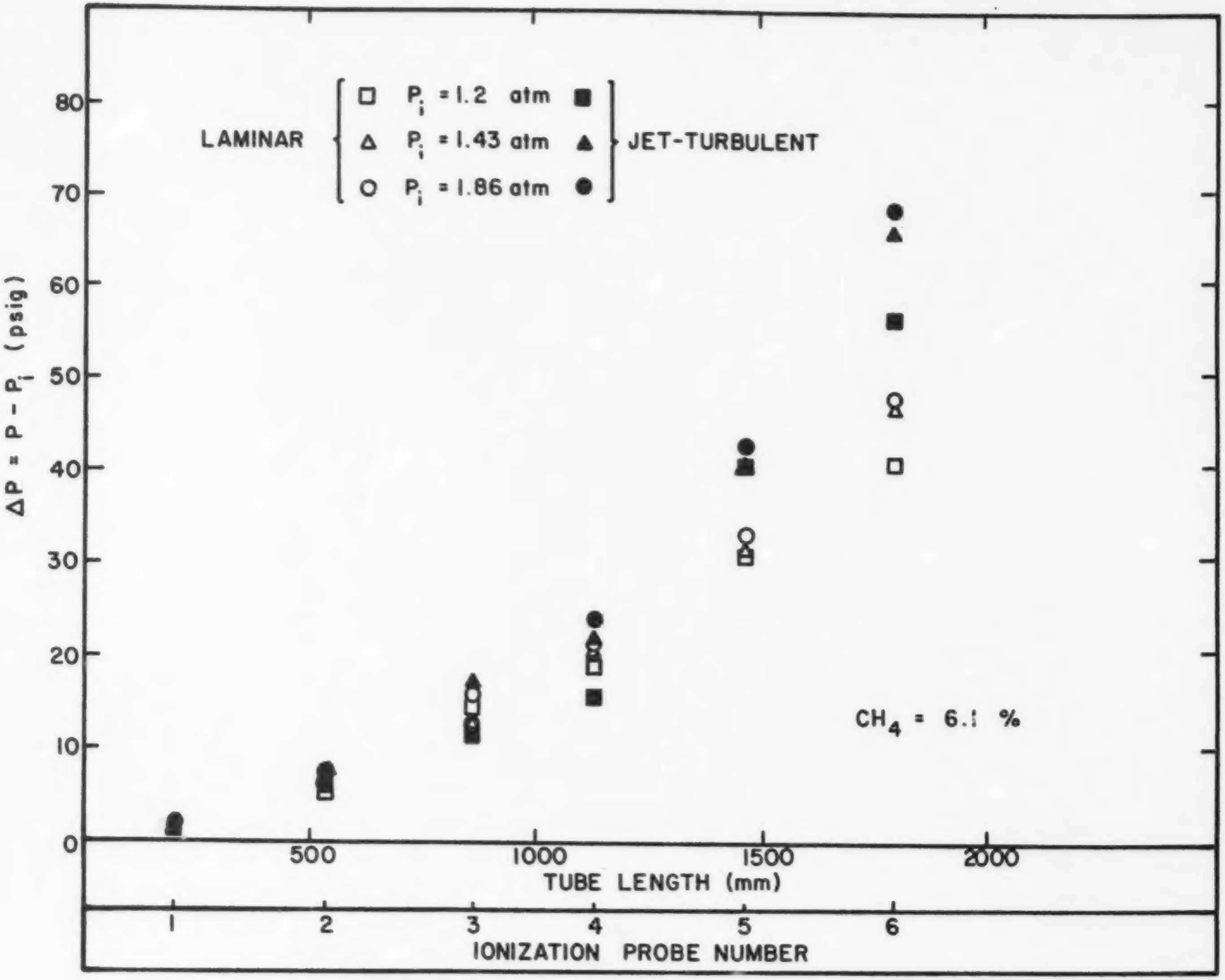

Fig. 32-(b) : Pressure as a function of location of flame along the tube for laminar and turbulent propagation (jet-induced turbulence).

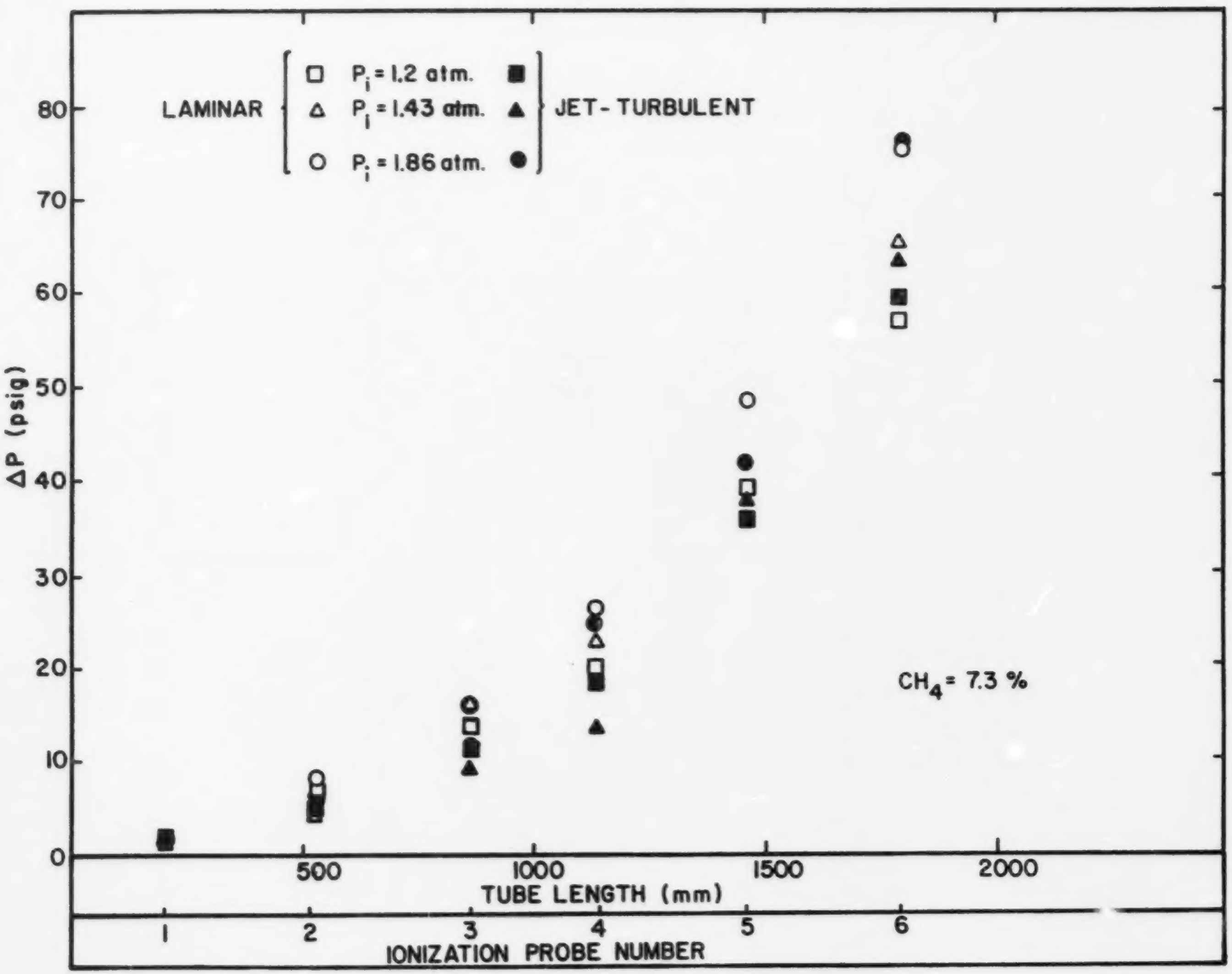

Fig. 32-(c) : Pressure as a function of location of flame along the tube for laminar and turbulent propagation (jet-induced turbulence).

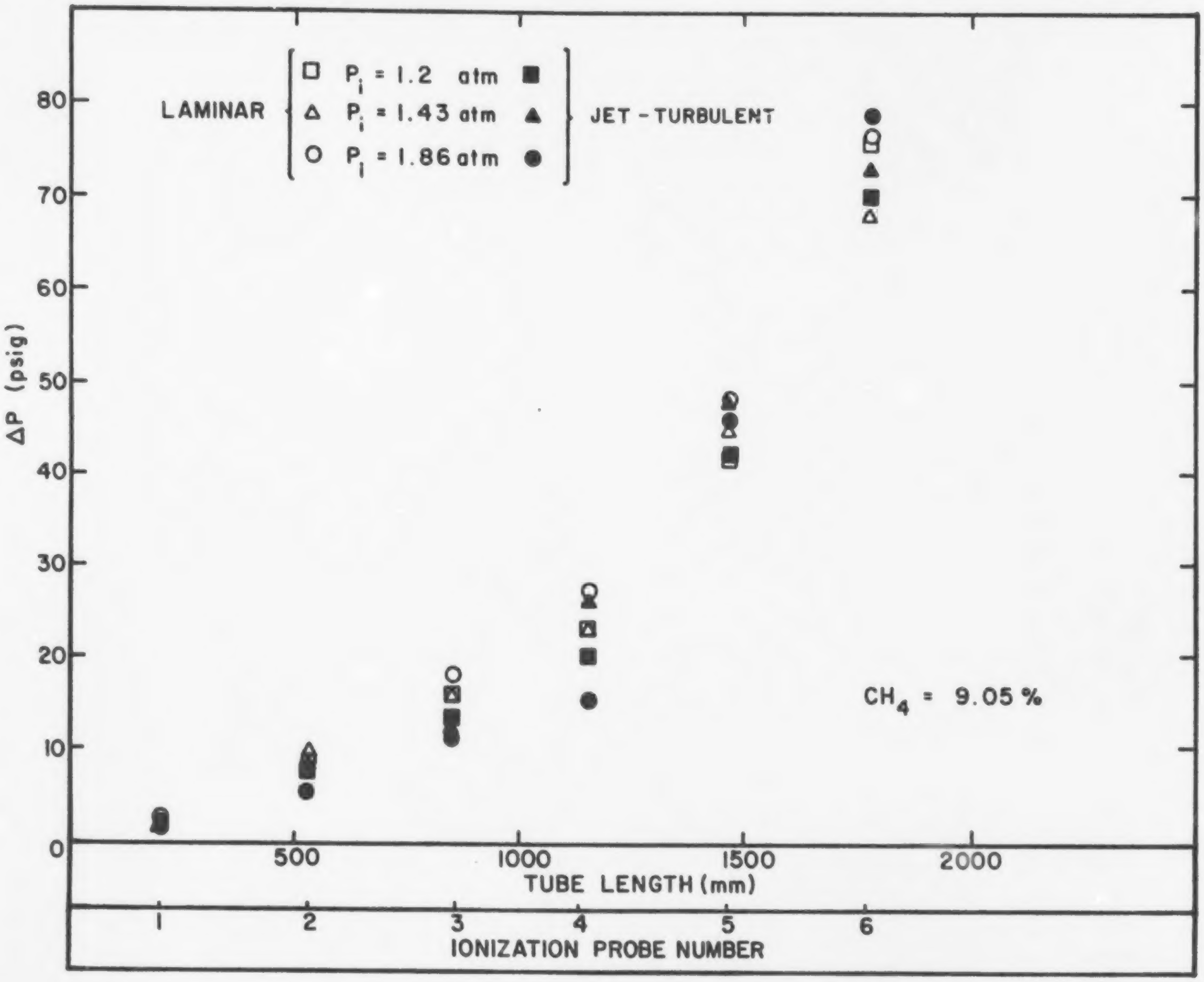

Fig. 32-(d) : Pressure as a function of location of flame along the tube for laminar and turbulent propagation (jet-induced turbulence).

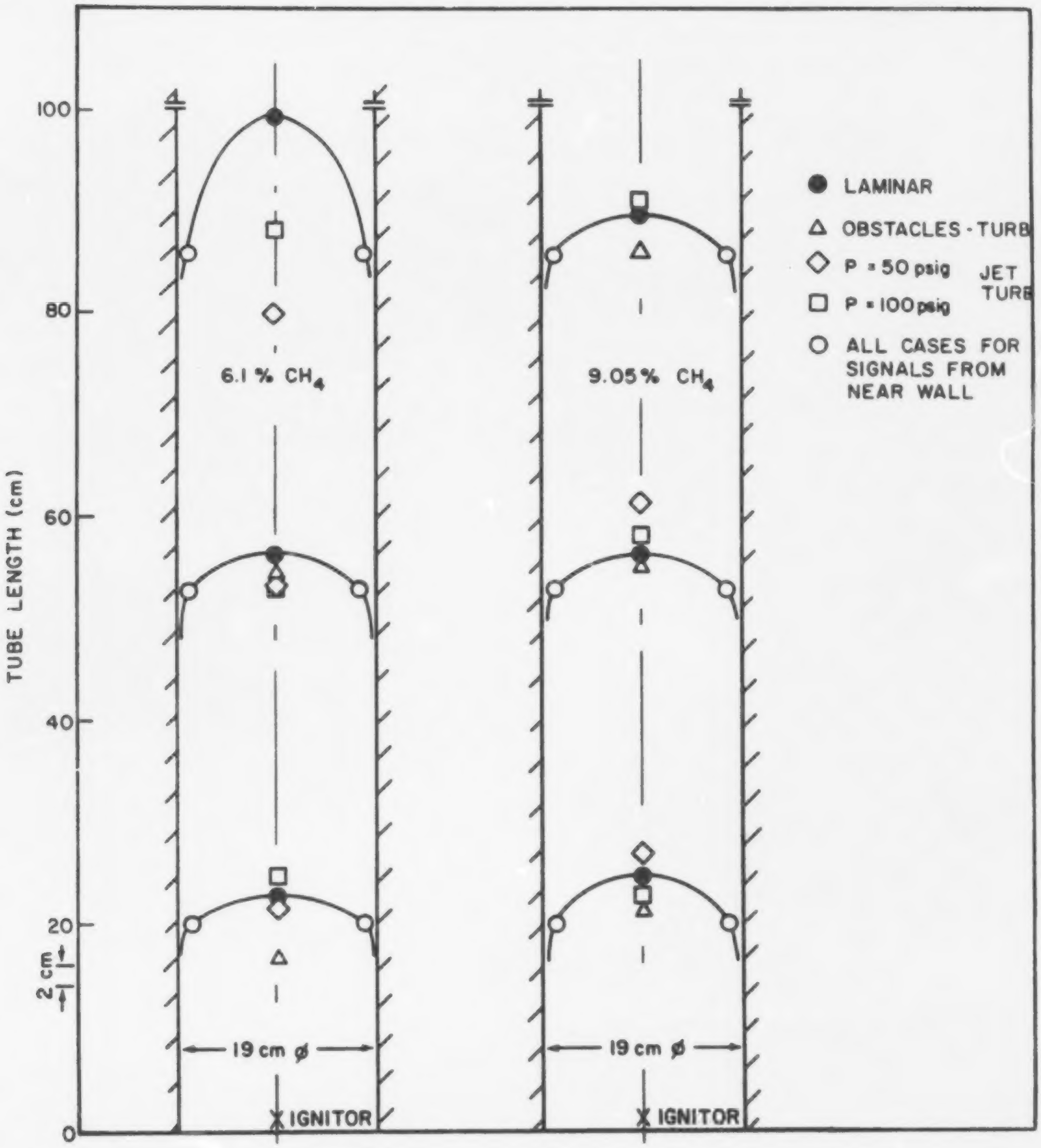

Fig. 33 : The shape of flame in the bottom section, while the flame propagating from the bottom end to the top of the tube (the data are estimated at the base of simultaneous measurements at the exit of the tube and near its wall when L/D is equal 9.6; D=19 cm).

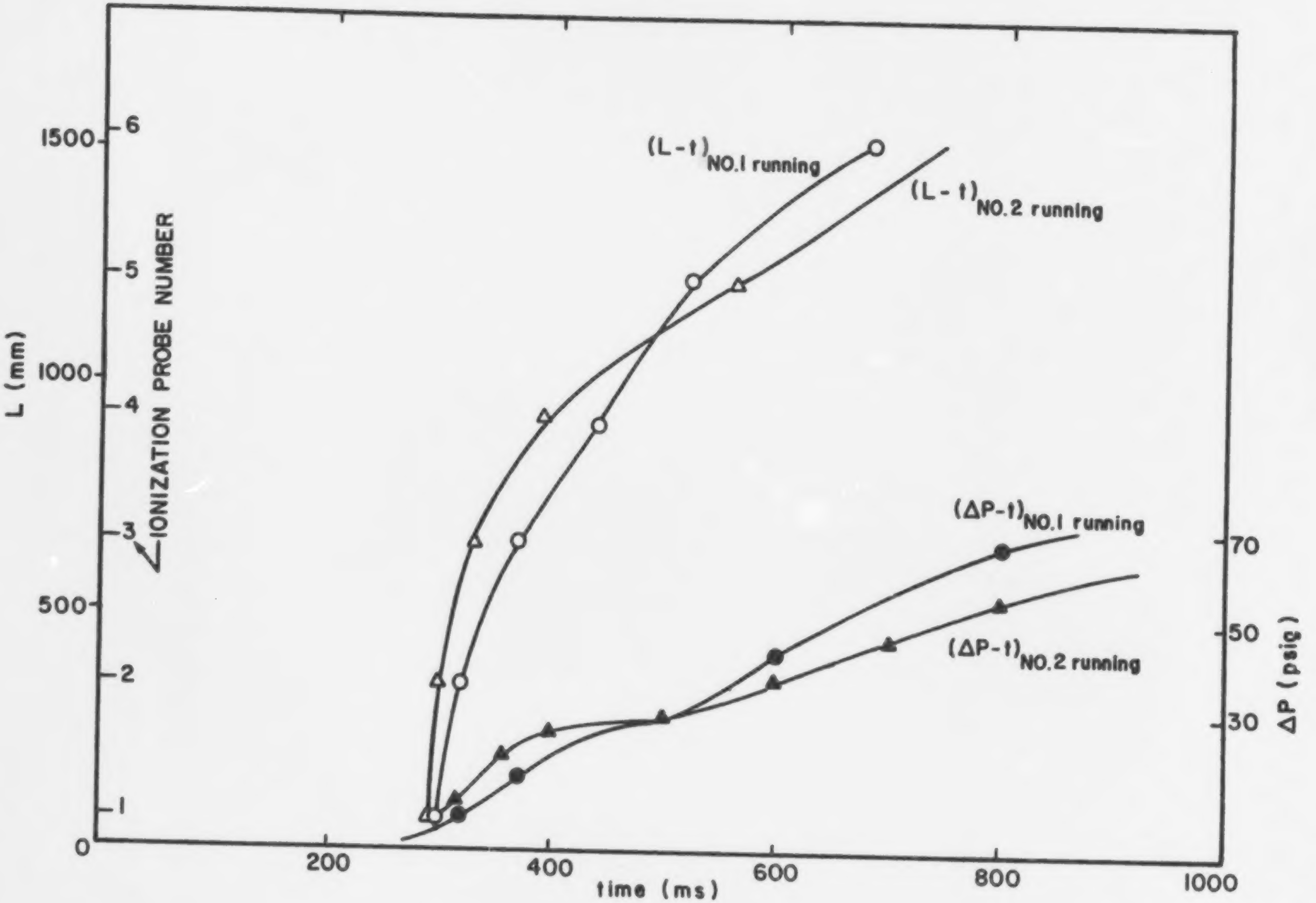

Fig. 34 : Pressure and location of the dust flame along the tube (L/D= 9.6, D= 19 cm) as a function of time for quasi-laminar case (cornstarch concentration : 480 g/m^3).

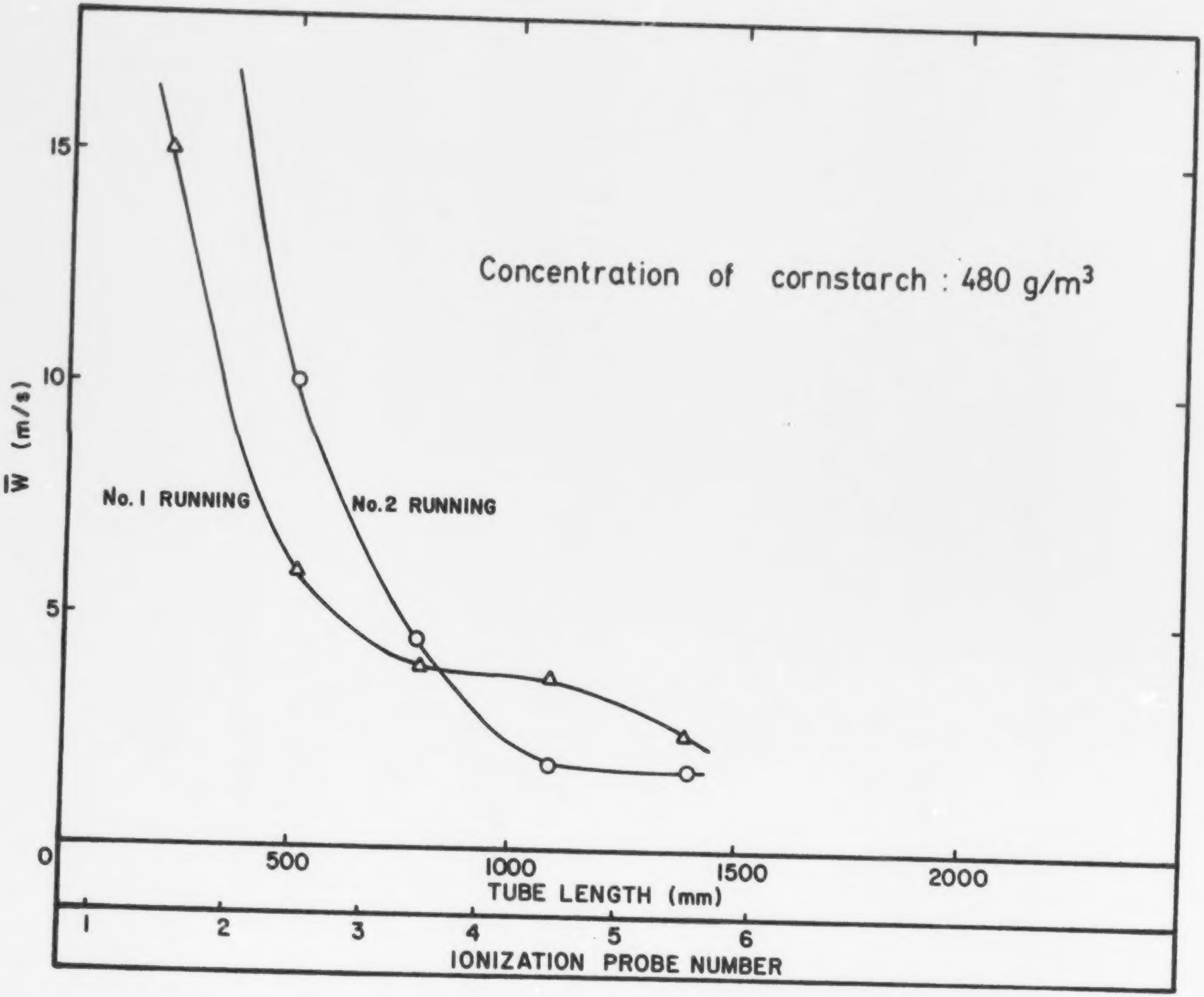

Fig. 35 : Propagation velocities as a function of location of dust flame along the tube (L/D= 9.6, D= 19 cm) in quasi-laminar case.

The Influence of Turbulence on Dust Flame Propagation

Yi Kang Pu, R. Knystautas and J.H. Lee

Department of Mechanical Engineering
McGill University
Montreal, Canada

The subject matter:
- Constant volume combustion
- Flame
- Turbulent combustion

Submitted for presentation at the 21st International Combustion Symposium
Munich, West Germany, August 3-8, 1986

ABSTRACT

The influence of turbulence on flame propagation in cornstarch dust-air mixture has been studied. The experiments were carried out in a tube 0.19 m inside diameter and 0.91 m long with two ends closed. In the present work a dispersion system has been developed with a good quality uniform dust suspension and very low level of dispersion-induced turbulence at the moment of ignition. The flame propagation velocity and pressure-time history were measured. The results of measurements of dust flames were compared with that of methane-air flames which were carried out in identical initial and turbulence conditions. The measurements show that the behavior of quasi-laminar dust flames is similar to that of the gas flames. The similarity is based on the similar processes controlling both gas and dust flames. The increase in the maximum overpressure and maximum rate of overpressure rise for dust flames by a factor of two times higher than for gas flames is explained by the increase of combustion efficiency as a result of transition from laminar near-wall combustion to turbulent more uniformly distributed combustion. It was found that the influence of turbulence on the combustion process in a closed tube is more effective in the initial stage of flame propagation along the tube.

I. Introduction

Dust combustion has become an increasingly important problem both in hazard evaluation in coal mines, powder industries, flour mills and grain elevators, as well as in the design of ventilation systems for installations handling combustible dusts. All situations of practical interest in the combustion of dust-air mixtures involve some degree of turbulence which also is an intrinsic property for dispersion, mixing and suspension. Therefore, the investigation of the influence of turbulence on dust combustion is becoming an important factor. Currently, there are two main types of combustion experiments carried out for dust-air mixtures; closed bomb experiments and stabilized open flames. A considerable amount of data has been accumulated on dust-air explosions, mainly in closed bombs of various shapes and sizes over the past few decades [1-7]. The accumulated data covers factors such as minimum ignition energy, minimum surface ignition temperature, +lean concentration limits, maximum overpressure, and the peak rate of overpressure rise (or the K_{st} factor when normalized with respect to the volume of the vessel). All the above mentioned experimental data are somewhat dependent on the apparatus and test procedures, as well as on the physical properties of the dust itself. Little information concerning the flame processes can be deduced from these closed bomb experiments. Furthermore, even less is known about the influence of turbulence on the burning rate of a dust flame [7]. In order to correlate these experimental data and achieve some meaningful assessment of the explosibility of a certain dust-air mixture, it is necessary to understand at least in a qualitative way the fundamental mechanisms of flame propagation (both laminar and turbulent). Experience with turbulent premixed gaseous flame has already shown that such understanding must be based upon a knowledge of laminar flames. It might be expected that an understanding of turbulent dust flames requires a similar foundation.

The nature of laminar dust flames has been studied in open flame experiments [8-12]. It is fairly difficult to make direct optical observations of the flame structure, since an explosive dust-air mixture is quite opaque. Experimentally, it is also very difficult to produce a uniform laminar flow of a dust mixture and to stabilize an adiabatic dust flame on a burner. In view of these difficulties, laminar dust flame structure and mechanism of laminar flame propagation have been insufficiently studied as compared to gas flame. The U.S. Bureau of Mines has developed a full-scale underground explosion testing facility (with one open end) to study how coal mine explosions are initiated and propagated [13, 14]. Although their experimental results show that the speed of the flame front is increased by turbulence significantly and satisfactory correlations can be developed between dust flame front speed and other flow parameters, it is still not possible to predict the flame front speed itself in terms of the initial conditions, because of the lack of data of the fundamental properties of dust flames and the modelling of dust flame propagation. Therefore, currently there is no satisfactory empirical relationship linking the burning rate and flame propagation to the relevant parameters of turbulence [15].

In the present study it was thought worthwhile to perform some exploratory experiments in a constant volume tube (L/D = 5) to investigate the influence of turbulence on dust flame propagation. The starting point is based upon a proposed structure and propagation mechanism of laminar dust flame by Bradley and Lee [16]. The assumption made by [16] is that laminar dust flame propagation for small particle sizes ($\simeq 15 \mu m$) and high volatile content is governed only by combustion of volatiles. For homogeneous gases, the fundamental parameters that characterize the explosibility of a mixture are well known and the physical picture of gas flame development in a constant volume tube was observed by Ellis [17, 18] and confirmed by the Bureau of Mines' experiments [3] as well as the effect of turbulence on the propagation of a gas flame is fairly well established [19, 20]. There is no doubt that comparing the experimental data of dust combustion in a constant volume tube to an identical gas combustion can help elucidate the structure and propagation mechanism of dust flame. Therefore, combustion of cornstarch-air mixture is comparable to the gas combustion if size of particles $\simeq 15\ \mu$m is used. Such a comparison is used as a means to assess in present investigation the influence of turbulence on dust flame propagation.

EXPERIMENTAL DETAILS

The apparatus used in the present study (Fig. 1) is a circular combustion chamber (190 mm in diameter and 910 mm long). The two ends of the chamber are closed by blind flange plates. There are two small tubes (each with a diameter of 14 mm and a length of 910 mm) running along the inner wall of the main combustion tube. One is the dispersion tube containing a series of small dispersion holes with diameters ranging from 1 to 2 mm; the other is the turbulence generating tube. The dispersion tube is connected upstream to a dust vessel (a small cavity of 10 cm^3), a solenoid valve and an air reservoir (230 cm^3). In this system, prior to dispersion, a measured quantity of dust is loaded into the dust vessel. The dispersion air reservoir is pressurized to 10 bar overpressure. When the solenoid valve is opened, the dust is injected from the cavity through the dispersion tube and into the combustion chamber. The dust loading air jets emerging from the dispersion holes blow the dust particles over a circular blockage bar, which is 0.95 mm in diameter and 910 mm long placed 4 mm away from the holes, uniformly throughout the whole test tube. The purpose of the bar is twofold: to prevent the particles from hitting the other side of the combustion tube by reducing their momentum and to obtain a more uniform particle distribution by deflecting the jets. The uniformity of the dust particle suspension along the test tube has been evaluated by light transmission measurements. Transmission data are obtained by a photo-multiplier with a laser beam passing through the dust-air mixture perpendicular to axis of the test tube. Results show that initially there is

20% more dust suspended in the top cross-section than in the bottom one. Experimental data also show that in both the top and bottom cross-sections, the dust particle suspension lasts at least 0.5 seconds. Therefore, a fairly uniform dust suspension is considered to be achieved for the duration of the dust combustion process which lasts about 0.5 seconds. The other 14 mm diameter tube in the combustion chamber is the turbulence tube. It contains four series of small holes along its length with diameters ranging from 0.5 to 1 mm. Four series of small holes are equally spaced on a 90° arc. The turublence tube is connected upstream to a solenoid valve and to another bigger air reservoir (1500 cm^3). In this system, the solenoid valve is opened and the pressurized air in the reservoir is released into the turbulence tube. The turbulence jets emerging from the holes cover a great percentage of the tube cross-sectional area. The intensity of the jet-induced turbulence is related to the initial pressure in the reservoir (3.5 to 10 bar) and can be determined from the mean velocities of the jets by the experimental correlations of Wygnanski and Fiedler [21]. The average velocities of the jet along the jet centre-line are determined in four positions by the experimental data of the dust particle time of arrival from the light transmission measurements. It is assumed that the dust particles have the same velocity as the air jet. The exit velocities of four line jets are derived from the measured data of average jet velocity gradient according to the profiles of the mean velocities along the jet centre-line which are given by the experimental studies of Wygnanski and Fiedler [21] and Knystautas [22]. As an example, a jet exit mean velocity of 20 m/sec, which corresponds 10 bar initial overpressure in the reservoir, decreases rapidly to 6 m/sec, 30 mm away from holes, to 2 m/sec at 60 mm, which is the center position of the test tube and decreases more slowly to 1 m/sec beyond half the tube diameter. The intensities of u', v', w' fluctutions in the jet centre-line decrease according to the same law as the mean velocity. All of these results are shown schematically in Fig. 2.

Ignition of the dust-air mixture at the centre of the bottom part of the tube is by a black powder ignitor. A dust flame starts to propagate and develops upwards along the constant volume tube. The air jet-induced turbulence can be added to the original dust combustion process after an appropriate time delay to investigate the influence of turbulence on dust flame propagation. The time delay between dispersion and ignition is controlled by means of an electronic timer and the time delay between ignition and turbulence addition is controlled by a mechanical timer. During the combustion process, the pressure-time history is measured by a PCB quartz pressure transducer. The maximum rate of overpressure rise is calculated from the slope of a tangent to the pressure-time curve through its inflection point. The flame front time of arrival is measured by ionization gauges which are located at three positions along the length of the tube.

III. RESULTS AND DISCUSSION

The study of the influence of turbulence on dust combustion appears to involve contradictory experimental requirements with respect to the dispersion system. To disperse the dust effectively for a uniform suspension of dust-air mixture at a definable and reproducible concentration, an intense flow producing turbulence in every dispersion system is required. On the other hand the investigation of the influence of turbulence on dust combustion requires a quiescent mixture at the initial conditions of dust combustion. Thus the coupling of the combustion process with dispersion-induced turbulence presents some difficulty isolating the influence of turbulence on dust combustion in the investigation. It is necessary to design a compromise dispersion system with good quality uniform dispersion of dust and as low level of dispersion-induced turbulence as possible at the moment of ignition. Such dispersion system satisfying these conditions has been systematically developed in the present study. Its influence of dispersion-induced turbulence on maximum overpressure and maximum rate of overpressure rise shown in Fig. 3. The peak overpressure approaches the maximum level in the range of ignition delay time from 50 to 100 ms (fluctuation can be attributed to nominal dust concentration variations), decreasing slowly thereafter. With ignition delay time of 250 ms, the peak pressure is at the level of 80% as compared to its maximum value. Because the data of peak pressure reflect the quantity of dust particles participating in combustion, it can be inferred that 80% of dust particles are still in suspension, and the dust particles settling can be ignored. For delay time longer than 500 ms, the maximum overpressure of dust combustion is also practically independent of dispersion-induced turublence. The dispersion-induced turbulence influences the maximum rate of overpressure rise of dust combustion in different degree depending on the ignition delay time and the concentration of the dust-air mixture. It approaches the maximum value when ignition delay time is 50 ms and decays very fast beyond this point, becoming equal to about 120% of its reference value when ignition delay time is 250 ms. The reference value corresponds to the ignition delay time of 700 ms which is determined by the gas combustion in an identical dispersion-induced turbulence condition. To meet the contradictory requirements of low dispersion-induced turublence level at an acceptable dust suspension level, the ignition delay time 250 ms has been chosen in the experiments as the baseline delay time because at this point the dust is effectively in an initial quasi-laminar suspension. Figure 4 displays the maximum pressure and K_{ST} factor, obtained at the chosen ignition delay time (i.e., 250 ms) versus the cornstarch concentrations against a background of experimental data of other researchers. The maximum overpressure which indicates the quality of the dust suspension is comparable in present work with that of the others. In contrast, the K_{ST} factor which is related to the intensities of the dispersion-induced turublence is much less at a very low level. It is evident from the expermental results presented in Fig. 4 that the developed dispersion system satisfies the requirement which is a good quality uniform dust suspension with very low level of dispersion-induced turbulence.

The flame conditions just at ignition whether for a dust or gas mixture at optimum delay time are arbitrarily designated as quasi-laminar for convenience. The experimental data for the speeds of the quasi-laminar flame for both gas (9.5% CH_4-air) mixture and cornstarch dust-air mixture (dust concentration at maximum pressure in closed vessel, $C_d \simeq 500$ g/m^3) show that the development of the flame in a closed tube with L/D = 5 is similar to that observed in the experiments of Ellis [17,18]. Three regions with different propagation velocities and different slopes in the pressure curves are distinguishable as a result of these measurements and are shown in Fig. 5. Combustion in the first stage is characterized by very high propagation velocity of the flame front and slight increase of pressure. In the second stage the slower propagation velocity is accompanied by a substantial pressure increase. In the third stage the increased propagation velocity is accompanied by a further pressure increase, very high for the gas flame and more moderate for the dust flame. The effect of jet-induced turbulence on the quasi-laminar dust flame, in these three different stages of its propagation, has been investigated. Figure 6 illustrates this influence on maximum overpressure and maximum rate of overpressure rise for both gas and dust flame propagation by adding turbulence in three different time delays indicated by η. The η factor is a ratio of the time delay of turbulence addition after ignition to the duration of the combustion process, which is a period between the time of the peak pressure arrival in the pressure-time history and the time of ignition. Three η values taken in the dust and gas flame propagation correspond to adding turbulence in three different regions previously mentioned. Two phenomena are observed in the above experiments. One is that the dust and gas flames are influenced by jet-induced turbulence to a different degree. The maximum overpressure is 1.5 times higher and the maximum rate of overpressure rise is 2-3 times higher for dust flames than for gas flames. The other is that in both gas and dust combustion the most effective influence of jet-induced turbulence on combustion is observed when turbulence is introduced in the first stages of flame propagation.

As a result of the present experiments, a physical model of quasi-laminar dust flame propagation in a constant volume tube has been suggested. The behavior of the dust flame in this model is similar to that of a gas flame. The similarity is based on the fact that the same processes, which are heat conduction and molecular diffusion, control both gas and dust flames. This similarity between gas and dust flame has been already suggested in the paper of Bradley and Lee [16]. In their physical model, valid for small particle size ($\simeq 15\ \mu$m) of fuel with high volatile content, the dust flame structure consists of rapid devolatilization process of particles in the preheat zone followed by a thin effective reaction zone where gas phase reactions occur. Slow burning of the char proceeds in the much longer "tail" of the reaction zone. This suggestion is supported by the recent works of Smoot et al [23] and by the recent measurements of quenching distance for cornstarch dust-air mixture by Jarosinski et al [24].

From the points of view of interaction of turbulence with a laminar flame in the closed tube the most interesting event in the present study is the first stage of combustion, both for gas and dust flame. The first stage provides the best conditions for the investigation of the interaction of the turbulence with the flame because they are characterized by a clear gas dynamics model of flame propagation and the small influence of pressure on the combustion process. The second and the third stages of combustion in the closed tube are influenced, according to Strehlow [25], by Taylor-Markstein instability phenomena which turbulize the flame and interfere with an additionally introduced turbulence. Therefore, it is only natural that the most effective influence of additional turbulence on combustion is in the initial stage of the flame propagation.

Relatively high growth of maximum overpressure and higher maximum rate of overpressure rise with increased jet-induced turublence for dust flame, which are observed from our experiments, can be explained by increase in combustion efficiency, which is defined as a ratio of the amount of energy released to the total amount of energy present in the fuel. It is known that in the quasi-laminar case, the flame shape looks like a paraboloid of revolution in the first stage of its propagation in the closed tube. Most of the dust-air mixture in this flame burns in the neighbourhood of the walls, where combustion is not completed. There are two reasons for incomplete combustion: the cooling effect of the wall and the divergence of streamlines and, hence of the trajectories of the particles. Therefore, some dust particles are settled out due to the effect of gravity before they get completely burned. If turbulence is introduced into the mixture early enough, the structure of the flame will change and its shape will become wrinkled and flatter. Therefore, in the turbulent flame most of the dust particles burn far from the wall and more dust can participate in the combustion process. The interaction of turbulence with the flame during the early stage of its propagation in a constant volume tube should be a subject for further research.

CONCLUSIONS

A dispersion system was developed which yields a medium of uniform dust suspension and very low level of dispersion-induced turbulence at ignition. This provides relatively quiescent initial conditions of flame propagation to study the influence of turbulence on dust combustion in constant volume tube. A physical three-stage model of quasi-laminar dust flame propagation in a constant volume tube has been proposed. The measurements show that the behavior of the dust flame in this model is similar to that of a gas flame. The similarity is based on the same processes controlling both gas and dust flames: heat conduction and molecular diffusion.

The influence of turbulence on the combustion process is most effective in the initial first stage of combustion. Increase in the maximum overpressure and the maximum rate of overpressure rise for dust flames is higher than for gas flames and can be explained by an increase of combustion efficiency as a result of transition from laminar near-wall combustion to turbulent more uniformly distributed combustion.

It was found that the first stage of combustion in the closed tube is most suitable to investigate the influence of turbulence on dust flame by virtue of clear gas dynamic model of its propagation. The advantage of this kind of investigation lies in its simplicity: the overpressure and the maximum rate of overpressure rise determine sufficiently the efficiency of the combustion process.

ACKNOWLEDGEMENTS

The work was supported by the Natural Sciences and Engineering Reserch Council of Canada under NSERC Grants A7091 and A3347 and by Energy, Mines and Resources of Canada under Contract OST-00119.

REFERENCES

1. Hartmann, I., Nagy, J., Brow, H.R., U.S. Bureau of Mines, Rept. of Inv. No. 3722, 1943.

2. Hartmann, I., Cooper, A.R., Jacobson, M., U.S. Bureau of Mines, Rept. of Inv. No. 4725, 1951.

3. Nagy, J., Seiler, E.C., Conn, J.W., Verakis, H.C., U.S. Bureau of Mines, Rept. of Inv. No. 7507, 1971.

4. Bartknecht, W., "Explosion-course-prevention-protection", Translated by Bung, H. and Almond, T., Springer-Verlag, New York, 1980.

5. Bartknecht, W., "Brenngas-Und Stousbexplosionen", Forschung-Bericht F45, Bundesinst. f. Arbeitschutz. Kobleng (1971).

6. Bartknecht, W., 18th Annual Loss Prevention Symp., AIChE, Philadelphia, Aug. 19-22.

7. Kauffman, C.W., Srinath, S.R., Tezok, F.I. etc., 20th Symposium (International) on Combustion, 1984.

8. Faraday, M., Lyell, C., Phil. May 26, 16 (1845).

9. Smoot, L.D., Horton, M.D., Prog. Energy Combust. Sci., Vol. 3, pp. 235-258, 1977.

10. Howard, J.B., Essenhigh, R.H., Ind. Eng. Chem. Proc. Des. and Devel. 6, 76 (1967).

11. Howard, J.B., Essenhigh, R.H., 11th Symposium (International) on Combustion, pp. 399-408, 1967.

12. Howard, J.B., Essenhigh, R.H., Combustion and Flame 9, 337 (1965), 10, 92 (1966).

13. Richmond, J.K., Liebman, I., "A Physical description of coal mine explosions", Bureau of Mines, U.S. Department of the Interior.

14. Richmond, J.K., Liebman, I., "A physical description of coal mine explosions Part II", Bureau of Mines, U.S. Department of the Interior.

15. Clark, D.P., Smoot, L.D., Combustion and Flame, 62: 255-269, 1985.

16. Bradley, D., Lee, J.H.S., "On the mechanism of propagation of dust flame", presented at the First International Colloquium on Explosibility of Industrial Dusts, Baranow near Sandomierz, 8-10 November, 1984.

17. Ellis, O.C. des. Fuel. Vo. 7., Nos. 5-12, 1928 (in 8 parts).

18. Ellis, O.C. des. Fuel. Vo. 7, No. 4, 1928, pp. 169-178.

19. Chomiak, J., Prog. Energy Combust. Sci., 5: 207-221, 1979.

20. Libby, P.T., Williams, F.A., Turbulent Reacting Flows, Springer-Verlag, 1980.

21. Wygnanski, I., Fiedler, H., J. Fluid Mech. (1969), Vol. 38, part 3, pp. 577-612.

22. Knystautas, R., The Aeronautical Quarterly, Vol. XV, Feb. 1964.

23. Smoot, L.D., Hedmen, P.O. and Smith, P.J., Prog. Energy Combust. Sci., 10: 359-441, 1984.

24. Jarosinski, J., Lee, J.H.S., Knystautas, R. and Crowley, J.D., Submitted for presentation at the 21st International Combustion Symposium.

25. Strehlow, R.A., Combustion Fundamentals, McGraw-Hill Book Company, 1984, p. 426.

FIGURE CAPTIONS

Fig. 1	Side view of the apparatus.
Fig. 2	The distribution of the mean velocities of the jet (U_m) and the intensities of the jet-induced turbulence of u', v', w' fluctuations in the jet centre-line (determined by [21], [22]).
Fig. 3	Maximum overpressure (ΔP_{max}) and maximum rate of overpressure rise ($[dp/dt]_{max}$) versus ignition delay time (t_d).
Fig. 4	The comparison between the present work and the work of the others of the maximum overpressure and K_{ST} factor versus cornstarch concentrations.
Fig. 5	The measurements of flame speeds and pressure-history in both quasi-laminar gas and dust flames propagation in the closed tube.
Fig. 6	The maximum overpressure (ΔP_{max}) and the maximum rate of overpressure rise ($[dp/dt]_{max}$) both in gas and dust flame propagation in the closed tube versus intensities of jet-induced turbulence (indicated by exit velocity of jet along its centre-line in this Figure).

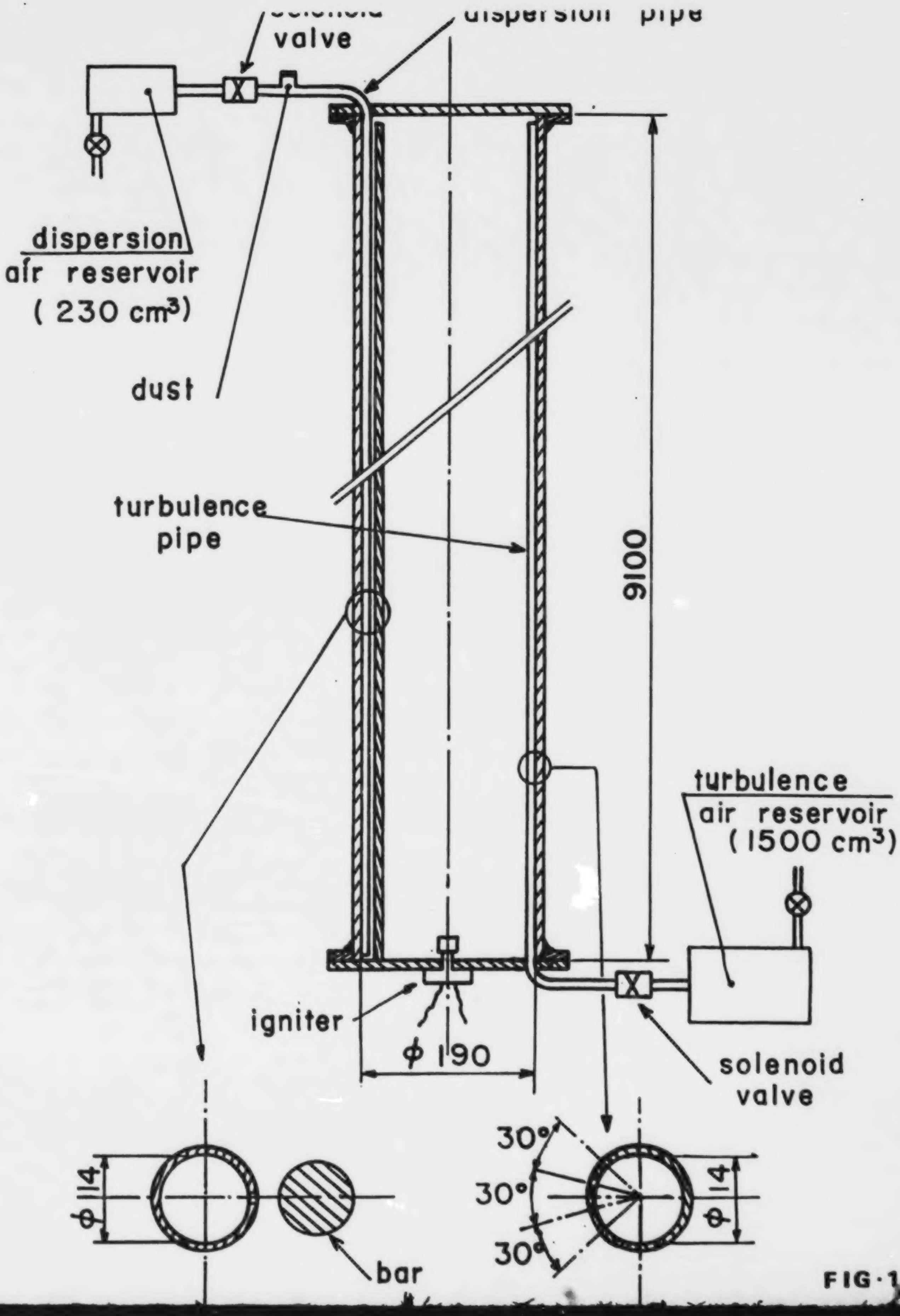
solenoid
valve
dispersion pipe
dispersion
air reservoir
(230 cm³)
dust
turbulence
pipe
9100
turbulence
air reservoir
(1500 cm³)
igniter
φ 190
solenoid
valve
φ 114
bar
30°
30°
30°
φ 14

FIG·1

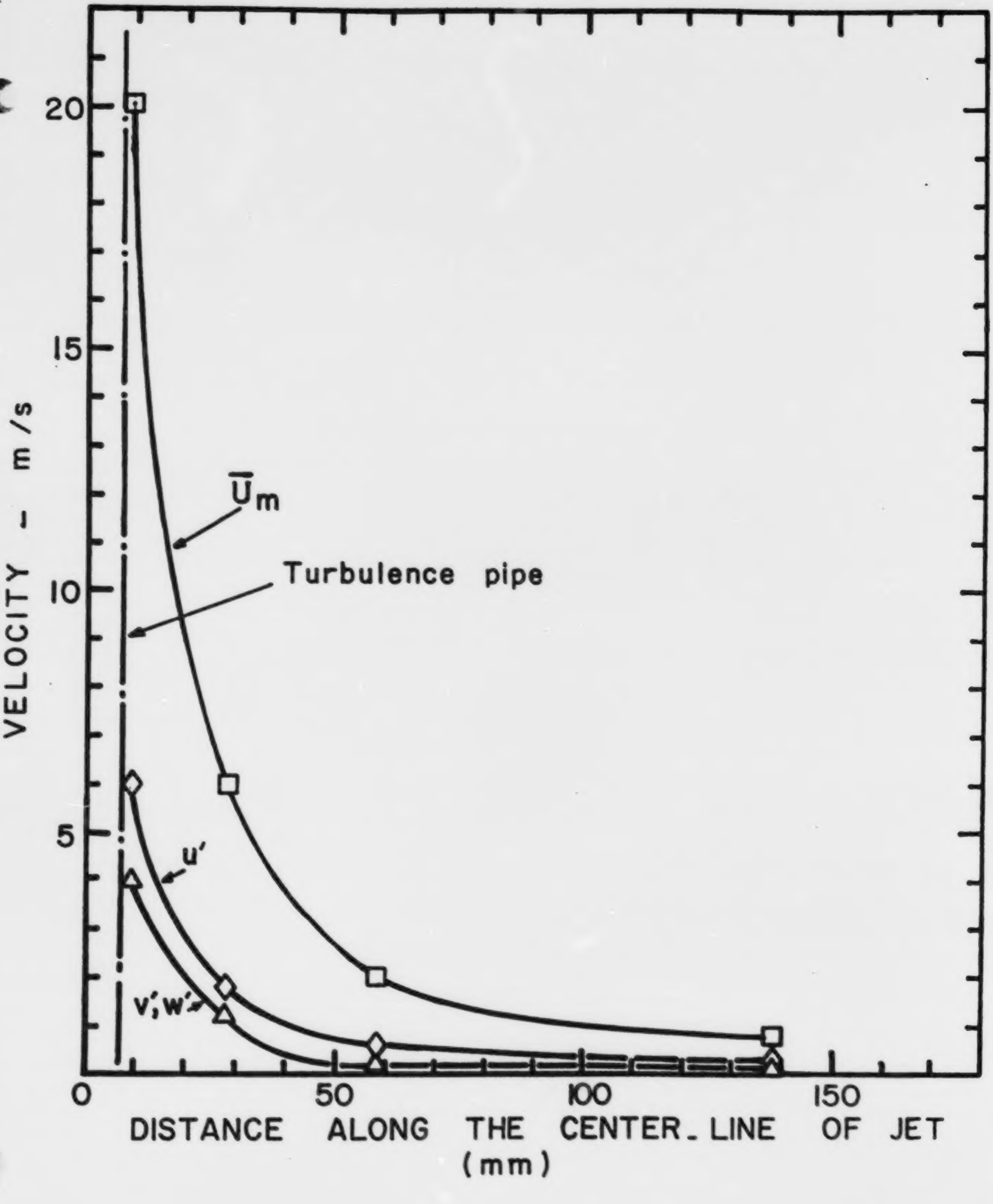
VELOCITY - m/s
20
15
10
5
0
50
100
150
DISTANCE ALONG THE CENTER-LINE OF JET (mm)
$\overline{U}_m$
Turbulence pipe
u'
v', w'

FIG·2

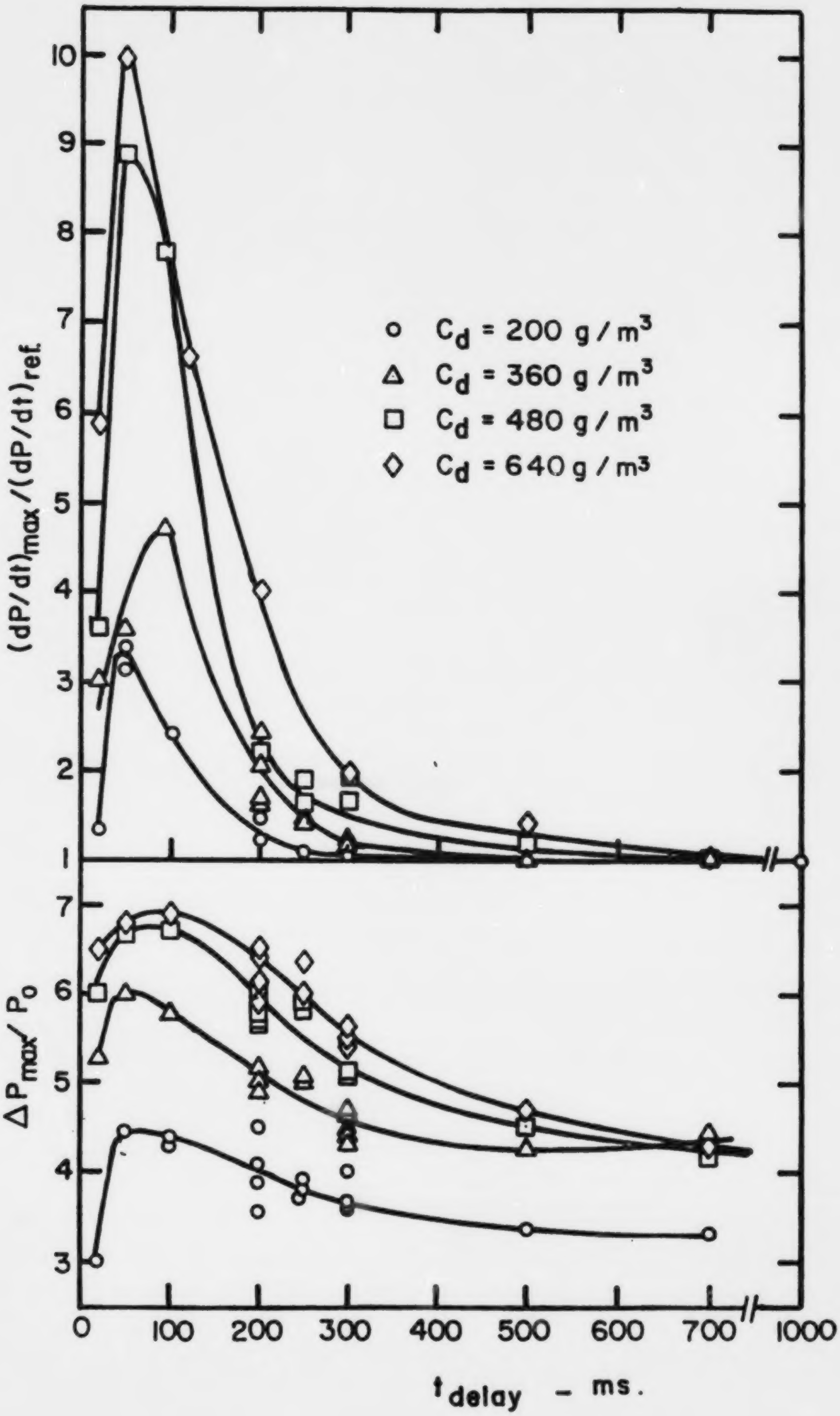

$(dP/dt)_{max}/(dP/dt)_{ref.}$
10
9
8
7
6
5
4
3
2
1
○ $C_d = 200\ g/m^3$
△ $C_d = 360\ g/m^3$
□ $C_d = 480\ g/m^3$
◇ $C_d = 640\ g/m^3$
$\Delta P_{max}/P_o$
7
6
5
4
3
0
100
200
300
400
500
600
700
1000
t_{delay} – ms.

FIG·3

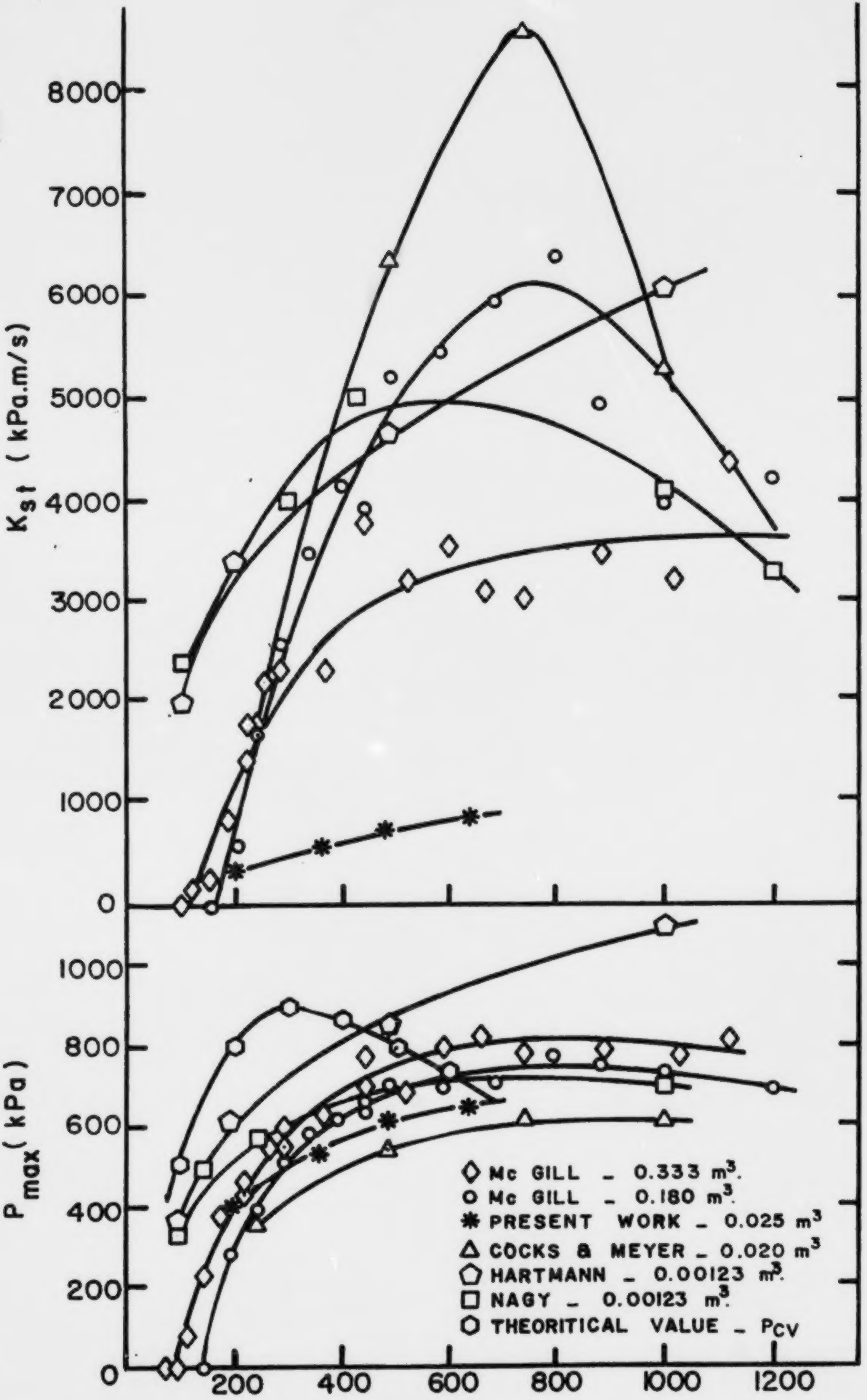

K$_{st}$ (kPa.m/s)
8000
7000
6000
5000
4000
3000
2000
1000
0
P$_{max}$ (kPa)
1000
800
600
400
200
0
200
400
600
800
1000
1200
CORNSTARCH CONCENTRATION
(g / m^3)
◇ Mc GILL _ 0.333 m^3.
○ Mc GILL _ 0.180 m^3.
✱ PRESENT WORK _ 0.025 m^3
△ COCKS & MEYER _ 0.020 m^3
⬠ HARTMANN _ 0.00123 m^3.
□ NAGY _ 0.00123 m^3.
⬡ THEORITICAL VALUE _ P$_{CV}$

FIG·4

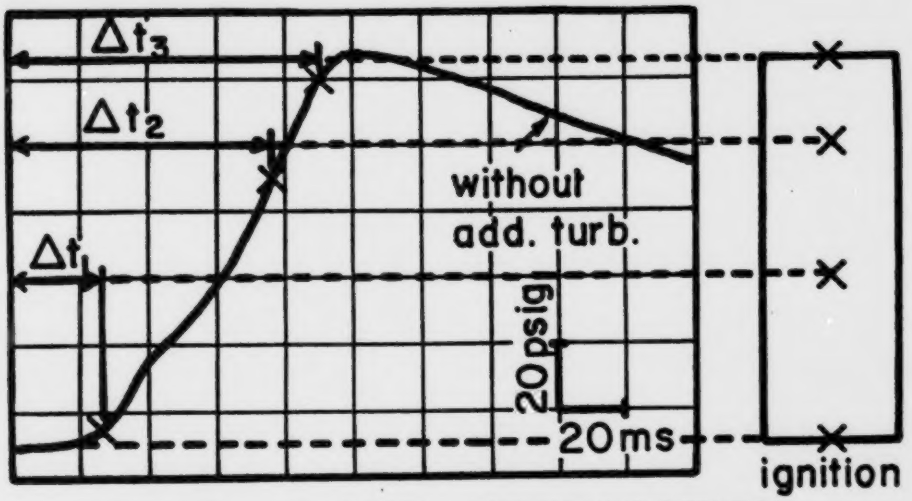

GAS FLAME PROPAGATION

9.5 % CH_4 - AIR

ELLIS' RESU

L = 91 cm	19.5 cm
ϕ = 19 cm	5 cm
L/ϕ = 4.8	3.9

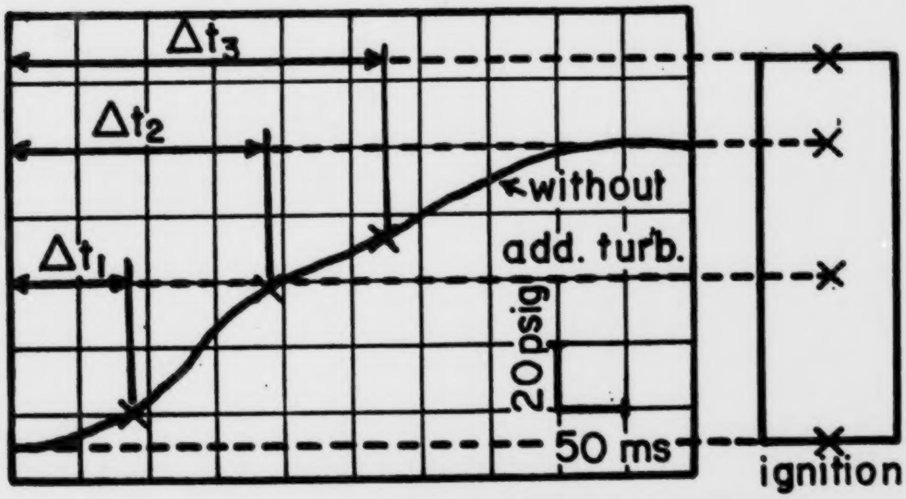

DUST FLAME PROPAGATION

CORNSTARCH - AIR , $C_d = 480 g/m^3$

FIG·5

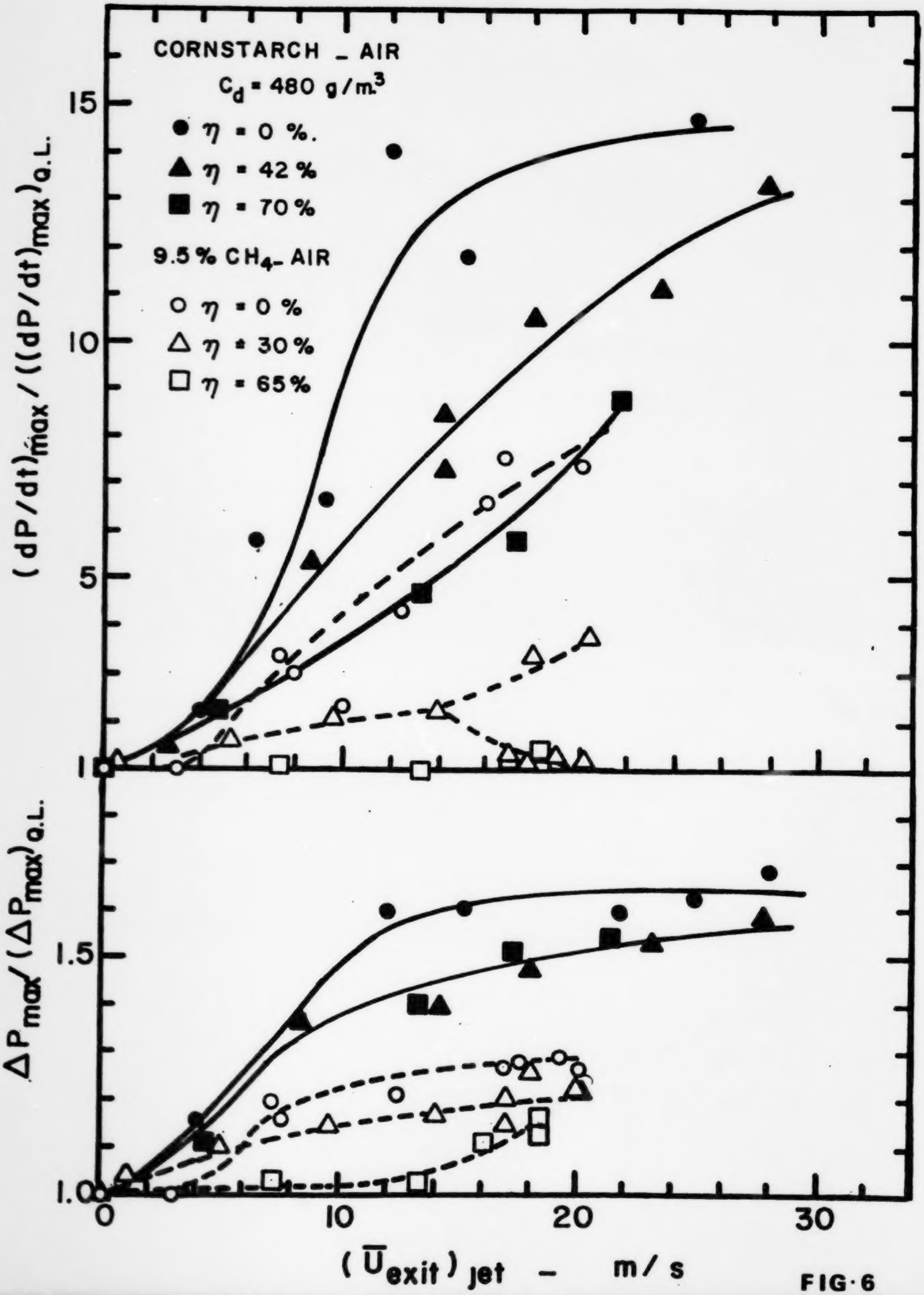
CORNSTARCH _ AIR
C_d = 480 g/m^3
● η = 0 %.
▲ η = 42 %
■ η = 70 %
9.5 % CH_4- AIR
○ η = 0 %
△ η = 30 %
□ η = 65 %
$(dP/dt)_{max} / ((dP/dt)_{max})_{a.L.}$
15
10
5
1
$\Delta P_{max} / (\Delta P_{max})_{a.L.}$
1.5
1.0
0
10
20
30
$(\overline{U}_{exit})_{jet}$ – m/s

FIG·6

THE INFLUENCE OF TURBULENCE ON DUST AND GAS EXPLOSIONS IN CLOSED VESSELS

Submitted by

J.F. Bond
J.H. Lee
R. Knystautas

McGill University
Montreal, Quebec

March 31, 1986

ABSTRACT

Experiments have been carried out to assess the influence of turbulence on the burning rate of cornstarch-air explosions in closed vessels. Different means of varying the turbulence were used, so as to investigate a substantial range of turbulence intensity and a variety of turbulent flow structures.

Since gas-air deflagrations are currently better understood than dust-air deflagrations, all experiments done with the cornstarch-air mixture were replicated with a methane-air mixture, in order to compare the influence of turbulence in explosions in the two media.

The most important finding of the study was that the ratio of the burning rate of the gas-air mixture to that of the dust-air mixture, observed under identical conditions of turbulence, was a constant, independent of the intensity of the turbulence and of the details of the structure of the turbulent flow. This suggests that this ratio is a function of the physico-chemical properties of the mixtures themselves.

RESUME

La présente étude a eu pour objet d'évaluer l'influence de la turbulence sur le taux de combustion d'une explosion se propageant dans un mélange amidon-air contenu dans une enceinte fermée. Dans ce but, nous avons utilisé diverses méthodes de génération de la turbulence afin d'en modifier la structure et de faire varier son intensité.

Les déflagrations dans les mélanges biphasiques étant moins bien connues que celles dans les mélanges gazeux, toutes les expériences réalisées avec le mélange amidon-air ont été reprises avec un mélange méthane-air, afin de comparer l'influence de la turbulence sur des explosions se produisant dans ces deux milieux. Cette étude comparative nous a permis de montrer que le rapport du taux de combustion du mélange gazeux sur celui du mélange biphasique mesurés dans les mêmes conditions expérimentales est constant. Il semble donc que ce rapport ne dépende ni de l'intensité de la turbulence, ni de sa structure, mais uniquement des propriétés physico-chimiques des mélanges eux-mêmes.

ACKNOWLEDGEMENTS

We would like to acknowledge the invaluable contributions of Mr. Marc Champagne, in building the electronic instrumentation, and of Messrs. Moris Fresko and Aris Makris, in performing some of the experimental work. The stimulating discussions with Mrs. Yi Kang Pu, Mr. Neil Craft, Mr. Theofanous Panayiotis, Mr. Michael Gaug and Dr. Olivier Peraldi are also gratefully acknowledged. This work was supported under the sponsorship of Energy Mines and Resources of Canada under contracts OSV82-00039 and OST85-00119 and under NSERC grants A-3347 and A-7091.

TABLE OF CONTENTS

PAGE

i- Nomenclature 6

I- Introduction 8
a) Introductory remarks 8
b) Outline of the report 11

II- Relevant physical mechanisms and review of previous research 13
a) Turbulence and turbulent combustion 14
b) Review of constant volume explosion theory 19
c) Previous research into turbulent dust and gas explosions 22

III- Experimental considerations and preliminary experiments 26
a) Apparatus 26
b) Properties of the combustible mixtures 29
c) Preliminary experiments on the effects of dust concentration 33

IV- Dispersion-induced turbulence 36
a) Influence of ignition delay 36
b) Influence of dispersion pressure 45

V- Jet-induced turbulence 53
a) Dispersion-induced turbulence and jet-induced turbulence 54
b) Influence of ring jet flow rate 56
c) Influence of pipe jet flow rate 57

VI- Summary and conclusion 59
a) Synthesis of the experimental results 59
b) General conclusions 62
c) Recommendations for future work 64

ii- References 66

iii- List of figures 70

iv- Figures 72

i- NOMENCLATURE

A	Area
D	Diameter
E	Energy
Ge	Turbulence decay number
K	Normalized burning rate
K'	Ratio of normalized burning rate to a reference value
M	Mass
P	Pressure
R	Universal gas constant
Re	Reynolds number
S	Burning velocity
T	Temperature
U	Internal energy
V	Volume
c	Specific heat
g	Acceleration of gravity
k	Thermal conductivity
l	Integral length scale of turbulence
m	Mass
r	Radius
u	Velocity or speed
u'	Turbulent r.m.s. velocity
γ	Specific heat ratio of gaseous mixture
$\bar{\gamma}$	Specific heat ratio of dust-air mixture
Δ	Difference
δ	Flame thickness
ε	Turbulence kinetic energy decay rate
ε'	Eddy diffusivity
η	Kolmogoroff microscale of turbulence
θ	Half-energy time of turbulence decay
κ	Ratio of dust mass to gas mass per unit volume of mixture
λ	Taylor microscale of turbulence
μ	Dynamic viscosity
ν	Kinematic viscosity
ρ	Density
τ	Characteristic time

Subscripts

a	Activation
b	Dispersion bottle
c	Combustion chamber
d	Developed
de	Decay
dev	Devolatilization
e	Enclosed
f	Final
g	Gas
i	Initial
l	Laminar
o	Reference
p	Constant pressure
set	Settling
st	Dust (staub)

t	Turbulent
u	Unburned
v	Constant volume
vr	Velocity rise
tr	Temperature rise

I- INTRODUCTION

a) Introductory remarks

All situations of practical interest in the combustion of dust-air mixtures involve a certain degree of turbulence. In pulverized coal burners, the coal-air mixture enters the burner as a turbulent jet, and additional means of inducing turbulence are often used to enhance the burning rate[1]. In a typical grain silo explosion, the initial ignition of a small dust-air pocket creates a flow field which raises more dust into suspension, and subsequent flame propagation takes place in this turbulent mixture[2]. Hence turbulence is an intrinsic feature of a dust explosion, and the study of the influence of turbulence on the burning rate of a dust-air mixture in an important area of dust combustion research.

An adequate understanding of the influence of turbulence on the burning rate of dust-air mixtures is especially important to those who are concerned with safety in coal mines, grain silos, and industrial process equipment where dust is handled. The proper design of explosion relief vents for grain silos, for example, requires an estimate of the maximum rate of pressure rise associated with the dust explosion. This type of problem has received considerable attention since the series of grain elevator explosions in the United States, in December 1977[3].

Renewed interest in the design of internal combustion engines fueled by coal dust is another subject for which a knowledge of the role played by turbulence could be of high importance[4]. A fair amount of research has been done on these engines in recent years and it appears at present that the burning rates achieved are too low to permit the construction of an engine with a r.p.m. sufficiently high for practical applications. Hence an understanding of the means by which increases in burning rates may be achieved is critical to further progress in this field.

In attacking the complex problem of dust explosion, it is wise to try to draw upon our knowledge of gas and vapor phase explosion. For homogeneous gases and vapors, the fundamental parameters that characterize the explosibility of a mixture (e.g. minimum ignition energy, laminar burning velocity, flammability limits, etc.) are well known and their value can be measured directly by experiments. The effects of turbulence on the propagation of a gas-air flame are also fairly well established, at least on a qualitative basis[5], and there exists enough reliable experimental data to permit engineering estimates of the burning rate under different flow conditions. By contrast, no reliable fundamental parameters are as yet known for explosive dust-air mixtures. Hence the study of gas explosion in conjunction with dust explosion under the same conditions can help elucidate the structure and propagation mechanisms of dust-air flames. In particular, it is worthwhile to compare the effect of turbulence on dust-air explosions to that on gas-air explosions occurring in the same apparatus, with identical flow fields. Such a comparison is the program of this study.

It is generally known that turbulence plays a strong role in the development of a dust-air explosion. As yet, however, the few experimental studies that have been performed have not yielded empirical relationships linking the burning rate to the relevant parameters of the turbulence. One reason for this is that it is difficult to define turbulence in the context of a closed vessel explosion without mean flow, and that measurement of fluctuating velocities in a dust-air suspension poses important experimental problems. Furthermore, even if one measures the flow velocity at a given point in the combustion chamber prior to ignition, compression of the unburned mixture and irregular fluid motions caused by the flame itself start to change this velocity as soon as the flame ball begins to propagate towards the walls of the vessel - it is therefore doubtful that such a measurement is of any value.

For these reasons, it was thought worthwhile to perform some rather crude experiments to investigate the influence of "turbulence" on the maximum burning rate of explosions inside closed vessels. "Turbulence", in the context of this study, will be taken to refer to any fluid motion in the combustible mixture, and the intensity of the turbulence will be characterized by the value of a relevant parameter of the device used to generate the fluid motions.

The experiments whose results are reported in this study were carried out in two vessels of similar dimensions: a 333 liter sphere and a 180 liter vertical cylinder with a height to diameter ratio of two. Cornstarch, an organic polymer with 100% volatile content, was used as fuel in all the dust experiments; a 7.5% methane-air mixture, whose energetics are similar to those of the starch-air mixture, was used in all the gas experiments. The experiments focussed on assessing how the initial flow field of the explosive mixture affected the maximum pressure developed, which is a measure of the extent of the reaction, and the maximum rate of pressure rise, which is a measure of the rate of the reaction.

b) Outline of the study.

The study begins by a discussion of the physical mechanisms that are thought to be relevant to the propagation of turbulent explosion flames and a review of the previous work that has been done in the area of turbulent dust and gas explosions (chapter 2). Such a discussion provides the necessary framework for the proper interpretation of all experimental results.

Chapter 3 describes the details of the apparatus and of the experimental procedures. The results of a preliminary series of experiments, in which the variation of maximum pressure (P_{max}) and maximum rate of pressure rise $(dP/dt)_{max}$ with cornstarch concentration was measured, are also presented in this chapter and are found to be in good agreement with those reported by other workers. This serves to establish some confidence in the quality of the apparatus and of the experimental method.

In chapter 4, the results of experiments measuring the effect of dispersion-induced turbulence are presented. Dispersion of the dust was achieved by an air blast from a small bottle charged to high pressure, directed at a dust bowl at the center of the vessel. Hence some turbulence is associated with the dispersion process itself and the features of this turbulence can be varied by adjusting either the initial pressure of the dispersion bottle or the delay between dispersion of the dust and ignition of the mixture. In this chapter it is seen that the burning rate of dust and gas respond to dispersion pressure variations in a similar manner, but that for a given dispersion pressure, the burning rate of a dust-air mixture decreases faster with ignition delay than does that of a gas-air mixture. Some possible explanations to this discrepancy are introduced.

Chapter 5 describes the results of experiments measuring the effect of jet-induced turbulence on dust and gas explosions in the 333 liter sphere. Additionnal turbulence of controllable intensity was introduced in the sphere by a series of air jets along a circular ring or along a vertical tube. In this case, the burning rate increases observed with the dust-air mixture are nearly equal to those obtained with the gas-air mixture.

The results of the study suggest that the ratio of the turbulent burning rates of mixtures of dust-air and gas-air observed under identical conditions of turbulence is not sensitive to differences in the detailed structure of the turbulence induced by the various devices used to generate it, but that it rather depends on the physico-chemical properties of the mixtures themselves. This idea is elaborated on in the concluding chapter (chapter 6), where some suggestions about useful future work on this subject are also made.

II- RELEVANT PHYSICAL MECHANISMS AND REVIEW OF PREVIOUS RESEARCH

To put the experimental results obtained in this study in the proper perspective, it is necessary to first establish a framework of the physical mechanisms which are thought to influence the propagation of a turbulent flame. This is the primary purpose of this chapter.

Some comments on the nature of homogeneous turbulence will first be introduced. A brief discussion of the mechanisms of flame folding and turbulent eddy transport will follow. This discussion will allow us to determine the length, time and velocity scales that are involved in the consideration of the burning rate. It will then be possible to compare, in a qualitative manner, the burning rate increases expected to follow from a given turbulence in gas-air flames and dust-air flames.

The Bradley-Mitcheson[6] model of explosion development in a spherical vessel, relating the experimentally observable values of pressure, rate of pressure rise and burnout time to the fundamental burning velocity of the mixture and the radius of the vessel, will be introduced and its validity will be assessed in the context of our experimental conditions. It will be seen that while the turbulent flame structure observed in our experiments is more complex than that assumed in the Bradley-Mitcheson model, the model is still of some use in converting tha apparatus-dependent value of maximum rate of pressure rise $(dP/dt)_{max}$ to the standard quantity of turbulent burning velocity (S_t), which can be compared to that of other researchers.

Finally, a brief review of the existing experimental work on turbulent dust and gas explosions will be made.

a) Turbulence and turbulent combustion

Turbulence, a random-like, disorganized flow pattern with a complex underlying structure, is usually studied in contexts where a mean flow can be identified, such as in jets, wakes or boundary layers. In these situations, it is natural to consider the flow velocity u to be made up of a time-averaged value $\bar{u}$, representing the mean flow at that point, plus a fluctuating quantity u', representing "turbulence". Because the equations governing the behavior of these fluctuations are outnumbered by the flow variables (closure problem), a complete mathematical description of turbulent fluid flow appears beyond reach. Hence to represent the phenomenon of turbulence for practical applications, a simplified physical model must be introduced.

A particularly fruitful line of thought, in the elaboration of such a model, is the consideration of the kinetic energy associated with the turbulent fluctuations. Consider, for example, the useful idealization of homogeneous, isotropic turbulence. On the macroscopically observable scale, this turbulence appears to consist in a collection of "eddies" or swirls, with characteristic length l and characteristic velocity u', which decay , or disappear, in time of the order of l/u' [7] . For steadiness, the rate of supply of energy from the mean flow to the fluctuating motions must equal the rate of decay of the energy associated with the large eddies. The order of magnitude of this rate is simply the kinetic energy per unit mass of eddy (u'^2) divided by the eddy lifetime (l/u'):

$$(1) \qquad \varepsilon = \frac{u'^2 u'}{l} = \frac{u'^3}{l}$$

The energy that "disappears" with the decay of the large eddies must either be recovered as kinetic energy of smaller scale motions, or be dissipated as thermal energy by viscous shear. The rate of energy dissipation by viscous shear that occurs on the length scale of the macroscopic eddies is simply estimated as the product of the viscous shear stress on a unit volume of fluid ($\frac{\mu u'}{l}$) times the strain rate (u'/l) divided by the mass of the volume (ρ):

$$(2) \qquad \frac{\mu u'}{l}\,\frac{u'}{l}\,\frac{1}{\rho} = \frac{\mu u'^2}{\rho l^2}$$

The ratio of the rate of energy supply to that of viscous dissipation occurring at the macroscale level is, therefore,

$$(3) \qquad \left[\frac{u'}{l}\right]^3 \frac{\rho l^2}{\mu u'^2} = \frac{u' l}{\nu} \equiv Re$$

Since in turbulent flow, Re is a very large number (typically, $Re > 10^3$), no significant dissipation takes place on the macroscopic scale: the energy is transfered to smaller scale motions through a cascading process that ends when the length scale of these motions is sufficiently small for viscous dissipation to be effective in converting organized motion into random, thermal motion. It follows from the above discussion that the length and velocity scale of the dissipative regions must be related to their characteristic dissipation rate by

(4) $\varepsilon_\eta = u_\eta{}^3/\eta = \nu(u_\eta/\eta)^2$ or (5) $\eta = (\nu^3/\varepsilon_\eta)^{\frac{1}{4}}$, (6) $u_\eta = (\nu\varepsilon_\eta)^{\frac{1}{4}}$

where η is called the Kolmogoroff scale.

On the basis of these arguments, and taking into account the experimentally observed fact, that viscous dissipation in turbulence is intermittent, i.e. occurs only in highly localized regions scattered throughout the flow, Tennekes[8] has proposed the following simplified model of turbulence. Turbulence consists in macroscopic swirls with a velocity of the order of the turbulent r.m.s. velocity and length scale of the order of the integral length scale, on which are superimposed dissipative vortex tubes with a diameter of the order of the Kolmogoroff microscale η and a spacing of the order of the Taylor microscale λ, i.e. a scale which relates the rate of turbulent kinetic energy dissipation per unit mass to the turbulent r.m.s. velocity. The model is depicted in figure 1, where we have also represented other length scales that are important in turbulent dust flame propagation along with the order of magnitude of these length scales as they occur typically in explosions of the type considered in this study.

The Tennekes model has been widely accepted in recent efforts to observe and model turbulent flame propagation, for example by Tabaczynski et al[9-11], Ohta[12], and Chomiak[13]. In the context of the Tennekes model, we now discuss the two physical mechanisms that are deemed responsible, in the current theories of turbulent flame propagation, for the burning rate increase due to turbulence: flame wrinkling and turbulent eddy transport.

Irregular wrinkling of the flame front because of velocity fluctuations in the flow field directly ahead of the flame causes an increase in the total burning area, and hence in the burning rate. Insofar as the laminar burning velocity of the mixture is not affected by the wrinkling process, the ratio of turbulent burning velocity to laminar burning velocity in wrinkled laminar flame propagation is simply given by

$$\frac{S_t}{S_l} = \frac{A_d}{A_e} \tag{7}$$

where A_d and A_e refer to the developed and enclosed flame areas, respectively. It stands to reason that the characteristic spacing of the flame wrinkles should be related to the integral length scale, and that the magnitude of the wrinkles should depend on the turbulent r.m.s. velocity, u'. Hence wrinkled laminar flame theories yield predictions of turbulent burning velocity in terms of the macroscopic features of the turbulence: $S_t = S_t\ (S_l, u', l)$. Velocity fluctuations on the microscopic scale, on the other hand, play an important role in the energy and mass transport processes inside the flame itself. If these fluctuations are significant, then the mechanism determining the rate of propagation of the flame front normal to itself is no longer molecular diffusion, but rather turbulent eddy transport. Damkohler[14] was the first to propose a theory of turbulent flame propagation based on turbulent eddy transport. Since thermal flame theory shows that laminar burning velocity is proportional to the square root of the diffusivity of the medium, Damkohler concluded that

$$S_t/S_l = (\varepsilon'/\nu)^{\frac{1}{2}} \tag{8}$$

where ε' is the eddy diffusivity of the turbulent flow field.

Recent models of turbulent flame propagation, such as the two-eddy theory of Abdel-Gayed and Bradley[15], have recognized that both of the abovementionned mechanisms play an important role in enhancing the burning rate. However, it is easy to see that the relative importance of the two mechanisms will depend critically on the relationship between the relevant chemical scales of the mixture on the one hand, and the fluid mechanical scales of the turbulence, on the other hand[16].

If the laminar flame thickness δ is smaller than the scale of the smallest turbulent fluctuations η, then turbulent eddy transport inside the flame is impossible and flame wrinkling alone is responsible for turbulent burning rate increase. If, on the other hand, the flame thickness spans many Kolmogoroff eddies, while being less than the integral scale, the two processes of turbulent burning rate increase will be important. Finally, if the flame is as thick as the characteristic dimension of the macroscopic turbulence, then wrinkling by the large eddies can only have a minimal impact on total burning rate, and only turbulent eddy transport can play a significant role. Hence, to predict the influence of turbulence on dust and gas explosions under the same experimental conditions, it is necessary to have some idea of their laminar flame thickness. The thickness of laminar gas-air flames has been the subject of extensive studies[17] and it is agreed that this thickness, measured as the depth of the temperature profile, varies in orders of magnitude between 10^{-4} and 10^{-3} m. By contrast, very little research has been done with laminar dust-air flames, partly owing to the difficulties in achieving a stable, laminar dust-air suspension for burner studies. Smoot[18] reports laminar coal-dust-air flames with a thickness of 10^{-2} m, while measurements of quenching distance performed by Mason and Wilson[19] indicate a thickness of approximately 3×10^{-3} m for a flame of lycopodium spores, a vegetable dust whose structure is probably similar to that of cornstarch. Hence a cornstarch flame is probably not a lot thicker than a methane-air flame, and this may imply that turbulence will have a similar effect on cornstarch-air and methane-air explosions. However, it must be stressed that this argument is highly speculative, since no study of the laminar flame structure of cornstarch-air mixtures has ever been done.

b) Review of constant volume explosion theory

In a closed vessel explosion, a centrally ignited flame propagates outward towards the walls of the vessel and combustion of the mixture results in final overpressure ratios typically of the order of 6 to 10.

Pressure measurements of dust explosion experiments performed in closed vessels allow us to obtain an estimate of the extent of the burning (from the maximum pressure developed, P_{max}) and of the rate of combustion (from the maximum rate of pressure rise, dP/dt_{max}). Models of explosive combustion in a closed vessel show that the burning velocity S, the pressure P and the rate of pressure rise dP/dt are related to each other in a simple manner. It is of interest to use the results of pressure measurements to obtain the burning velocity, because this quantity can serve as a basis for comparing our data with those obtained by other researchers in a variety of experimental set-ups. Bradley and Mitcheson[6] have recently reviewed the problem of spherical vessel explosion and concluded that a very good approximate, analytical solution to the pressure development can be derived with the help of a few simplifying assumptions. The most important assumptions are the following:

1- Regular, spherical flame propagation without heat loss.

2- The burned and unburned mixtures behave as perfect gases.

3- The unburned mixture is being compressed isentropically by the propagating flame.

4- The pressure rise is directly proportional to the mass fraction burned.

The burning velocity formula obtained from these assumptions is

$$(9) \qquad S = \frac{\frac{dP}{dt}}{\frac{3}{r}\left[\frac{P}{P_i}\right]^{1/\gamma_u} (P_f - P_i) \left[1 - \left[\frac{P_i}{P}\right]^{1/\gamma_u} \left(\frac{P_f - P}{P_f - P_i}\right)\right]^{2/3}}$$

where P = Pressure

P_i = Initial pressure

P_f = Final explosion pressure

S = Burning velocity

r = Vessel radius

γ_u = Specific heat ratio of the unburned mixture.

From the above expression, the maximum rate of pressure rise is obtained when

$$(10) \qquad P = P_f$$

i.e. at the very end of the flame travel. This stands to reason, because the last shell of fuel-air mixture of thickness Δr that burns, has the biggest volume and the highest density of all such shells. Furthermore, as P approaches P_f, the rate of pressure rise is related to the scale of the vessel by

$$\frac{dP}{dt} = \left(\frac{dP}{dt}\right)_{max} = \frac{3}{r} (P_f - P_i) S \tag{11}$$

Hence the maximum rate of pressure rise in two vessels with radiuses r_1 and r_2, and with identical burning velocity and final and initial pressure, should be related by

$$\left(\frac{dP}{dt}\right)_{max\ 1} r_1 = \left(\frac{dP}{dt}\right)_{max\ 2} r_2 = \text{constant} \tag{12}$$

Bartknecht[20] has found experimentally a scaling law applicable to the burning of many dust-air and gas-air mixtures in vessels of different sizes and shapes:

$$\left(\frac{dP}{dt}\right)_{max} V^{1/3} = K_{st} \tag{13}$$

where V is the vessel volume and K_{st} is a constant of the dust-air mixture (st stands for "staub", which is german for dust. The term K_g is used when a gas mixture is being considered). This law reduces to equation 11 in the case of a spherical vessel. Equation 11 also makes clear that the maximum rate of pressure rise is directly proportional to the burning velocity.

Out of all the assumptions made in the Bradley-Mitcheson model, that of regular, spherical flame propagation without heat loss is probably the one that is least satisfied in the experimental conditions of this study. As we have seen before, a turbulent flame front is wrinkled by the turbulent velocity fluctuations and this wrinkling can be so severe as to create a situation, such as has been observed by Shchelkin[21] in circular tubes, where pockets of unburned mixture are left behind the propagating flame front. Such a situation can even be considered likely if, as appears to be the case in our experiments, the turbulent r.m.s. velocity is very much larger than the laminar burning velocity of the mixture. It goes without saying that such a flame structure destroys the validity of the theoretical formula, equation 9. In chapter 4, we will present experimental evidence regarding the mode of flame development which indicates that flame propagation is highly irregular.

c) Previous research into turbulent dust and gas explosions

Since it is difficult to achieve stationary, adiabatic dust flames for detailed observations, dust combustion has traditionnally been studied in constant volume bombs of various sizes and shapes, with emphasis being put of classifying dusts by such criteria as minimum explosible concentration, minimum auto-ignition temperature, etc., to allow for the design of safety measures appropriate for the safe handling of each dust. A number of people have attempted to measure the influence of turbulence by varying the delay between dispersion of the dust and ignition of the mixture. Turbulence associated with the dust dispersion process is not supported and hence must decay as the delay between dispersion and ignition is increased. This type of experiments have been done by Moore [22,23], Bartknecht [24], Eckhoff [25], Cocks and Meyer [26], Swift [27] and Reeh [28]. These people found that the maximum pressure is affected very little by the ignition delay, but that the maximum rate of pressure rise decreases by a factor as high as 6, as the dispersion turbulence is allowed to decay. The rate of decay of the turbulence appeared to be closely connected with the minimum dimension of the combustion chamber, i.e. the maximum eddy size. This will be explored further in chapter 4, where we discuss the results of our own experiments with ignition delay variation. In a few of the abovementionned studies, the experiments were replicated with gas-air mixtures, i.e. the combustion chamber and dispersion bottle were filled with explosible gas-air mixture and the dispersion bottle was discharged, without any dust in the system at all. Here again, the maximum pressure, which in principle depends only on the energetics of the mixture, varied very little, but the K_g factor relaxed towards a laminar value as the ignition delay was increased. In the studies by Bartknecht and Moore, the ratio of the K factors of the dust and gas, K_{st}/K_g, was approximately constant over all the ignition delays studied, which indicates that the burning rate increase brought about by turbulence in dust is equal to that obtained in gas. In the experiments by Reeh, this pattern could not be so clearly observed.

Experiments in which the degree of turbulence was varied by adjusting the initial pressure of the dispersion bottle, while keeping the ignition delay constant, were performed by Nagy and Portman [29] with a coal-dust-air mixture and with a hybrid mixture of coal-dust, methane and air in a 9.3 liter chamber. With the coal dust, the maximum rate of pressure rise increased linearly with dispersion pressure until a peak of 25,000 kPa/s was reached. Further dispersion pressure increases caused the K_{St} to drop. With the hybrid mixture, the maximum rate of pressure rise increased linearly over the whole range of dispersion pressures studied.

The influence of fan-generated turbulence on gaseous explosions in closed vessels has been studied by Harris[30] and more recently by Abdel-Gayed et al.[31] In Harris' study the maximum rate of pressure rise of pentane-air explosions in a 1.7 m^3 sphere increased linearly with fan speed. Measurements of pressure fluctuations in the turbulent premixture flow showed in turn that the turbulence intensity was directly proportional to the fan speed. This suggests the following simple correlation for the turbulent burning velocity:

(14)
$$\frac{S_t}{S_l} = 1 + k\,\frac{u'}{S_l}$$

Abdel-Gayed et al. measured burning velocity directly by the double kernel technique in a 22.2 liter cylindrical bomb fitted with four fans generating near-isotropic turbulence. For low turbulence intensities ($0 < u' < 2$ m/s) the burning velocity increased linearly with the turbulent r.m.s. velocity, in agreement with equation 14. For higher turbulence intensities the curves of S_t versus u' begin to flatten out, and with some mixtures, quenching of the flame was obtained with a sufficiently high value of u'. Because this extensive study has been performed with gas-air mixtures similar to ours, and with state-of-the-art techniques of turbulence and burning velocity measurements, we will want to use its results to assess the features of the turbulent flow field in our own experiments.

Kauffman et al.[32] have recently studied turbulent dust explosions in a 1 m^3 spherical vessel in which the dust-air mixture was fed from six ports located symmetrically on the surface of the sphere. The turbulence intensity was adjusted by varying the air flow rate through the ports and, to a very good approximation, the turbulent r.m.s. velocity was directly proportional to the flow rate. The burning velocity of cornstarch-air mixtures, deduced from pressure measurements, was found to be directly proportional to the turbulent r.m.s. velocity.

III- EXPERIMENTAL CONSIDERATIONS AND PRELIMINARY EXPERIMENTS

a) Apparatus

A spherical vessel of 333 liter volume (figure 2), of 0.9 m diameter, and a cylindrical vessel of 180 liter volume, with 1 m height and 0.5 m diameter, were used in the present study to assess the influence of turbulence on dust and gas explosions in closed vessels.

In the spherical vessel, the dust was placed in a bowl at the bottom of the vessel and dispersion was achieved by an air blast from a 1.57 liter dispersion bottle discharging through a half-inch diameter tube nozzle directed at the center of the dust bowl. The dispersion was triggered by opening a solenoid valve in the dispersion circuit. Ignition was achieved by either an exploding fuse wire or a bare magnesium flashbulb filament located at the center of the vessel. The delay between dispersion and ignition could be controlled by means of an electric timer.

The features of the dispersion system provide us with two means of varying the intensity of the turbulence of the dust-air mixture at the moment of ignition. With a fixed initial pressure in the dispersion bottle, we can vary the delay between opening the dispersion solenoid valve and igniting the mixture; the longer the ignition delay, the more the flow field will have relaxed towards a quiescent state. Alternatively, with a fixed delay between dispersion and ignition, the dispersion bottle initial pressure can be varied; the higher the pressure, the bigger the swirl induced in the combustion chamber. Both these means of turbulence variation were studied in the spherical bomb and the results are presented in chapter four.

The cylindrical vessel was fitted with accessories similar to those of the spherical one. Additionnal turbulence was generated in the cylindrical vessel by a 3.0 liter "turbulence bottle" which discharged through a port on the circumference of the vessel, near its center. The turbulence bottle was charged to the same pressure as the dispersion bottle and discharged simultaneously with it. Since it was desired to study explosions occurring at atmospheric initial pressure, it was necessary, in the cylindrical vessel experiments, to first evacuate the vessel to a level such that atmospheric pressure would just be recovered upon injection of gas by the turbulence and dispersion bottles. In the spherical vessel, this precaution was not taken because the mass injected by the dispersion bottle was a very small fraction of that initially present in the vessel. The results of experiments, performed in the cylindrical bomb, in which the pressure of the dispersion and turbulence bottles was varied, are presented in chapter 4.

It was desired to study the influence of jet-induced turbulence in conjunction with dispersion-induced turbulence in the spherical vessel. For this purpose, the vessel was fitted with two different turbulence-producing mechanisms and series of experiments were performed with each. One was a 45 cm diameter copper tubing ring (figure 4a) on which 16 holes of 1.1 mm diameter were drilled. The other was an 80 cm long vertical pipe (figure 4b), positioned 12 cm away from the vertical axis of the sphere, on which 12 holes of 9.5 mm diameter were drilled. The holes were arranged in four stations, spaced 20 cm away from each other, each station comprising three holes spread at 120 degree intervals along the circumference of the tube.

The turbulence ring and turbulence pipe were fed by a high pressure (690 kPag) air supply and the level of turbulence generated by the jets could be controlled by varying the mass flow rate of air through the holes. In the case of the turbulence ring, the flow was choked at the orifices, so that the flow rate could be adjusted by varying the static pressure in the ring itself. In the case of the pipe, the hole area was too large to permit choking, hence the flow rate was modulated by a globe valve in the air supply circuit and measured from the time required to attain a certain pressure rise in the sphere.

The sequence of operations for dust explosion experiments with jet-induced turbulence was as follows. The dust was first weighed into the cup at the bottom of the vessel. The vessel was then put under a vacuum of 400 mm Hg. The air jets were turned on, and air addition from the jets caused the vessel pressure to increase again. When atmospheric pressure was restored, the dispersion air blast was activated and ignition followed after a predetermined delay. In the experiments done with methane-air mixtures, the vessel was first evacuated (to 600 mm Hg) and then filled by partial pressure with an amount of methane resulting in the desired composition. The air jets were then turned on, and the dispersion process was triggered when the vessel reached atmospheric pressure, followed by ignition. It is believed that the intense swirl generated by the jets was sufficient to mix the methane and air adequately.

A PCB quartz pressure transducer was used to record the pressure-time history in both the spherical and the cylindrical vessels; the maximum rate of pressure rise was calculated from the slope of a tangent to the pressure-time curve through its inflection point. An ion gauge was mounted on the surface of the spherical vessel, to monitor the time of flame arrival on the vessel wall. A typical oscilloscope record of a turbulent dust explosion is shown in figure 5.

b) Properties of the combustible mixtures

The dust used in the present study was cornstarch, a natural polymer of dextrose, with formula $(C_6H_{10}O_5)_n$. Peraldi[33] has measured its heat of combustion to be 631.5 kcal/mole and its heat of formation 222 kcal/mole. The literature seems to contain no information on the devolatilization properties (i.e. products, rate and enthalpy of devolatilization) of cornstarch. However, these properties should be very similar to those of cellulose, since these two compounds are identical in structure and vary only by the number of monomers making up a polymer chain. Devolatilization of thin strips (100 micron thickness) of cellulose fiber, with moderate heating rates and short residence time, has been studied by Lewellen et al.[34] who achieved complete devolatilization (i.e. no residual char) and found that the process could be described by the simple Arrhenius formula

$$\frac{dM}{dt} = -k \exp\left(\frac{-E_a}{RT}\right) M \qquad (15)$$

where M = mass of cellulose present in the sample

$k = 6.79 \times 10^{-9}\ s^{-1}$

$E_a = 33.4$ kcal/mole

R = universal gas constant

T = temperature

From the above formula, a characteristic time of devolatilization is determined to be

$$\tau_{dev} = k^{-1} \exp\left(\frac{E_a}{RT}\right) \qquad (16)$$

Table 1 shows how the time required for devolatilization varies as a function of temperature.

T, °K	τ_{dev}, sec
1000	2.2×10^{-3}
1200	1.4×10^{-4}
1400	1.9×10^{-5}
1500	8.8×10^{-6}
1600	4.4×10^{-6}
1800	1.4×10^{-6}
2000	5.6×10^{-7}

Table 1. Characteristic time of devolatilization as a function of temperature.

From this we can conclude that complete devolatilization of cornstarch occurs well before a temperature of about 1500 degrees K has been reached. Since the flame temperature of cornstarch-air mixtures (as calculated by the NASA code[35]) is of the order of 2000 degrees K, and since chemical reactions do not start occurring at a significant rate until the temperature reaches the vicinity of the flame temperature[36], it seems likely that the burning will not start occurring before devolatilization is complete, i.e. burning will occur completely in the gas phase.

Commercially available starch usually contains about 10% moisture by weight. In the present study, the cornstarch was placed in an oven at 90 degrees C for about 18 hours prior to an experiment, to eliminate the moisture and thus help produce a more uniform dispersion. In a number of experiments, a fluidizing agent (CAB-O-SIL) was mixed with the cornstarch in the proportion of 0.5% of fluidizing agent per unit mass of mixture, to further improve the dispersion. A particle size analysis obtained via direct imaging with an optical image analyzer showed the average size of the particles to be 14.7 microns, with a standard deviation of 5.1 microns. Scanning electron micrographs (figure 6) showed the particles to be remarkably spheroidal in shape.

The laminar burning velocity of cornstarch-air mixtures has never been measured. Kauffman et al.[32] estimate the laminar burning velocity to be 0.40 m/s for a 300 gm/m^3 mixture and 0.70 m/s for a 700 gm/m^3 mixture, from extrapolation of their results of burning velocity versus turbulence intensity. This estimate, however, is highly sensitive to the method of determining the turbulent burning velocity and to the extrapolation scheme used to abstract the laminar burning velocity.

Marble [37] has shown that, from the thermodynamic point of view, a dust-air suspension, whose particles are so small that the velocity and temperature difference between the solid and gas phase is negligible, can be treated as a perfect gas whose properties reflect a weighted average of the solid and gas phase. Since the characteristic velocity rise time of the particles in our suspension (i.e. the time required for any slip velocity to be reduced to 1/e times its original value as a result of Stokes drag), which can be shown to be

$$\tau_{vr} = \frac{2}{9} \frac{\rho_{dust}\, r^2_{dust}}{\mu} \tag{17}$$

and their characteristic temperature rise time (i.e. the time required for any temperature difference to be reduced to 1/e times its original value), which can be shown to be

$$\tau_{tr} = \frac{\rho_{dust}\, r^2_{dust}\, c_p}{3\, k_{air}} \tag{18}$$

are both of the order of milliseconds, i.e. a time span very short compared to the duration of an explosion, the assumptions of no slip and no temperature lag are valid, and the specific heat ratio of the dust-air mixture, which enters into the calculation of the burning velocity from pressure measurements (equation 9), can be taken as

$$\bar{\gamma} = \frac{c_{p\,air} + \kappa\, c_{dust}}{c_{v\,air} + \kappa\, c_{dust}} \tag{19}$$

where κ is the ratio of dust mass to gas mass per unit volume. For a 300 gm/m^3 mixture at 20 degrees C, we have

$$\bar{\gamma} = \frac{1.006 \frac{kJ}{kg\ ^oC} + \frac{300\ gm/m^3}{1209\ gm/m^3} \times 1.55 \frac{kJ}{kg\ ^oC}}{0.718 \frac{kJ}{kg\ ^oC} + \frac{300\ gm/m^3}{1209\ gm/m^3} \times 1.55 \frac{kJ}{kg\ ^oC}} \tag{20}$$

$\bar{\gamma} = 1.26$

Table 2 summarizes the properties of cornstarch that are relevant to its combustion characteristics.

Chemical formula: $(C_6H_{10}O_5)_n$
Mol. wt. of monomer: 162
Density: 1.5 gm/cm^3
Stoichiometric concentration: 253.7 gm/m^3
Heat of combustion: 631.5 kcal/mole
Heat of formation: 222 kcal/mole
Specific heat: 0.37 kcal/kg-C

Table 2. Properties of cornstarch that are relevant to its combustion characteristics.

The methane used in the present study was of the commercially pure grade. The laminar burning velocity of a 7.5% methane-air mixture is reported by Andrews and Bradley[38] to be 0.28 m/s.

c) Preliminary experiments on the effects of dust concentration

To establish some confidence in the ability of the apparatus to produce repeatable and trustworthy results, the effect of varying dust concentration with a fixed ignition delay, fixed dispersion bottle pressure and without extra means of inducing turbulence was investigated. The dispersion bottle pressure was 1379 kPa and the ignition delay was set at 0.5 seconds after a few preliminary runs showed that this gave the highest value of P_{max} and $(dP/dt)_{max}$.

Figures 7 and 8 show maximum overpressure and K_{st} factor, respectively, as a function of cornstarch concentration for the 333 liter sphere and the 180 liter cylinder. For comparison purposes, results from Nagy[39], Hartmann[40] and Cocks and Meyer[26] are also shown. The peak overpressures are found to be in fair agreement with one another, in spite of the widely different properties of the cornstarch used and of the different characteristics of the experimental apparatuses. The K_{st} factor, on the other hand, is found to vary over a wider range. All the data for P_{max} show a similar trend, with P_{max} rising sharply from a lean limit concentration of about 100 gm/m^3 and asymptote to about 700 kPa when the concentration reaches 500 gm/m^3. No rich limit was observed up to a concentration of 1000 gm/m^3. The peak overpressure in the 333 liter sphere was consistently higher than that obtained in the 180 liter cylindrical vessel. This may be due to more severe heat losses to the walls in the cylindrical vessel since the flame is already in contact with the cylinder wall prior to complete consumption of the mixture at the ends of the vessel. For both vessels, the maximum pressure is far less than predicted from an equilibrium calculation[35] when the concentration is smaller than stoichiometric, but the theoretical and experimental curves seem to cross in the vicinity of 600 gm/m^3. The discrepancies could be caused by heat loss, settling or by the inability to predict pressure rise correctly from mere chemical equilibrium arguments.

The K_{st} from the cylindrical bomb show a maximum value of about 6000 kPa-m/s at a dust concentration of 200 gm/m^3 and then decreases with a further increase in concentration. The K_{st}

from the spherical vessel does not show the same trend: it simply increases asymptotically to a peak value of about 3500 kPa-m/s. Thus the burning rate in the cylindrical vessel, as indicated by the K_{st} factor, is generally higher than that from the spherical vessel.

IV- DISPERSION-INDUCED TURBULENCE

a) Influence of ignition delay

i- Influence of ignition delay on dust and gas explosions

Since the discharge of the dispersion bottle is a sudden, discrete event, the turbulence induced by the dispersion process will start to decay immediately after the dispersion bottle has been completely emptied and the fuel-air mixture will relax back towards a laminar state.

Figures 9 and 10 show the results of experiments in which the delay between dispersion and ignition was varied to try to elucidate the role played by the transient turbulence of the dispersion process. The experiments were done with a 450 gm/m^3 cornstarch-air mixture in the spherical vessel, with a 300 gm/m^3 cornstarch-air mixture in the cylindrical vessel and with a 7.5% methane-air mixture in the spherical vessel. The dispersion pressure used was 1379 kPa.

Figure 9 shows the maximum pressure developed, while figure 10 shows the ratio of K_{st} and K_g to the maximum K factor observed (this maximum value is given in the table below). This provides a convenient way of normalizing the data to compare the influence of the flow field on gas-air flames and dust-air flames.

Spherical bomb Methane-air	Spherical bomb Cornstarch-air	Cylindrical bomb Cornstarch-air
$(dP/dt)_{max}$:	$(dP/dt)_{max}$:	$(dP/dt)_{max}$:
16 456 kPa/s	6 895 kPa/s	4 496 kPa/s
K_g:	K_{st}:	K_{st}:
11 406 kPa-m/s	4765 kPa-m/s	2539 kPa-m/s

Table 3. Reference values for figure 10.

For both the cylindrical and the spherical vessels with dust and gas, the maximum overpressure and the maximum K factor are obtained with an ignition delay of approximately 0.5 seconds. Transient measurements of the dispersion bottle pressure show that this is just the time required for the bottle to become completely discharged. With shorter ignition delays, it appears that the dust and air have had insufficient time to mix homogeneously, while for longer delays, the turbulence of the dispersion has begun to die down and is less effective in enhancing flame propagation.

For both the 180 liter cylinder and the 333 liter sphere, the K_{st} factor measured with an ignition delay of 1.0 second is roughly 25% of the maximum K_{st} recorded.

Two causes can explain this sudden, violent decrease in the burning rate: settling of the dust particles, on the one hand, and decay of the dispersion-induced turbulence, on the other hand.

If we assume that the typical settling velocity of the dust particles is equal to their Stokes free fall velocity, then the characteristic settling time of the dust suspension, defined as the ratio of the average falling distance to the settling velocity, is calculated to be

$$\tau_{set} = \frac{9\,\mu\,r}{2\,r_{dust}^{2}\,\rho_{dust}\,g} \qquad (21)$$

where r is the sphere radius, in the case of the spherical vessel, or one half the cylinder height, in the case of the cylindrical vessel. Since this quantity is approximately equal to 50 seconds for single starch particles of 15 micron diameter, then it appears unlikely that significant settling can take place with ignition delays of the order of one second, if the suspension is made up of single particles. However, Bryant[41] has found that dust suspensions of the type studied here often consist of agglomerated particles whose settling time can be far less than that of single particles. Our experimental observation, that a 450 $\mathrm{gm/m^3}$ starch-air mixture could not be ignited in the 333 liter sphere with an ignition delay of 1.0 second or longer (only one shot, with 1.5 second ignition delay, ignited and gave minimal pressure rise), seems to support this idea. In what concerns the shots that did ignite, however (ignition delay less than or equal to 0.9 seconds), the pressure deviation from the value observed with 0.5 seconds ignition delay was at most 30%, while the decrease in the maximum rate of pressure rise was by a factor of four. Referring back to figures 7 and 8, it seems unlikely that such a large decrease in the burning rate could result in such a relatively small decrease in the peak pressure, if it were caused primarily by a decrease in concentration.

We conclude that there is uncertainty as to whether settling or turbulence decay cause the observed variations. It is probably true that both mechanisms affect combustion of the dust-air mixture, and that settling and turbulence decay are coupled processes.

It will be observed that in the 333 liter sphere, the ratio K/K_{max} falls far more steeply with time for the dust-air mixture than for the gas-air mixture. Although this could be due to settling of the dust particles, as discussed above, another cause can be cited. Dust remains in suspension in a gas by virtue of the viscous and pressure forces exerted by the gas on the suspended particles. In a turbulent dust-air suspension, therefore, energy is being dissipated not only by the shearing forces in the small-scale motions, but also by the work being done against the dust-suspending forces. Beer et al.[42] have estimated that the ratio of the kinetic energy dissipation rate in a dust-air mixture due to this effect (ε_p) to the dissipation rate that would be observed in the absence of dust particles (ε) was of the order of the mass fraction of dust present in the gas, i.e. $\varepsilon_p / \varepsilon = \kappa$. In our particular case, the mass fraction is κ = (450 gm/m^3)/(1230 gm/m^3) = 37%. Hence the dissipation rate is significantly higher in the dust-air mixture than in the gas-air mixture.

ii- Characterization of the decay of the dispersion turbulence

In a closed vessel, decomposition of the fluid velocity into a mean and a fluctuating quantity is not possible since the closed boundaries do not allow the existence of a mean flow. Hence, in discussing the influence of "turbulence" on explosions in closed vessels, one has to be a little bit more specific regarding what is meant by "turbulence" in this context.

The phenomenon of the decay of turbulence in a closed vessel has been studied experimentally by Tsuge et al.[43,44] who performed the following simple experiment. Tsuge et al. dragged a perforated plate, at a fixed speed, across a cylinder and measured the fluid speed, generated by the motion of the plate, at a hot-wire anemometer spaced 10 cm away from the wall of the cylinder (cylinder length: 60 cm), along its axis.

The flow pattern identified by Tsuge et al. consisted in large scale motions with a regular decay rate (Tsuge calls these motions "flow components"), on which were superimposed small, irregular, jagged motions whose amplitude decayed along with that of the flow components. The Fourier spectrum of these motions had a sharply peaked distribution, i.e. most of these motions corresponded to a fairly well-defined eddy size. Tsuge et al. made a parametric study of the factors which affected the decay rate of the flow components by varying the perforated plate hole spacing and diameter, the viscosity of the fluid, the piston speed and the diameter of the cylinder (diameters of 50, 100 and 150 mm were investigated). It was found that the method of generating the "turbulence", i.e. hole diameter and spacing, had very little influence on the decay rate, but that cylinder diameter was very important in controlling that rate. The best fit of the experimental data was obtained with

(22) $$Ge = k\,Re^{0.70} \quad \text{where}$$

(23) $$k = 1.73,$$

(24) $$Re \equiv \frac{uD}{\nu} ,$$

(25) $$Ge \equiv \left(\frac{\varepsilon D^4}{\nu^3}\right)^{1/4} ,$$

(26) $$\varepsilon \equiv \frac{u^2(t)}{2\,\theta(t)}$$

$\theta \equiv$ half-energy time, i.e. the time required for the kinetic energy, per unit mass of fluid, to be reduced by a factor of 1/2.

From equation 22, a relationship between u_0, the flow component speed at time zero, and u(t), the speed at any subsequent time, can be derived as follows:

(27) $$Ge = \left(\frac{u^2\ D^4}{2\ \theta\ \nu^3}\right)^{1/4} = k\left(\frac{uD}{\nu}\right)^{0.7}$$

(28) $$\frac{u^2 D^4}{2\ \theta \nu^3} = \frac{k^4 u^{2.8} D^{2.8}}{\nu^{0.8}}$$

(29) $$\theta\ u^{0.8} = \frac{D^{1.2}}{2\ k^4 \nu^{0.2}} \equiv J$$

where J is a dummy variable used to regroup terms.

If we consider t to be a function of u, this gives

(30) $$t\ (\ u_i/2^{1/2}) - t\ (\ u_i) = J\ u_i^{-0.8}$$

Let us assume a relationship of the type

$$t = \alpha + \beta u_i^{-0.8} \tag{31}$$

where α and β are undetermined constants. Then

$$t(u_i/2^{1/2}) - t(u_i) = \left(\alpha + \frac{\beta u_i^{-0.8}}{\sqrt{2}^{-0.8}}\right) - \left(\alpha + \beta u_i^{-0.8}\right) = J u_i^{-0.8} \tag{32}$$

This is satisfied identically if

$$\beta = \frac{J}{\left(\frac{1}{\sqrt{2}^{-0.8}} - 1\right)} \text{ . Hence} \tag{33}$$

$$t = \alpha + \frac{J}{\left(\frac{1}{\sqrt{2}^{-0.8}} - 1\right)} u^{-0.8} \equiv \alpha + J' u_o^{-0.8} \tag{34}$$

At $t = 0$, $u = u_o$, so that $\alpha = -J' u_o^{-0.8}$:

$$t = J' u_o^{-0.8}\left[\left(\frac{u}{u_o}\right)^{-0.8} - 1\right] \tag{35}$$

$$\left(\frac{u}{u_o}\right)^{-0.8} = \left(\frac{t}{J' u_o^{-0.8}}\right) + 1 \tag{36}$$

$$\frac{u}{u_o} = \left[1 + \left(\frac{t}{J' u_o^{-0.8}}\right)\right]^{-1/0.8} \tag{37}$$

Absorbing the constants, with $\nu = 1.5 \times 10^{-5}$ m^2/s, this gives

$$u = u_o\left[1 + \left(\frac{0.6207 u_o^{0.8}}{D^{1.2}}\right) t\right]^{-1.25} \tag{38}$$

Hence it seems that the quantity $t/D^{1.2}$ is the parameter governing the decay of the flow components. This can be interpreted to mean that the decay rate is governed by the size of the largest eddy in the vessel, i.e. the vessel diameter. If the dispersion turbulence decay in closed bombs follows the pattern identified in Tsuge's experiments, and if the "flow components" can be associated with a turbulence intensity, then there should be a relationship between the burning rate observed with a given ignition delay, and the amount by which the turbulence induced by the dispersion process has been allowed to decay. Since the ignition delay, τ_{do}, corresponding to the observation of the maximum K_{st}, also corresponds to the greatest intensity of turbulence, then closed vessel experiments should show a relationship between $K_{st}/K_{st\ max}$, the normalized burning rate, and $(\tau_d-\tau_{do})/D^{1.2}$, the normalized turbulence decay time.

In figures 11 and 12, we have attempted to see whether such a relationship existed. It is seen in figure 12 that all the data fall fairly well on a single curve, despite the wide variety of the vessel sizes and shapes and of the dust-air mixtures under study. The figure makes clear the simple relationships linking vessel size, turbulence decay and dust combustion rate.

In the methane-air explosions performed in the 333 liter spherical vessel, the characteristic decay time of the turbulence, which we define to be the interval over which the measured K factor decreases by 1/e times its original value, is seen to be (figure 10)

(39) $$\tau_{de} = \tau_d (K_g = K_{g\,max}/e) - \tau_d (K_g = K_{g\,max}) = 2.0\ \text{s} - 0.6\ \text{s} = 1.4\ \text{s}$$

Let us try to see whether this agrees with the prediction of the characteristic decay time from Tsuge's work. From equation 31, this predicted time is given by

(40) $$\frac{1}{e} = \frac{u}{u_o} = \left[1 + \left(\frac{0.6207\ u_o^{0.8}}{D^{1.2}}\right)\tau_{de}\right]^{-1.25}$$

(41) $$\tau_{de} = \frac{1}{0.6207}\left[\left(\frac{1}{e}\right)^{-4/5} - 1\right]\frac{D^{1.2}}{u_o^{0.8}}$$

(42) $$\tau_{de} = 1.97\ \frac{D^{1.2}}{u_o^{0.8}}$$

u_o, the turbulent velocity corresponding to the observation of $K_{g\,max}$, can be estimated by comparing the ratio S_t/S_l (or, equivalently, K_{gmax}/K_{gl}) obtained in our experiments with the results of Abdel-Gayed et al.[31] Since $K_{gmax}/K_{gl} = 16500/3100 = 5.3$, we have

(43) $$S_t = \left(\frac{S_t}{S_l}\right) S_l = 5.3 \times 0.28\ \text{m/s} = 1.5\ \text{m/s}$$

Abdel-Gayed et al. have shown that this is obtained in 8% methane-air with $u_o = 1.2$ m/s. Hence

(44) $$\tau_{de} = \frac{1.97 \times (0.9)^{1.2}}{1.2^{0.8}} = 1.50\ \text{seconds}$$

The experimentally observed turbulence decay rate, as measured by explosion burning rates, corresponds nearly exactly to that predicted by Tsuge's results.

iii- Flame regularity

It was pointed out in chapter 2 that if flame propagation is regular, then in the case of a spherical vessel, the time of flame arrival on the vessel surface, the time at which the maximum rate of pressure rise is observed, and the time at which maximum pressure is reached, should all coincide. Yet our experiments with both dust and gas mixtures show that this is not the case. In general, the maximum rate of pressure rise occurs when the overpressure ratio $(P_f - P_i)/P_i$ is about half its final value, and the time of flame arrival on the vessel surface, as measured by an ionization probe on the wall, corresponds loosely to the time of maximum rate of pressure rise (figure 5).

In figure 13, we have plotted the ratio of time of flame arrival to the time at which 95% of the final pressure is attained, as a function of the ignition delay for 7.5% methane-air in the 333 liter sphere. As the ignition delay is increased and the burning relaxes towards a laminar state, the time of flame arrival approaches that of maximum pressure, indicating a more regular flame development.

For very turbulent flames, however, the development appears highly irregular. This behavior of dust explosion flames has also been noted by Kauffman et al.[32] It appears, then, that estimates of turbulent burning velocity based on pressure measurements can only be of limited validity.

b) Influence of dispersion pressure

i- Spherical bomb

With a fixed ignition delay, the intensity of the turbulence in a closed explosion vessel will be determined by how the features of the dispersion system are matched with those of the vessel. To be more specific, the intensity of the turbulence will be proportional to the dispersion bottle pressure and volume, since an increase in either of these two factors increases the "swirl" induced by the dispersion discharge, and will vary in inverse proportion to the vessel volume, since an increase in this increases the mass of fluid which must be swirled.

Figures 14 and 15 show the results of a series of experiments in which the dispersion bottle pressure was varied in the 333 liter sphere with a 300 gm/m^3 cornstarch-air mixture and a 7.5% methane-air mixture. The ignition delay in these experiments was set to be 0.5 seconds, as this has been previously shown to result in the least amount of decay. Figure 14 shows the maximum pressure developed as a function of pressure in the dispersion bottle. For the methane-air mixture there is very little variation in the maximum pressure developed: it is nearly constant at about 560 kPa , 18% below the theoretically calculated value of 684 kPa for adiabatic combustion.[35] For the starch-air mixture, there is a slight increase of P_{max} with dispersion bottle pressure: it goes from 475 kPa at 690 kPa dispersion pressure, to 655 kPa at 2069 kPa dispersion pressure. On the average, the observed maximum pressure is 587 kPa , 37% below the theoretically calculated value of 932 kPa for adiabatic combustion. The fact that the deviation from adiabatic behavior is more pronounced in the case of dust than in that of gas is probably linked to the slower burning velocity of the dust-air mixture. Since flame development is irregular, the flame contacts the wall early in the flame travel and heat loss starts well before the maximum pressure has been reached - hence the total amount of heat loss depends on the time required for complete combustion, and since this time is larger for dust than it is for gas, the deviation from adiabatic pressure is also larger for dust than for gas.

It seemed appropriate to normalize the burning rates with respect to that observed in a "reference" laminar explosion of 7.5% methane-air. Hence in figure 15, we have plotted the ratio $K' \equiv K/K_{g\ lam}$, where $K_{g\ lam}$ is the K of a laminar gas-air explosion, versus pressure in the dispersion bottle. The value of $K_{g\ lam}$ was measured in the spherical bomb to be 2575.9 kPa-m/s. The formula of Bradley and Mitcheson[6] (equation 9) for spherical vessel explosion shows that this value corresponds to a laminar burning velocity of 33 cm/sec, in good agreement with the value of 28 cm/sec reported by Andrews and Bradley[38], especially if a correction is made to account for the burning velocity increase associated with adiabatic compression of the mixture. Both K_g' and K_{st}' increase monotonously with bottle pressure, although it seems that the increase begins to taper off when the dispersion pressure has reached about 1724 kPa. For a given intensity of turbulence, methane-air seems to burn much faster than cornstarch-air, the ratio K_g'/K_{st}' having a value of about four. The scatter in the values of K' is much more important than that observed in the maximum overpressures (figure 14). This is understandable, since P_{max} is primarily determined by the concentration of fuel, whereas K' is highly sensitive to the random fluctuations in the turbulent flow field from one explosion to the next.

ii- Cylindrical bomb

Experiments similar to the ones described above were performed in the 180 liter cylindrical vessel. Here, turbulence of the dispersion bottle was supplemented by that of a 3.0 liter "turbulence bottle", charged at the same pressure as the dispersion bottle and discharging simultaneously with it through a port on the circumference of the vessel, near its center. A 300 gm/m^3 cornstarch-air mixture and a 7.5% methane-air mixture were investigated, with the ignition delay set at 0.5 seconds.

Figure 16 shows the maximum pressure developed as a function of bottle pressure, while figure 17 shows K', the normalized burning rate, versus bottle pressure. The results are qualitatively similar to those obtained with the spherical vessel. The maximum overpressure is affected very little by the bottle pressure, and the dust-air mixture deviates more from adiabatic behavior than does the gas-air mixture. Here again, a monotonous increase of K_g' and K_{st}' with increased bottle pressure is evident and K_g' is roughly 3 to 4 times larger than K_{st}' at a given bottle pressure. Thus the explosions behave in a manner similar to those performed with dispersion pressure variation in the spherical vessel, even though the structure of the turbulent flow induced by the two bottles in the cylindrical geometry must be different from that induced by the single bottle in the spherical geometry. On comparing figures 15 and 17, we see that the K' factor obtained at a given bottle pressure, for both dust and gas, is roughly twice in the cylinder what it is in the sphere. The explanation could lie in the fact that a given bottle pressure induces a much bigger swirl in the cylinder than in the sphere, because the ratio of bottle volume (i.e. the volume responsible for the swirling) to combustion chamber volume (the volume being swirled) is higher in the cylinder: this ratio has a value of (1 l + 3 l)/180 l = 0.0222 for the cylinder and 1.57 l/333 l = 0.0047 for the sphere.

iii- Correlation of burning rate increases in different apparatuses

The burning rate increase due to the dispersion process in vessels with different sizes and dispersion systems can be quantitatively assessed by making a simple thermodynamic study of the parameters affecting the turbulent r.m.s. velocity induced by the dispersion.

Consider the following system:

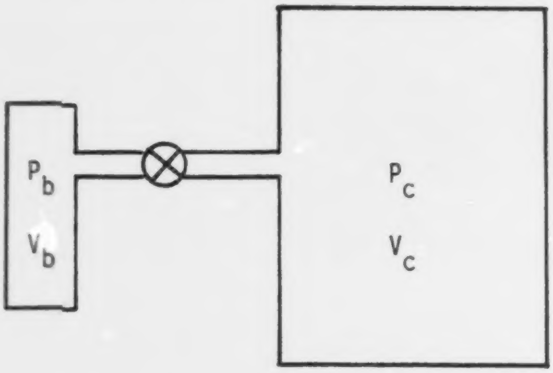

Let the subscripts i denote initial condition

f denote final condition

b denote the dispersion bottle

c denote the combustion chamber

We assume that the result of discharging the dispersion bottle is to impart a flow speed u' to the whole gas, without viscous dissipation taking place before the discharge if complete. Conservation of energy then requires

$$(45) \qquad U_{bi} + U_{ci} = U_{bf} + U_{cf} + \frac{1}{2}(m_{bi} + m_{ci})\, u'^2$$

With $U = m\, c_v\, T$ and $PV = mRT$, this gives

$$(46) \quad P_{bi}V_bc_v + P_{ci}V_cc_v = P_{bf}V_bc_v + P_{cf}V_cc_v + \frac{1}{2}\,\frac{(P_{bi}V_b + P_{ci}V_c)}{T_i}\, u'^2$$

$$(47) \qquad u'^2 = 2\, c_vT_i\left[\frac{V_b\,(P_{bi} - P_{bf}) + V_c\,(P_{ci} - P_{cf})}{P_{bi}V_b + P_{ci}V_c}\right]$$

$$(48) \qquad u'^2 = 2\, c_vT_i\left[1 - \left(\frac{P_{bf}V_b + P_{cf}V_c}{P_{bi}V_b + P_{ci}V_c}\right)\right]$$

If the dispersion bottle volume is small compared to the vessel volume, then the initial and final chamber pressures will be nearly equal. Since the flow stops when the bottle pressure equals the vessel pressure, this gives

$$(49) \qquad P_{cf} \simeq P_{ci} = P_{bf} \equiv P_c$$

Hence

$$(50)\qquad u'^2 = 2\,c_v T_i\left[1 - \left(\frac{P_c\,(V_b + V_c)}{(P_{bi} - P_c)\,V_b + P_c\,(V_b + V_c)}\right)\right]$$

$$(51)\qquad u'^2 = 2\,c_v T_i\left[1 - \left(1 + \frac{(P_{bi} - P_c)\,V_b}{P_c V_c}\right)^{-1}\right]$$

With the assumptions that $P_{bi} >> P_c$, $V_c >> V_b$, this gives

$$(52)\qquad u'^2 = 2\,c_v T_i\left[1 - \left(1 - \frac{P_{bi}V_b}{P_c V_c} \cdots\right)\right]$$

In first approximation, then, u' and $(P_{bi}V_b/P_cV_c)^{\frac{1}{2}}$ vary in direct proportion with each other. If the burning rate is linked to the turbulence intensity in a simple manner, such as

$$(53)\qquad \frac{S_t}{S_l} = 1 + k\,u'$$

then results of closed vessel experiments in which the explosion of a gas-air mixture is accelerated by dispersion-induced turbulence should show the pattern

$$(54)\qquad \frac{K_{gmax}}{K_{glam}} = 1 + k(P_{bi}V_b/P_cV_c)^{1/2}$$

In figure 18, we have plotted the ratio K_{gmax}/K_{glam} versus $(P_{bi}V_b/P_cV_c)^{\frac{1}{2}}$ obtained by different researchers with bombs of various sizes and shapes and dispersion systems with different pressures and volumes. Since some researchers did not perform truly laminar explosions in their experiments, we approximated K_{glam} to be the K factor obtained with an ignition delay equal to five times the ignition delay corresponding to the observation of the maximum K factor. The observation of K_{gmax} corresponds to the smallest possible amount of viscous dissipation in the particular apparatus, and thus corresponds most closely to the conditions of analysis described above. A linear increase of K_{gmax}/K_{glam} with $(P_{bi}V_b/P_cV_c)$ is observed. Thus the burning rate increase due to the turbulence of the dispersion process is simply related to the size and pressure of the dispersion bottle and of the combustion chamber.

V- JET-INDUCED TURBULENCE

It has been seen that the turbulence associated with the dispersion process has a transient, decaying nature. In experiments in which the delay between dispersion and ignition was varied, it was difficult to decouple the effects of dust settling on the one hand, and of turbulence decay on the other hand. Hence it was thought worthwhile to study the effect of a turbulent flow which would not have any direct impact on the dust-air suspension.

A convenient means of achieving this is by blowing air from a series of jets into the combustion chamber. For this purpose, two different devices were constructed and installed in the 333 liter spherical vessel: we shall designate them by the names of "turbulence ring" and "turbulence pipe". The turbulence ring was installed vertically in the center of the vessel. Because eight of the sixteen holes on the ring were drilled on one side of the copper tube, while the other eight were on the opposite side, the flow of air through the ring induced a tangential swirl in the combustion chamber. Hence it is sensible to think that only a small portion of the kinetic evergy flux $1/2\ \dot{m}\ c^2$ into the sphere went into "turbulent" random velocity fluctuations. The rest was going to support the swirling motions which, since they were perpendicular to the direction of flame propagation, did not directly contribute to acceleration of the flame. The dispersion bottle pressure used in experiments done with the turbulence ring was 1034 kPa and the ignition delay was 0.5 seconds; total ring flow rates varying from 0 to 14.9 g/s were investigated.

The purpose of constructing the turbulence pipe was to investigate higher turbulence intensities than had been achieved with the turbulence ring. The total hole surface in the turbulence pipe was 6.25 times greater than that in the turbulence ring - this allowed us to achieve total flow rates as high as 38.7 g/s with the same air supply system. In the turbulence pipe, the holes were drilled at 120 degree intervals on the surface of the copper tube: this geometry does not induce a tangential swirl and it is thought that the turbulence pipe is a more effective means of inducing turbulence than the turbulence ring. In experiments done with the turbulence pipe, the dispersion bottle pressure was increased to 2069 kPag, in an attempt to further increase turbulence intensity. The ignition delay was kept at 0.5 seconds.

Kauffman et al.[32] have measured that the turbulent r.m.s. velocity induced by blowing jets through six ports located symmetrically on the circumference of a 1 m^3 sphere was, to a very good approximation, directly proportional to the total jet flow rate. Hence a similar dependence can be expected in this study.

a) Dispersion-induced turbulence and jet-induced turbulence

Before comparing the influence of jet-induced turbulence on dust-air and gas-air explosions, it was thought instructive to acquire a feel for the relative importance of the dispersion-induced turbulence and the jet-induced turbulence in the 333 liter sphere. For this purpose, the following experiment was devised: the influence of ring jet flow rate on the maximum rate of pressure rise was studied with a 7.5%

methane-air mixture. In one case, the dispersion bottle was not used: turbulence was due to the ring jets alone. In the other case, the dispersion bottle was charged with methane-air mixture up to a pressure of 1034 kPa, hence the burning rate increase was due both to ring and jet turbulence. The results of the experiments are shown in figures 19 and 20. For both series of shots, the observed maximum rate of pressure rise, and therefore the turbulent burning velocity, increases linearly with jet mass flow rate. For such low turbulent burning velocities, Abdel-Gayed et al. have found a linear dependence of S_t on u'. Hence it appears that, both with and without dispersion, the turbulent r.m.s. velocity induced by the jets is directly proportional to the jet flow rate - a result similar to that obtained by Kauffman et al. The maximum rate of pressure rise, for a given ring flow rate, was consistently higher with the dispersion than without - clearly indicating the additional role played by the dispersion in enhancing the burning rate. The discrepancy between the two sets of results diminishes as we go to higher and higher flow rates, indicating that at high flow rates, the influence of the dispersion has faded and the flow field is dominated by the influence of the ring jets.

It is seen that the maximum pressure is significantly higher in the experiments without dispersion-induced turbulence than in those with it. This may at first appear paradoxical, since the faster burning in the experiments with the dispersion should reduce heat losses, and since the extra mass of mixture in the dispersion bottle should yield an additional pressure of

$$(55) \qquad \Delta P_f = \frac{P_f}{P_i} \Delta P_i = \frac{P_f}{P_i} P_d \frac{V_d}{V_c} \simeq \frac{785}{101} \times 1135 \text{ kPa} \times \frac{1.57}{333} = 41.6 \text{ kPa}$$

However, a close examination of the experimental records indicates that flame development is much more regular in experiments without dispersion-induced turbulence than in those with it. As seen in figures 21a and 21b, the flame arrives on the vessel wall just before combustion is complete when the dispersion is not used, whereas it arrives much earlier when it is used. The greater time of flame contact with the walls, in the experiments with dispersion turbulence, results in greater heat losses which explain the measured discrepancies of peak pressure. The simplest explanation is that the tangential swirl of the ring jets alone promotes regular, orderly flame development, whereas the random, irregular motions from the dispersion tend to destroy it.

b) Influence of ring-jet flow rate

We performed a series of experiments with 300 gm/m^3 cornstarch-air and 7.5% methane-air, in which the turbulence of the dispersion process was supplemented by that generated by air jets blowing into the combustion chamber from the turbulence ring. This has the effect of altering both the intensity and the detailed structure of the fluid motions. The results for maximum overpressure and rate of pressure rise as a function of mass flow rate through the ring are presented in figures 22 and 23 respectively.

Both for dust and methane, the maximum overpressure remains remarkably constant with mass flow rate. This firmly establishes the fact that the mass of dust consumed in an explosion is insensitive to the ring jet flow rate and that the effects of jet flow rate on the maximum rate of pressure rise, displayed in figure 23, are not caused by changes in the effective dust concentration, but rather by turbulence itself. In figure 23, K_g ' and K_{st} ' increase monotonously, K_g ' is typically 3 to 4 times higher than K_{st} ' and the relative increase in burning rate due to increased mass flow rate, which we define as $\Delta K'/K'\Delta\dot{m}$, is about the same for the dust-air as for the gas-air. These results parallel the situations observed with dispersion pressure variation in the sphere (figure 15) and bottle pressure variation in the cylinder (figure 17). The scatter observed in the values of K' is much higher for dust-air than for methane-air, perhaps owing to the difficulty in achieving a consistently homogeneous mixture of dust and air with the kind of dispersion system used in this study.

c) Influence of pipe jet flow rate

The experiments done with the turbulence ring were repeated with the vertical turbulence pipe, with the objective of investigating the effect of modifying the geometry of the jets and of studying a range of turbulence intensities higher than those which could be achieved with the turbulence ring. For this specific purpose, the turbulence pipe was designed to handle total air flow rates as high as 40 gm/s and the experiments were performed with a dispersion pressure of 2069 kPag. The results for maximum overpressure and K' as a function of mass flow rate are presented in figures 24 and 25 respectively.

The results are qualitatively similar to those obtained with the turbulence ring. The maximum overpressure of methane-air deviates very little from an average of 635 kPa. This is somewhat higher than the average value from previous experiments, probably owing to the additionnal mass of mixture associated with the high bottle pressure.

In this case again, K_g' and K_{st}' increase monotonously with turbulence intensity, K_g' is typically 3 to 4 times higher than K_{st}' and the relative increase in burning rate due to increased mass flow rate, $\Delta K'/K'\Delta\dot{m}$, is about the same for the dust-air mixture as for the gas-air. There was no evidence of turbulent quenching either for dust-air or methane-air, even for the highest K' ($K_g'=10.8$, $K_{st}'=3.77$) observed at a mass flow rate of 38.7 g/s.

VI - SUMMARY AND CONCLUSION

a) Synthesis of the experimental results

The experimental results presented in chapters four and five show that, for a substantial variety of turbulent flow structures and turbulence intensities, the relative burning rate variations caused by variation of the turbulence intensity are equal in a cornstarch-air mixture and a methane-air mixture. This result has been obtained with all methods of turbulence generation studied with the exception of ignition delay variation, where we have seen that the discrepancies between dust and gas behavior could be explained in terms of the settling of the dust particles or of the faster decay of turbulence in a dust-air mixture because of the work being done against the dust-suspending forces.

The finding that dust and gas respond to turbulence in a similar manner suggests that we use K_g' as a scale against which to compare K_{st}'. In figure 26, we have attempted to present a unified picture of the experimental results by plotting the relationship between the quantities K_g' and K_{st}' obtained under identical conditions of turbulence in each of the following four experimental set-ups: dispersion pressure variation in the sphere, bottle pressure variation in the cylinder, ring and pipe mass flow rate variation in the sphere. It is seen that K_g' and K_{st}' vary in linear proportion with each other, the data being best represented by the formula

$$K'_{st} = 0.30\ K'_g \qquad (56)$$

This suggests that the ratio of the burning rates of the dust-air mixture and the gas-air mixture is not sensitive to differences in the detailed structure of the turbulence induced by the various devices used, but that it rather depends on the physico-chemical properties of the mixtures themselves. Although we would need to know more about the fundamental characteristics of the cornstarch-air mixture (in particular, its laminar burning velocity and its laminar flame thickness) to draw a more definite conclusion from the results shown in figure 26, two possible explanations can be put forward at this time.

The first hypothesis is that the laminar burning velocity of the cornstarch-air mixture is about 0.30 times smaller than that of the methane-air and that the physical mechanisms responsible for the burning rate increase are the same in the two mixtures. Since it is known that, for the relatively small intensities of turbulence studied in this investigation, the main effect of turbulence on gas-air flames is to wrinkle the flame front so as to increase the total burning area, this hypothesis would imply that the dust-air flame and the gas-air flame are being wrinkled in the same proportion, so that the ratio of their turbulent velocities ($S_{st}/S_g = K_{st}'/K_g' = 0.30$) would simply be equal to the ratio of their laminar burning velocities. This "wrinkled laminar flame" regime of turbulent dust flame propagation would require that the thickness of the laminar dust-air flame be smaller than the smallest characteristic length scale of the velocity fluctuations.[16]

The second hypothesis is that, while the laminar burning velocities of the two mixtures may be close to one another, the laminar dust-air flame is much thicker than the gas-air flame, and consequently, the modes of action of turbulence are different in the two media. If the laminar dust-air flame is thicker than the smallest length scale of the velocity fluctuations, its area can only be minimally affected by these fluctuations, and the more significant effect of turbulence will be to increase the rate of the transport processes taking place within the flame itself. This might be a less efficient mechanism of burning rate increase than flame wrinkling, and this could explain the observed discrepancies in the combustion rates of cornstarch-air and methane-air.

The approach used in this study has been to relate the maximum rate of pressure rise observed in an explosion to a parameter characterizing the intensity of the turbulence in the explosion (e.g. ignition delay, dispersion pressure, etc.) In order to make our results comparable with those of other workers, however, we need to express them in terms of more fundamental quantities: the burning rate should be expressed as a turbulent burning velocity and the turbulence should be described either by its r.m.s. velocity or by a quantity, such as the turbulent Reynolds number, representing both its intensity and its characteristic length scale.

A fair estimate of the turbulent burning velocity at the moment of maximum rate of pressure rise can be obtained through the use of the formula of Bradley and Mitcheson[6], equation 9. Since Abdel-Gayed et al.[31] have measured the turbulent burning velocity in a 22.2 liter cylindrical vessel where isotropic turbulence was being generated by four fans, it is possible to infer the turbulent r.m.s. velocity in our apparatus by comparing our ratio of turbulent to laminar burning velocity of methane-air in a particular situation to the results of Abdel-Gayed et al. This allows us to show, in figure 27, the burning velocity as a function of turbulent r.m.s. velocity. The results are presented for jet-induced turbulence only, since it is obvious that experiments with jet-induced turbulence would show the same trend.

Although it is admitted that this method of data reduction has definite shortcomings (the correlation of S_t and u' obtained for methane by Abdel-Gayed et al. may not be applicable to our apparatuses where the structure of the turbulent flow is different; the Bradley-Mitcheson formula assumes spherical, regular flame development which is known not to be obtained in practice, to name but two), it is still thought to be of some use to obtain a rough estimate of the dependence of burning velocity on turbulent r.m.s. velocity. The relationship between S_t and u' for the dust-air mixture appears linear, although the scatter in the data is too large to notice a definite trend. It is unsafe to extrapolate from our results a value for the laminar burning velocity of 300 gm/m^3 cornstarch-air, although it appears that this value cannot be higher than about 30 cm/s.

b) General conclusions

From the results of our experiments, we are now in a position to draw a few definite conclusions regarding the validity of the approach we took to attack the problem and regarding the nature of the problem itself.

Although the crudeness of the method of dispersing dust used in our experiments creates uncertainties as to the homogeneity of the mixture and the constancy of the total amount of dust in suspension, the fact that maximum overpressures remained practically constant as we varied the intensity of the turbulence, while the maximum rates of pressure rise varied by a factor as high as eight, is proof that the extent of the reaction in our experiments was insensitive to whatever inhomogeneities may have been present and that the observed burning rate variations were associated with turbulence itself. We conclude that the crude experimental set-ups we used to study turbulent dust explosions are adequate for their intended purpose and that efforts to improve the means of suspending the dust by the use of more sophisticated devices can only be of marginal usefulness.

We have established that the relative burning rate increases brought about by turbulence in dust-air explosions are equal to those observed in gas-air explosions performed under identical conditions of turbulent flow. This result is not obvious a priori, since the structure and propagation mechanisms of turbulent flames are expected to differ widely in the two media. Although the proper physical interpretation of this result woud require further studies, it is felt that the result itself demonstrates the usefulness of studying gas-air explosions in conjunction with dust-air explosions. Since the turbulent flow field ahead of a turbulent explosion flame is constantly evolving, and since, in any case, a precise definition of turbulence in the context of a closed vessel without mean flow is difficult, it is felt that it is more meaningful to relate the burning rate of a dust-air explosion to that of a gas-air explosion taking place under identical conditions, than to relate it to some characteristic value of the velocity fluctuations in the unburned mixture prior to ignition.

c) Recommendations for future work

The interesting results obtained in the course of this study have raised more questions than they have answered. While a strong correlation has been observed between the effects of turbulence on dust-air and gas-air explosions in closed vessels, the central questions of the structure and propagation mechanisms of a dust-air flame remain unanswered. It appears, however, that the use of gas explosion as a probe to study dust explosion can help speed up the learning process for the elucidation of these important issues.

A knowledge of the fundamental characteristics of laminar dust-air flames is required before the effects of turbulence on dust explosions displayed in this study can be properly interpreted. It is suggested that flat flame burner studies, concentrating on measurement of the laminar flame thickness and the laminar burning velocity, and evaluation of the modes of energy transport of cornstarch-air flames, could help clarify the relationship between the relevant length and velocity scales of dust-air flames and gas-air flames, and therefore constitute the next logical step in this area of research. While the difficulties of generating a uniform, stable dust-air suspension have plagued this type of studies in the past, it now appears that the fluidized bed techniques developed by

Veyssiere[45] and Peraldi[33] can help overcome these problems and lead to rapid progress in this field.

ii- REFERENCES

1- Corey, R.C. Chemical Engineering, 16 January 1978, pp. 111-119.

2- Sliz, J. First National School on Explosibility of Industrial Dusts. Karpacz, Poland, 1978, pp. 119-126.

3- Kauffman, C.W. Proc. International Meeting on Fuel-Air Explosions, SM Study 16, Eds. C.M. Guirao and J.H. Lee, University of Waterloo Press, Waterloo, 1982.

4- Tipler, W. Power Plants and Future Fuels. Institution of Mechanical Engineers, London, 1976.

5- Andrews, G.E., Bradley, D. and Lwakabamba, S.B. Combustion and Flame, 24, 285-304 (1975).

6- Bradley, D. and Mitcheson, A. Combustion and Flame, 26, 201-217 (1976).

7- Tennekes, H. and Lumley, J.P. A First Course in Turbulence. MIT Press,Cambridge, Massachusetts, 1972.

8- Tennekes, H. Physics of Fluids, 11, 669-670 (1968).

9- Tabaczynski, R.J., Ferguson, C.R. and Radhakrishnan,K. SAE Paper no. 770647, 1977.

10- Hires, S.D., Tabaczynski, R.J. and Novak, J.H. SAE Paper no. 780232, 1978.

11- Tabaczynski, R.J., Trinker, F.H. and Shannon, B.A. Ford Motor Company, 1978.

12- Ohta, Y. Proceedings of Workshop on the Gas Flame Structure, Novosibirsk, U.S.S.R., 1984.

13- Chomiak, J. Prog. Energy Combust. Sci., 5, 207-221 (1979).

14- Damkohler, G. Zeitschrift Electrochemie Angewandte Phys. Chem., 46, 601 (1940). (English translation NACA TM 1112 (1947))

15- Abdel-Gayed, R.G. and Bradley, D. Phil. Trans. Roy. Soc. London, 301, A1457, 1981.

16- Williams, F.A. Combustion and Flame, 26, 269-270 (1976).

17- Gaydon, A.G. and Wolfhard, H.G. Flames - Their Structure, Radiation and Temperature. Chapman and Hall, London, 1960.

18- Smoot, L.D. Private communication.

19- Mason, W.E. and Wilson, M.J.G. Combustion and Flame, 11, 195-200 (1967).

20- Bartknecht, W. Explosions - Course - Prevention - Protection. Springer Verlag, New York, 1980.

21- Karlovitz, B. 4th Symposium (International) on Combustion, Cambridge, Massachusetts, 1952.

22- Moore, P.E. Chemistry and Industry, p. 430, 1979.

23- Moore, P.E. I. Chem. E. Symposium Series no. 58, Rugby, 1980.

24- Bartknecht, W. Staub Reinhaltung der Luft, 31, 28 (1971).

25- Eckhoff, R.K. First International Colloquium on the Explosibility of Industrial Dusts. Baranow, Poland, 1984.

26- Cocks, R.E. and Meyer, R.C. Fabrication and Use of a 20 liter Spherical Dust Testing Apparatus. Process Specialties Section, Engineering Division, Procter and Gamble, Cincinnati, Ohio.

27- Swift, I. Proc. International Meeting on Fuel-Air Explosions, SM Study 16, Eds. C.M. Guirao and J.H. Lee, University of Waterloo Press, Waterloo, 1982.

28- Reeh, D. Staub Reinhaltung der Luft, 31, 12-21 (1971).

29- Nagy, J. and Portman, W.M. U.S. Bureau of Mines R.I. 5815, 1961.

30- Harris, G.F.P. Combustion and Flame, 11, 17-25 (1967).

31- Abdel-Gayed, R.G., Al-Khishali, K.J. and Bradley, D. Proc. Roy. Soc. London, A391, 393-414 (1984).

32- Kauffman, C.W., Srinath, S.R., Tezok, F.I., Nicholls, J.A. and Sichel, M. 20th Symposium (International) on Combustion, Ann Arbor, Michigan, 1984.

33- Peraldi, O. These de Docteur Ingenieur, Universite de Poitiers, 1985.

34- Lewellen, P.C., Peters, W.A. and Howard, J.B. 16th Symposium (International) on Combustion, Cambridge, Massachusetts, 1976.

35- Gordon, S. and McBride, B.J. Computer Program for Calculation of Complex Chemical Equilibrium Compositions, Rocket Performance, Incident and Reflected Shocks, and Chapman-Jouguet Detonations. National Aeronautics and Space Administration, Washington, 1971.

36- Lee, J.H.S. Phenomenology of Gas Explosions. McGill University, Montreal, 1980.

37- Marble, F.E. Proc. 5th AGARD Colloq. Combust. Propul., Braunschweig, pp. 175-213, 1962.

38- Andrews, G.E. and Bradley, D. Combustion and Flame, 19, 275-288 (1972).

39- Nagy, J., Seiler, E.C., Conn, J.W. and Verakis, H.C. U.S. Bureau of Mines R.I. 7507, 1971.

40- Hartmann, I., Cooper, A.R. and Jacobson, M. U.S. Bureau of Mines R.I. 4725, 1951.

41- Bryant, J.T. Combustion and Flame, 20, 138-139 (1973).

42- Beer, J.M., Chomiak, J. and Smoot, L.D. Prog. Energy Combust. Sci., 10, 177-208 (1984).

43- Tsuge, M., Kido, H. and Yanagihara, H. Bulletin of the J.S.M.E., 16, 244-251 (1973).

44- Tsuge, M., Kido, H., Kato, K. and Nomiyama, Y. Bulletin of the J.S.M.E., 17, 587-594 (1974).

45- Veyssiere, B. These de Docteur Ingenieur, Universite de Poitiers, 1978.

iii- LIST OF FIGURES

1- Length scales involved in turbulent dust flame propagation

2- 333 liter spherical apparatus (schematic)

3- 180 liter cylindrical vessel

4a- Turbulence ring

4b- Turbulence pipe

5- Scope record of dust explosion

6- S.E.M. picture of cornstarch

7- Maximum explosion overpressure versus cornstarch concentration

8- K_{st} versus cornstarch concentration

9- Variation of maximum explosion pressure with ignition delay

10- Variation of normalized K factor with ignition delay

11- Effect of turbulence decay time on K_{st} ratio

12- Effect of normalized turbulence decay time on K_{st} ratio

13- Comparison of time of flame arrival and time of maximum pressure for 7.5% methane-air explosions with varying ignition delay

14- Effect of dispersion bottle pressure on P_{max} in the 333 liter spherical vessel

15- Effect of dispersion bottle pressure on maximum burning rates in the 333 liter spherical vessel

16- Effect of bottle pressure on P_{max} in 180 liter cylindrical vessel

17- Effect of bottle pressure on maximum burning rates in the 180 liter cylindrical vessel

18- Effect of dispersion characteristics on maximum K factor observed in gas-air experiments

19- Effect of ring jet flow rate on P_{max} in 7.5% methane-air explosions in the 333 liter spherical vessel

20- Effect of ring jet flow rate on maximum rate of pressure rise in 7.5% methane-air explosions in the 333 liter spherical vessel

21a- Scope record of 7.5% methane-air explosion with ring jets, without dispersion blast

21b- Scope record of 7.5% methane-air explosion with ring jets, with dispersion blast

22- Effect of ring jet flow rate on P_{max} in the 333 liter spherical vessel

23- Effect of ring jet flow rate on maximum burning rates in the 333 liter spherical vessel

24- Effect of pipe jet flow rate on P_{max} in the 333 liter spherical vessel

25- Effect of pipe jet flow rate on the maximum burning rates in the 333 liter spherical vessel

26- Relationship between dust burning rate and methane burning rate in identical turbulent flow situations

27- Variation of turbulent burning velocity with turbulent r.m.s. velocity, for starch and methane explosion in the 333 liter spherical vessel with jet-induced turbulence

iv- FIGURES

FIGURE 1 - LENGTH SCALES INVOLVED IN TURBULENT DUST FLAME PROPAGATION

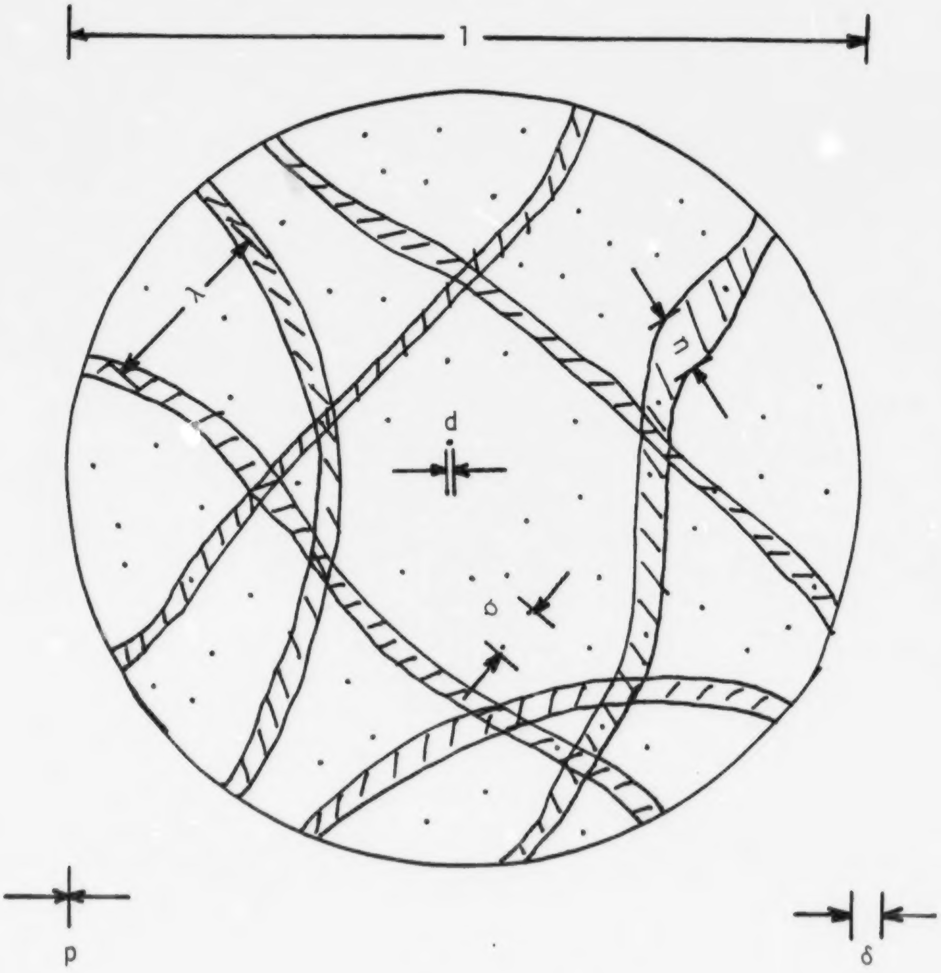

LENGTH SCALE	SYMBOL	ORDER OF MAGNITUDE
INTEGRAL LENGTH SCALE	1	10^{-2} m
TAYLOR MICROSCALE	λ	10^{-3} m
KOLMOGOROFF SCALE	η	10^{-4} m
PARTICLE SIZE	d	1.5×10^{-5} m
INTER-PARTICLE SPACING	σ	1.5×10^{-4} m
THICKNESS OF LAMINAR GAS FLAME	δ	10^{-4} m
MOLECULAR MEAN FREE PATH	p	10^{-8} m

TEST APPARATUS
$(V = 0{,}333\ m^3)$

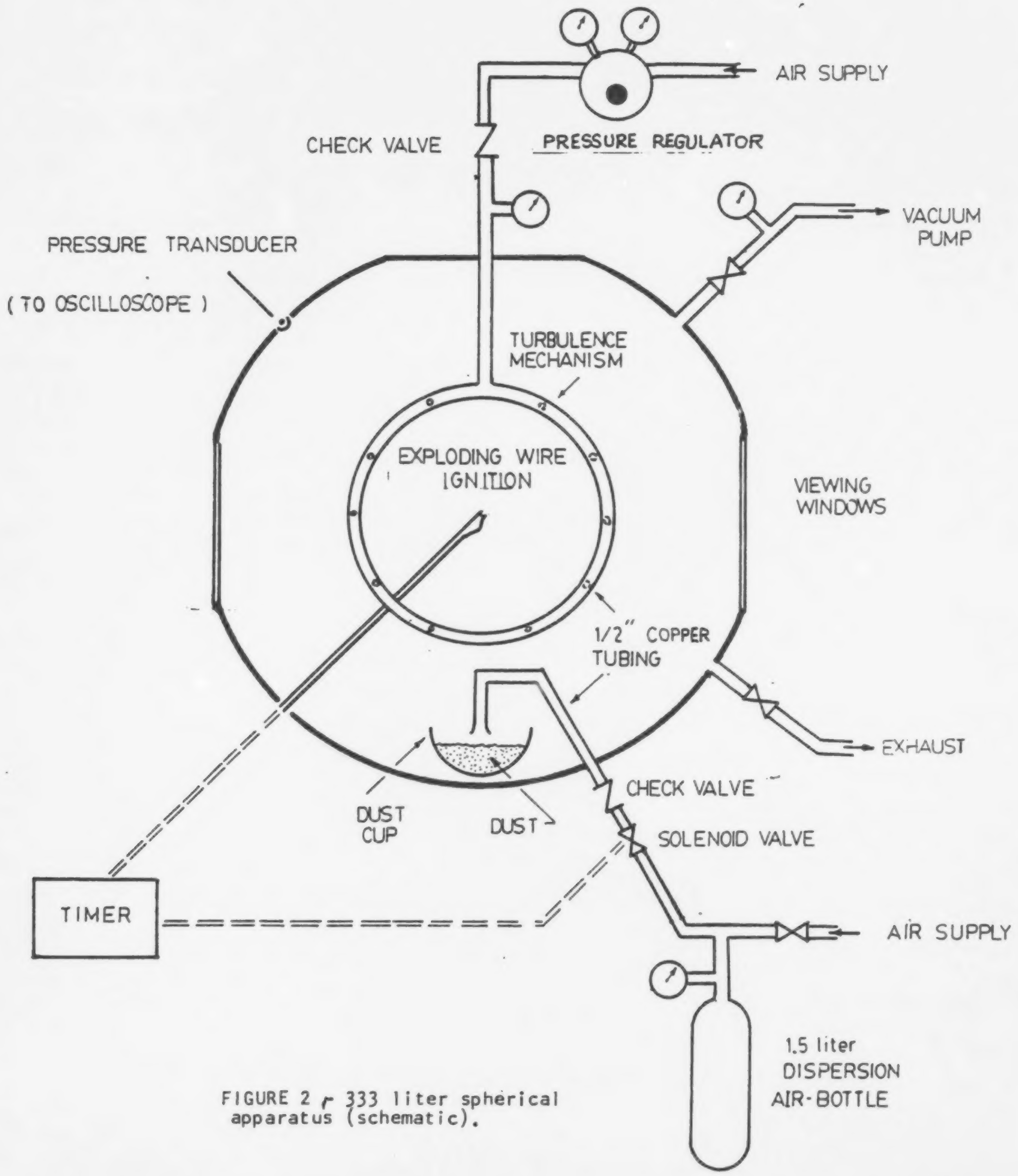
AIR SUPPLY
CHECK VALVE
PRESSURE REGULATOR
VACUUM PUMP
PRESSURE TRANSDUCER
(TO OSCILLOSCOPE)
TURBULENCE MECHANISM
EXPLODING WIRE IGNITION
VIEWING WINDOWS
1/2" COPPER TUBING
EXHAUST
CHECK VALVE
DUST CUP
DUST
SOLENOID VALVE
TIMER
AIR SUPPLY
1.5 liter DISPERSION AIR-BOTTLE

FIGURE 2 - 333 liter spherical apparatus (schematic).

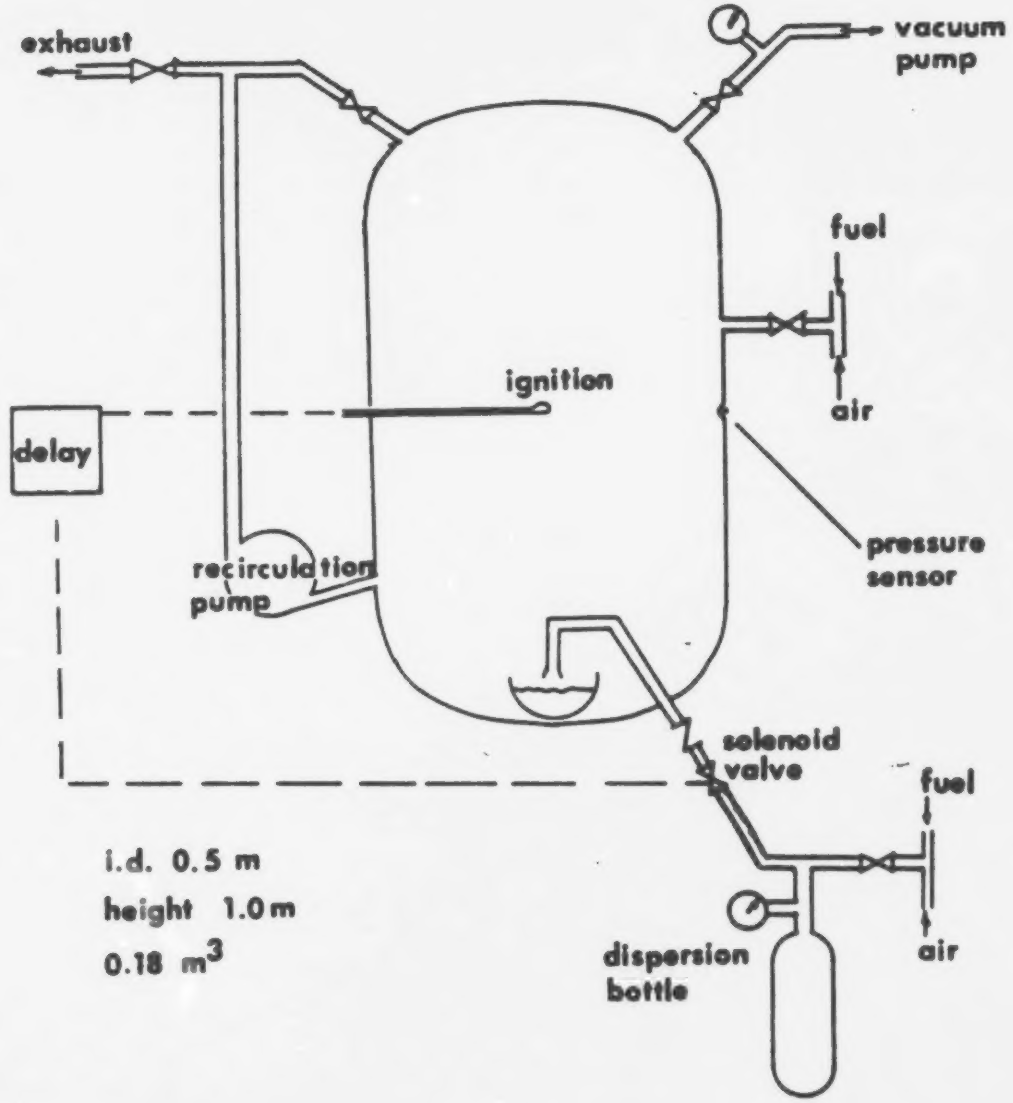
exhaust
vacuum pump
fuel
air
ignition
delay
pressure sensor
recirculation pump
solenoid valve
fuel
air
dispersion bottle
i.d. 0.5 m
height 1.0 m
0.18 m³

FIGURE 3 - 180-liter cylindrical vessel

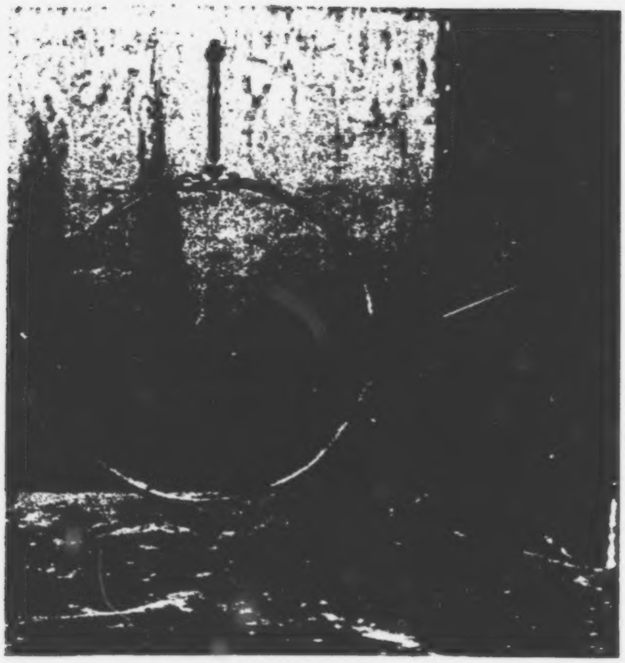

FIGURE 4a - Turbulence ring

FIGURE 4b - Turbulence pipe

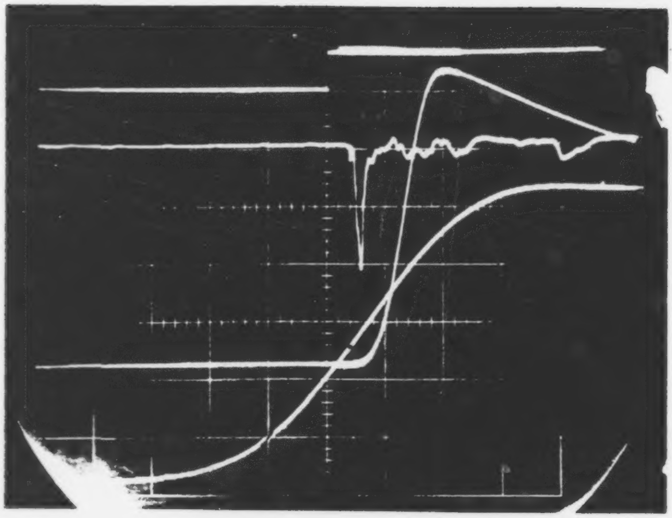

FIGURE 5 - Scope record of a dust explosion. The first and third trace (starting from the top) are triggered upon dispersion and sweep at 0.1 second per division. The second and fourth trace are triggered 0.5 seconds after dispersion and sweep at 0.01 second per division. Trace 1 is a witness trace showing the moment of ignition. Trace 2 is the ion probe record. Traces 3 and 4 show pressure, at 100 kPa per vertical scope division.

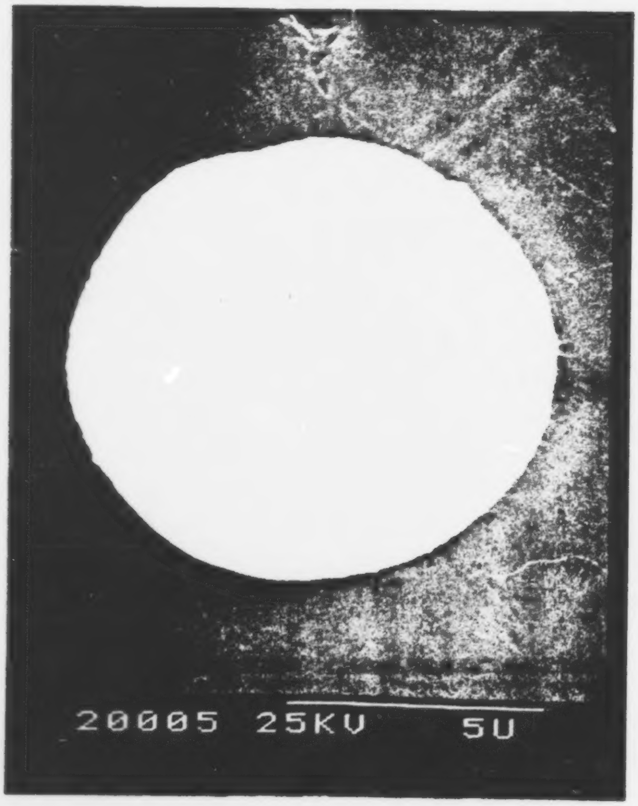

FIGURE 6 - S.E.M. photograph of cornstarch particle.

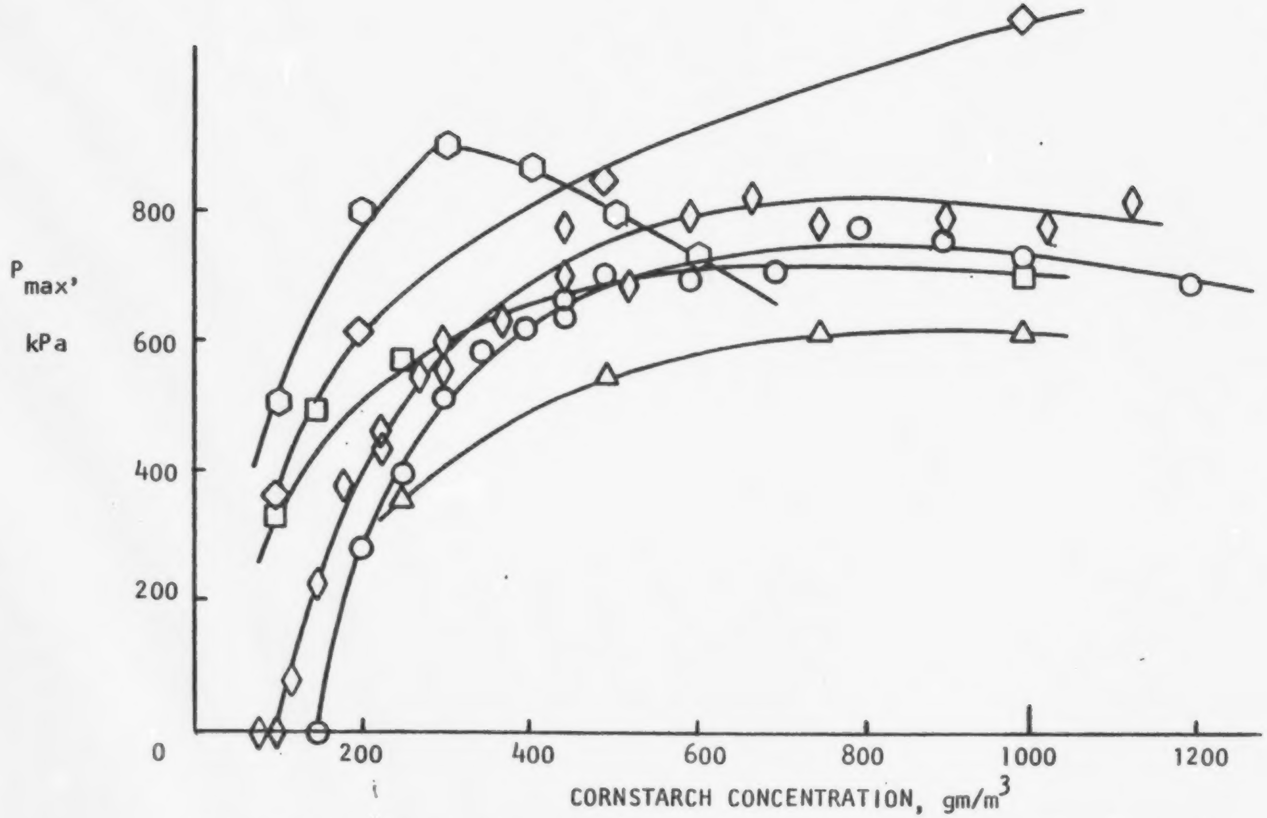

FIGURE 7 - Maximum explosion overpressure versus cornstarch concentration. ◊ McGill 0.333 m^3. ○ McGill 0.180 m^3. △ Cocks and Meyer 0.020 m^3. ◇ Hartmann 0.00123 m^3. □ Nagy 0.00123 m^3. ⬡ Theoretical value calculated from NASA code for adiabatic combustion.

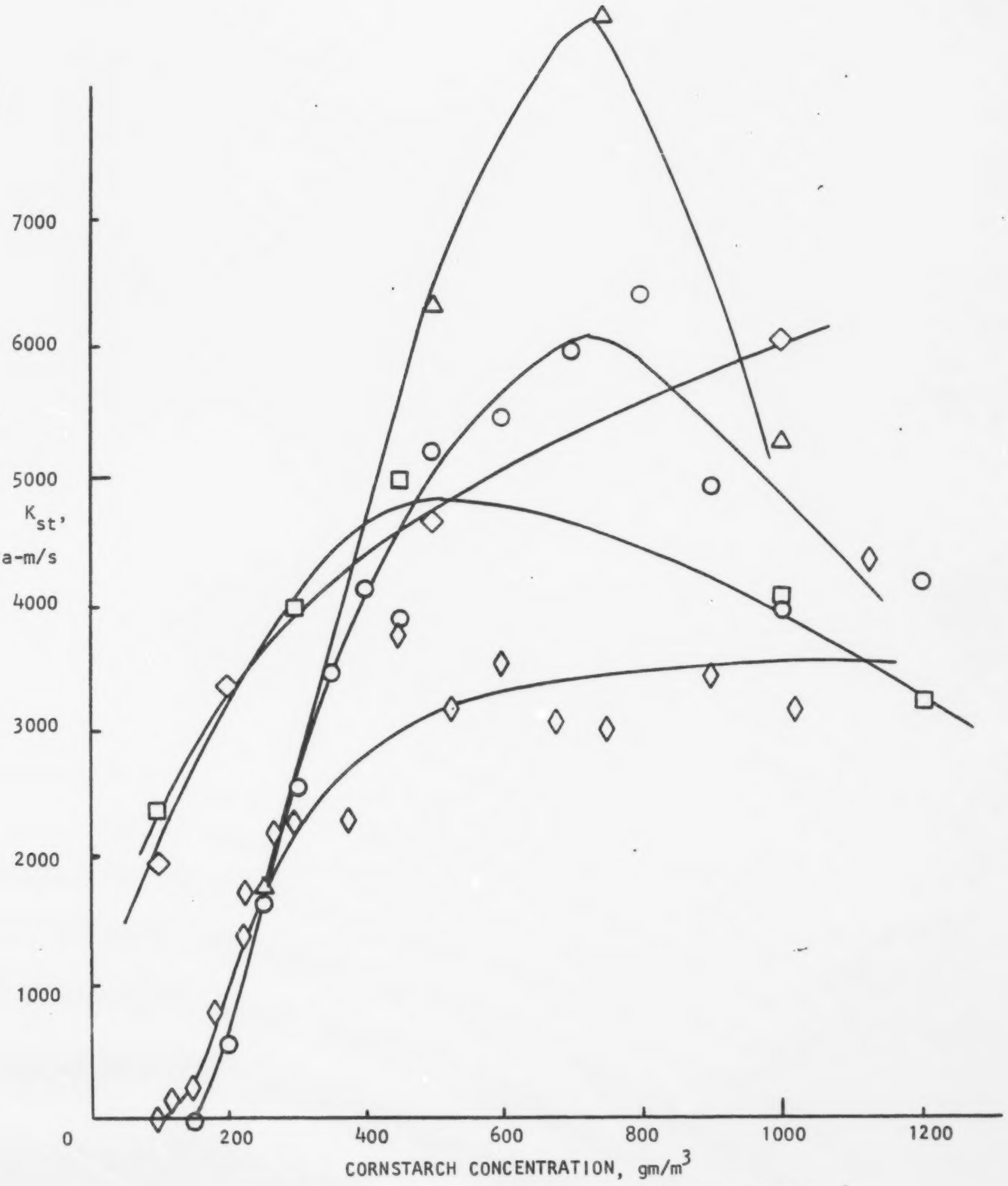

FIGURE 8 - K_{st} versus cornstarch concentration. ◊ McGill 0.333 m^3. ○ McGill 0.180 m^3. △ Cocks and Meyer 0.020 m^3. ◇ Hartmann 0.00123 m^3. □ Nagy 0.00123 m^3.

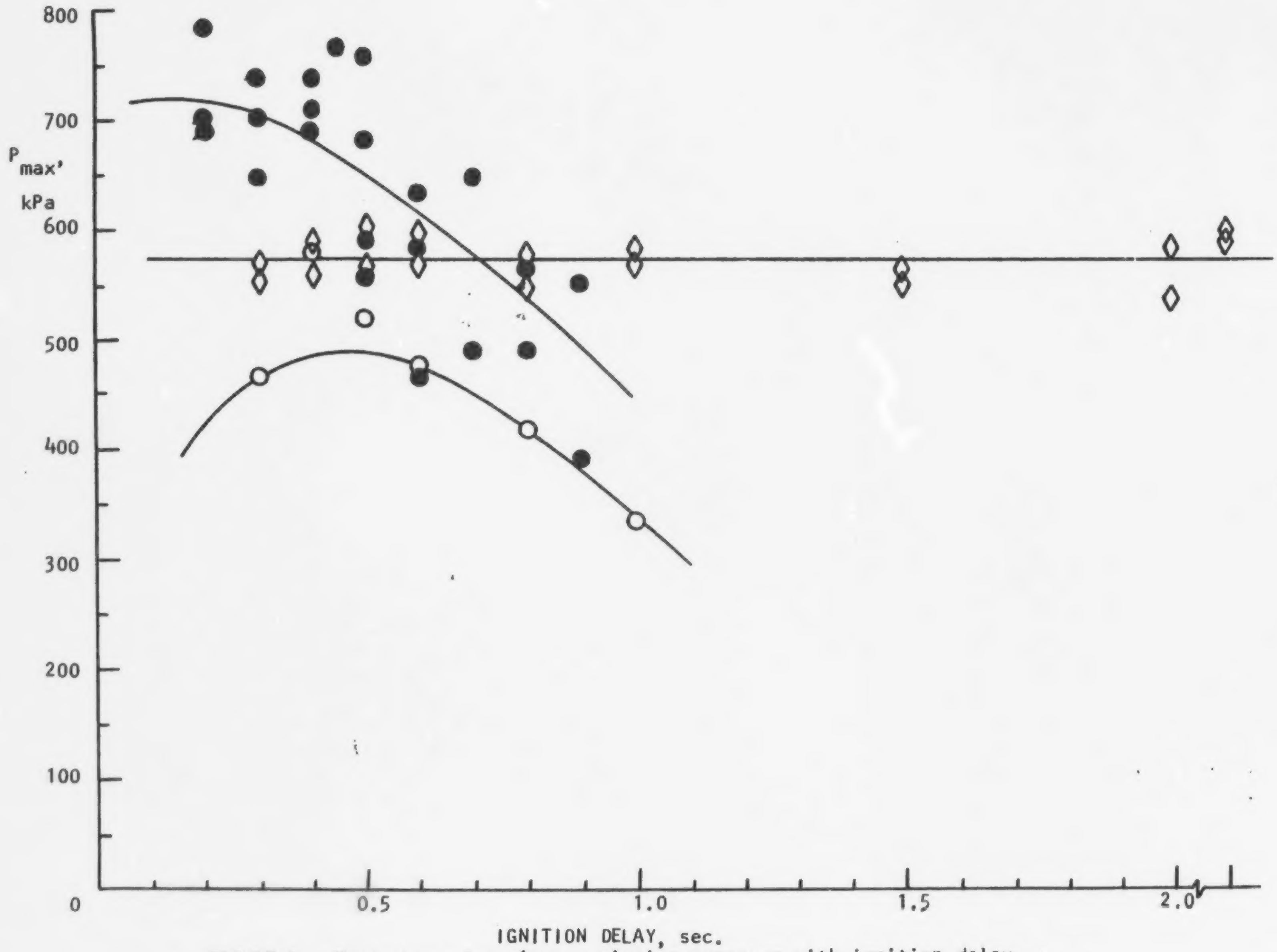

FIGURE 9 - Variation of maximum explosion pressure with ignition delay. ● 450 gm/m^3 starch-air in 333 liter sphere. ◊ 7.5% methane-air in 333 liter sphere. ○ 300 gm/m^3 starch-air in 180 liter cylinder.

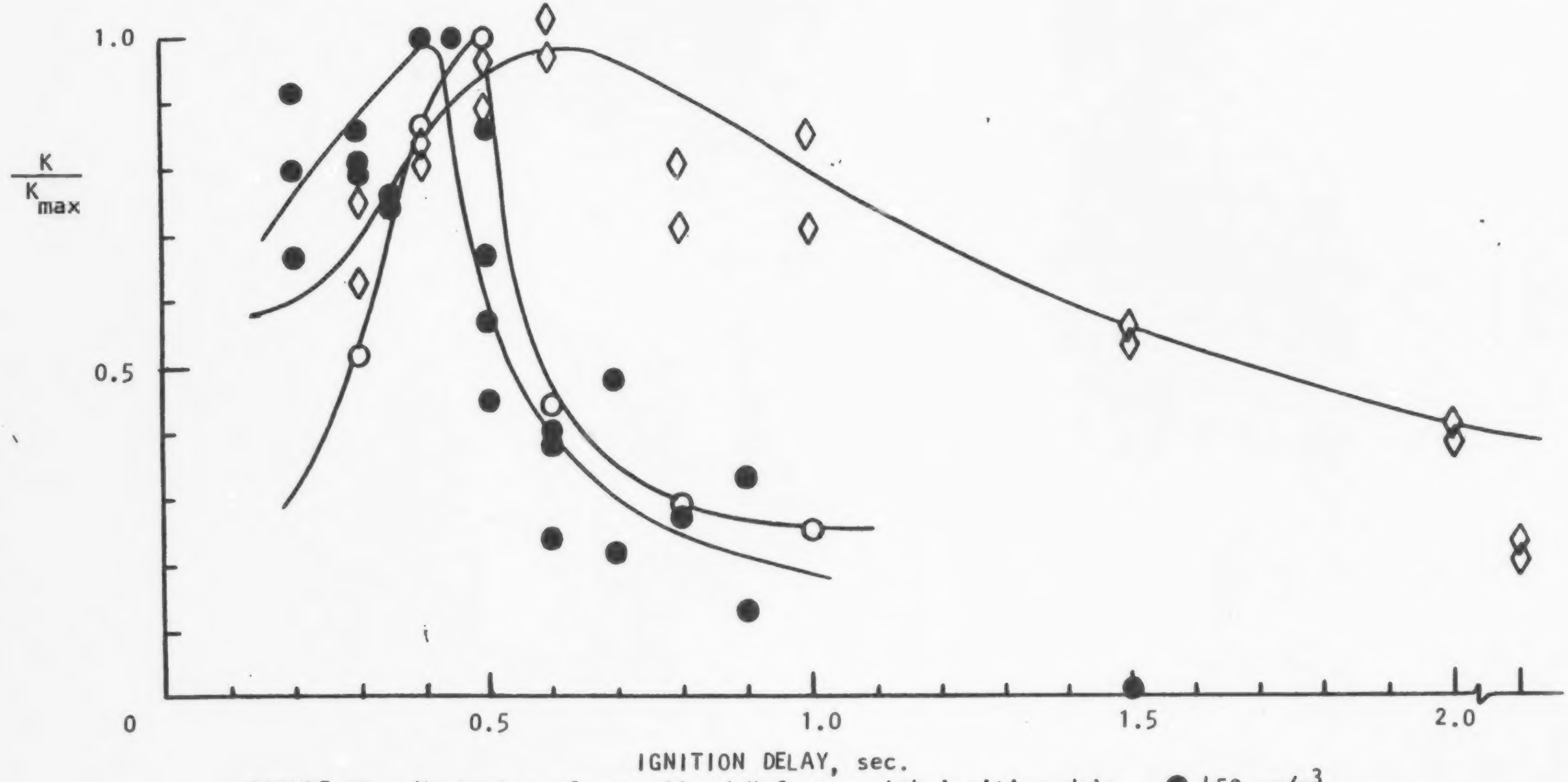

FIGURE 10 - Variation of normalized K factor with ignition delay. ● 450 gm/m^3 starch-air in 333 liter sphere. ◇ 7.5% methane-air in 333 liter sphere. ○ 300 gm/m^3 starch-air in 180 liter cylinder.

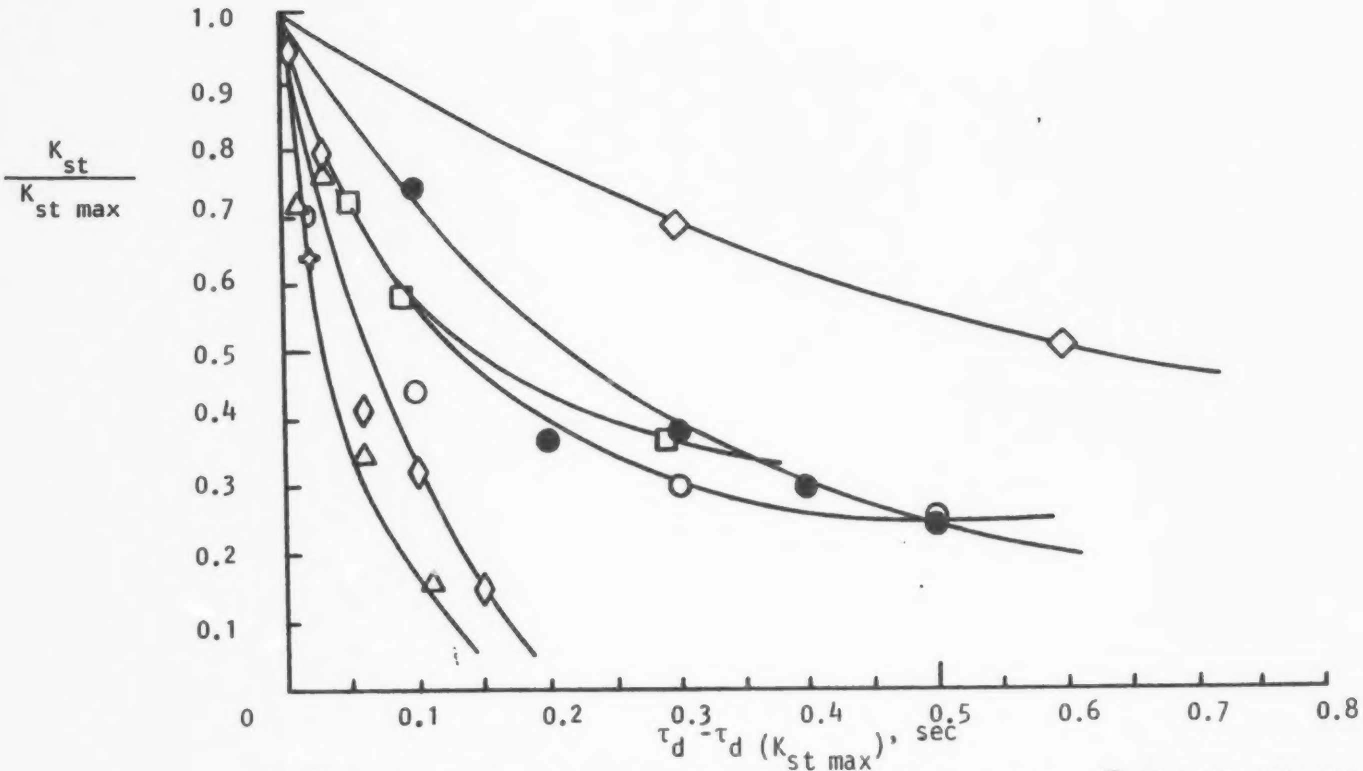

FIGURE 11 - Effect of turbulence decay time on K_{st} ratio. ● McGill, 333 liter sphere (D=0.90 m). ○ McGill, 180 liter cylinder (D=0.50 m). □ Moore, 43 liter sphere (D=0.435 m). ◇ Bartknecht, 1 cu. meter cylinder (D=1.084 m). △ Eckhoff, 1.2 liter cylinder (D=0.07 m). ◊ Moore, 1.75 liter cylinder (D=0.136 m). ✥ Cocks and Meyer, 20 liter sphere (D=0.337 m). O Swift, 26 liter sphere (D=0.368 m).

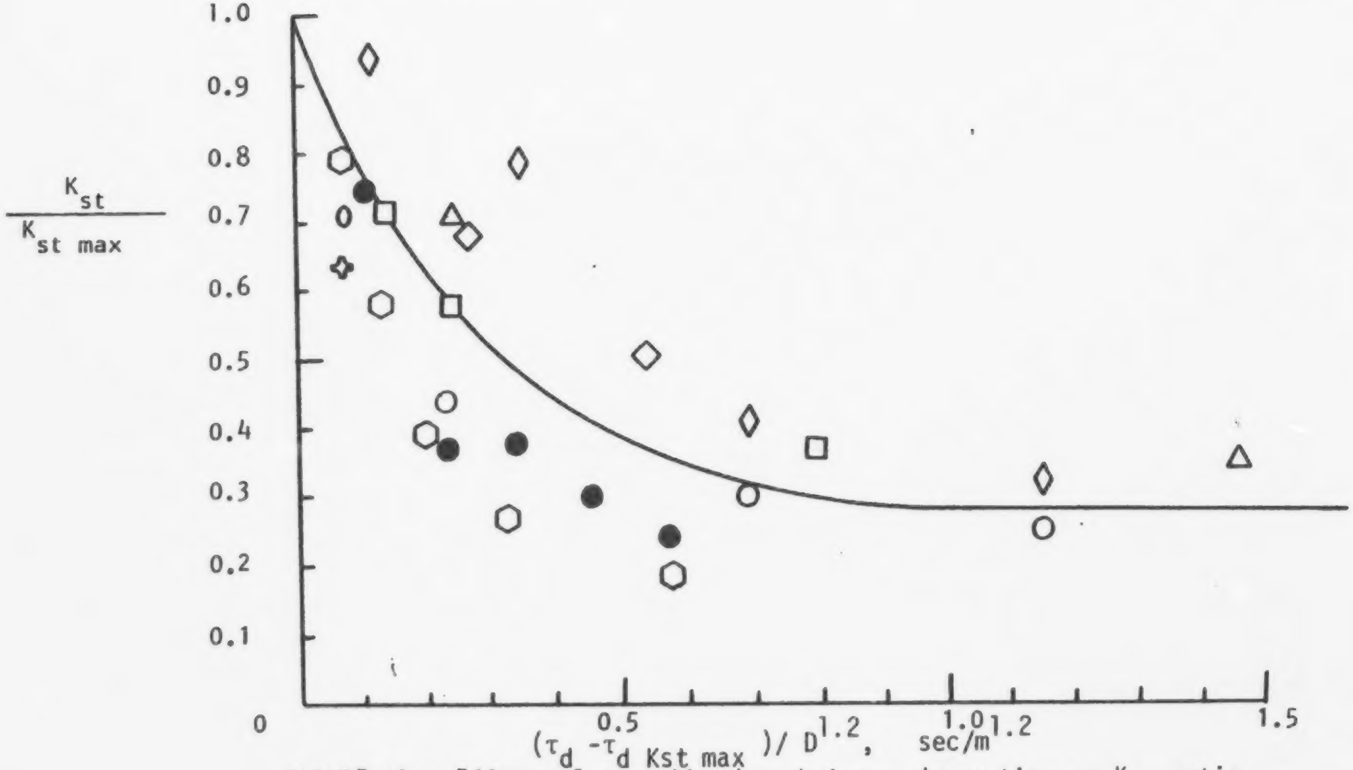

FIGURE 12 - Effect of normalized turbulence decay time on K_{st} ratio. ● McGill, 333 liter sphere (D=0.90 m). ○ McGill, 180 liter cylinder (D=0.50 m). □ Moore, 43 liter sphere (D=0.435 m). ◇ Bartknecht, 1 cu. meter cylinder (D=1.084 m). △ Eckhoff, 1.2 liter cylinder (D=0.07 m). ◊ Moore, 1.75 liter cylinder (D=0.136 m). ✤ Cocks and Meyer, 20 liter sphere (D=0.337 m). 0 Swift, 26 liter sphere (D=0.368 m). ⬡ Reeh, 115 liter cylinder (D=0.46 m).

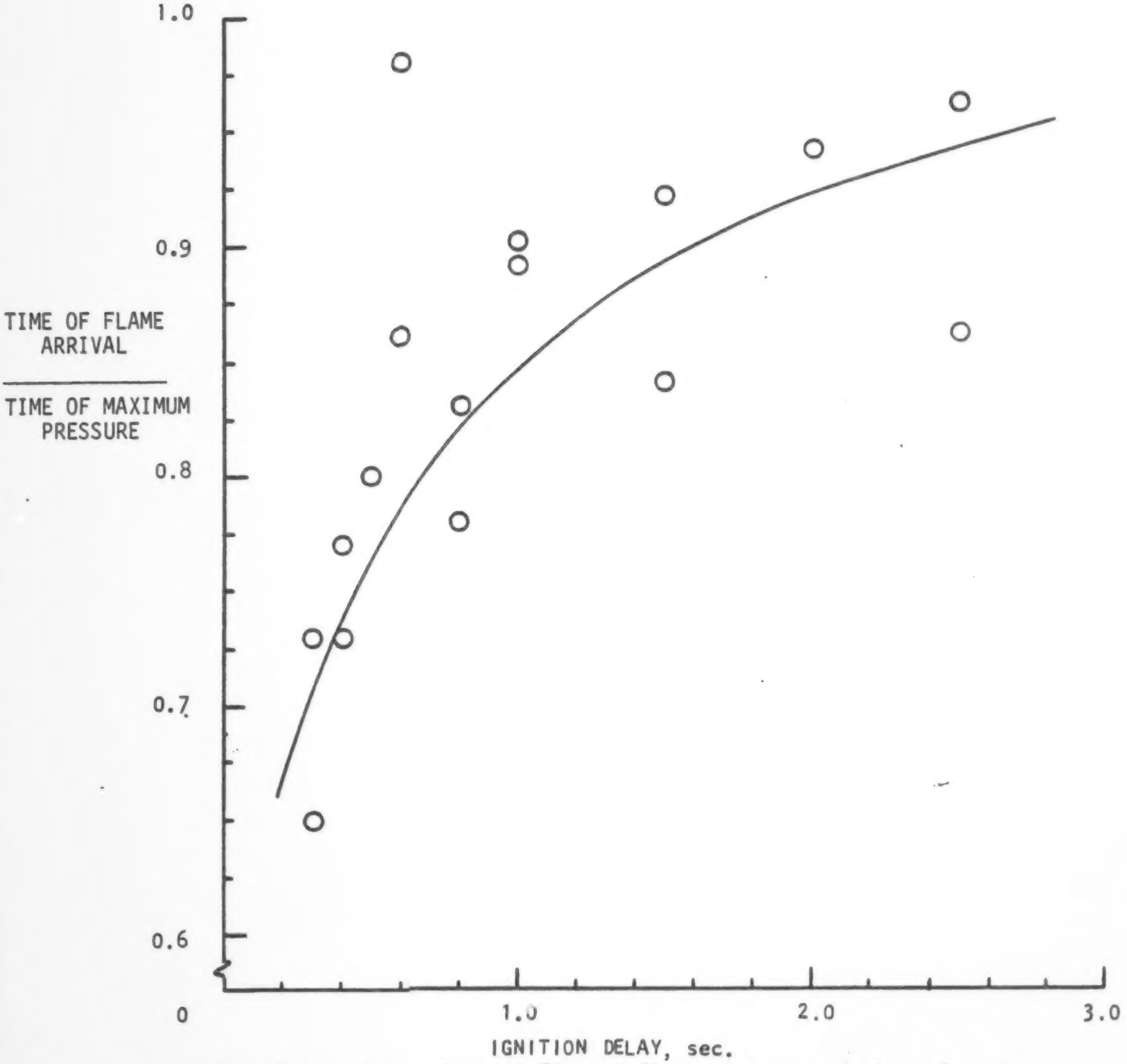

FIGURE 13 - Comparison of Time of flame arrival and time of maximum pressure for 7.5% methane-air explosions with varying ignition delay.

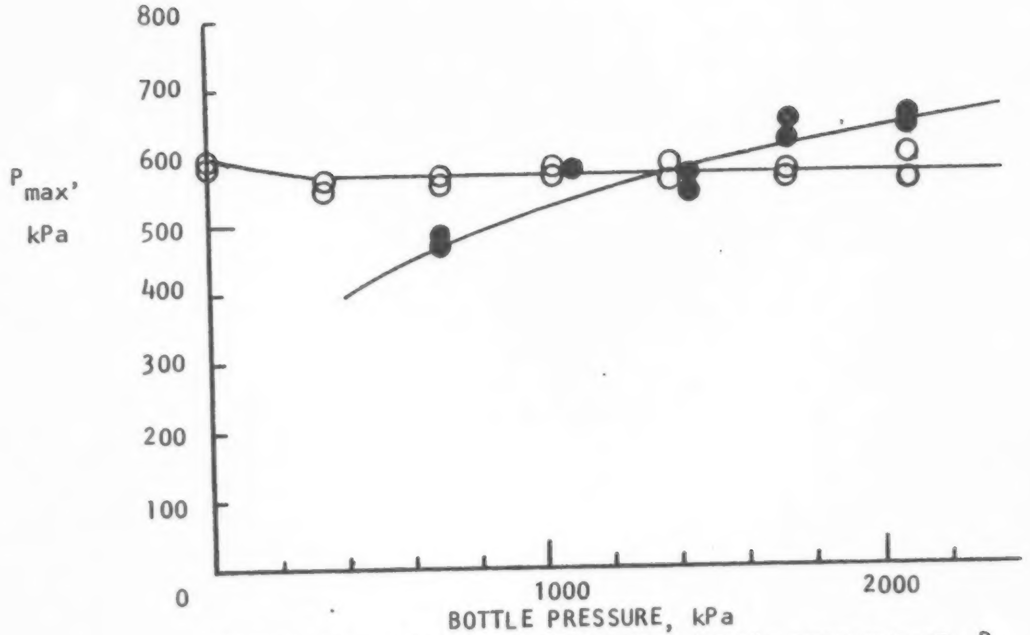

FIGURE 14 - Effect of dispersion bottle pressure on P_{max} in the 333 liter spherical vessel. ○ 7.5% methane-air. ● 300 gm/m^3 cornstarch-air.

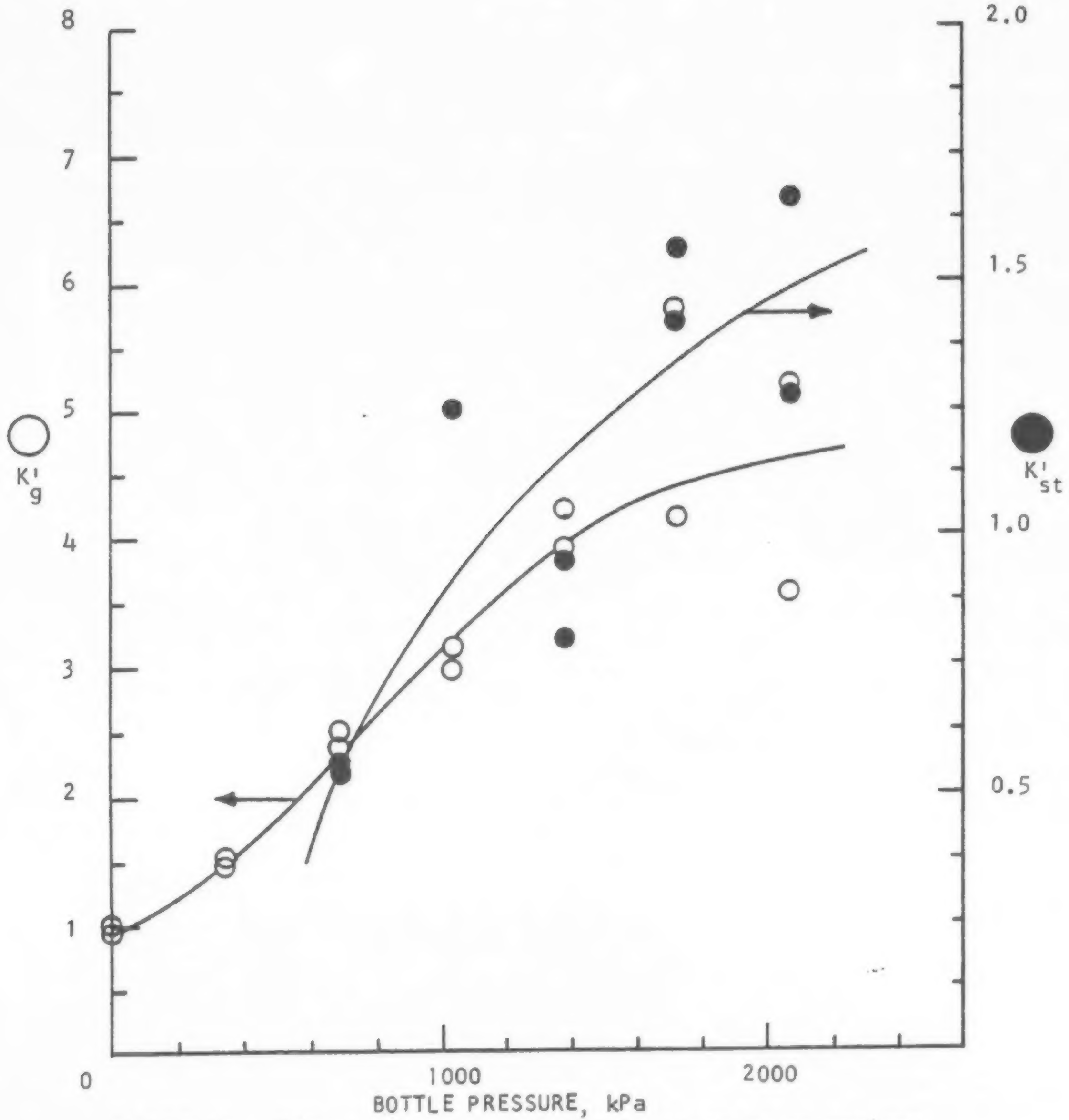

FIGURE 15 - Effect of dispersion bottle pressure on maximum burning rates in 333 liter spherical vessel. ○ 7.5% methane-air. ● 300 gm/m^3 cornstarch-air.

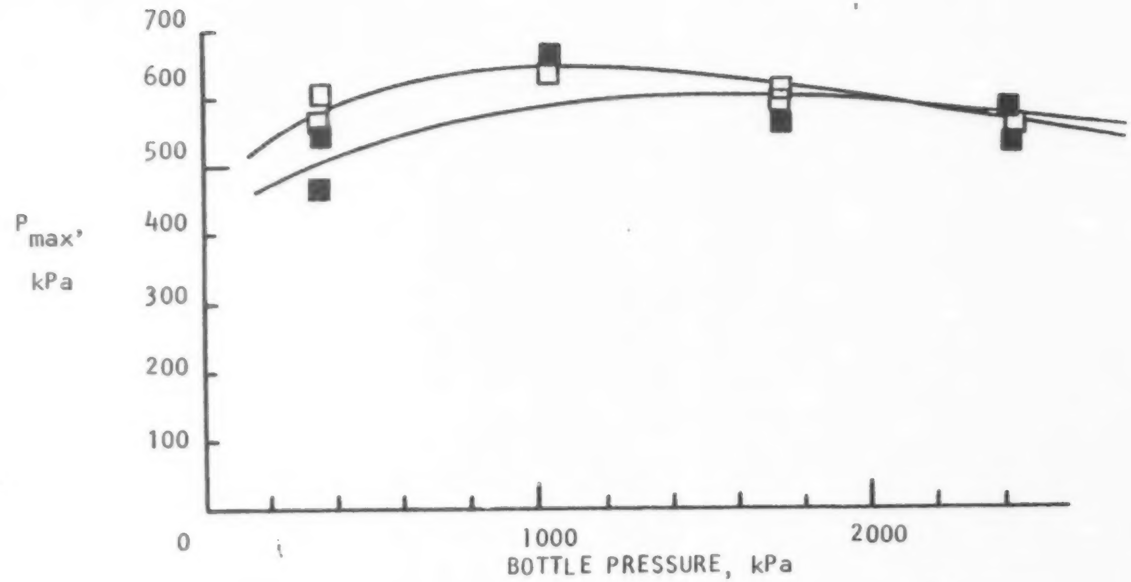

FIGURE 16 - Effect of bottle pressure on P_{max} in 180 liter cylindrical vessel. □ 7.5% methane-air. ■ 300 gm/m^3 cornstarch-air.

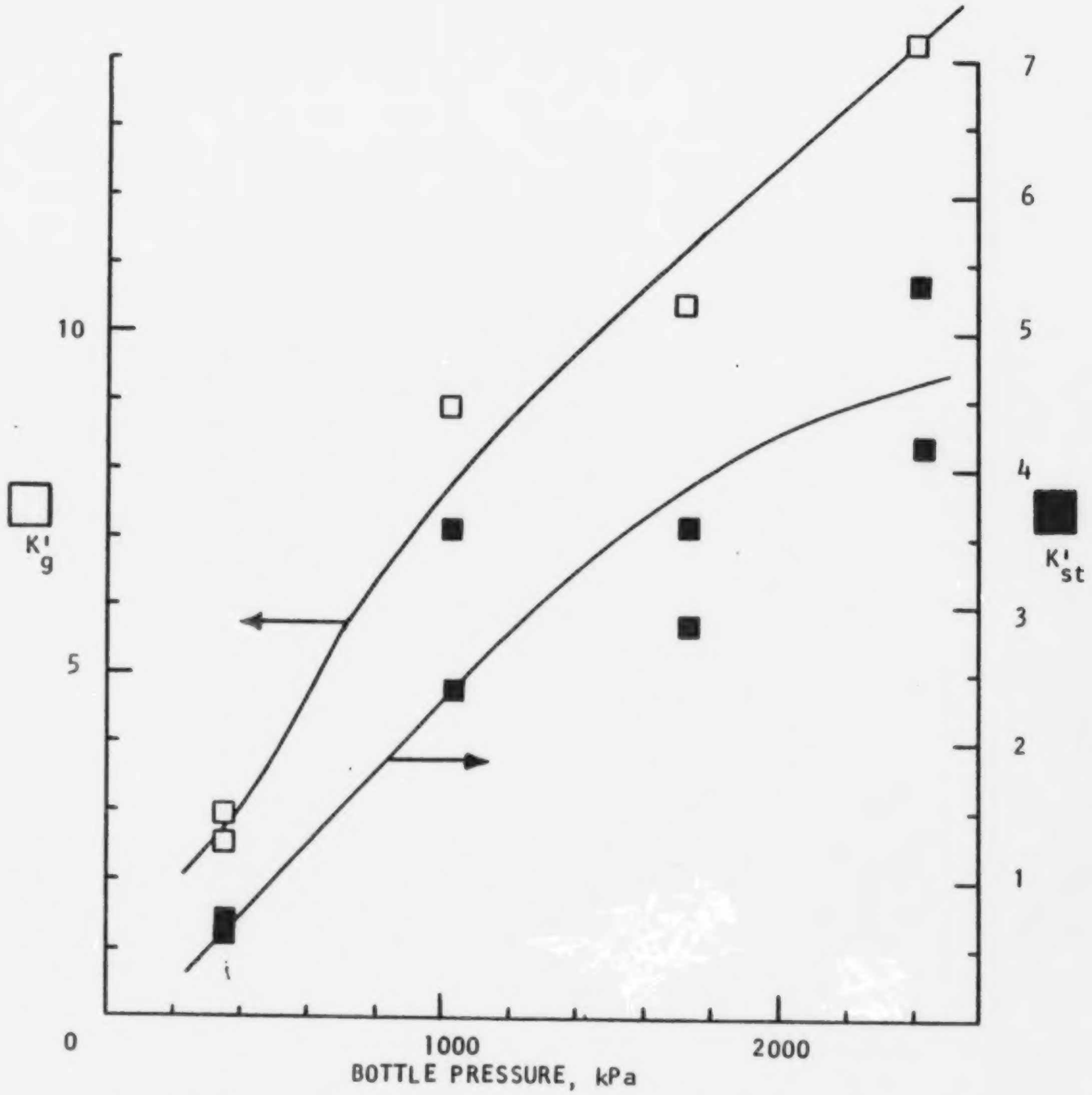

FIGURE 17 - Effect of bottle pressure on maximum burning rates in the 180 liter cylindrical vessel. □ 7.5% methane-air. ■ 300 gm/m^3 cornstarch-air.

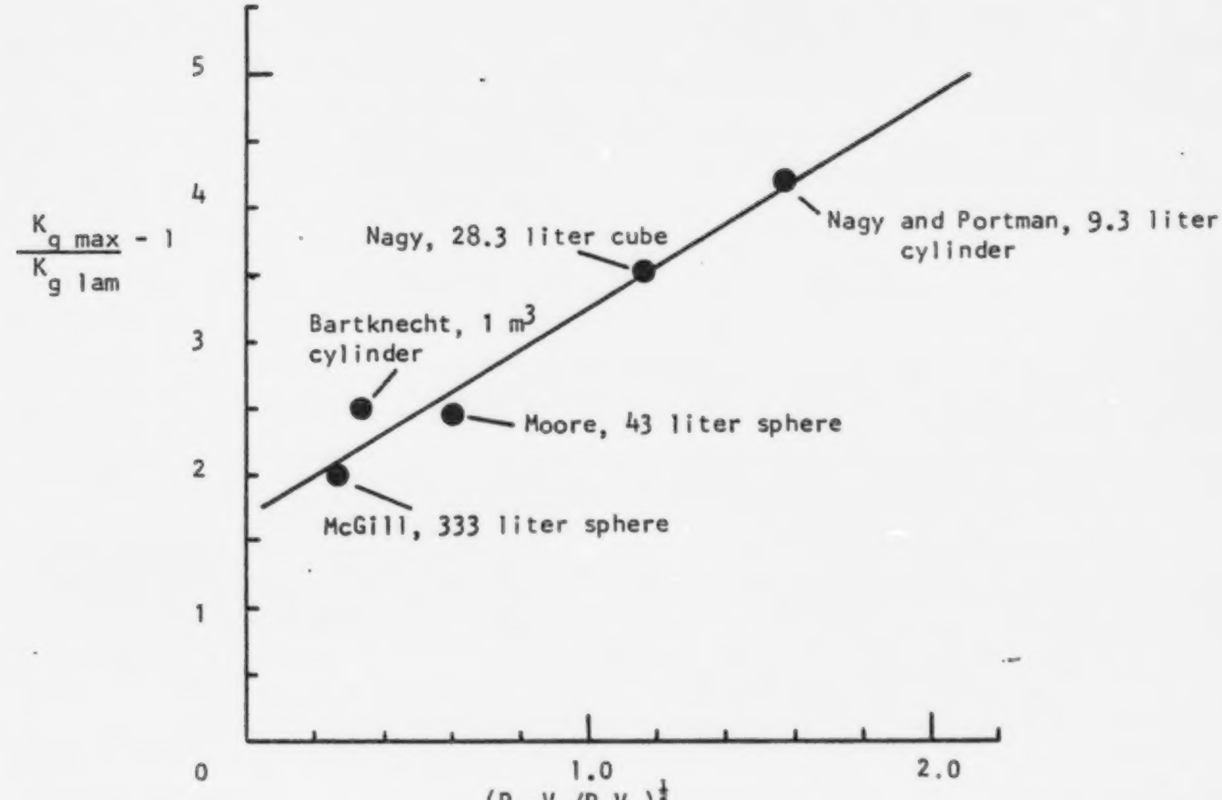

FIGURE 18 - Effect of dispersion characteristics on maximum K_g factor observed in gas-air experiments.

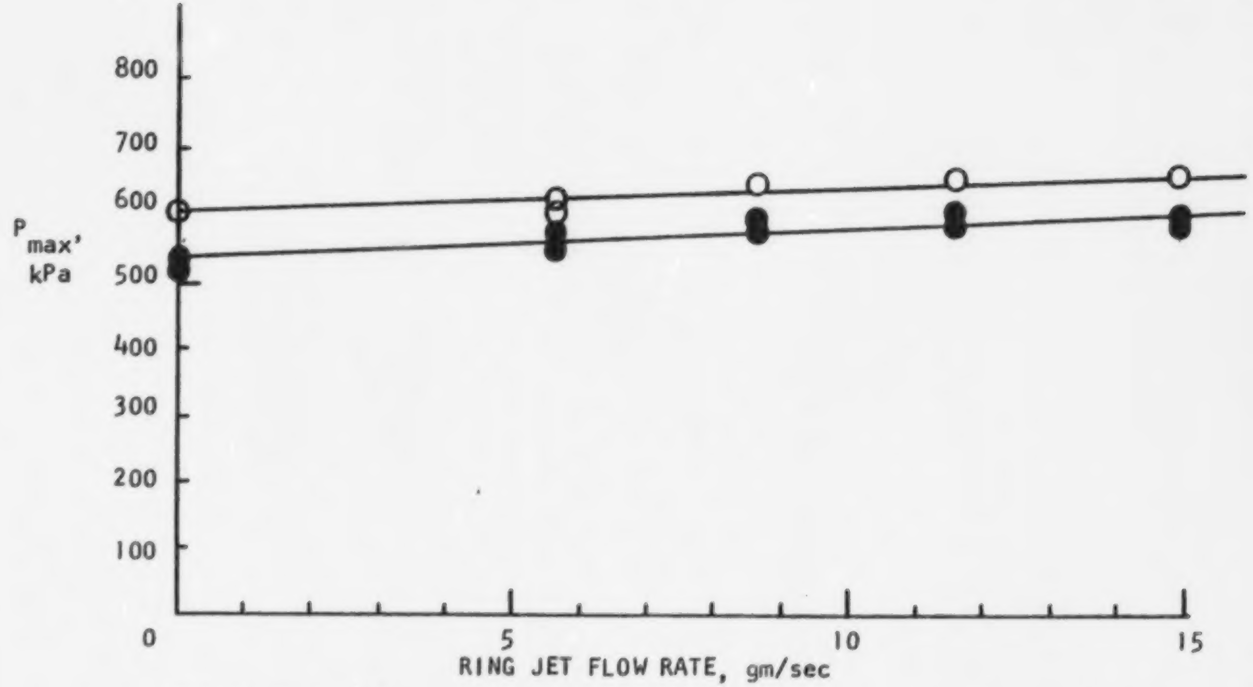

FIGURE 19 - Effect of ring jet flow rate on P_{max} in 7.5% methane-air explosions in the 333 liter spherical vessel. ● with dispersion blast. ○ without dispersion blast.

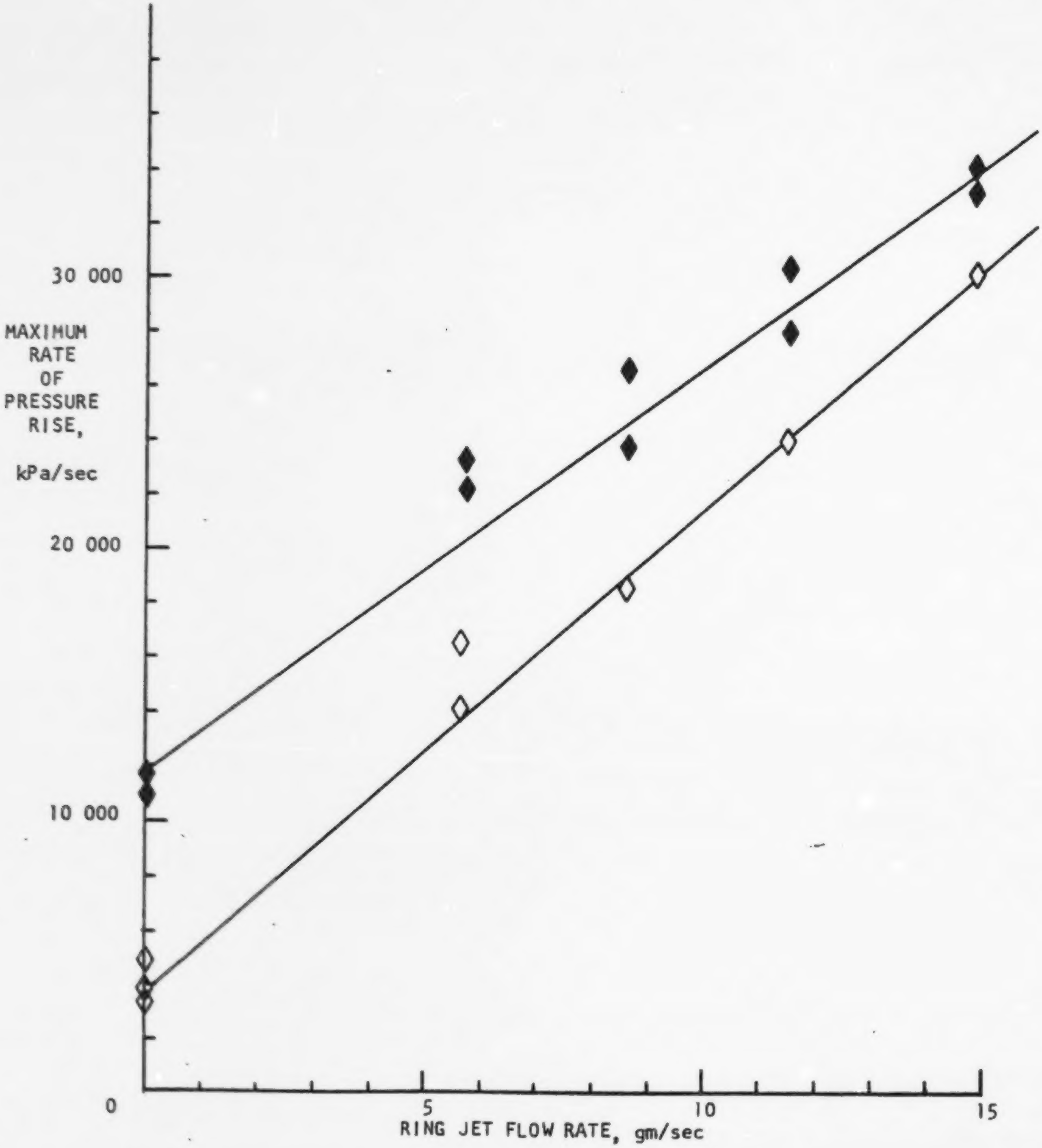

FIGURE 20 - Effect of ring jet flow rate on maximum rate of pressure rise in 7.5% methane-air explosions in the 333 liter spherical vessel. ◆ with dispersion blast. ◇ without dispersion blast.

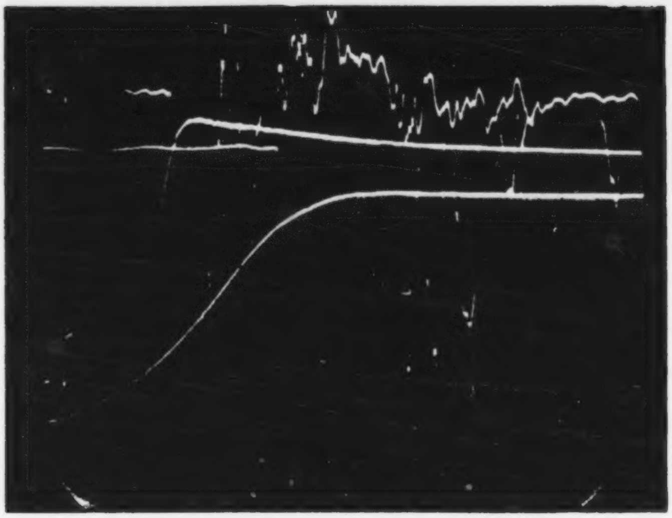

FIGURE 21a - Scope record of 7.5% methane-air explosion with ring jets, without dispersion blast.

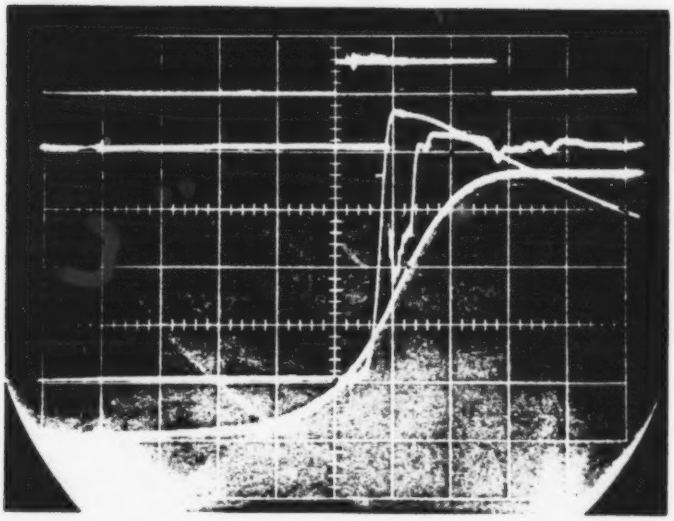

Figure 21b - Scope record of 7.5% methane-air explosion with ring jets, with dispersion blast.

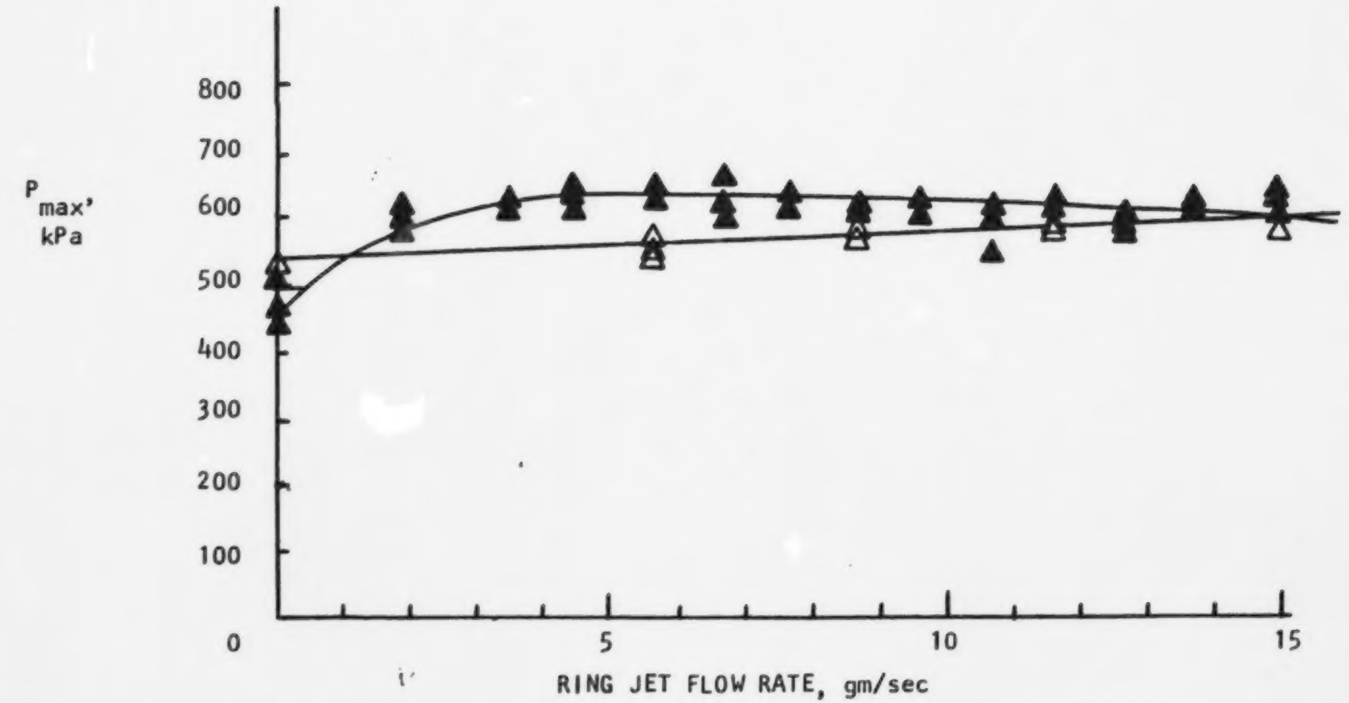

FIGURE 22 - Effect of ring jet flow rate on P_{max} in the 333 liter spherical vessel. △ 7.5% methane-air. ▲ 300 gm/m^3 cornstarch-air.

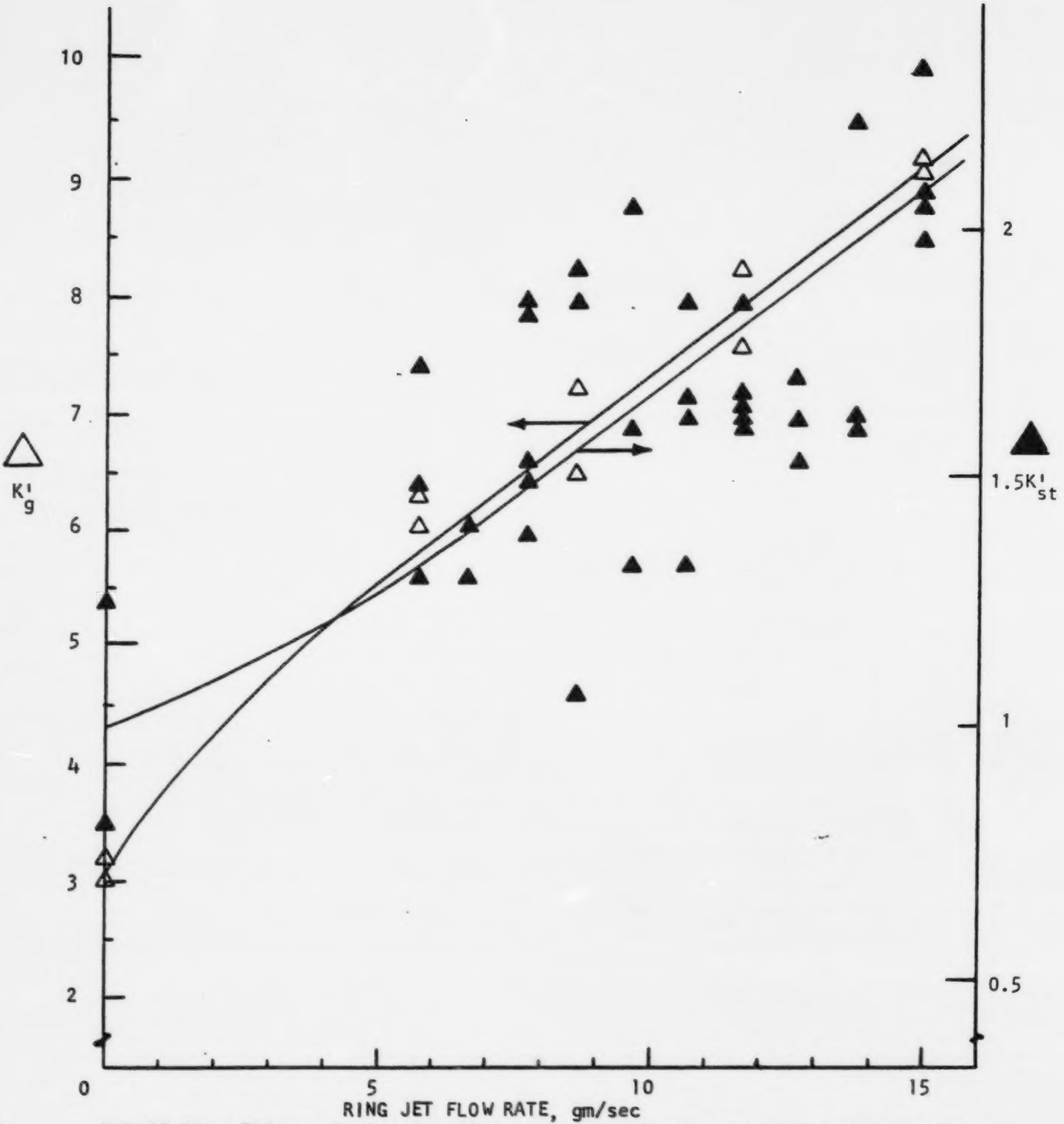

FIGURE 23 - Effect of air mass flow rate through the turbulence ring on the maximum burning rates in the 333 liter spherical vessel. △ 7.5% methane-air. ▲ 300 gm/m^3 cornstarch-air.

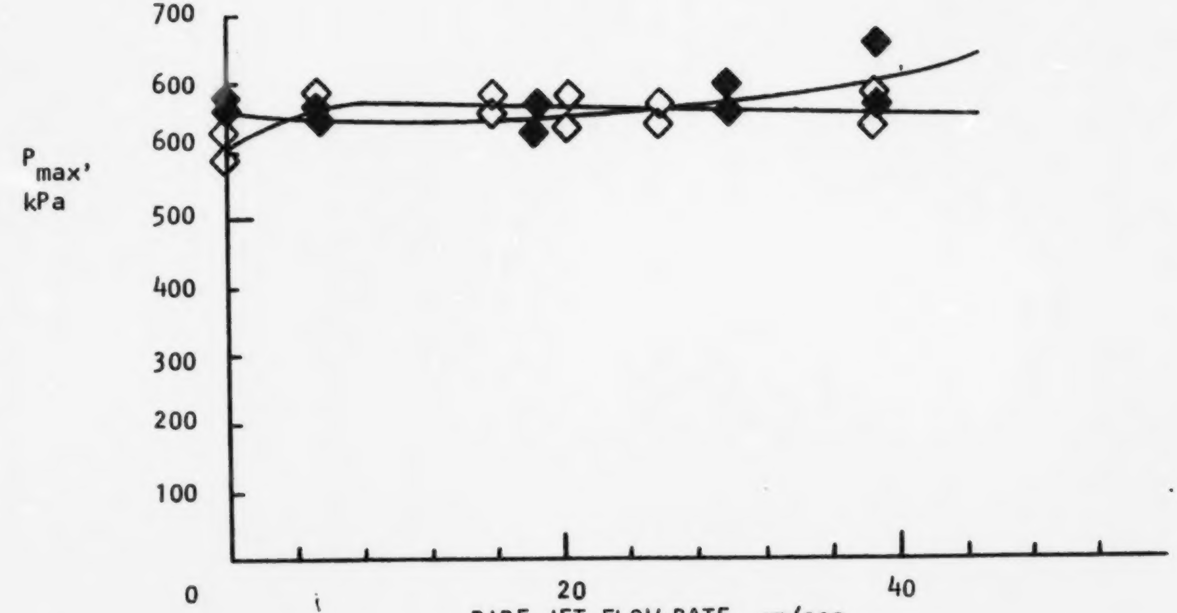

FIGURE 24 - Effect of pipe jet flow rate on P_{max} in the 333 liter spherical vessel. ◇ 7.5% methane-air. ◆ 300 gm/m^3 cornstarch-air.

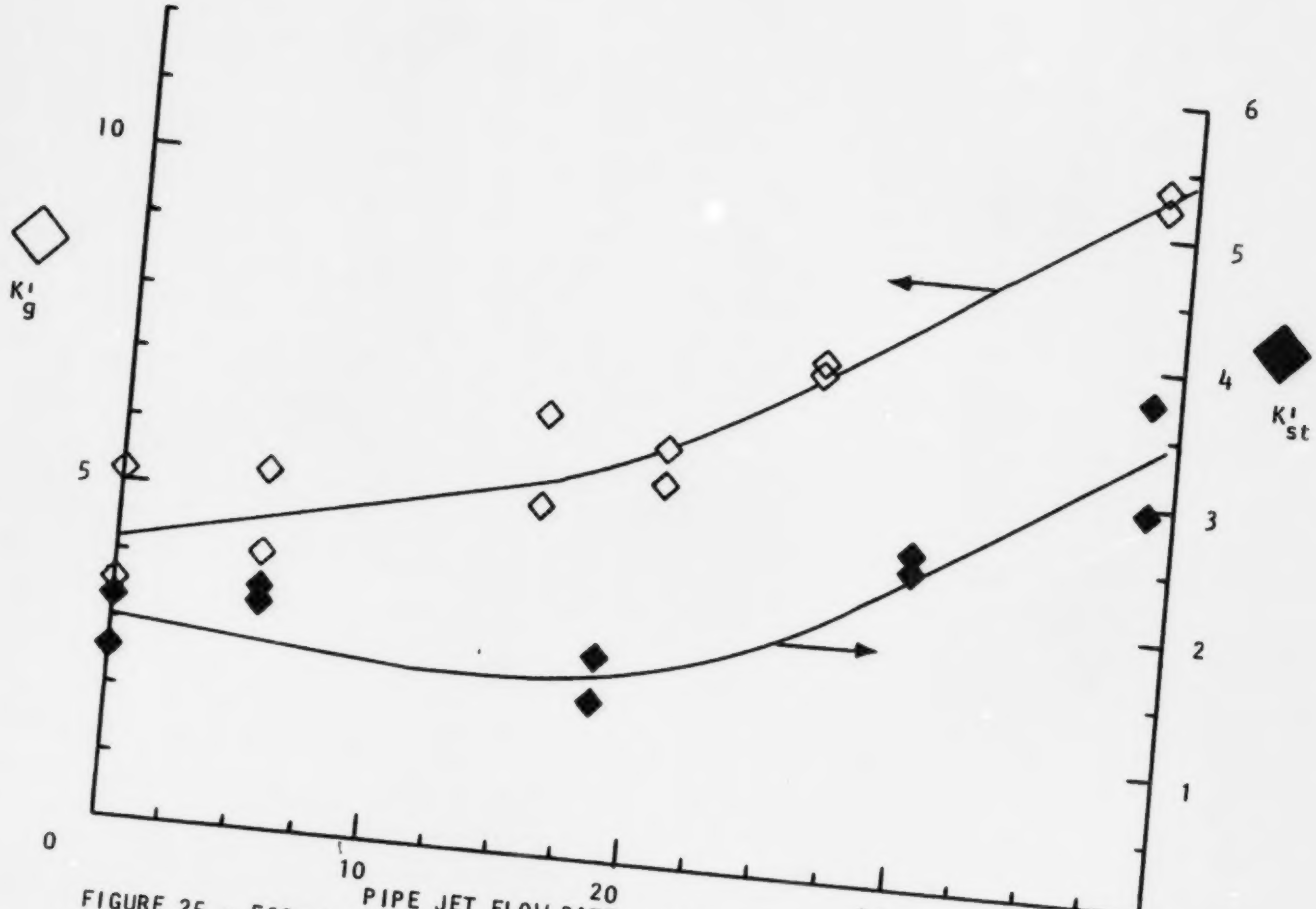

FIGURE 25 - Effect of pipe jet flow rate on the maximum burning rates in the 333 liter spherical vessel. ◇ 7.5% methane-air. ◆ 300 gm/m^3 cornstarch-air.

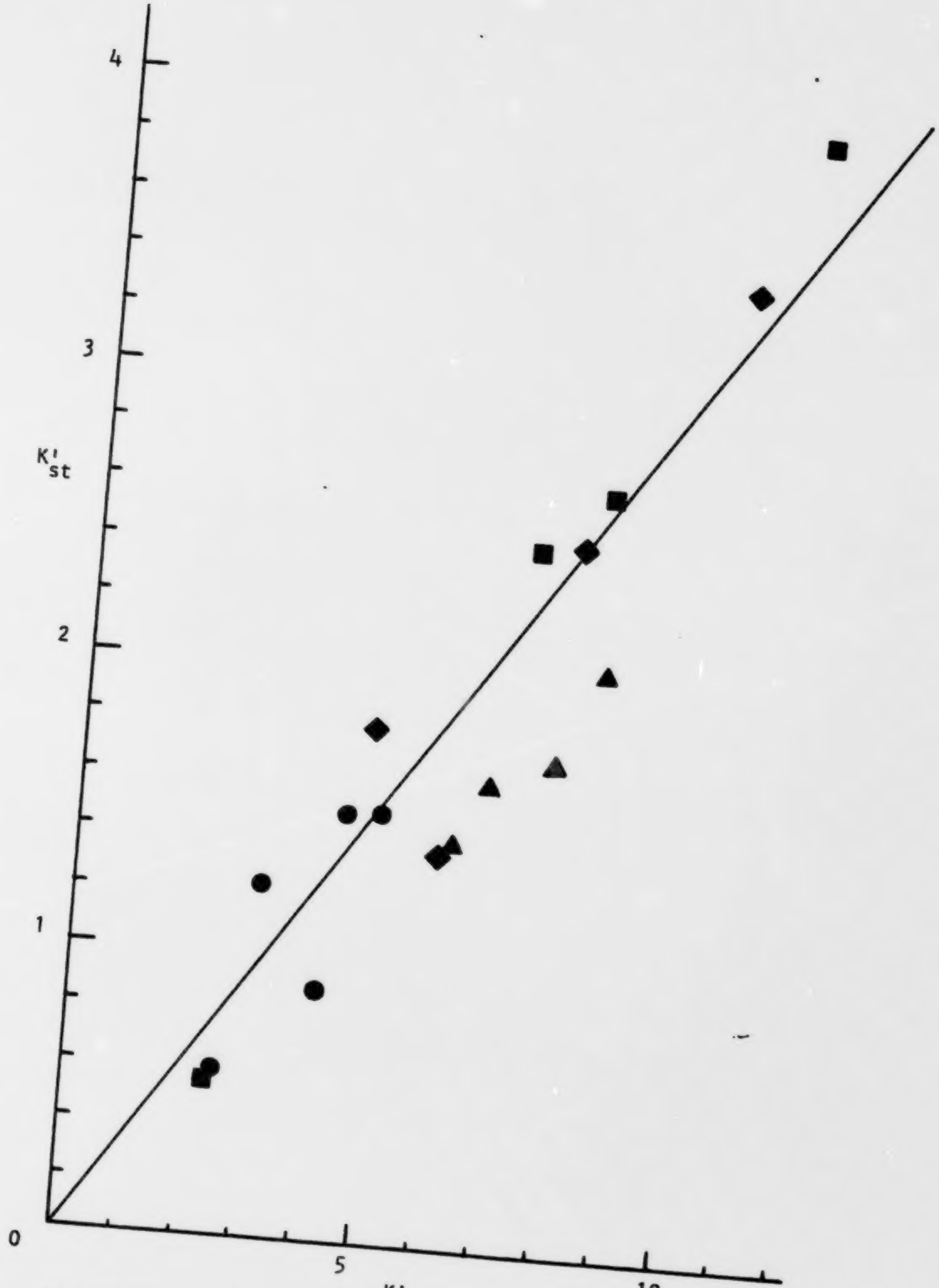

FIGURE 26 - Relationship between dust burning rate and methane burning rate in identical turbulent flow situations. ● Dispersion pressure in 333 liter sphere. ■ Bottle pressure in 180 liter cylinder. ◆ Turbulence pipe in 333 liter sphere. ▲ Turbulence ring in 333 liter sphere.

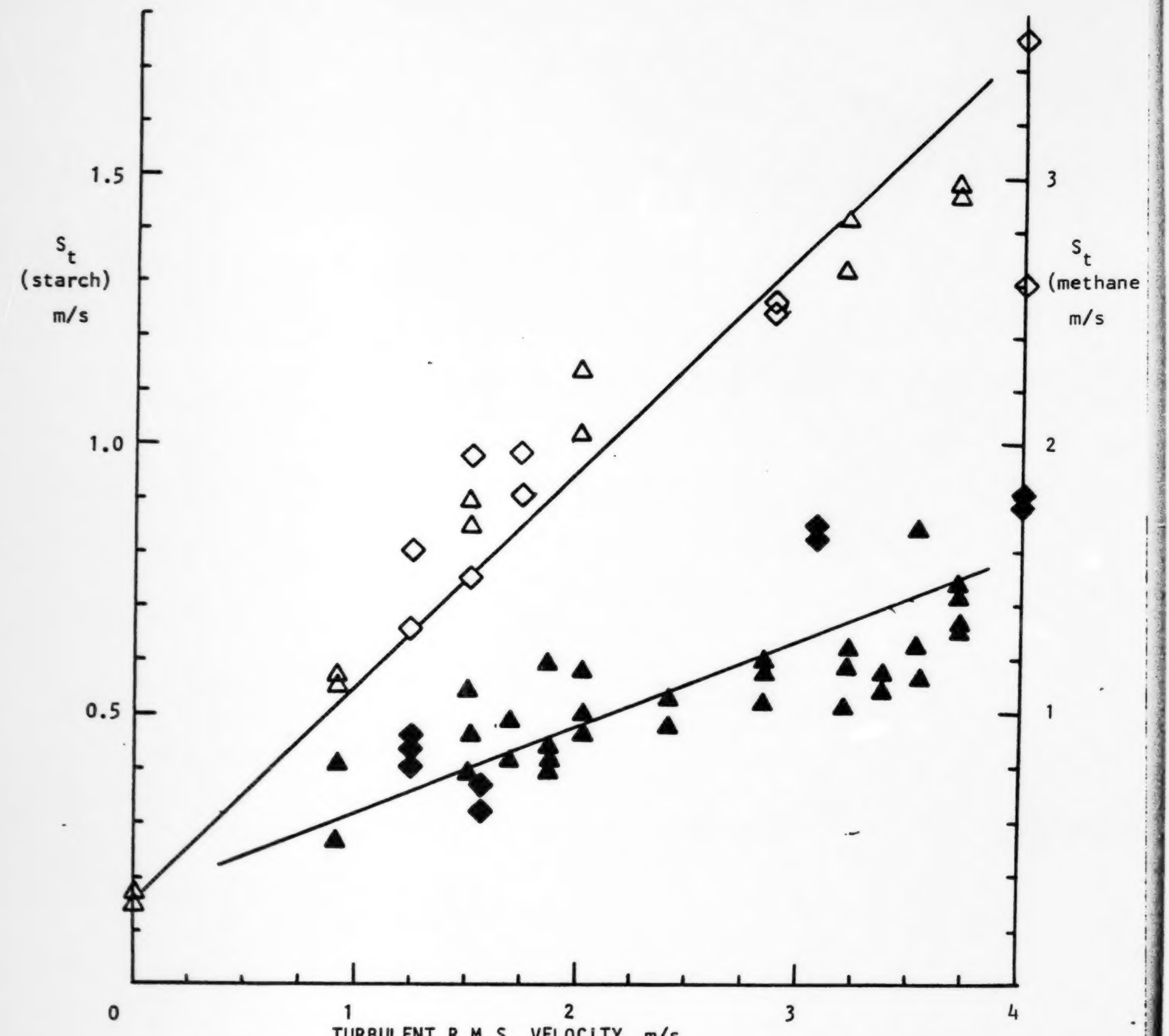

FIGURE 27 - Variation of turbulent burning velocity with turbulent r.m.s. velocity, for starch and methane explosions in 333 liter spherical vessel with jet-induced turbulence. ◇ 7.5% methane-air. ◆ 300 gm/m^3 cornstarch-air. (pipe-induced turbulence) △ 7.5% methane-air. ▲ 300 gm/m^3 cornstarch-air. (ring-induced turbulence).

The Influence of Turbulence on Dust and Gas Explosions in Closed Vessels

J.F. Bond,* R. Knystautas,† and J.H.S. Lee†
McGill University, Montreal, Canada

Presented at the 10th ICDERS, Berkeley, California, August 4-9, 1985.

Copyright © 1986 by the American Institute of Aeronautics and Astronautics, Inc. All rights reserved.

* Research Assistant, Department of Mechanical Engineering

† Professor, Department of Mechanical Engineering

Abstract

Experiments have been carried out to assess the influence of turbulence on cornstarch-air explosions in two closed bombs. The turbulence of the combustible mixture was adjusted by varying the pressure of the dispersion system and by blowing air into the combustion chambers from different devices at a variable flow rate. For the purpose of comparing the effect of turbulence on dust-air explosions to that on gas-air explosions occurring in the same apparatus with identical flowfields, all experiments done with the cornstarch-air mixture were replicated with a 7.5% methane-air mixture. The burning rate of both mixtures was seen to increase monotonically with the intensity of the turbulence. The ratio of the burning rates of the two mixtures, in a given turbulent flowfield, was a constant for all the different means of generating turbulence that were used. This suggests that this ratio is not sensitive to the intensity or to the detailed structure of the turbulence, but rather depends on the physicochemical properties of the mixtures themselves. It appears that the use of gas-air explosions as a reference against which to compare dust-air explosions can help elucidate the structure and propagation mechanisms of turbulent dust-air flames, as the effects of turbulence displayed in the two media are strongly correlated.

Introduction

It is generally known that turbulence plays a strong role in the development of a dust-air explosion. As yet, however, the few experimental studies that have been performed have not yielded empirical relationships linking the burning rate to the relevant parameters of the turbulence (Bartknecht 1980; Nagy and Portman 1961; Moore 1980; Reeh 1971). Since it is difficult to achieve stationary, adiabatic dust flames for detailed observations, these studies have concentrated on observing explosions in constant volume bombs of various sizes and shapes. The "turbulence," in these studies was generally that produced by the air blast used to disperse the dust.

A unique definition of turbulence in the context of a closed vessel explosion without mean flow is difficult. Furthermore, even if one measures the flow velocity at a given point in the combustion chamber prior to ignition, as soon as the flame ball starts to propagate toward the walls of the vessel, compression of the unburned mixture and irregular fluid motions caused by the flame itself alter the flow velocity ahead of the flame. It is therefore doubtful that such a measurement is of any value.

For these reasons, the present authors thought it would be worthwhile to first perform some rather crude experiments to investigate the influence of "turbulence" on the maximum burning rate of dust explosions inside closed vessels. "Turbulence," in the context of this study, will be taken to refer to any fluid motion in the combustible mixture. To generate such motion, the dispersion air jets were used, as well as additional jets of controllable intensity from external sources. The experiments focused on measuring the maximum burning rate in the dust explosions expressed by the K_{st} factor, which is simply the maximum rate of pressure rise normalized with respect to vessel size (Bartknecht 1980):

$$K_{st} = \left(\frac{dP}{dt}\right)_{max} V^{1/3}$$

where $(dP/dt)_{max}$ is the maximum rate of pressure rise in the explosion and V is the volume of the vessel.

Since the current understanding of turbulent dust-air deflagration lags considerably behind that of gas-air deflagration, it was felt that the most meaningful way to attack the problem of the influence of turbulence on dust explosions would be to compare the K_{st} of a dust explosion to the K_g (the analog of K_{st} for a gas explosion) of a gas explosion taking place under identical conditions of turbulence. Since the effect of turbulence on gas-air flames is well established, at least on a qualitative basis (Andrews et al. 1975), such a comparison could yield some information regarding the structure and propagation mechanisms of a dust-air flame.

This paper presents the results of a series of experiments on turbulent explosions of a 300 g/m^3 cornstarch-air mixture and a 7.5% methane-air mixture in a 333-liter spherical vessel and in a 180-liter cylindrical vessel with a height to diameter ratio of 2.

Experimental Apparatus and Procedure

A spherical vessel of 333 liter volume (Fig. 1) and a cylindrical vessel of 180 liter volume (Fig. 2) were used in the present study to assess the influence of turbulence on dust and gas explosions in closed vessels.

In the spherical vessel, the dust was dispersed by an air blast from a 1.57-liter compressed air bottle discharging through a nozzle directed at the center of a small bowl at the bottom of the vessel, in which the dust had been loaded. The dispersion was triggered by opening a solenoid valve in the dispersion circuit. Ignition was achieved by either an exploding wire or a bare magnesium filament from a flashbulb. The delay between dispersion and ignition was set at 0.5 s, as some preliminary experiments showed that this delay resulted in maximum pressure and maximum rate of pressure rise, for a given set of experimental conditions.

The intensity of the turbulence induced by the dispersion blast obviously increases with the pressure in the dispersion bottle, and our first series of experiments looked at the effect of varying the dispersion bottle pressure.

Two devices were constructed to investigate the effect of jet-induced turbulence in the 333-liter sphere. We shall designate them by the name of "turbulence ring" and "turbulence pipe." The turbulence ring was a 45-cm-diam copper tubing ring, on which 16 holes of 1.1 mm diameter were drilled. It was installed in a vertical plane going through the center of the sphere, and the geometry of the holes (eight holes drilled on one side of the tube, with the remaining eight on the other side) induced a tangential swirl to the dust-air mixture. The turbulence pipe was an 80-cm-long vertical section of copper tube, on which 12 holes of 9.5 mm diameter were drilled. The holes were arranged in four stations, spaced 20 cm away from each other, each station comprised of three holes spread evenly along the circumference of the tube. The turbulence ring and pipe were fed from a high-pressure air supply, and the level of turbulence induced by the jets was altered by varying the total mass flow rate of air.

The sequence of operations for dust explosion experiments with jet-induced turbulence in the 333-liter sphere was as follows. The dust was first weighed and placed into the bowl at the bottom of the vessel. The vessel was then evacuated to 400 mm Hg. The air jets were then turned on, and air addition from the jets caused the pressure to increase. When atmospheric pressure was restored, the dispersion air blast was activated. Ignition followed 0.5 s thereafter. For the methane-air experiments, the vessel was evacuated to 600 mm Hg and filled by partial pressure with an amount of methane, resulting in the desired composition. The air jets were then turned on, and when atmospheric pressure was restored, dispersion of an identical mixture stored in the dispersion bottle was triggered, followed by ignition.

Similar accessories and experimental procedures were used in the cylindrical vessel. In this vessel, we studied the effect of dispersion-induced turbulence supplemented by additional turbulence generated by a 3.0-liter "turbulence bottle" which discharged through a port on the circumference of the vessel, near its center. The dispersion and turbulence bottles were charged to the same pressure and discharged simultaneously. Since it was desirable to study explosions occurring at atmospheric initial pressure, it was necessary, in the cylindrical vessel experiments, to first evacuate the vessel to a level such that atmospheric pressure would just be recovered upon discharge of the bottles. This precaution was not taken in the spherical vessel because the mass injected by the dispersion bottle was a negligible fraction of that initially present in the vessel.

The dust used in the present study was cornstarch, a natural organic polymer of dextrose. Prior to an experiment, the cornstarch was placed in an oven at 90°C for about 18 hours, to eliminate the moisture and thus help to produce a more uniform dispersion. In a number of experiments, a fluidizing agent (CAB-O-SIL) was mixed with the cornstarch in the proportion of 0.5% of fluidizing agent per unit mass of mixture, to further improve the dispersion. A particle size analysis obtained via direct imaging with an optical image analyzer showed the average size of the particles to be 14.7 μm, with a standard deviation of 5.1 μm. Scanning electron micrographs showed the particles to be remarkably spheroidal in shape.

A PCB quartz pressure transducer was used to record the pressure-time history inside the vessels.

Results and Discussion

The intensity of the turbulence induced by the dispersion process increases with the initial pressure in the dispersion bottle. In our first series of experiments, we studied the influence of bottle pressure on the maximum overpressure ΔP_{max} developed in the 333-liter sphere by explosions of a 300 g/m^3 cornstarch-air mixture and a 7.5% methane-air mixture. Nagy and Portman (1961) have observed, in a 9.3-liter cylindrical vessel that ΔP_{max} for a 600 g/m^3 coal-air mixture showed a significant variation (roughly 25%) with dispersion bottle pressure. In principle, ΔP_{max} should depend only on the energetics of the mixture, but in practice, it can be affected by heat losses to the walls of the vessel. These losses, in turn, depend on the duration of the explosion, and hence on the burning rate. ΔP_{max} can also be affected by the total amount of dust consumed by the explosion. It is therefore important to observe the influence of the intensity of the dispersion turbulence on ΔP_{max} before the question of the influence of turbulence on the burning rate can be addressed.

Figure 3 shows ΔP_{max} as a function of pressure in the dispersion bottle. For the methane-air mixture, there is little fluctuation of ΔP_{max} as the intensity of the dispersion-induced turbulence is varied: It is nearly constant at 560 kPa, 18% below the theoretical value of 684 kPa for adiabatic, isochoric combustion (Gordon and McBride 1971). The maximum overpressure for starch-air, by contrast, shows a slight increase from 475 kPa with a dispersion pressure of 690 kPa, to 655 kPa with a bottle pressure of 2069 kPa. The average ΔP_{max} is 587 kPa. This value is in good agreement with the results of Cocks and Meyer (1980), Nagy and Verakis (1983), and Hartmann et al. (1951); it is 37% below the theoretical value of 932 kPa (Gordon and McBride

1971).

The fact that the deviation from adiabatic behavior is more pronounced for the cornstarch-air than for the methane-air is probably linked to the slower burning rate of the dust-air mixture. This increases the time available, between ignition and completion of the burning, for heat to be lost by radiation and turbulent convection to the walls of the vessel. By the same token, the faster burning caused by increasing the intensity of turbulence reduces heat losses, and this could account for the observed increase in ΔP_{max} for cornstarch-air when the dispersion pressure is increased. It is also possible that the higher intensity of turbulence at high dispersion pressure increases the amount of dust in suspension and hence available for combustion.

The main objective of our investigation was to study how turbulence generated by different devices affects the burning rate of dust and gas explosions. In Figs. 4 through 7, we show the variation of the burning rate in 300 g/m^3 cornstarch-air and 7.5% methane-air mixtures. It seemed appropriate to normalize the burning rates with respect to that observed in a "reference" laminar explosion of 7.5% methane-air. Hence we have plotted the ratio $K' = K/K_{g\ lam}$, where $K_{g\ lam}$ is the K of a laminar gas-air explosion versus the parameter characterizing the turbulence in each of the particular setups. The value of $K_{g\ lam}$ was measured in the spherical bomb to be 2575.9 kPa-m/s. The formula developed by Bradley and Mitcheson (1976) for spherical vessel explosion shows that this value corresponds to a burning velocity of 33 cm/s, in good agreement with the value of 28 cm/s reported by Andrews and Bradley (1972) for atmospheric conditions, especially if a correction is made to account for adiabatic compression of the mixture.

Figure 4 shows K' as a function of the dispersion bottle pressure in the 333-liter sphere. Both K'_g and K'_{st} increase monotonicallly with bottle pressure, although it seems that the increase begins to taper off when the dispersion pressure has reached about 1724 kPa. For a given intensity of turbulence, methane-air seems to burn much faster than cornstarch-air, the ratio K'_g/K'_{st} having a value of about 4. The scatter in the values of K' is much more important than that observed in the maximum overpressures (Fig. 3). This is understandable, since ΔP_{max} is primarily determined by the concentration of fuel, whereas K' is highly sensitive to the random fluctuations in the turbulent flowfield from one explosion to the next.

Figure 5 shows K' as a function of the pressure in the dispersion and "turbulence" bottles in the 180-liter cylinder. Here again, a monotonic increase of K'_g and K'_{st} with increased bottle pressure is evident, and K'_g is roughly three to four times larger than K'_{st} at a given bottle pressure. Thus the explosions behave in a manner similar to those performed with dispersion pressure variation in the spherical vessel, even though the structure of the turbulent flow induced by the two bottles in the cylindrical geometry must be different from that induced by the single bottle in the spherical geometry. On comparing Figs. 4 and 5, we see that the K' factor obtained at a given bottle pressure, for both dust and gas, is roughly twice in the cylinder to what it is in the sphere. The explanation could lie in the fact that a given bottle pressure induces a much bigger swirl in the cylinder than in the sphere, because the ratio of bottle volume (i.e., the volume responsible for the swirling) to the combustion chamber volume (the volume being swirled) is higher in the cylinder: This ratio has a value of (1 L + 3 L)/180 L = 0.0222 for the cylinder and 1.57 L/333 L = 0.0047 for the sphere.

In a further series of experiments, the turbulence of the dispersion process in the spherical vessel was supplemented by that generated by air jets blowing into the combustion chamber from a circular "turbulence ring." This has the effect of altering both the intensity and the detailed structure of the fluid motions. Figure 6 shows the effect of turbulence induced by the turbulence ring jets on the burning rate of 300 g/m^3 cornstarch-air and 7.5% methane-air in the 333-liter sphere. K' has been plotted as a function of the total mass flow rate of air through the ring, a measure of the intensity of the turbulence. The dispersion pressure, in this series of experiments, was 1034 kPa. Once again, K'_g and K'_{st} increase monotonically with turbulence intensity; K'_g is typically three to four times higher than K'_{st}; and the relative increase in burning rate due to increased mass flow rate, $\Delta K'/K'\Delta\dot{m}$, is about the same for the dust-air as for the gas-air. The scatter observed in the values of K' is much higher for dust-air than for methane-air, perhaps owing to the difficulty in achieving a consistently homogeneous mixture of dust and air with the kind of dispersion system used in this study.

The experiments done with the turbulence ring were repeated with the vertical turbulence pipe, with the objective being to investigate the effect of modifying the geometry of the jets and of studying a range of turbulence intensities higher than those that could be achieved with the turbulence ring. For this specific purpose, the turbulence pipe was designed to handle total airflow rates as high as 40 g/s, and the experiments were performed with a dispersion pressure of 2069 kPa. K'_g and K'_{st} responded to turbulence in a manner that was qualitatively similar to that shown in Figs. 4-6. There was no evidence of turbulent quenching either for dust-air or methane-air, even for the highest K' (K'_g = 10.8, K'_{st} = 3.77) observed at a mass flow rate of 38.7 g/s.

The results presented in Figs. 4-7 indicate that there is a direct correlation between K_g' and K_{st}' obtained in a given turbulent flow situation, and this suggests that we use K_g' as a scale against which to compare K_{st}'. In Fig. 8, we have attempted to present a unified picture of all our experimental results by plotting the relationship between the quantities K_g' and K_{st}' obtained under identical conditions of turbulence in each of the four experimental setups studied. K_g' and K_{st}' are seen to vary in linear proportion to each other, the data being best represented by the formula $K_{st}' = 0.30\ K_g'$. This strongly suggests that the ratio of the burning rates of the dust-air mixture and the gas-air mixture is not sensitive to differences in the detailed structure of the turbulence induced by the various devices used, but that rather it depends on the properties of the combustible mixtures themselves. Although we would need to know more about the fundamental characteristics of the cornstarch-air mixture (in particular, its laminar burning velocity and its laminar flame thickness) to draw a more definite conclusion from the results shown in Fig. 8, two possible explanations come to mind in the light of the present state of knowledge.

The first hypothesis is that the laminar burning velocity of the cornstarch-air mixture is about .30 times that of the methane-air and that the physical mechanisms responsible for the burning rate increase are the same in the two mixtures. Since it is known that, for the relatively small intensities of turbulence studied in this investigation, the main effect of turbulence on gas-air mixtures is to wrinkle the flame so as to increase the total burning area, this hypothesis would imply that the dust-air flame and the gas-air flame are being stretched by turbulence in the same proportion, so that the ratio of their turbulent burning velocities ($S_{st}/S_g \simeq K_{st}'/K_g' = 0.30$) would simply be equal to the ratio of their laminar burning velocities. This would require that the thickness of the laminar dust-air flame be smaller than the smallest characteristic length scale of the velocity fluctuations (Williams 1976).

The second hypothesis is that, while the laminar burning velocities of the two mixtures may be very close to one another, the laminar dust-air flame is much thicker than the gas-air flame, and consequently, the modes of action of turbulence are different in the two media. If the dust-air flame is thicker than the smallest length scale of the velocity fluctuations, the area of the dust-air flame can only be minimally affected by these fluctuations, and the only significant effect of turbulence will be to increase the rate of the transport processes taking place within the flame itself. This might be a less efficient mechanism of burning rate increase than flame stretching, and this could explain the observed discrepancies in the combustion rates of cornstarch-air and methane-air.

Conclusions

The influence of dispersion-induced and jet-induced turbulence on dust and gas explosions has been studied experimentally in two closed vessels with different geometries. It has been found that, under all the conditions studied, the relative burning rate variations caused by turbulence are equal in a 300 g/m^3 cornstarch-air mixture and a 7.5% methane-air mixture. The ratio of the burning rates of the dust-air mixture and the gas-air mixture observed under the same conditions of turbulence appears to be insensitive to the detailed structure of turbulence.

A better knowledge of the fundamental characteristics of laminar dust-air flames (especially the flame thickness and the burning velocity) is required before this interesting finding can be properly interpreted. It appears that the use of gas explosion as a reference against which to compare dust explosion can help speed up the learning process for the elucidation of the structure and propagation mechanisms of turbulent dust-air flames, as the effects of turbulence observed in the two media appear to be correlated.

Acknowledgments

The authors would like to gratefully acknowledge the assistance of M. Fresko and A. Makris in performing some of the experimental work and of L. Nelson and J. Shepherd of Sandia National Laboratories for procuring information on the physical characteristics of cornstarch. The work was supported by the Natural Sciences and Engineering Research Council of Canada under grants A-3347 and A-7091 and by Energy, Mines and Resources of Canada under contract number OSV82-00039.

References

Andrews, G.E. and Bradley, D. (1972) The burning velocity of methane-air mixtures. Combust. Flame 19, 275-288.

Andrews, G.E., Bradley, D., and Lwakabamba, S.B. (1975) Turbulence and turbulent flame propagagion--A critical appraisal. Combust. Flame 24, 285-304.

Bartknecht, W. (1980) Explosions: Cause, Prevention, Protection (translated by H. Burg and T. Almond). Springer-Verlag, New York.

Bradley, D. and Mitcheson, A. (1976) Mathematical solutions for explosions in spherical vessels. Combust. Flame 26, 210-217.

Cocks, R.E. and Meyer, R.C. (1980) Fabrication and use of a 20-liter spherical dust testing apparatus. Process Specialties Division, Procter and Gamble, Cincinnati, Ohio.

Gordon, S. and McBride, B.J. (1971) Computer program for calculation of complex chemical equilibrium compositions, rocket performance, incident and reflected shocks, and Chapman-Jouguet detonations. NASA.

Hartmann, I., Cooper, A.R., and Jacobson, M. (1951) Recent studies on the explosibility of cornstarch. US Bureau of Mines Report of Investigation 4725.

Moore, P.E. (1980) Dust explosion hazard assessment. Chemical Process Hazards with Special Reference to Plant Design, I.Chem. E. Symposium Series, No. 58, pp. 77-88.

Nagy, J. and Portman, W.M. (1961) Explosibility of coal dust in an atmosphere containing a low percentage of methane. US Bureau of Mines Report of Investigation 5815.

Nagy, J. and Verakis, H.C. (1983) Development and Control of Dust Explosions. Dekker, New York.

Reeh, D. (1971) Tests on the development of coal dust explosions in pressur chambers and in a 200-m-long pipe of 1800-mm inner diameter. Staub-Reinhalt. Luft 31 (3), 12-21.

Williams, F.A. (1976) Criteria for existence of wrinkled laminar flame structure of turbulent premixed flames. Combust. Flame 26, 269-270.

Figure Captions

Fig. 1 333-liter spherical vessel.

Fig. 2 180-liter cylindrical vessel.

Fig. 3 Effect of dispersion bottle pressure on P in the 333-liter spherical vessel. ○ 7.5% methane-air; ● 300 g/m^3 cornstarch-air.

Fig. 4 Effect of dispersion bottle pressure on maximum burning rates in 333-liter spherical vessel. ○ 7.5% methane-air; ● 300 g/m^3 cornstarch-air.

Fig. 5 Effect of pressure in the dispersion and "turbulence" bottles on maximum burning rates in the 180-liter cylindrical vessel; □ 7.5% methane-air. ■ 300 g/m^3 cornstarch-air.

Fig. 6 Effect of air mass flow rate through the turbulence ring on the maximum burning rates in the 333-liter spherical vessel; △7.5% methane-air. ▲ 300 g/m^3 cornstarch-air.

Fig. 7 Effect of air mass flow rate through the turbulence pipe on the maximum burning rates in the 333-liter spherical vessel. ◇ 7.5% methane-air; ◆ 300 g/m^3 cornstarch-air.

Fig. 8 Relationship between dust burning rate and methane burning rate in identical turbulent flow situations. ● Dispersion pressure in 333-liter sphere; ■ bottle pressure in 180-liter cylinder; ◆ turbulence pipe in 333-liter sphere; ▲ turbulence ring in 333-liter sphere.

RUNNING HEADS

J.F. BOND ET AL.

DUST EXPLOSIONS

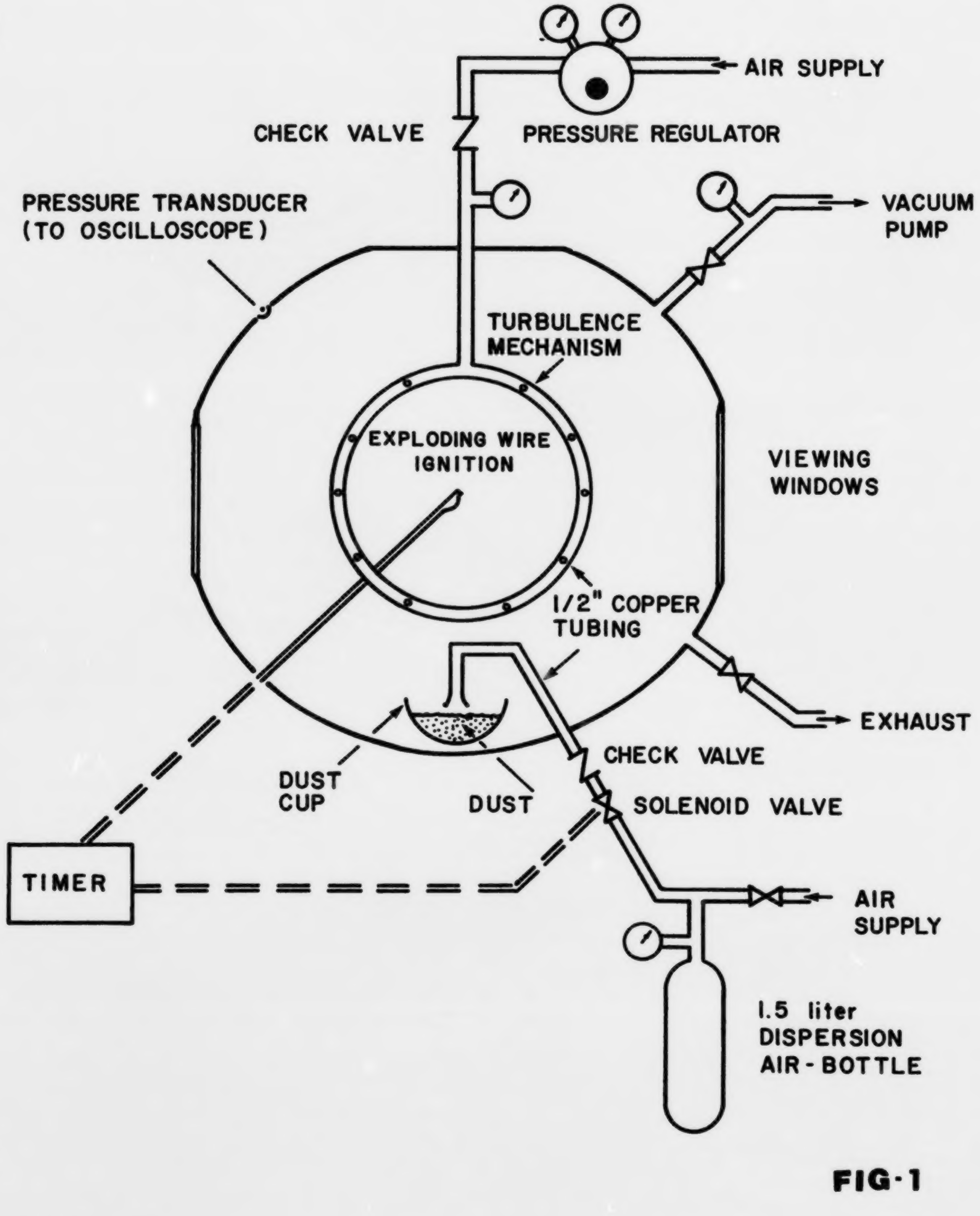
AIR SUPPLY
CHECK VALVE
PRESSURE REGULATOR
PRESSURE TRANSDUCER (TO OSCILLOSCOPE)
VACUUM PUMP
TURBULENCE MECHANISM
EXPLODING WIRE IGNITION
VIEWING WINDOWS
1/2" COPPER TUBING
EXHAUST
CHECK VALVE
DUST CUP
DUST
SOLENOID VALVE
TIMER
AIR SUPPLY
1.5 liter DISPERSION AIR-BOTTLE

FIG-1

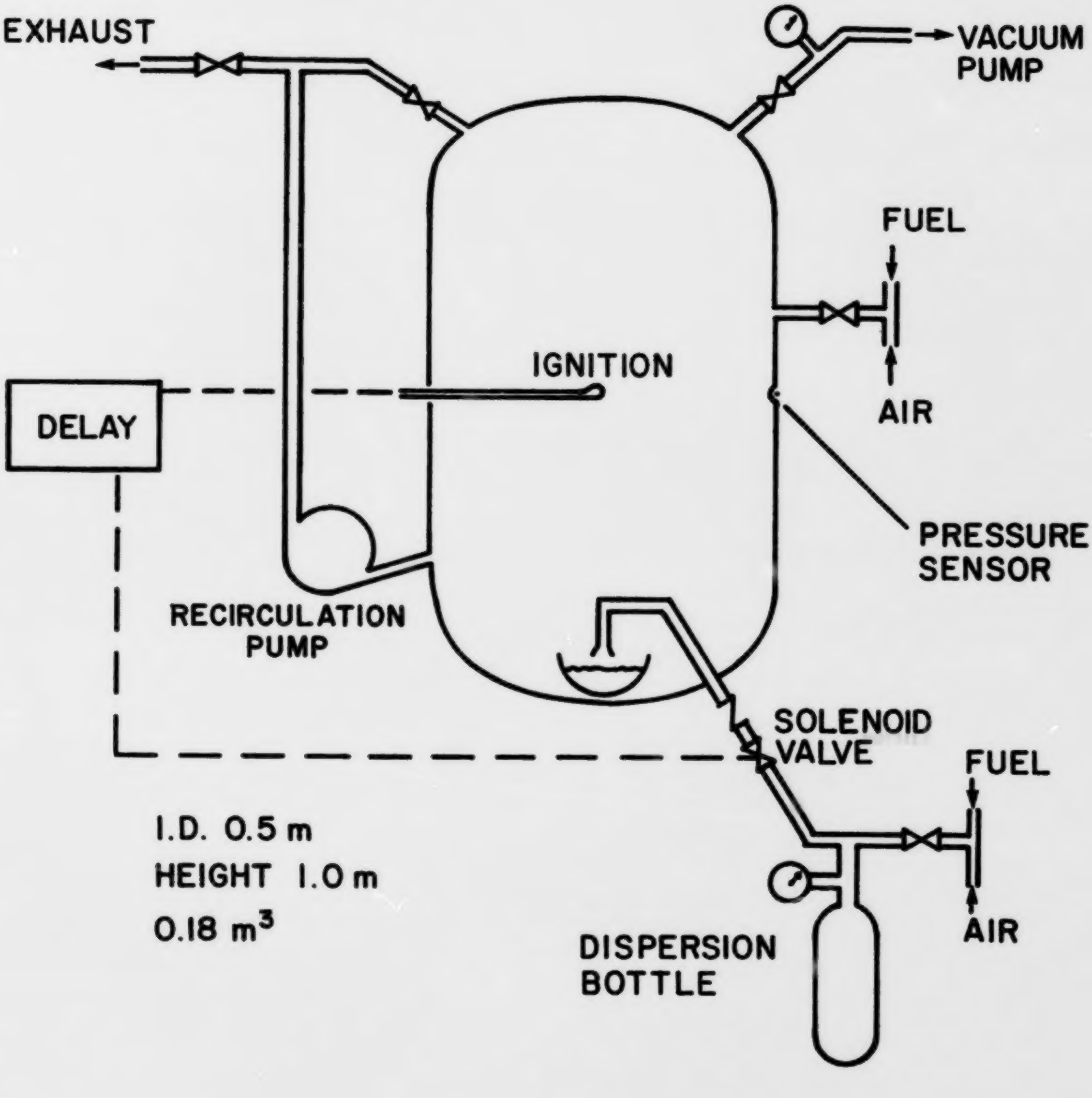
EXHAUST
VACUUM PUMP
FUEL
AIR
IGNITION
DELAY
PRESSURE SENSOR
RECIRCULATION PUMP
SOLENOID VALVE
FUEL
AIR
I.D. 0.5 m
HEIGHT 1.0 m
0.18 m³
DISPERSION BOTTLE

FIG-2

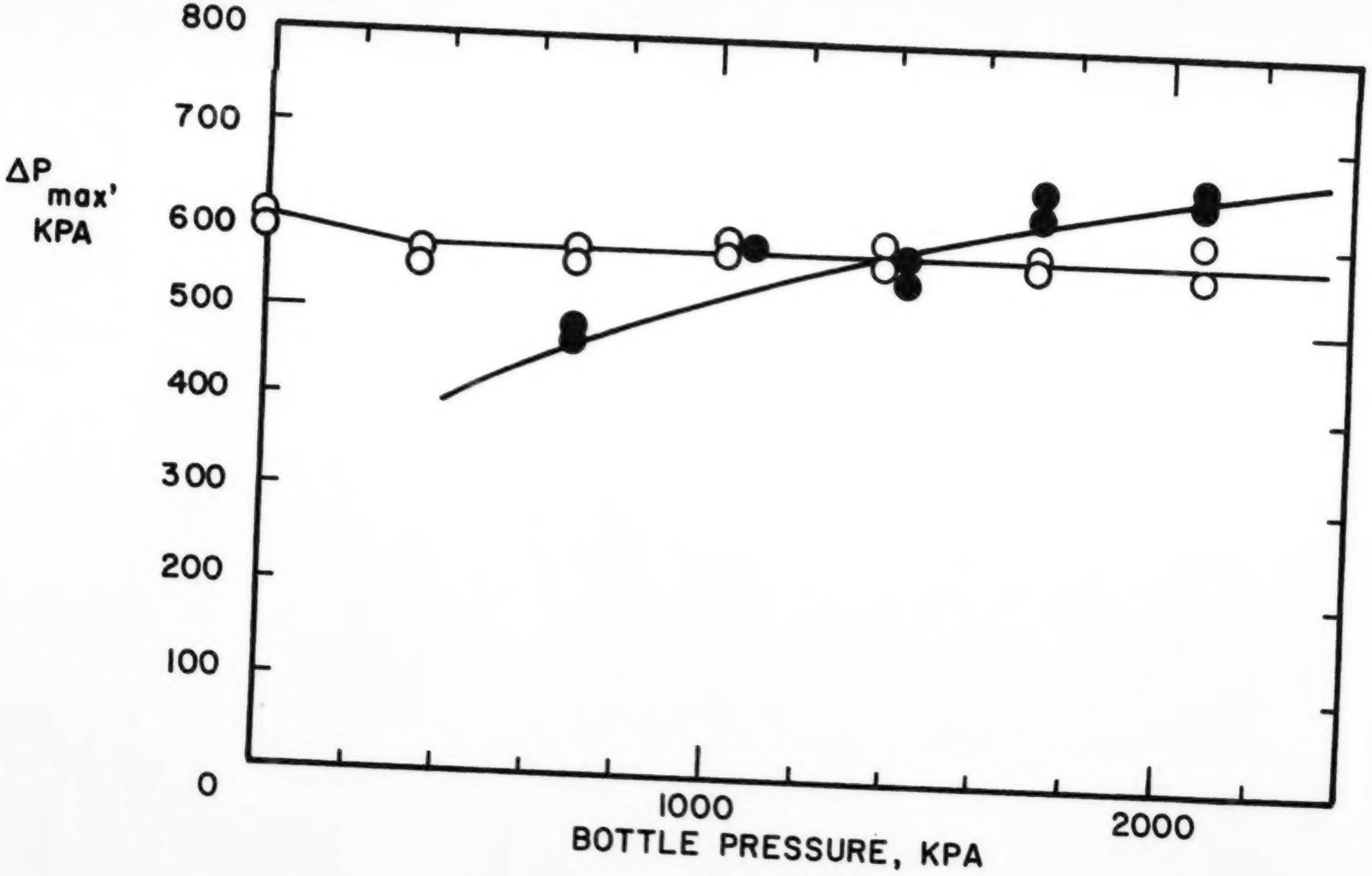
ΔP_{max}, KPA
800
700
600
500
400
300
200
100
0
1000
2000
BOTTLE PRESSURE, KPA

FIG·3

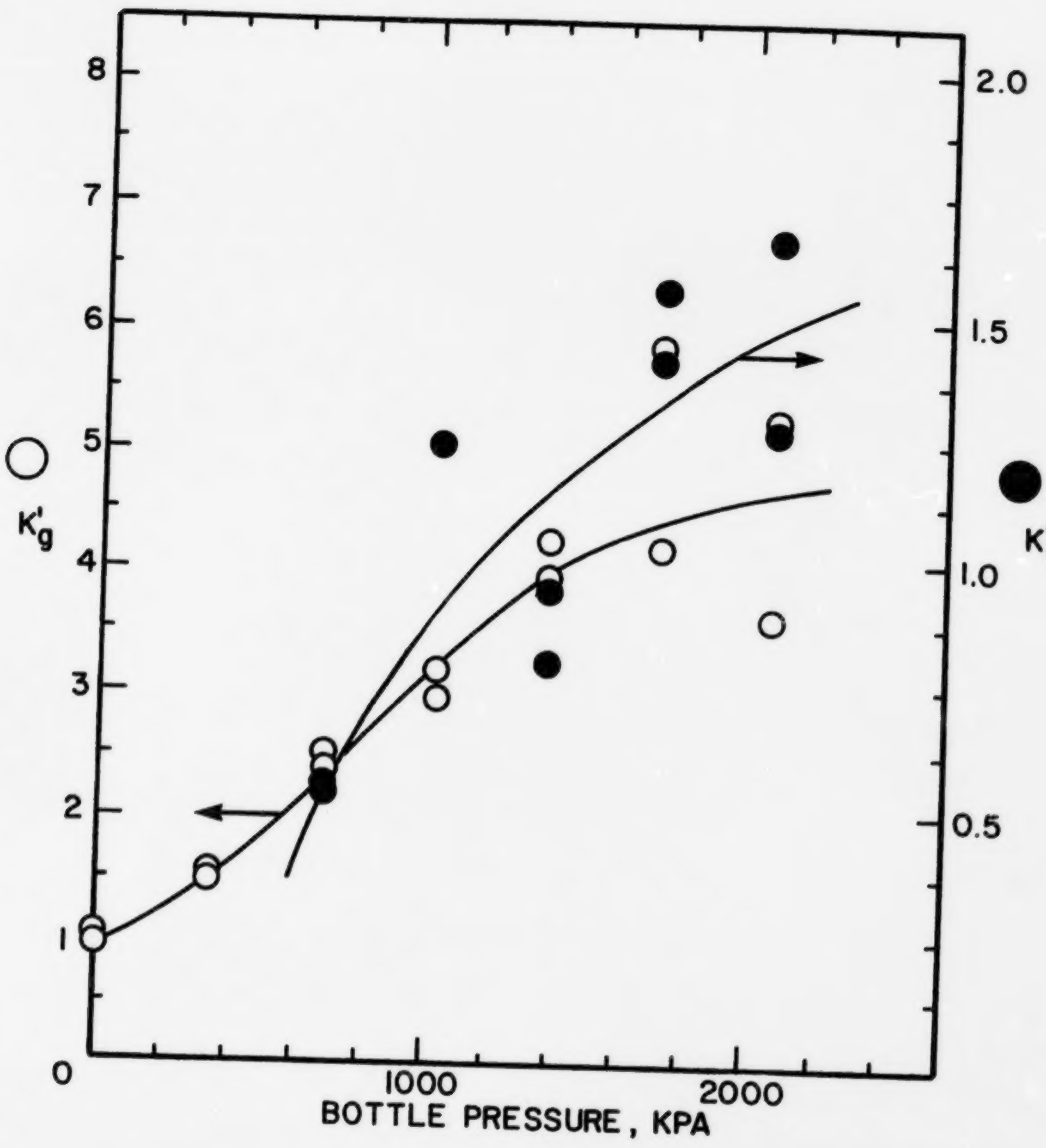

FIG ·4

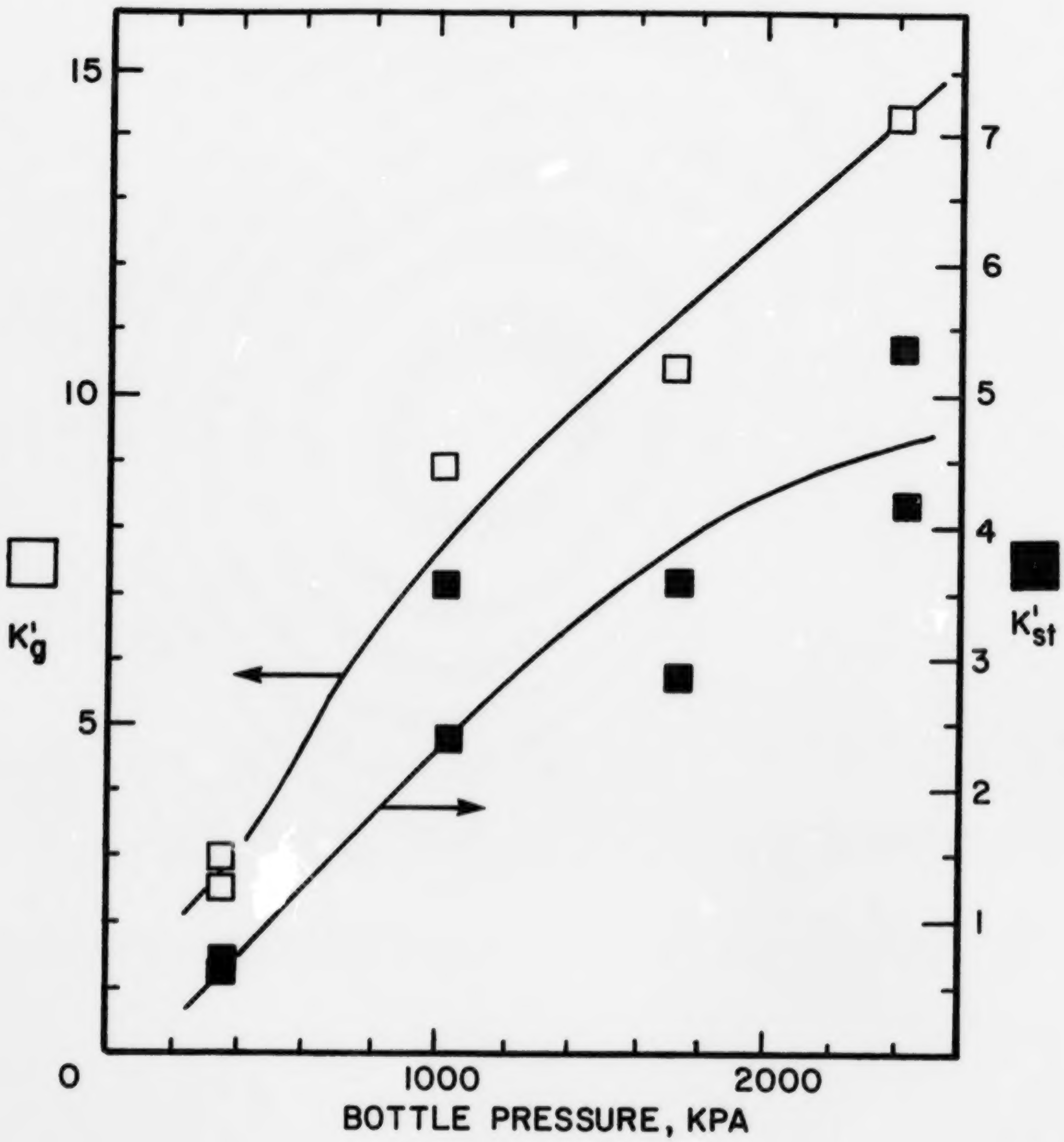

FIG·5

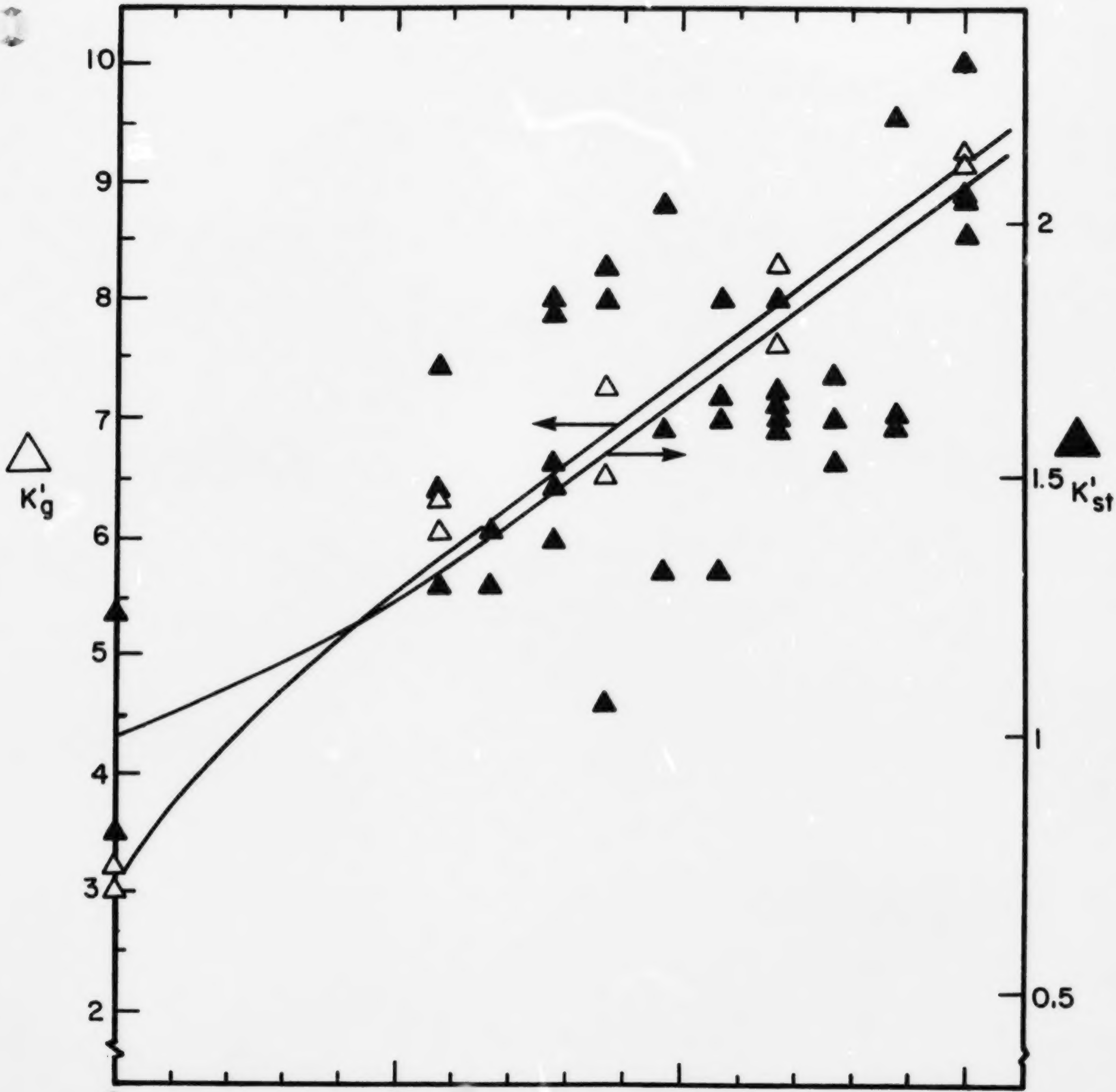

FIG-6

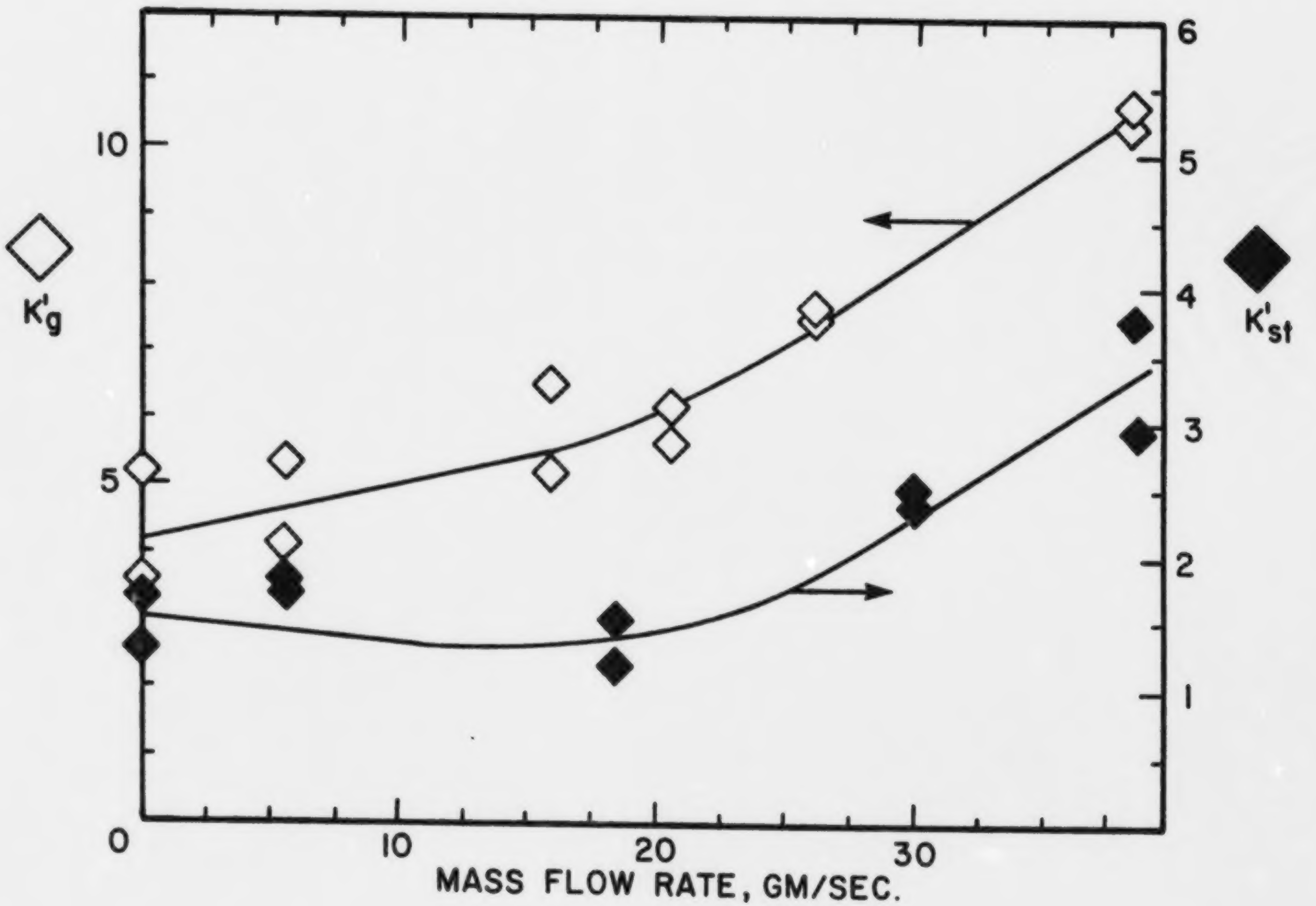

FIG · 7

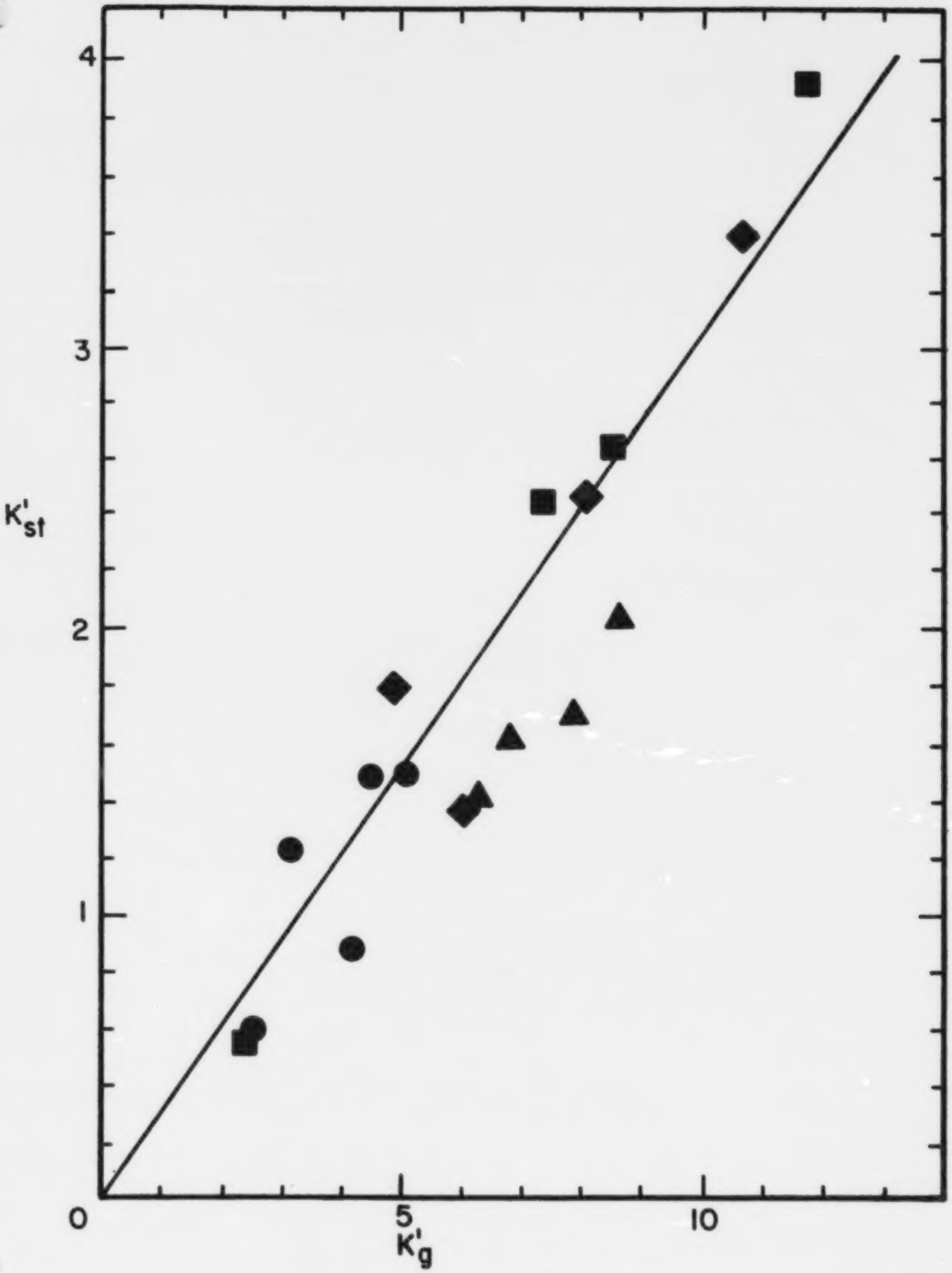

FIG · 8

The Lean Flammability Limits of Hybrid Mixtures

M. Gaug,* R. Knystautas,** and J.H.S. Lee**
McGill University, Montreal
Canada

L.S. Nelson,† W.B. Benedick,‡ and J.E. Shepherd§
Sandia National Laboratories, Albuquerque
New Mexico

Presented at 10th ICDERS, Berkeley, California
August 4-9, 1985

Copyright © 1986 by the American Institute of Aeronautics and Astronautics, Inc. All rights reserved.

* Research Engineer, Dept. of Mechanical Engineering; currently with SPAR Aerospace

**Professor, Dept. of Mechanical Engineering

† Research Scientist, Severe Accident Containment Response Division

‡ Research Scientist, Shock Wave and Explosive Physics Division

§ Research Scientist, Fluid Mechanics and Heat Transfer Division

Abstract

This paper investigates the lean flammability limits of gaseous fuel-dust-air mixtures. The gaseous fuels used were methane and hydrogen. Two different dusts were used in an attempt to determine the influence of volatile content on hybrid limits. Cornstarch was selected for its high volatile content, while iron dust was chosen for its complete lack of volatiles. The experiments were performed in two different apparatus: a 0.18-m^3 cylindrical vessel, and to investigate the effects of scaling, a 5.1-m^3 cylindrical tank. The dust was dispersed by means of an air blast into a hemispherical dust receptacle placed at the bottom of the apparatus. The criterion for self-sustained flame propagation was the evidence of an overpressure in excess of an arbitrarily set limit. For hydrogen-air-cornstarch mixtures, the lean limit of H_2 alone was found to be 4.25% by volume, while that of cornstarch alone was observed to be 70 g/m^3. A line joining these two limits on a graph represents the Le Chatelier limit law (formulated for gaseous homogeneous fuels), which is based on energetics. For the range of mixtures studied, the extension of Le Chatelier's law to hybrid mixtures was shown to be invalid. The deviation of the results from the Le Chatelier law indicates that hybrid lean limits depend more on the mechanism of propagation than on energetics. In fact, it can be seen that in traversing the entire hybrid mixture range from pure dust to pure gas, a crossover region can be identified in which the mode of propagation switches from dust to gas.

Introduction

The study of flammability limits and combustion behavior of dust-gas hybrid mixtures is of great practical importance. It is well known that coal dust and methane gas mixtures can produce violent explosions although the individual concentrations of both fuels may be below their respective lean flammability limits. This has been shown by Nagy and Portman (1960), who demonstrated that the minimum explosive concentration of coal dust decreases almost linearly as the concentration of methane increases from 0% to 5%. Bartknecht (1981) observed similar behavior for mixtures of PVC dust and either methane or propane. He demonstrated that for hybrid mixtures, the peak explosion pressure, and the maximum burning rate do not occur at the same mixture composition, which is generally true for premixed gas explosions.

Generally, however, comparatively few investigations have been carried out for hybrid lean flammability limits. Although Le Chatelier formulated a rule for determining flammability limits for homogeneous gas mixtures in the late

1800's, no such formulation exists today for determining hybrid mixture flammability limits. However, Le Chatelier's rule has been used as a point of departure for examining the behavior of hybrid limits. Le Chatelier's law is based on energetics and can be stated as follows: given a mixture of flammable gases, if the sum of all individual fuel concentrations C_i divided by their respective lean limit concentrations L_i is greater than or equal to 1, then that particular mixture is flammable ($\sum_i C_i/L_i > 1$). Due to its normalizing character, this law may be readily extended to include dust-gas hybrid mixtures. The linear behavior of this law has been shown by Nagy and Portman (1960) as mentioned previously. Hertzberg et al. (1981) also observed linear trends for the flammability limits of methane gas admixed with various coal dusts. However, both Nagy and Hertzberg performed their investigations in very small volume apparatus, a 0.33-ft^3 cylinder and 8-liter cylinder, respectively. The size of these apparatus raises serious doubts as to whether a true self-sustained flame propagation was observed. Thus, the present study was performed in both small-scale (.18 m^3) and large-scale (5 m^3) apparatus for the purposes of determining the influence of chamber volume and geometry on the flammability limits of the mixtures studied. The large-scale apparatus was the principal apparatus of interest, as its dimensions with respect to a dust flame thickness were considered to be large enough to eliminate the adverse effects of small scale. However, due to the difficulties and extreme costs involved with running tests in a 5-m^3 vessel, the majority of tests were performed in the small-scale .18-m^3 chamber. An attempt was made to investigate and explain the mechanisms inherent in determining the flammability limits for hybrid mixtures. Based on these results, a simple model is proposed to explain the flammability limit behavior for hybrid dust-gas mixtures.

Experimental Details

The present study was performed in two separate apparatus, one large scale (5.1 m^3) and one laboratory scale (.18 m^3).

The laboratory scale apparatus has a volume of 180 liters and is cylindrical in shape with rounded dome shaped ends. The cylinder itself consists of a straight portion (48.2 cm in diameter, by 54.2 cm long) capped by two dome-shaped ends that are each 48.2 cm in diameter, with a mean equivalent cylindrical length of approximately 22 cm each. An overall view of the apparatus is shown schematically in Fig. 1. In a given experiment, the gaseous mixture in the vessel is prepared by manometric measurements of partial pressures. The contents are recirculated for 30 min with a Bellows type pump to ensure a uniform mixture. The dust is deposited in a circular cup and placed at the bottom of the vessel. The dust is then dispersed with an air blast from a 1-liter vessel pressurized to 1.5 MPa. The composition of the gas in the dispersion vessel is exactly that of the vessel itself. Ignition is achieved centrally via a glow wire wrapped with 1 g of black powder. Diagnostics involved pressure measurement in the explosion vessel via a PCB 113A24 piezoelectric transducer. A solid state delay generator was used to vary the time between dispersion and ignition. All tests were performed at atmospheric pressure.

The large scale experiments were performed in a subterranean steel pressure vessel, 5.1 m^3 in volume and cylindrical in shape. The tank measures 1.2 m in diameter by 4.8 m in height and is oriented vertically. Its ends are dome shaped. The 5.1-m^3 tank is equipped with an array of six aerosol dispersal cups mounted in racklike fashion along two vertical columns of three cups each about 50 cm off-axis. The cups have a vertical separation of 1.2 m with the uppermost being about 30 cm below the upper flange (Fig. 2). The dispersal is achieved by the discharge of a 100-liter pressurized vessel (2 MPa) through a tube array into the cups. The dispersal system contains the same mixture as that in the 5.1-m^3 tank under the test conditions. All experiments were performed at standard atmospheric pressure. The mixture composition was determined by partial pressure measurements. The gas was then mixed with a sparkless air-driven fan installed in the upper dome of the tank, for a period of 30 min. Ignition was achieved via an exploding length of pyrofuse (aluminum-palladium wire) typically 100 cm in length and tightly coiled. A delay of 1 s was used between dispersion and ignition. Diagnostics included 18 thermocouple stations dispersed throughout the volume of the tank and six Koolite pressure sensors along the walls of the tank.

In the small-scale tests, both hydrogen and methane were used as gaseous fuels. For the large-scale tests, hydrogen alone was used. For both small-and large-scale tests, both cornstarch and sponge iron powder were used as the dust fuels. The cornstarch dust used had a mean particle size of 15 μm. The mean particle size for the iron dust used was in the range of 30-50 μm.

Results and Discussion

Constant-volume combustion properties of explosive mixtures as well as their flammability limits are strongly dependent on the apparatus and criteria used. Thus, it is important to first carry out a number of tests well within the flammability limits to determine the characteristics of the current apparatus. For the homogeneous gas mixtures, the particular cases of 15% H_2 in air and 9.5% methane in air were investigated. Peak overpressures of 4 and 7 bars respectively, were recorded as compared to the theoretical values of 4.57 and 7.82 bars (Lee et al. 1979). Researchers using similar apparatus have reported comparable values. Nagy and Portman (1960) have obtained overpressures of 6.3 bars for 9.5% methane-air in a .3-ft^3 cylinder. In a separate study, Nagy et al. (1971) reported an overpressure of 6.8 bars for a turbulent mixture of 9.5% methane in a 1-ft^3 cube. Benedick et al. (1984), obtained overpressures of 3.8 bars for a turbulent mixture of 15% hydrogen-air and 3.75 bars for the quiescent case in a 5-m^3 cylindrical tank (1.2 m diam, 4.8 m long). Given the range of geometries and volumes used, along with the degree of turbulence present during combustion, the range of values reported is quite reasonable.

It should be noted, that in the present experiments mixtures were burned in a turbulent environment to simulate the initial conditions of the hybrid mixtures studied later, where turbulence is necessary to suspend the dust. Following this, a pure dust mixture, also well within the limits (i.e., 250 g/m^3 of cornstarch in air) was burned under the same initial conditions of ignition and turbulence. The peak overpressure recorded was 5.6 bars. Cocks and Meyer (1979) reported a value of 3.6 bars for the same concentration in a 20-liter sphere. Jacobson et al. (1961) obtained overpressures of 5.6 bars in a 1.23 liter cylinder (Hartmann bomb). Previous work performed at McGill University (Bond et al. 1984) in a 333-liter sphere, indicated overpressures of 5.4 bars. It is evident that for the case of dust combustion, where the uniformity of concentration is very difficult to guarantee, relatively larger scatter of results is expected. Nonetheless, the results obtained in the present apparatus, compare very favorably with those previously mentioned.

Flammability limits of the individual fuel components were first determined using strong pyrotechnic igniters (100-g black powder ignited by a glow wire). The order of magnitude of energy deposited by these igniters was about 1 kJ, determined from the overpressure generated in the vessel by the igniter alone. The level of ignition energy was rendered sufficiently high to ensure that true limits of flammability were being measured (as opposed to the relative ignitability of a dust for a given ignition energy). In selecting the flammability criteria, it was noted that overpressures decreased rapidly with decreasing concentration. At some point near the lean limit, the overpressures leveled off, essentially registering the pressure generated by the pyrotechnic igniter. An overpressure of 20.7 KPa was then selected as the criterion to establish the flammability limit. This value was chosen because it corresponded to the pressure generated by a quiescent mixture of 4.0% hydrogen in air in the present apparatus. 4.0% is the lean upward propagation limit for hydrogen in air as reported by Coward and Jones (1952) and Hertzberg (1981). Similar pressures were also obtained for limit mixtures of 5.0% methane-air (Coward and Jones 1952; Hertzberg 1981).

Having established the quiescent flammability limits for the gas components, limits were then determined under the conditions of the turbulence level generated by the dispersion bottle discharge (henceforth referred to as dispersion turbulence). For the case of hydrogen, flammability limits were found to be narrower. With the dispersion turbulence present, the hydrogen lean limit was found to be 4.5% using the same pyrotechnic ignition source. However, for the case of methane-air mixtures, the same lean limit of 5.0% was found for both the initially quiescent and turbulent cases. This can be explained by examining the structure of a lean limit H_2-air. At the lean limit, H_2-air flames are inherently unstable and propagate as a collection of individual flamelets. These pockets of hot gas enriched by selective diffusion are surrounded by cold unburned mixture. In a turbulent environment, the convection of large quantities of cold unburned gas into the flamelets would lower the effective concentration and hence quench the flame. This is not the case for the lean limit methane flame. At its limit, the methane-air flame was observed to still propagate as a uniform flame sheet. Hence, the increase in transport rate would tend to manifest itself as an increase in burning rate. Of course, given a high enough level of turbulence, the lean limit flame can also be quenched.

Based on the same limit criterion, the lean flammability limit of cornstarch was found to be 80 g/m^3. This is approximately double the value obtained by Jacobson et al. (1961) in a 1.23-liter Hartmann bomb. However, in the small volume of the Hartmann bomb used by Jacobson and coworkers, it is not at all certain that a self-sustained flame is present. Therefore, it is to be expected that a slightly higher lean limit dust concentration will be evident in a larger bomb. The lean limit for Fe dust in air was found to be 400 g/m^3, roughly four times that listed by Field (1982). However, Field does not report the details of vessel size or configuration, or the particle size range. It should be noted that all results are largely dependent on apparatus geometry, volume, and on ignition energy and placement. Thus, there is always a certain degree of arbitrariness associated wtih any flammability limit criterion. However, results obtained with a given criterion are meaningful within the context of its selection.

Similar steps were followed in establishing the lean limit criteria for tests performed in the large-scale 5-m^3 cylindrical tank. The criterion required to establish the lean flammability limits was much more straightforward than that for the 180-liter vessel. In all tests performed, there was a very sharp distinction noted between a "go" and a "no go." Namely, either a large overpressure was noted, or no overpressure was evidenced whatsoever. In the 5-m^3 tank, the igniter is located near the bottom of the bomb. Along with its high length to diameter ratio of about 4, the 5-m^3 tank more closely resembles a vertical flammability tube than a closed volume spherical bomb. As expected, this resulted in higher percentages of the bomb volume being burned for a given mixture by the upward propagating flame than was the case for the .18-m^3 square cylindrical bomb.

Numerous tests performed previously in the tank showed that the lean limit for quiescent H_2-air mixtures was approximately 4.1% H_2. When the turbulence required to suspend the dust was introduced, a 4.25% H_2 mixture was found to be the minimum H_2 concentration to support combustion. The lean limits for cornstarch dust and iron dust were 70 and 275 g/m^3, respectively. Both of these values were slightly below those determined for the 180-liter bomb as expected. Evidently, more of the mixture is available for burning due to the slightly different geometry. Before determining flammability limits for hybrid mixtures, homogeneous gaseous mixtures of hydrogen and methane in air were first investigated in the present apparatus to check the validity of the Le Chatelier limit law.

Fig. 3 displays the results of flammability limit studies done in a turbulent environment for mixtures of hydrogen and methane. It can be seen that within the limits of experimental error, Le Chatelier's law is adhered to very closely. For gaseous fuels, Nagai (1929) has shown that Le Chatelier's limit law holds primarily for mixtures whose components have approximately the same lean limit flame temperature, or in terms of energetics, roughly the same limit heat of combustion per unit volume. The hydrogen-methane results shown here would seem to violate the observation of Nagai, since the theoretical lean hydrogen limit flame temperature is approximately 700 K, while that of methane is 1500 K. These temperatures and the energetics they represent are quite disparate. This can be explained in part by examining the mechanism by which a 4.0% H_2 flame propagates. At this concentration H_2 flames cannot propagate as uniform flame sheets; instead, they propagate as a collection of individual flamelets. Due to the very high mass diffusivity of hydrogen as compared to air, any convex curvature of the flame, however slight, will allow the hydrogen molecules to diffuse preferentially and consequently enrich the flame locally. This process of selective diffusion is believed to play a major role in the propagation of lean limit H_2 flames up to the downward propagation limit of 8.0%. This is the minimum concentration required for propagation as a flame sheet rather than as a collection of flamelets. In a hydrogen-methane air limit flame, selective diffusion will play a role, along with the kinetic characteristics of hydrogen, in allowing a flame to propagate below the energetics requirement dictated by the methane lean limit.

Figs. 4 and 5 display the results of a series of hybrid mixture flammability tests performed for both small and large scale. In both the case of H_2-Fe-air and H_2-cornstarch-air, the trends displayed in the small-scale results are amplified in the large-scale results, largely due to the greater ease in determining the presence of a self-sustained flame in the large-scale apparatus. The greater L/D ratio and volume result in higher overpressures for near limit flames, thus lowering the determinable dust limit. The obvious conclusion reached upon examination of the large-scale results is that Le Chatelier's law is simply not valid for dust-gas hybrid mixtures. The data are normalized with respect to the individual fuel components lean limit concentration in a particular apparatus. Although the dust lean limits differ for large and small scale, normalizing the data eliminates any arbitrariness associated with geometry or scale. Both large-and small-scale results demonstrate conclusively that hybrid lean flammability limits are not dependent on energetics alone. In fact, while energetics most certainly play a role, the mechanisms of propagation inherent in the hybrid flame determine flammability limit behavior.

This can be shown in Figs. 6 and 7, where the large-scale results have been plotted over flame temperature isotherms calculated for adiabatic isochoric combustion of the hybrid mixture. If we examine the hybrid region near the dust limit, we see that the results fall on isotherms corresponding to the lean limit flame temperature of the dust component alone, up to the point where the dust is no longer the primary fuel. Evidently, the addition of gas to a dust flame does not alter the mechanisms of propagation at all. In short, it simply ensures that the minimum flame temperature required for the propagation of the dust flame is maintained. This is analogous to what was shown by Nagai (1929) for gas flames, that all things being equal, the lean limit flame temperature is the critical parameter. Thus, for mixtures which contain fuels with two very different propagation mechanisms, as long as the dust propagation mechanism is dominant, the amount of gas fuel required to ensure the flammability of the mixture is that which will maintain the dust lean limit flame temperature. Comparing mixtures whose dust components either do or do not contain volatiles, the trend is the same. Therefore, the influence of volatiles is visible only insofar as it influences the lean limit of the dust itself. Once the dust is part of a hybrid mixture, the aforementioned mechanism is the crucial one.

For small-scale methane-iron and methane-cornstarch hybrid tests (Figs. 8 and 9), the same behavior is noted, leading to the conclusion that large-scale trends would match those of H_2-Fe and H_2-cornstarch. It becomes evident therefore, that in attempting to analyze hybrid behavior, small-scale results can be misleading. This is plausible and, in fact, sensible when one considers the thickness of a dust flame in comparison to the integral length scale of a small-scale Hartmann-bomb-type apparatus.

Conclusion

An extension of Le Chatelier's limit law to include hybrid mixtures has been shown to be invalid for the hybrid mixtures studied. However, much can be learned about the propagation mechanisms inherent in hybrid mixtures in examining the degree of departure from the law evidenced by the particular mixtures studied. The dust lean limit flame temperature has been shown to be an important parameter in assessing the lean flammability limits of hybrid mixtures near the pure dust limit. In addition, it has been determined that results culled from small-scale apparatus may be very misleading when dust mixtures are studied due to the approach of the lean limit dust flame thickness to the integral vessel dimension. It is recommended that large-scale apparatus be used whenever possible when studying dust or dust-gas hybrid lean flammability limits.

Acknowledgements

The authors are grateful to A. Makris and C. Daniel for their help in the experiments. At McGill University, the work was sponsored by the National Sciences and Engineering Research Council (NSERC) of Canada under grants A-7091 and A-3347 and by Energy, Mines and Resources (EMR) of Canada under contract number OSV82-00039. At Sandia Laboratories, the work was supported by the Nuclear Regulatory Commission.

References

Bartknecht, W. (1981) Explosions. Springer-Verlag, Berlin.

Benedick, W.B., Cummings, J.C., and Prassinos, P.G. (1984) Combustion of Hydrogen Air Mixtures in the VGES Cylindrical Tank. SAND 83-1022, Sandia National Laboratories, Albuquerque, N.M.

Bond, J.F., Fresko, M., Knystautas, R., and Lee, J.H.S. (1984) Influence of Turbulence on Dust Explosion. Proc. First International Colloquium on Explosibility of Industrial Dusts, Warsaw, Poland.

Cocks, R.E. and Meyer, R.C. (1979) Fabrication and use of a 20-liter Spherical Dust Testing Apparatus. Process Specialties Section, Engineering Division, Proctor & Gamble, Cincinnati, Ohio.

Coward, H.F. and Jones, G.W. (1952) Limits of Flammability of Gases and Vapors. Bulletin 503, US Bureau of Mines, Pittsburgh.

Field, P. (1982) Dust Explosions. Elsevier Scientific Publishing Co., Amsterdam.

Hertzberg, M., Richmond, J.K. and Cashdollar, K. (1981) Flammability and the Extinguishment of Explosions in Gases, Dust and their Mixtures. Colloque International Berthelot-Vieille-Mallard-Le Chatelier, Universite de Bordeaux, France, pp. 202-210.

Hertzberg, M. (1981) The Flammability Limits of Gases, Vapors and Dusts: Theory and Experiment. Proc. International Conference on Fuel-Air Explosions, McGill University, Montreal, Canada. University of Waterloo Press, pp. 3-48.

Jacobson, M., Nagy, J., Cooper, A.R., and Ball, F.J. (1961) Explosibility of Agricultural Dusts. RI 5753, US Bureau of Mines, Pittsburgh.

Lee, J.H.S., Guirao, C.M., Chiu, K.W., and Bach, G.G. (1979) Blast Effects from Vapor Cloud Explosions. Proc. AIChE Loss Prevention Symposium, Houston, Tex.

Nagai, Y. (1929) Flame Propagation in Gaseous Mixtures. J. Fuel Soc., Jpn. 8 (2), 17-18.

Nagy, J. and Portman, W.M. (1960) Explosibility of Coal Dust in an Atmosphere Containing a Low Percentage of Methane. RI 5815, US Bureau of Mines, Pittsburgh.

Nagy, J., Seiler, E.C., Conn, J.W., and Verakis, H.C. (1971) Explosion Development in Closed Vessels. RI 7507, US Bureau of Mines, Pittsburgh.

FIGURE CAPTIONS

Fig. 1 0.18 m^3 cylindrical dust bomb.

Fig. 2 5 m^3 cylindrical apparatus.

Fig. 3 Lean flammability limits of turbulent H_2-CH_4-air mixtures.

Fig. 4 Flammability limits of H_2-Fe-air hybrid mixtures for large and small scale.

Fig. 5 Flammability limits of H_2-cornstarch-air hybrid mixtures for large and small scale.

Fig. 6 5 m^3 H_2-cornstarch flammability limits with flame temperature isotherms.

Fig. 7 5 m^3 H_2-Fe flammability limits with flame temperature isotherms.

Fig. 8 Flammability limits of CH_4-Fe-air hybrid mixtures.

Fig. 9 Flammability limits of CH_4-cornstarch-air hybrid mixtures.

RUNNING HEADS

M. GAUG ET AL.

DUST EXPLOSIONS

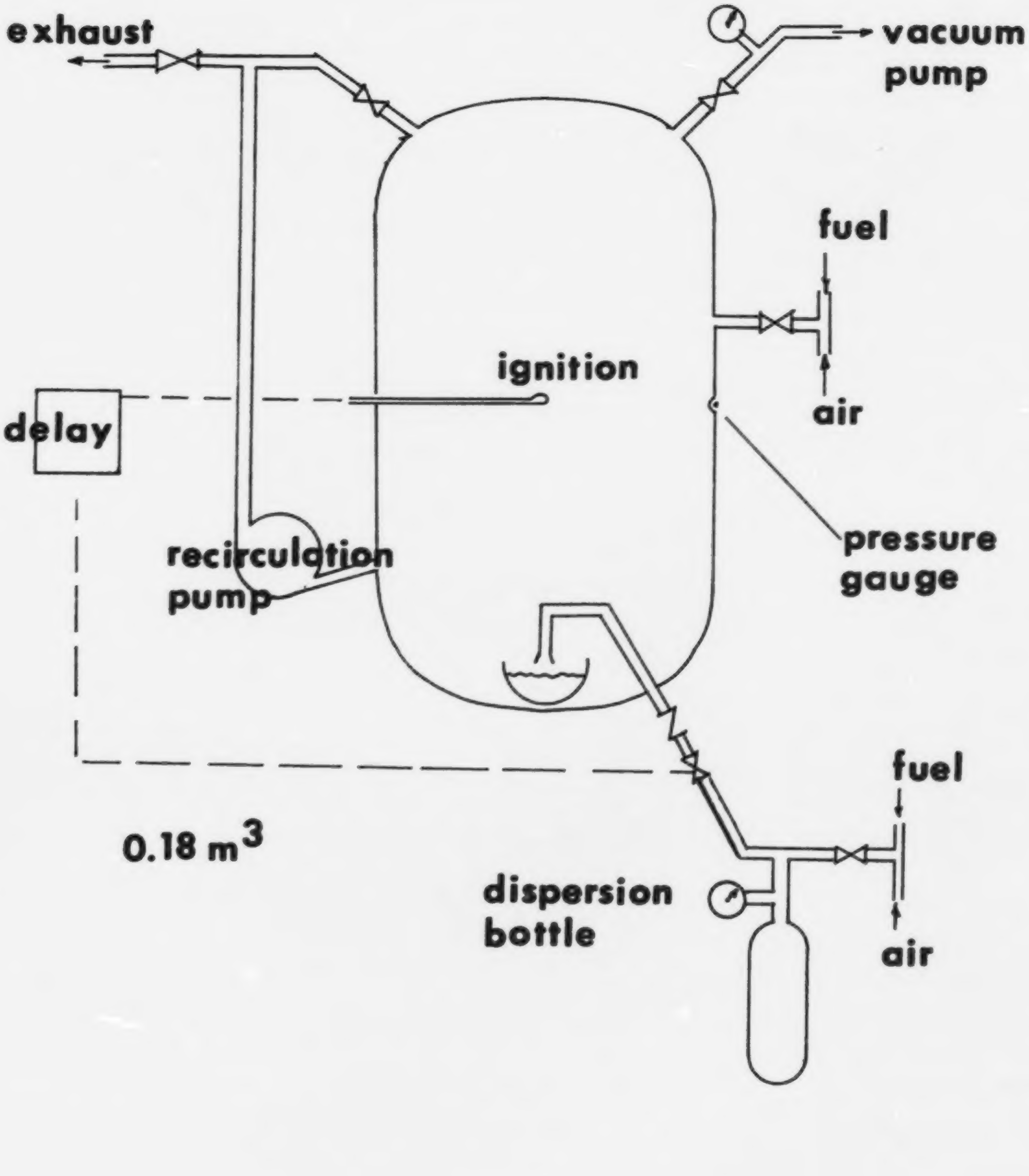
exhaust
vacuum pump
fuel
air
ignition
delay
pressure gauge
recirculation pump
fuel
0.18 m^3
dispersion bottle
air

FIG · 1

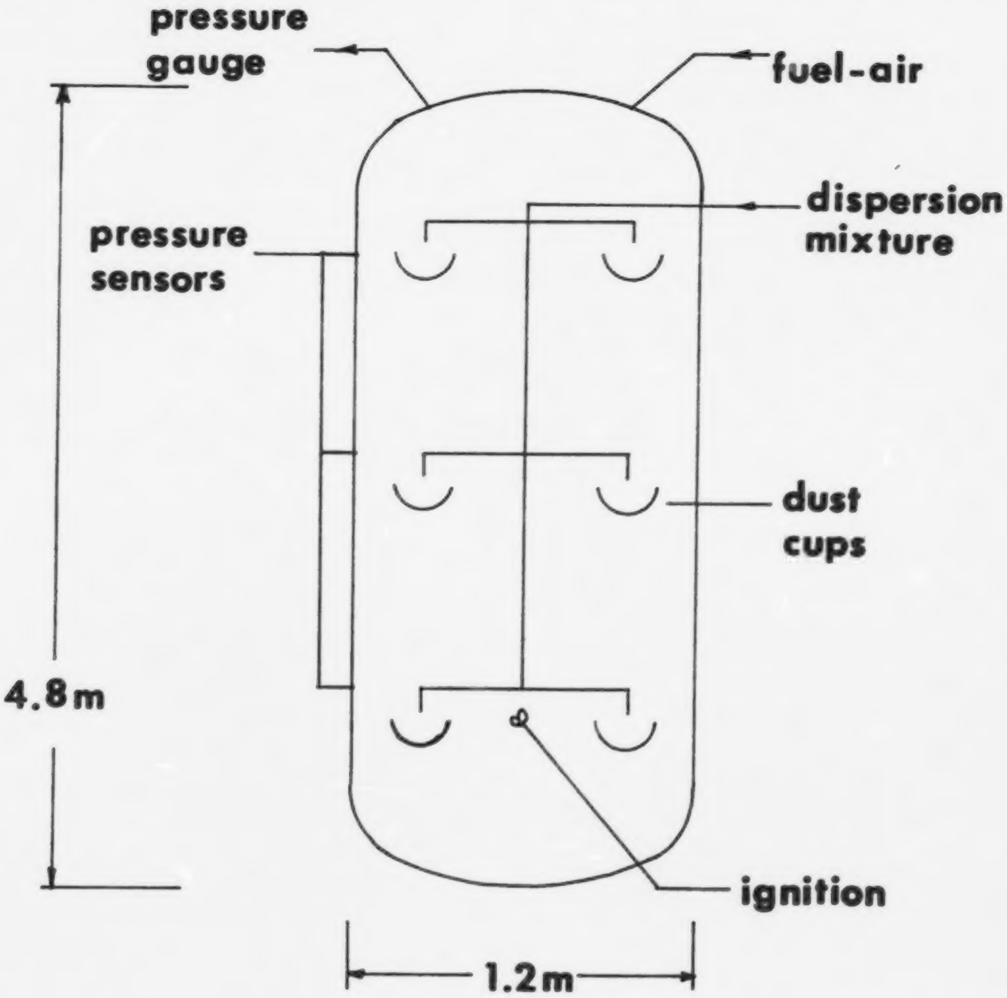
pressure gauge
fuel-air
dispersion mixture
pressure sensors
dust cups
4.8m
ignition
1.2m

5.1 m^3

FIG · 2

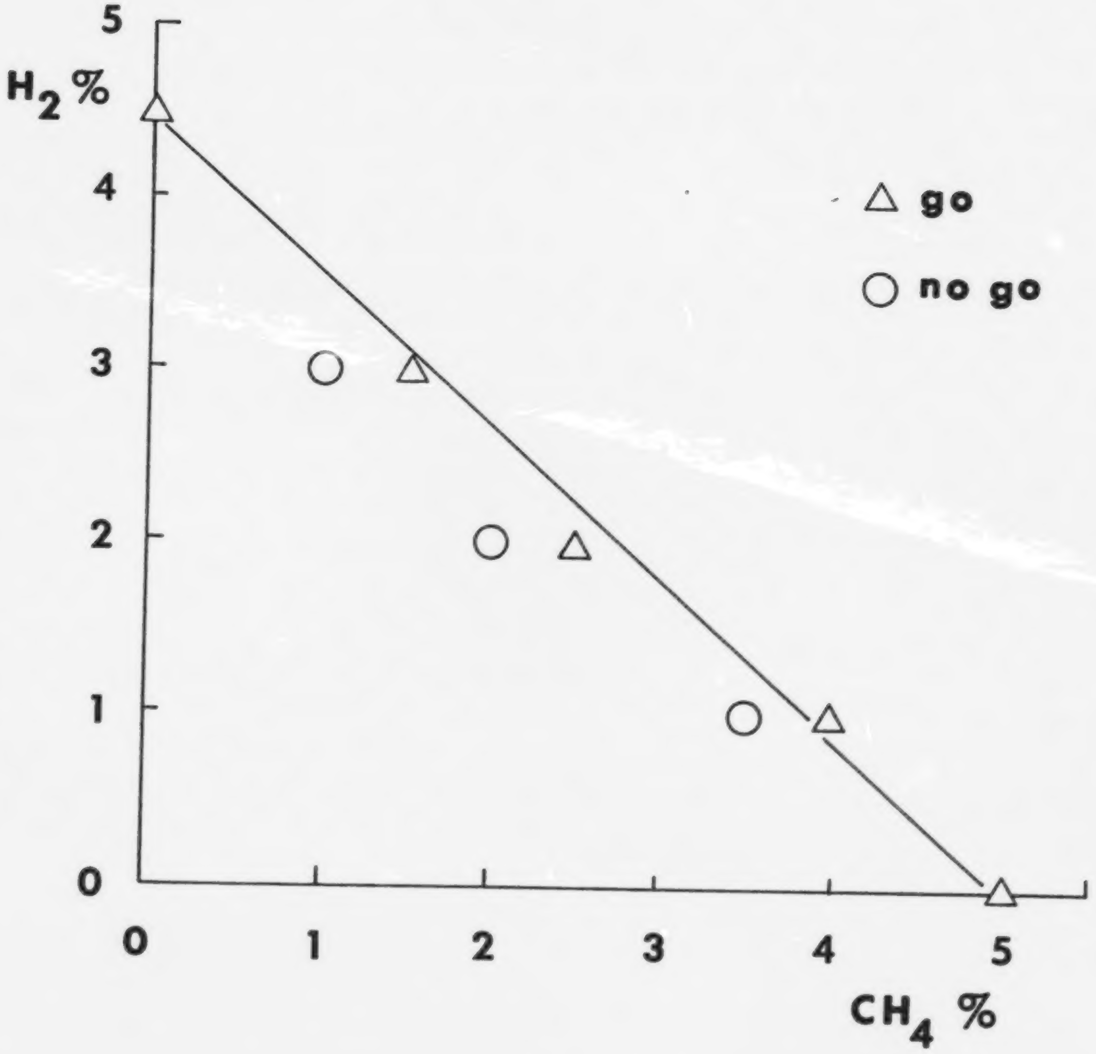

FIG·3

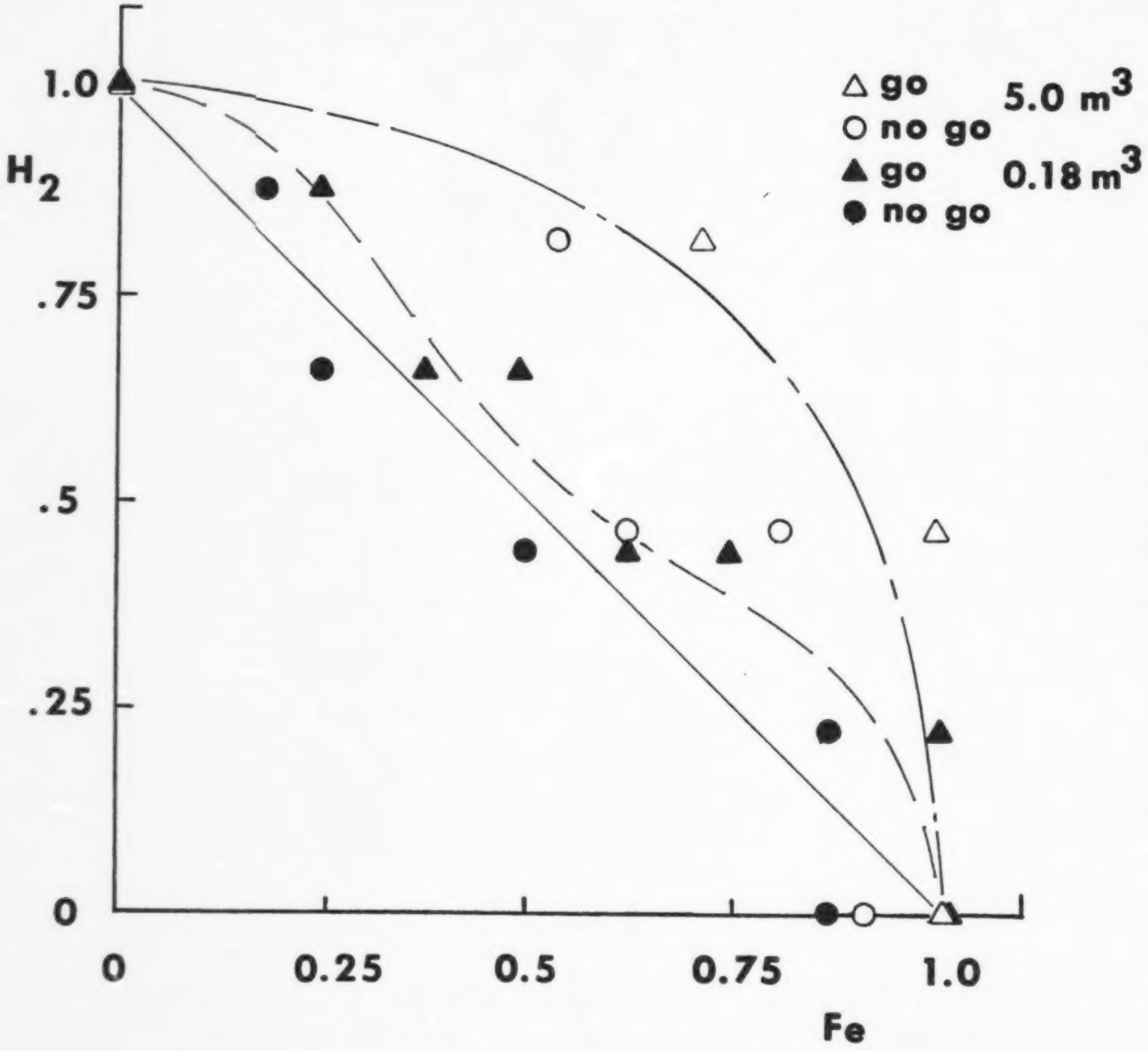

FIG·4

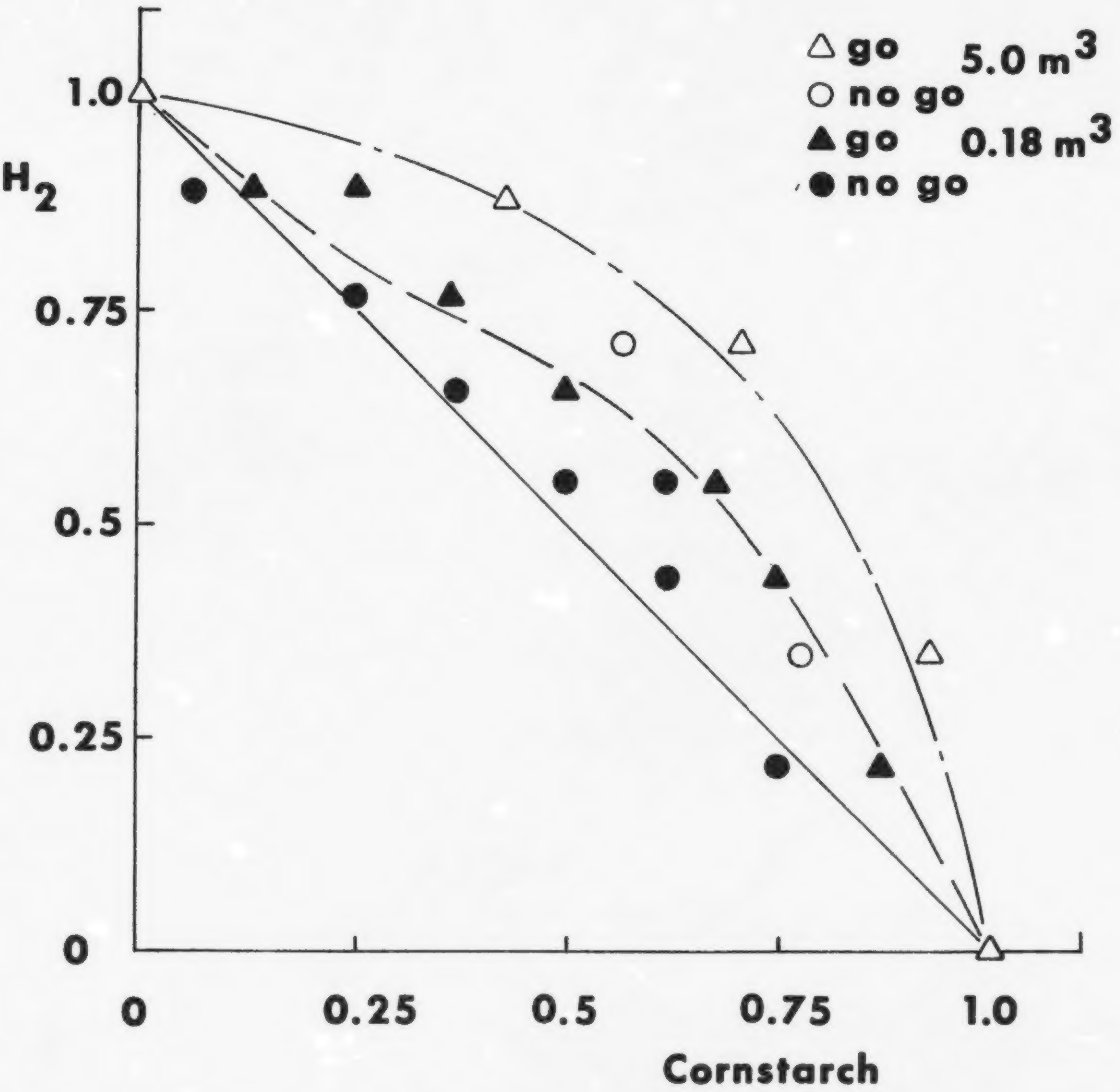
△ go
○ no go
5.0 m^3
▲ go
● no go
0.18 m^3
H$_2$
1.0
0.75
0.5
0.25
0
0
0.25
0.5
0.75
1.0
Cornstarch

FIG ·5

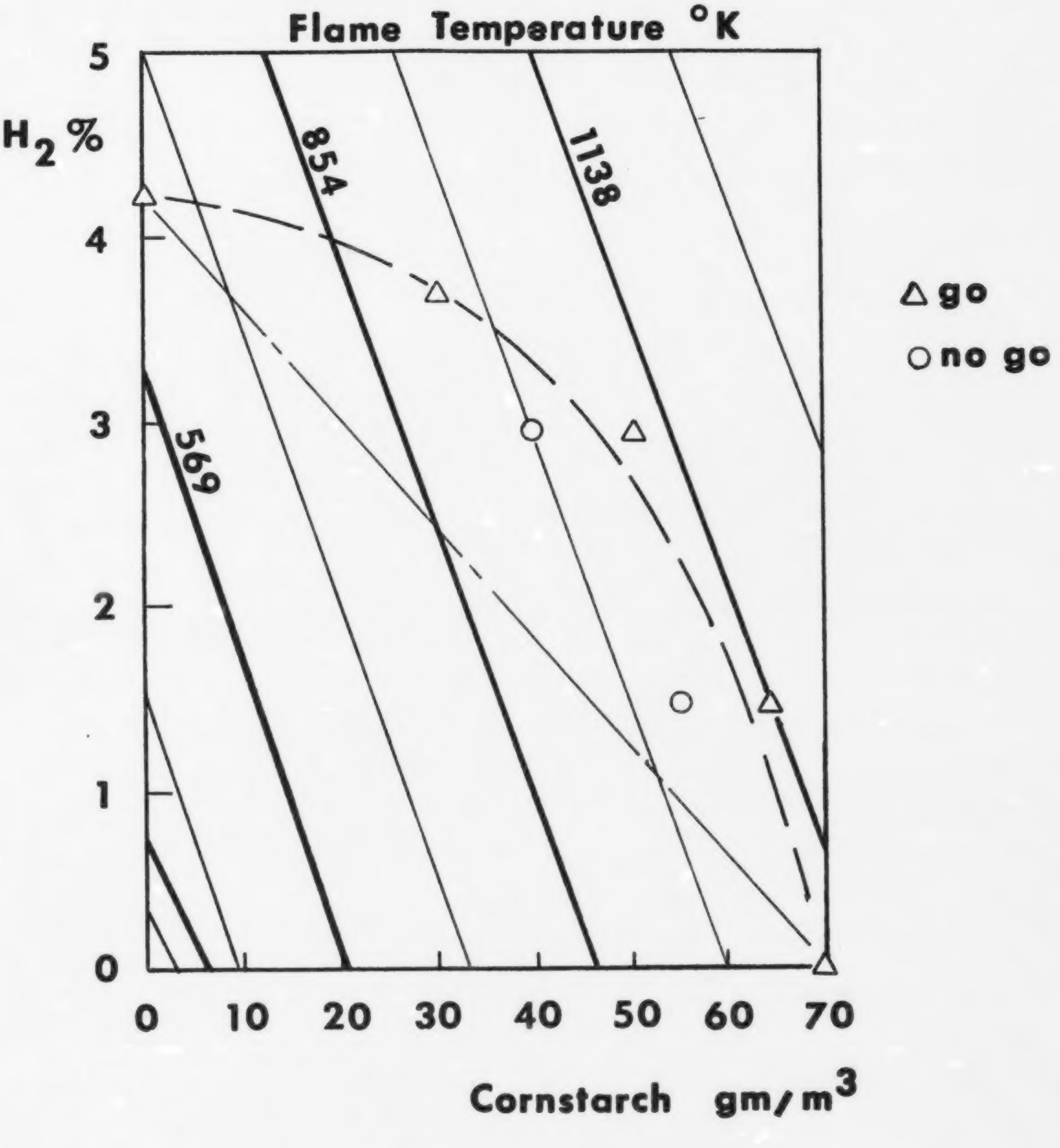
Flame Temperature °K
H$_2$ %
5
4
3
2
1
0
854
1138
569
0
10
20
30
40
50
60
70
Cornstarch gm/m^3
△ go
○ no go

FIG. 6

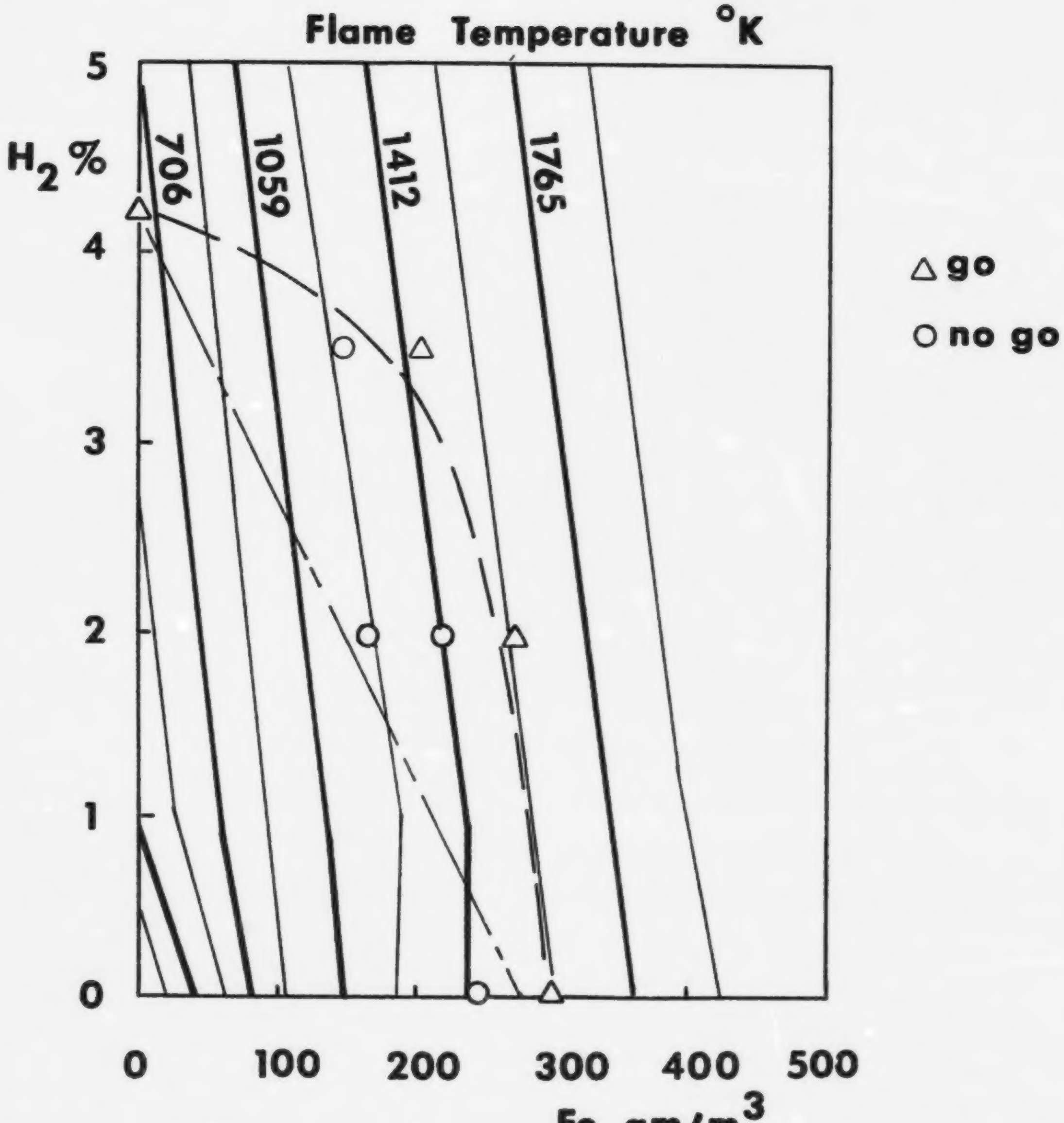

Flame Temperature °K
H2 %
706
1059
1412
1765
5
4
3
2
1
0
0
100
200
300
400
500
Fe gm/m3
△ go
○ no go

FIG· 7

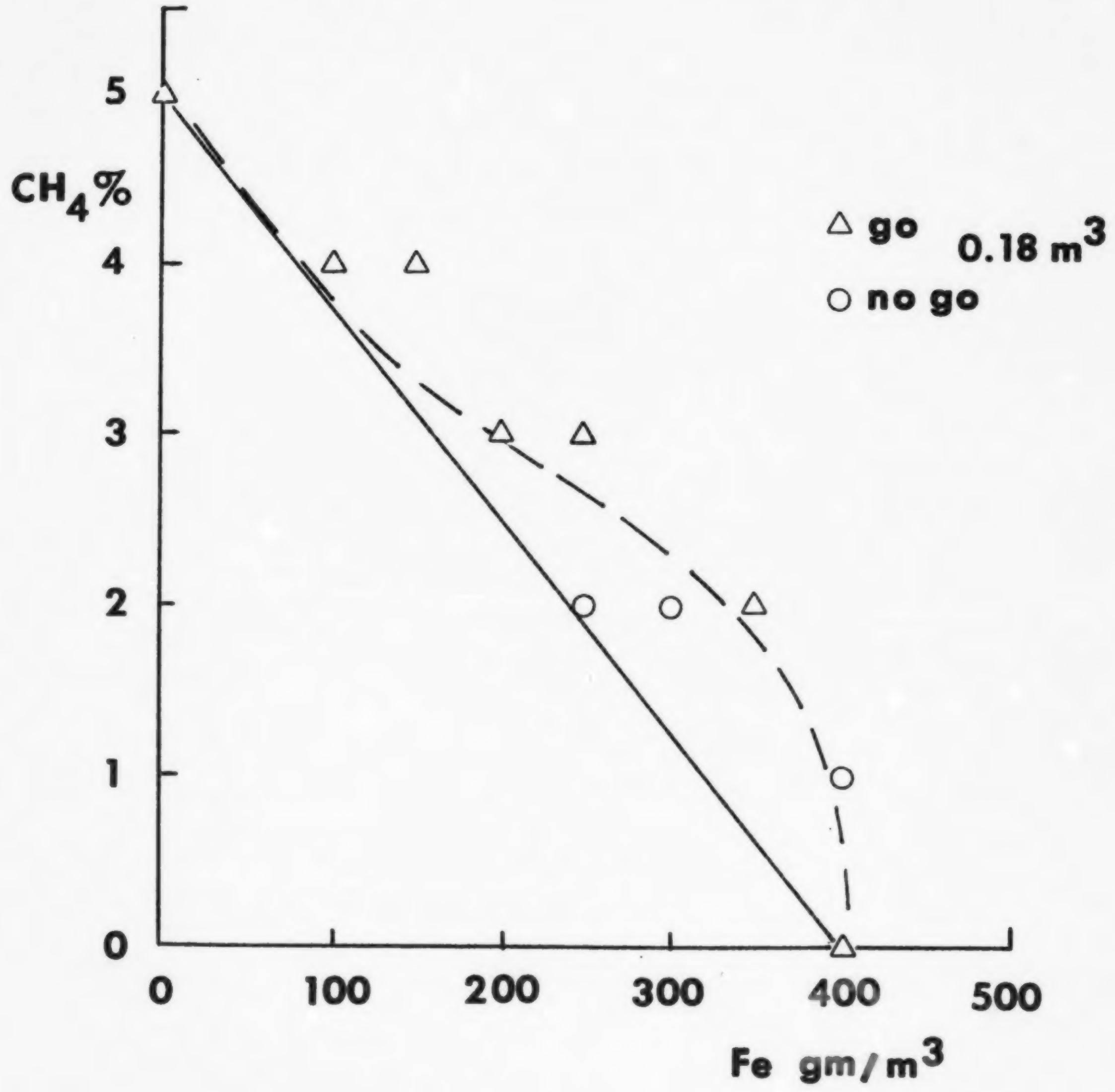

FIG · 8

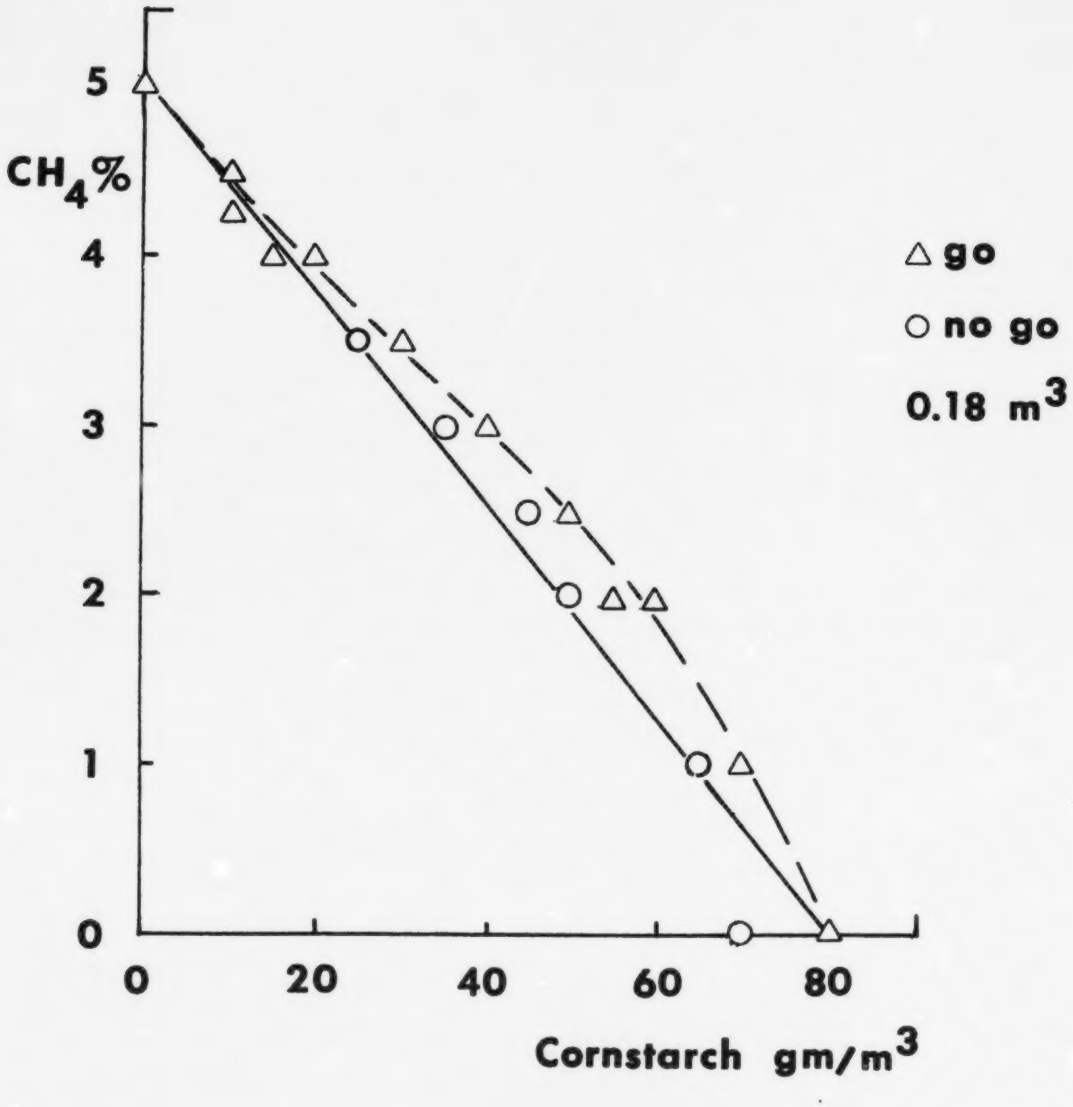

FIG·9

QUENCHING OF DUST-AIR FLAMES

J. Jarosinski*, J.H. Lee, R. Knystautas and J.D. Crowley
Department of Mechanical Engineering
McGill University
Montreal, Canada

The subject matter:

- Flames
- Property Measurements
- Quenching

Submitted for Presentation at the 21st International Combustion Symposium
Muchich, West Germany, August 3-8, 1986

---

* Permanent address: Institute of Aeronautics, Al. Krakowska 110/114, 02-256 Warszawa, Poland

ABSTRACT

Flame quenching in mixtures of cornstarch, aluminum and coal dusts with air has been studied. The experiments were carried out in a vertical tube 0.190 m inside diameter and 1.8 m long with quenching plates held in the middle part. The lean flammability limit determined under constant pressure conditions appears to be several times greater than that determined in constant volume for all dust-air mixtures investigated. The quenching distance was measured in conditions of upward freely propagating flame from the open bottom end of the tube. The minimum quenching distance for flames propagating through dust-air mixtures is 5.5 mm for cornstarch, 10.4 mm for aluminum and about 190 mm for coal dust as compared with 2.0 mm for a stoichiometric methane-air mixture. Because the order of magnitude of the measured quenching distance in cornstarch and aluminum dust flames is the same as in gas flames, it is inferred that processes controlling the flame propagation in all of these flames should be similar. The large value of the quenching distance for coal dust-air mixture can be explained by the large particle size of the coal dust used in the experiments. The quenching distance can be used to identify the controlling processes in laminar premixed coal dust-air flames and hence is one of the most fundamental quantities. This is due to the fact that such quantities as burning velocity and minimum ignition energy are apparatus dependent. Quenching distance determined in limit quenching conditions should not be apparatus dependent.

INTRODUCTION

Unlike dust combustion, the combustion of gas mixtures is now well understood. The main controlling processes of gas combustion have been identified and theories of laminar gas flames have been established. Such fundamental quantities as laminar burning velocity, flame thickness, quenching distance and minimum ignition energy, which have unique values for a given mixture composition, have been measured for most gases.

While research on dust combustion has been in progress for many years, the detailed mechanisms of the dust combustion process are still not fully understood. Insufficient knowledge of premixed laminar dust flame properties and the mechanism of their propagation inhibit the development of modeling of dust combustion processes as well as the development of theories. Detailed recent reviews of research into propagation of laminar premixed coal dust-air flames may be found in the work of Smoot et al. [1] and Krazinski et al. [2] Although past research and analysis has identified the general characteristics of laminar premixed coal dust-air flames, the details of the processes in the flame have not been resolved. The influence of the general dust parameters (size of particle, volatile part, dust concentration, physical nature of the particle) and the processes (radiation, conduction, diffusion, heterogeneous reaction) on the fundamental characteristics of the flame (burning velocity, flame thickness, minimum ignition energy, quenching distance) are the subject of continuing interest.

Numerous experiments reported in [1-3] have been carried out to measure the burning velocity and flame thickness on open burners. Experimental observations reveal that burning velocity and flame thickness depend not only on the coal dust characteristics, but also on the apparatus (scale shape, dispersion and stabilizing system, etc.). Analysis in [3] shows that flame speeds have been reported from 3 to 200 cm/s, depending on the type of apparatus in which the investigation was conducted.

Measurements of minimum ignition energy in dust mixtures have been recently reported by Ballal [4,5] and Hertzberg et al. [6]. Ballal carried out his experiments in dust clouds of carbon, graphite, coal, aluminum and magnesium. He found qualitative similarity between ignition and quenching of dust clouds and of liquid droplet sprays and mists. He modified the theory developed earlier [7] to predict the experimental results in dust-air flames, the quenching diameter in particular. Energy requirements for the spark ignition in air of polyethylene powder, lycopodium, and Pittsburgh coal dust have been determined by Hertzberg et al. [6]. The minimum ignition energies measured at room temperature for all three dusts studied occured at relatively high concentration of dust, several times higher than the stoichiometric concentration. The authors reported that the accurate determination of the minimum ignition energy of a dust involves extraordinary complications. The most important one is producing a quiescent dust-air mixture with reproducible concentration. They illustrated the complications with available data of minimum ignition energy for lycopodium which changed in different Bureau of Mines studies from 25 mJ to 50 mJ. In contrast a value of about 10 mJ was determined by Eckhoff using the optimum characteristics of the spark discharge [8]. They concluded that a reliable determination of a minimum ignition energy that reflects intrinsic flammability behaviour for dust mixtures is dubious.

Recently, Smoot and co-workers [9] reported a series of parametric predictions to identify the controlling processes in premixed fine coal dust-air flame. The model has been systematically developed since 1976 [10] and in its present state can predict the magnitude of burning velocity and flame thickness, together with dependence of burning velocity on dust parameters. It has been found, as a result of this prediction, that the rate of flame propagation is controlled by the rate of streamwise molecular diffusion of oxygen and volatiles, together with heat conduction from the hot gas to the particles. It also has been found that radiation, heterogeneous reaction, the rates of coal devolatilization and volatiles oxidation in the gas phase play a secondary role in the propagation of analyzed flames. The calculated results based on model of Slezak et al. [11] are different from those of Smoot [9]. There are still divergent opinions on the processes controlling the flame propagation which indicate that it is not known clearly what is the mechanism of flame propagation in premixed laminar dust-air mixtures. Smoot and co-workers consider radiation unimportant in the mechanism of flame propagation and report that the thickness of premixed laminar coal-dust flame is in the range of 0.5-4.0 cm [9]. Krier and co-workers consider radiation important in the mechanism of flame propagation and report that the thickness of premixed laminar coal dust flame is very large compared to gas flame and may even approach a meter [3, 11]. Smoot and Ballal who accept conduction and molecular diffusion as the controlling processes of flame propagation in dust-air mixture differ in quantifying the role of heterogeneous reaction and gas phase chemical reaction of volatiles in coal dust flames [5,9].

Much more reliable experimental data are required to verify the mechanism of flame propagation in laminar premixed dust-air mixture. Burning velocity and minimum ignition energy are not sufficiently fundamental - they are apparatus dependent. It is important to measure not only burning velocity, and minimum ignition energy, but also quenching distance which is linked directly to flame thickness, and by definition, is determined at the limit quenching conditions. Until now, nobody has tried to determine the quenching distance for dust-air flames, which can be measured with relative ease and which if properly measured should not be dependent on the apparatus. For gas mixtures the quenching distance is closely related to flame thickness. If the order of magnitude of measured quenching distance in dust flames is the same as for gas flames, the processes controlling dust-flame propagation should be similar to those of gas flames. Therefore, measuring the quenching distance can provide valuable insight into the mechanism of flame propagation in dust-air mixtures.

The purpose of this study is to investigate the quenching distance of a dust-air flame and its relation to laminar flame thickness. Because the controlling processes in laminar gas and dust-air flames are similar in the light of the analysis of Smoot, one should expect that the relation between fundamental quantities characterizing premixed laminar dust flames and gas flames should also be similar.

EXPERIMENTAL DETAILS

All experimental work was carried out in a vertical steel tube, 0.190 m inside diameter and 1.880 m long (volume = 53.3 L). The apparatus consists of two sections bolted together in the middle as shown in Fig. 1. A grid of quenching plates is held in the middle of the test apparatus between the two sections. For constant volume experiments the top cover-flange completely seals the top of the vessel. For constant pressure experiments this flange is replaced by a 28.6 mm orifice. The orifice is used to damp vibrations while allowing the flame to propagate toward what is effectively a closed end.

The flange on the bottom end of the tube holds the igniter. For constant volume experiments the flange is bolted in place to close the vessel. For constant pressure experiments the same flange is free-floating on three 100 mm long bolts so that it can either close or open the bottom of the tube.

Before an experiment the vessel is first evacuated to 150 torr. The experiment begins with the opening of a solenoid valve causing the dispersion of the dust by an air blast from a 0.23 L compressed air reservoir. The air passes through the dust reservoir where it entrains the dust which then dispersed by a perforated tube located inside the test vessel. Ignition with a 1.2 gram black powder match follows dispersion by 200 msec. Both the mixture introduced by the dispersion system and the gas evolution due to combustion cause the pressure to increase. The increasing pressure releases the cap at the top end of the tube and the cover-flange at the bottom end of the tube. Once the tube is open the pressure remains constant, the combustion products vent to the atmosphere and the flame propagates upward freely. After each test the dispersion system is purged of any residue and the tube is opened and swept clean.

The time delay between dispersion and ignition is controlled by a mechanical timer which permits time delays of up to 250 ms. Two limit switches control the opening and closing of the solenoid valves, and one limit switch controls the time of ignition. A mechanical timer is used instead of an electronic timer because of the inherent insensitivity of the mechanical timer to electromagnetic pulses caused by the operation of the solenoid valves and to stray signals caused by other laboratory equipment. While not as precise as an electronic device, calibration tests show the timer to have a fluctuation of less than 4 ms.

The flame arrival is detected at the axis of the test vessel by three ionization probes biased at a 400 VDC potential. The ionization probes are located at $y = 0.540$ m, $y = 0.870$ m, and $y = 1.155$ m from the bottom flange of the tube and their signal is recorded on an oscilloscope.

For experiments at constant volume a piezoelectric transducer (PCB113A24) is used to determine the pressure history inside the vessel. The sensitivity of this transducer is approximately 5 mv/psi. Experiments conducted at a constant pressure are monitored with a microphone under the assumption that a laminar flame velocity profile will not produce vibrations and should be relatively quiet.

The quenching distance of the flame is measured by varying the composition of the fuel-air mixture until the limit concentration is found for a particular gap. The quenching plates measure 1.5 mm x 75 mm x 130 mm and are arranged to form a 130 mm square grid with the 75 mm edge parallel to the axis of the tube. The quenching distance is adjusted by varying the size of the spacers placed between the quenching plates. The number of plates used varies with the size of the spacers.

The gaseous fuel-air mixture is made by blending air and gas with calibrated rotameter-type flow meters. The air flow rate is left constant and the mixture composition is varied by changing the flow rate of the fuel. Because the gas-air mixture is buoyant in air, it is introduced from the top end of the tube. To ensure that the mixture is homogeneous, a volume of mixture three times the volume of the test vessel is flushed through prior to ignition.

The dust-air mixture composition is varied by changing the mass of dust placed in the dispersion vessel. To ensure that there is dust-air mixture between the quenching plates the initial air pressure of the lower dispersion system is 25-35% greater than that of the upper system. Typical dispersion pressures are 1.03 MPa upper and 1.37 MPa lower (gauge). Upon dispersion, air and dust sweep through the plates as the pressure in the vessel goes to equilibrium. Turbulence due to dispersion is assumed to not affect the flame because the decay time is relatively short compared to about 1.0 s required for the flame to reach the quenching plates. Cornstarch, aluminum, and coal dusts were used in experiments.

Cornstarch ($C_6H_{10}O_5$) consists mostly of volatiles with little fixed carbon or ash. The particles are nearly spherical in shape and are fairly uniform in size with a mean size of 15 μm. The method of preparing the cornstarch fuel adopted for the present investigation consisted of mixing the cornstarch with 1% by mass of fumed silica gel and storing it in an open jar in an oven at 40^oC.

Aluminum dust consists of aluminum flakes of the average size of the particles about 15 μm x 0.1 μm.

The bituminous coal dust (DEVCO No. 26) used in experiments was supplied by the Canada Centre for Mineral and Energy Technology (CANMET). It contains a broad distribution of particle sizes. Its properties in comparison with the standard Pittsburgh bituminous coal dust determined by the same CANMET laboratory are presented in Table I. The samples were screened by passing them through a 200 mesh sieve.

RESULTS

In a closed vessel the increase in specific volume of the product gases behind the flame front tends to displace mixture in front of the flame and pushes the flame. Tests with methane-air mixture indicate that the apparatus is unsuited for constant volume experiments since a pushed flame would pass through a 1.5 mm spacing between the quenching plates even in lean limit mixtures. Since the quenching distance of freely propagating gas flames is well documented it was decided to calibrate the vessel with methane-air flames in constant pressure conditions with the bottom end of the tube open and the flame propagating toward the closed end. Under these conditions the propagation velocity of the flame front is effectively controlled by the velocity of the ascending buoyant gases rather than by the relatively small burning velocity of the mixture. The surface at the flame adjusts itself to the velocity of the leading point and to the laminar burning velocity in such a manner that $Su_L = Fu$, where S is the flame area, F the cross-sectional area of the tube, u_L the laminar burning velocity and u flame speed [12].

Methane-air tests at constant pressure indicate that the geometry of the test vessel makes it an excellent acoustic resonator. This problem was suppressed by converting the top flange into a tuned damper. With the amplitude of the acoustic vibrations measured with a microphone placed near the quenching grid, tests indicate that the optimum orifice size is 28.6 mm.

Tests of the apparatus indicate the quenching behaviour of upward freely propagating methane-air flames to be typically U-shaped as expected. As shown in Fig. 2, the results are similar to those obtained earlier in a 50 mm square tube [13]. The minimum quenching distance for methane-air is 2.0 mm and occurs at the stoichiometric mixture. Differences at the limit concentration are attributed to the difference in scale of the two experiments.

It was found that the lean flammability limit of cornstarch-air mixture is different when determined at constant volume as compred to constant pressure. In the constant volume cylindrical bomb (0.18 m^3) this limit was found to be 70 gm/m^3 [14], while in constant pressure experiments it was about 380 g/m^3. Lean limit dust concentration at constant pressure conditions was considered the leanest dust concentration at which a flame was observed to propagate the entire length of the tube.

The apparent discrepancy between the reported lean flammability limit and the results of the present investigation is explained by tests made with the apparatus under constant volume conditions. These tests indicate that cornstarch-air flames propagate easily and have substantial pressure rise with a concentration as low as 200 g/m^3, well below the constant pressure lean limit of 380 g/m^3. Thus the series of experiments made in the same apparatus, but in the different conditions of constant volume and constant pressure, confirm the existence of two difference lean flammability limits for cornstarch dust-air mixture.

The quenching distance as a function of the cornstarch dust-air mixture concentration is shown in Fig. 3. The graph shows two distinct regions for the sensitivity of the flame quenching distance on the dust concentration. For concentrations less than 500 g/m^3, a small change in dust concentration results in a large change in quenching distance. At 500 g/m^3 there is an abrupt change in the slope of the graph followed by a second region less sensitive to a change in dust concentration. The minimum quenching distance for cornstarch-air mixture is 5.5 mm at a dust concentration of 800 g/m^3 which is 3.4 times the theoretical stoichiometric mixture.

For quenching distances near the minimum there is some indication of rich limit behaviour. A flame in a mixture with a cornstarch concentration of 890 g/m^3 was quenched by plates with a 5.5 mm spacing, and flames propagating in mixtures with concentrations of 1000 g/m^3 and 1110 g/m^3 were quenched by plates with a 6.0 mm spacing. Since the flame was able to propagate as far as the test section, these three results must be due to quenching by the plates rather than to suppression by the non-reacting dust. While it is expected that the rich quenching trend should continue, present data indicate that there is no rich quenching for a spacing of 6.5 mm.

The next experiments were conducted with dust clouds of aluminum flake powder. Figure 4 presents the experimental results on quenching distance of aluminum flake. The lean flammability limit for flames propagating freely through aluminum dust-air mixtures in constant pressure conditions appears to be 330 g/m^3, approximately 2.4 times the lean limit in Ballal's experiments [5] and slightly higher than the stoichiometric composition. The quenching diameter for this kind of dust is reported by Ballal to be of the order of 4.0 mm. However, careful investigation shows that the minimum quenching distance for a freely propagating flame in aluminum dust-air mixture is 10.4 mm at a dust concentration of 670.0 g/m^3, which is 2.17 times the theoretical stoichiometric mixture.

In experiments with coal dust-air mixtures, new and unexpected behaviour of the flame has been observed. In spite of exhaustive attempts to obtain freely propagating flames through the mixture, the flame failed to propagate inside this size apparatus regardless of mixture concentration. Increasing the content of volatile matter by the addition of 5% by mass of cornstarch to the coal dust made it possible for the flame to propagate. Propagation was ascertained for coal dust concentrations ranging from 500 g/m^3 to 1100 g/m^3. The flame could pass the entire length of the tube only in the absence of any quenching plates between the two sections of the tube. It is evident from this description of experiments that the 19.0 cm tube diameter was very close to the quenching diameter for the coal dust-air mixture investigated.

DISCUSSION

Lean limits determined in constant pressure conditions appear to be several times greater than those determined in constant volume for all the dust-air mixtures investigated. One of the possible and the most natural explanation is that below the lean limit concentration the burning velocity is too low to form a self-propagating flame. It is known for different combustion gases in mixtures with air that the limit burning velocities are about 3 cm/s for ammonia, about 5 cm/s for methane, and about 7 cm/s for propane. The limit burning velocities for dust mixtures are not known, but should be of the same order of magnitude. The differences in lean limit concentration at constant volume and constant pressure could be explained by the observation that when a flame is pushed by hot gases it can propagate with a lower burning velocity [15].

Results of experiments show that the quenching distances of cornstarch-air and aluminum-air mixtures are comparable to the quenching distances of gas flames. For methane-air mixture, for example, the quenching distance is equal to 2.0 mm for stoichiometric mixtures, 9.2 mm for lean limit mixture, and even more for the rich limit, so it is in the same range as the dust-air flames investigated.

Because the quenching distances of flames propagating in cornstarch-air and aluminum-air mixtures are comparable with quenching distances of methane-air mixtures, the processes controlling flame propagation in all these mixtures should be similar, although these two dust mixtures have very different physical properties. In both dust-air flames heat conduction from the high temperature combustion zone raises the particle temperature to start volatilization or vaporization. The flame propagation is controlled in this case by heat conduction from hot gas to the particles and by the rate of streamwise molecular diffusion of oxygen and volatiles or aluminum vapour.

It is known for flames propagating in gas mixtures that the quenching distance is twice the flame thickness [13]. From the point of view of similarity of processes in the flames under consideration, the same relation should be valid for both dust-air flames. It follows from this that the flame thickness which corresponds to the minimum value of quenching distance for cornstarch with air is approximately 2.75 mm and for aluminum with air it is approximately 5.2 mm.

It was shown in [16] that for real flames the relation between the flame thickness δ_L (as defined in [17]) and the characteristic thickness $\Delta = \lambda / C_p \rho_u u_L$ is $\delta_L \simeq 8\Delta$, where λ is the thermal conductivity, C_p the specific heat at consant pressure, ρ_u the density of unburned mixture and u_L the burning velocity, λ/C_p should be calculated as a mean value for the temperature range across the flame front. This relation makes it possible to estimate the burning velocity at the quenching conditions. For cornstarch air mixture $u_L \simeq 14.5$ cm/s and for aluminum air mixture $u_L \simeq 11$ cm/s (λ/C_p was calculated at the base of data for air).

Experimental results of aluminum dust-air flames can be compared with those of Ballal [4,5] only on a limited scale. Ballal made his experiments in the range of concentration of 140 to 330 g/m^3, while experiments reported in this paper were made in the concentration range of 330 g/m^3 (lean flammability limit for freely propagating flame in apparatus used in experiments) to 700 g/m^3. The quenching distance defined in [5] is the minimum diameter which develops the flame initiated by a spark with near-limit ignition energy. The quenching distance measured in the present work is the maximum spacing between the walls for which heat outflow to the walls is able to quench the fully developed freely propagating flame. For gas mixture the quenching distance and minimum flame diameter are almost equal [18]. From this point of view the minimum flame diameter for methane-air mixture determined by Ballal and cited in [5] is surprisingly small and disagrees with [18] ($\simeq$ 0.6 mm compared to more than 2.0 mm according to Lewis and Elbe's measurements). Quenching distance as determined in the present study for aluminum dust-air flame appears to be 10.4 mm as compared to the quenching diameter of 4 mm reported by Ballal [5]. Because his quenching diameter for methane-air mixture is also less than that which is commonly accepted, one must conclude that the method used by Ballal lowers the value of the quenching diameter.

For coal dust-air mixtures the quenching distance appears to be unexpectedly large, which can be explained by the relatively large particle sizes used in the experiments. There is some agreement of data in the present work with that reported by Slezak et al. [3]. The distribution of particle sizes in both dusts was similar. The lean flammability limit with the added 5% of cornstarch dust was practically the same as in [3]. The behaviour of flame during its propagation along the tube was also similar. However, the interpretation of the results is different. In the present work the difficulty with flame propagation inside the tube may be due to a low burning velocity which is below the limit burning velocity. In the paper of Slezak et al. [3], the burning velocity is very high, much higher than usually estimated. The method used to determine its value is doubtful. According to Zeldovich this kind of flame propagation is highly influenced by buoyancy which determines the velocity of the leading point of the flame [12]. The surface of the flame adjusts itself to both the velocity of the leading point and the laminar burning velocity. Accuracy in calculating the burning velocity depends on the accuracy in determining the flame surface. The authors used a two-dimensional parabola to measure the surface of the flame front, which as they observed themselves was "bushy" and three-dimensional. As a result the measured burning velocity appears very high. Also, their temperature records show that the burning velocity cannot be high. The flame temperature in their experiments must have been very close to the limit temperature from the point of view of flammability limits. For most of the gases the limit temperature below which the flame cannot propagate is about 1200-1250°K. In conclusion it can be said that the burning velocity described in [3] appears to be overestimated and in reality may be rather small.

CONCLUSIONS

Quenching distance has been measured in a relatively large scale apparatus for freely propagating flames in dust-air mixtures of cornstarch, aluminum and coal. Minimum quenching distances for fine cornstarch and aluminum dust with air appear to be 5.5 mm and 10.4 mm respectively. These values are comparable with experimental data for gas flames. The quenching distance as determined in methane-air mixture is 2.0 mm for the stoichiometric mixture, 9.2 mm for the lean limit, and about 20.0 mm for the rich limit. Because the order of magnitude of measured quenching distance in cornstarch and aluminum dust flames is the same as in gas flames, the processes controlling flame propagation in all of these flames should be similar.

Quenching distance in coal dust-air mixtures with broad distribution of particle sizes was indirectly inferred to be 19.0 cm. Such a large value of quenching distance can be explained by the large size of the particles in coal dust used in the experiments. Increasing size of particles increases the flame thickness and decreases the burning velocity (i.e., increases the quenching distance).

The experimental study of the present paper offers the quenching distance as the most fundamental quantity which can be used to identify the controlling processes in dust combustion. Such quantities as burning velocity, flame thickness, and minimum ignition energy depend on the apparatus and are thereby not sufficiently fundamental. Quenching distance, linked directly with flame thickness, determined by definition in limit quenching conditions, if properly measured, should not be dependent on the apparatus.

ACKNOWLEDGEMENTS

This work was supported by the Natural Sciences and Engineering Research Council of Canada under NSERC Grants A7091 and A3347 and by Energy, Mines and Resources of Canada under Contract OST 85-00119.

REFERENCES

1. Smoot, L.D. and Horton, M.D., Prog. Energy, Combust. Sci., 3: 235-258, 1977.

2. Krazinski, J.L., Buckius, R.O. and Krier, H., Prog. Energy Combust. Sci., 5: 31-71, 1979.

3. Slezak, S.E., Fitch, D.J., Krier, H., Buckius, R.O., Combustion and Flame, 54: 103-119, 1983.

4. Ballal, D.R., Proc. R. Soc. London, A369: 479-500, 1980.

5. Ballal, D.R., Proc. R. Soc. London, A385: 1-19, 1983.

6. Hertzberg, M., Conti, R.S., Cashdollar, K.L., Twentieth Symposium (International) on Combustion, pp. 1681-1990, 1984.

7. Ballal, D.R. and Lefebre, A.H., Combustion and Flame, 35: 155-168, 1979.

8. Eckhoff, R.K., Combustion and Flame, 24: 53-64, 1975.

9. Smoot, L.D., Hedman, P.O. and Smith, P.J., Prog. Energy Combust. Sci., 10: 359-441, 1984.

10. Smoot, L.D., Hecker, W.C. and Williams, G.A., Combustion and Flame, 26: 323-342, 1976.

11. Slezak, S.E., Buckius, R.O. and Krier, H., Combustion and Flame, 59: 251-265, 1985.

12. Zeldovich, Ya.B., Combustion and Flame, 40: 225-234, 1981.

13. Jarosinski, J., Combustion and Flame, 50: 167-175, 1983.

14. Gaug, M., Knystautas, R., Lee, J.H.S., Nelson, L, Benedick, W.B. and Shepherd, J., "The Lean Flammability Limits of Hybrid Mixtures". 10th ICODERS, Berkeley, August 1985. To be published in AIAA Progress in Astronautics and Aeronautics.

15. Jarosinski, J., Strehlow, R.A., and Azarbarzin, A., Nineteenth Symposium (International) on Combustion, pp. 1549-1557, 1982.

16. Jarosinski, J., Combustion and Flame, 56: 337-342, 1984.

17. Andrews, G.E. and Bradley, D., Combustion and Flame, 19: 275-288, 1972.

18. Lewis, B. and von Elbe, G., Combustion, Flame and Explosion of Gases, New York, Academic Press, 1964.

Table I

Properties of Coal Dust Samples

Source	Proximate Analysis %				Specific Surface Area cm^3/g	Minimum Explosive Concentration g/m^3
	Moisture	Ash	V.M.	F.C.		
DEVCO NO. 26	0.70	4.47	32.09	62.74	2190	67
PITTSBURGH (Std.)	1.44	4.91	37.52	56.23	2670	70

FIGURE CAPTIONS

Fig. 1	Side view of the apparatus.
Fig. 2	Quenching distance as a function of methane concentration in methane-air mixture.
Fig. 3	Quenching distance as a function of cornstarch concentration.
Fig. 4	Quenching distance as a function of aluminum concentration.

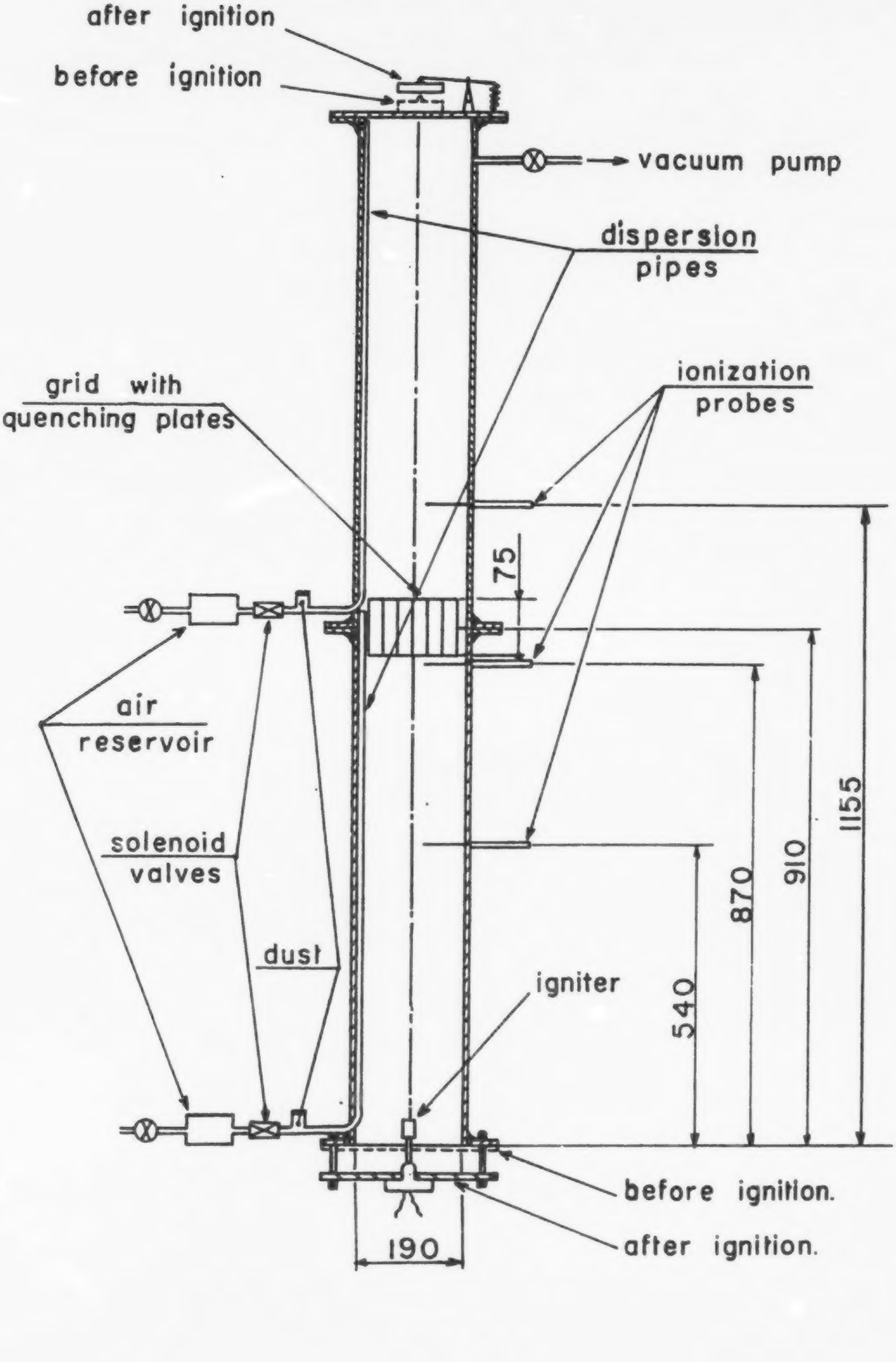
after ignition
before ignition
vacuum pump
dispersion pipes
ionization probes
grid with quenching plates
75
air reservoir
solenoid valves
dust
igniter
540
870
910
1155
before ignition.
after ignition.
190

Fig. 1.

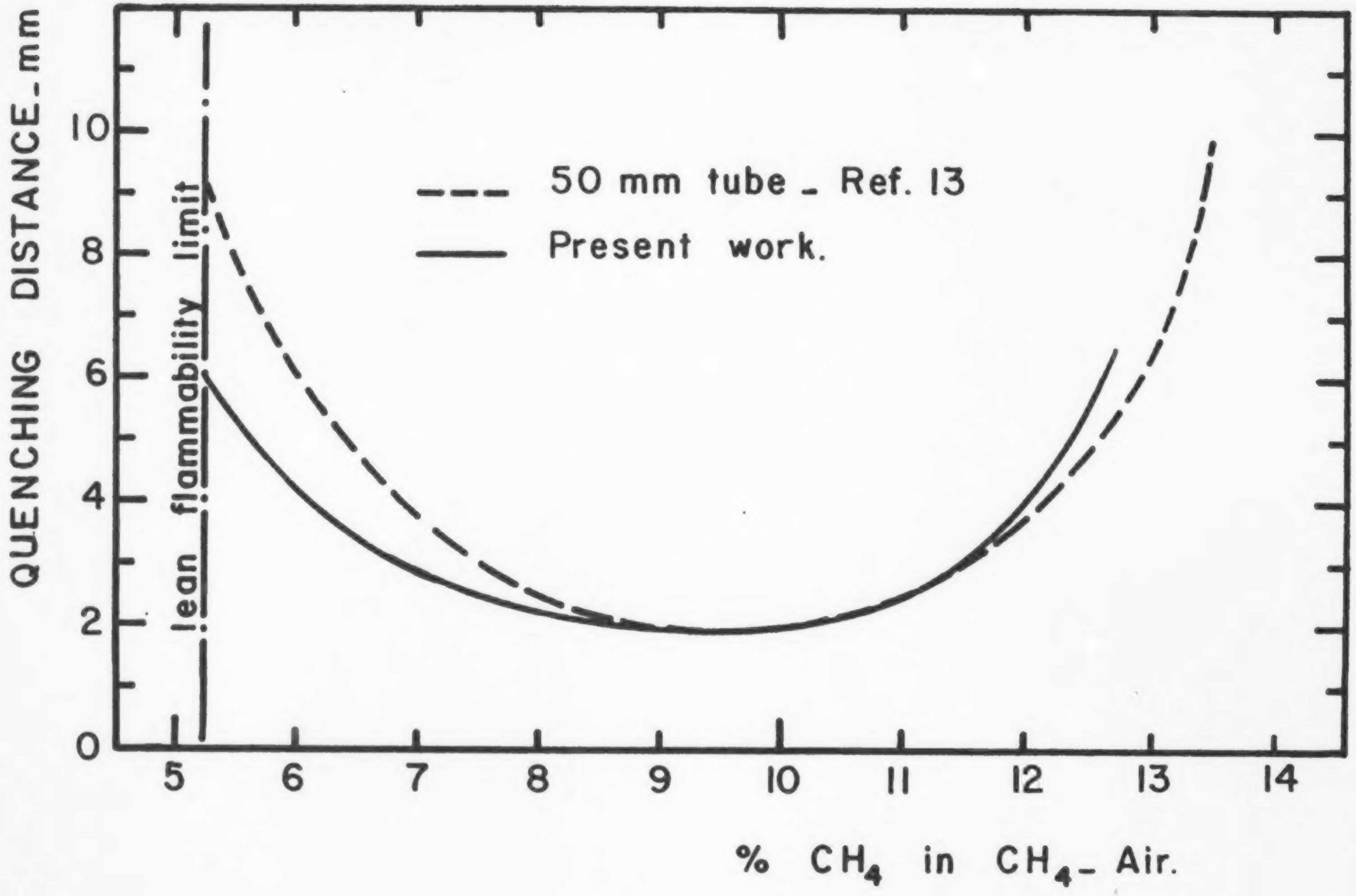
QUENCHING DISTANCE_mm
0
2
4
6
8
10
5
6
7
8
9
10
11
12
13
14
% CH_4 in CH_4- Air.
50 mm tube _ Ref. 13
Present work.
lean flammability limit

Fig. 2.

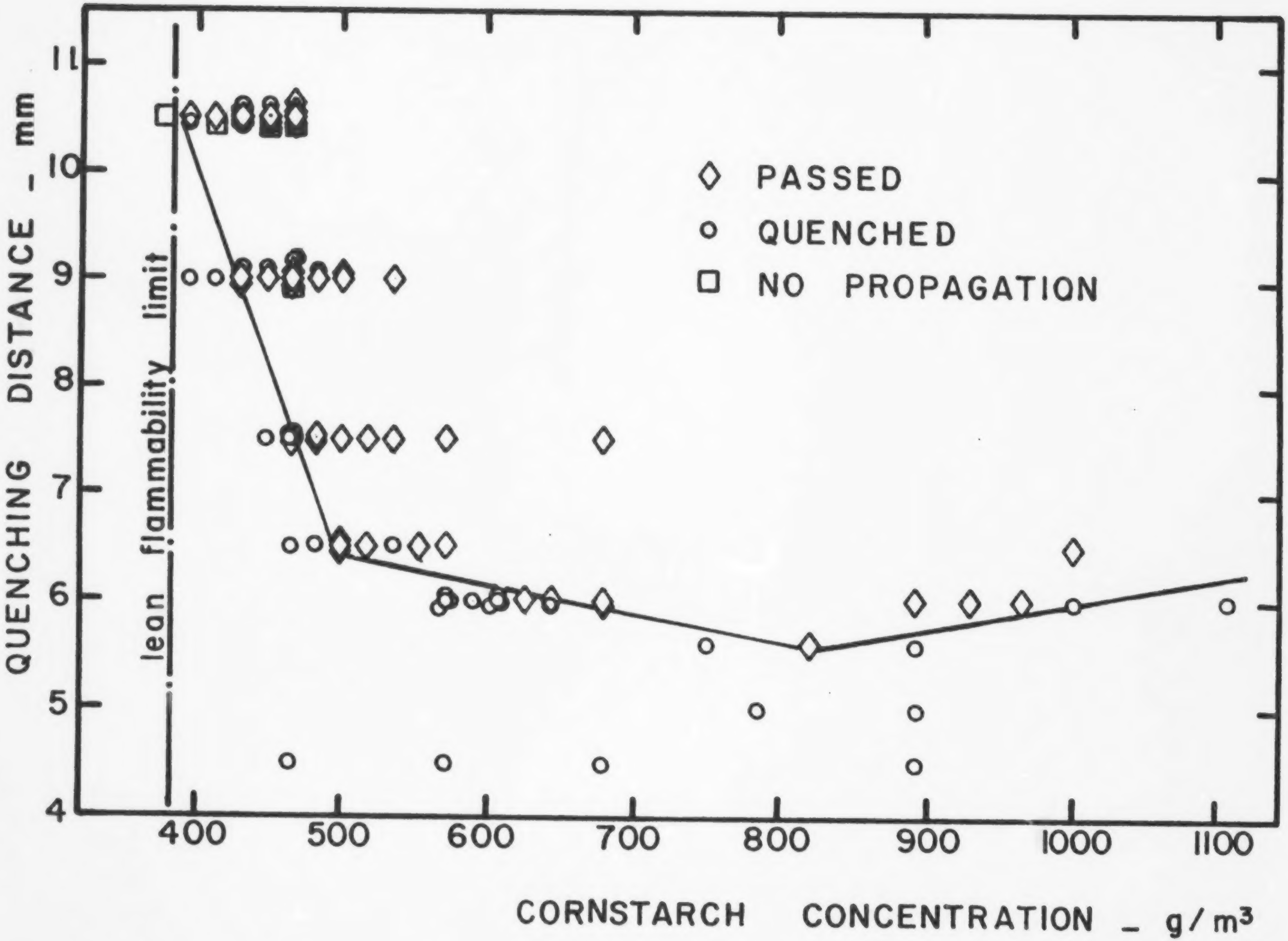
QUENCHING DISTANCE - mm
11
10
9
8
7
6
5
4
400
500
600
700
800
900
1000
1100
CORNSTARCH CONCENTRATION - g/m³
lean flammability limit
◇ PASSED
○ QUENCHED
□ NO PROPAGATION

Fig. 3.

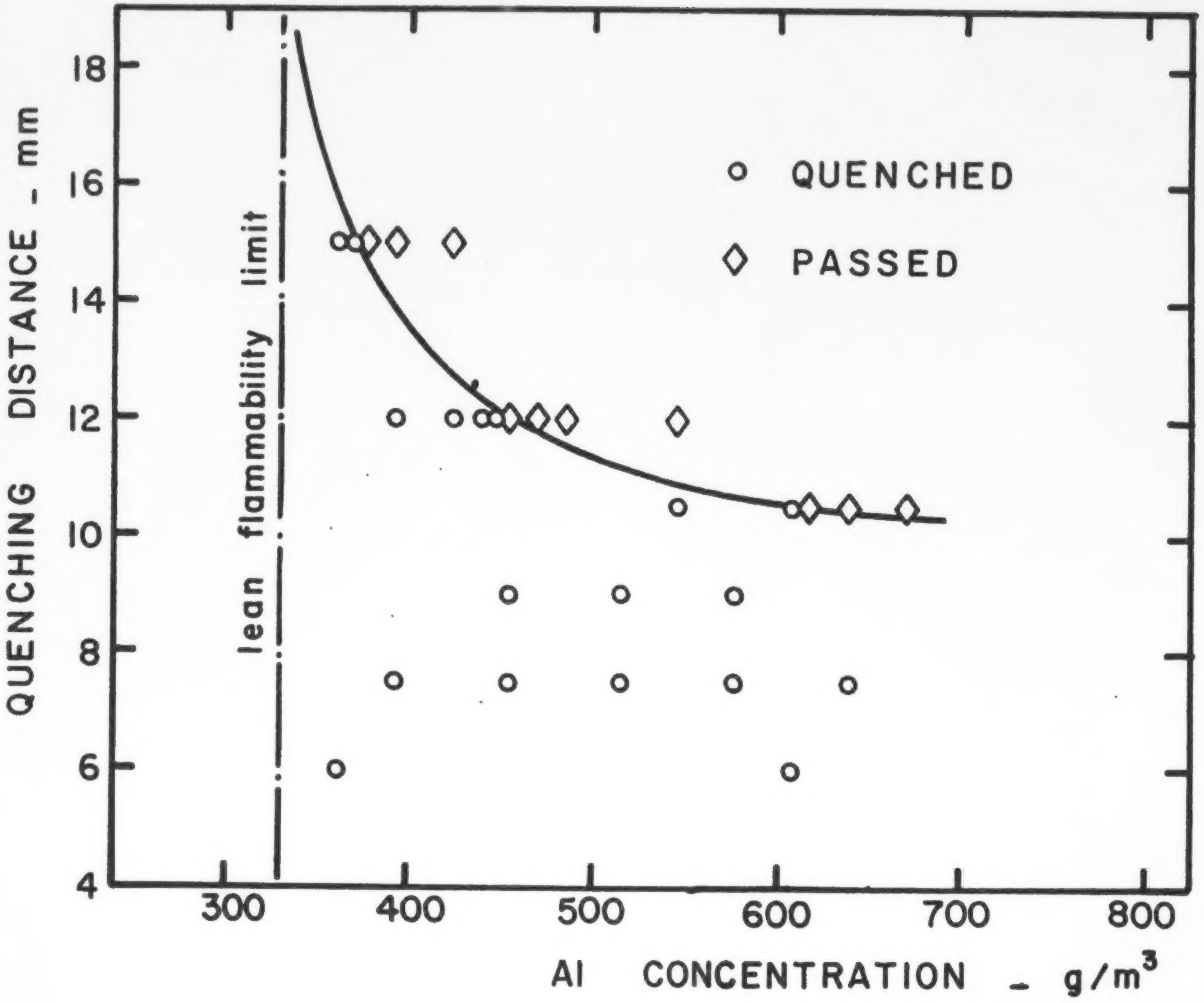
QUENCHING DISTANCE - mm
18
16
14
12
10
8
6
4
300
400
500
600
700
800
Al CONCENTRATION - g/m³
○ QUENCHED
◇ PASSED
lean flammability limit

Fig. 4.